THE *PLASMODIUM FALCIPARUM* EXPORTED HSP40 CO-CHAPERONE, PFA0660w

A thesis submitted in fulfillment of the requirements for the degree

of

DOCTOR OF PHILOSOPHY IN BIOCHEMISTRY

of

RHODES UNIVERSITY

in

THE FACULTY OF SCIENCE

DEPARTMENT OF BIOCHEMISTRY, MICROBIOLOGY AND BIOTECHNOLOGY

By

DANIYAN, Michael Oluwatoyin

B.Pharm, MSc (Pharmacology)

April 2013

ABSTRACT

Plasmodium falciparum is the pathogen that is responsible for the most virulent, severe and dangerous form of human malaria infection, accounting for nearly a million deaths every year. To survive and develop in the unusual environment of the red blood cells, the parasite causes structural remodelling of the host cell and biochemical changes through the export of virulence factors. Among the exportome are the molecular chaperones of the heat shock protein family, of which Hsp40s and Hsp70s are prominent. PFA0660w, a type II *P. falciparum* Hsp40, has been shown to be exported in complex with PfHsp70-x into the infected erythrocyte, suggesting possible functional interactions. However, the chaperone properties of PFA0660w and its interactions with proteins of parasite and human origin are yet to be investigated. Using a codon optimised coding region, PFA0660w was successfully expressed in *E. coli* M15[pREP4] cells. However, the expressed protein was largely deposited as insoluble pellet, and analysis of the pellets revealed a high percentage of PFA0660w, characteristic of inclusion body formation. PFA0660w was purified from inclusion bodies using additive enhanced solubilisation and refolding buffers followed by nickel affinity chromatography. SDS-PAGE and western analysis revealed that the purified protein was of high purity. Size exclusion chromatography showed that the protein existed as a monomer in solution and the secondary structure analysis using Fourier transformed infrared spectroscopy (FTIR) confirmed the success of the refolding approach. Its monomeric state suggests that PFA0660w may be functionally different from other Hsp40 that form dimers and that for PFA0660w, dimer formation may not be needed to maintain the stability of the protein in solution, but may occur in response to functional necessities during its interaction with partner Hsp70. PFA0660w was able to significantly stimulate the ATPase activity of PfHsp70-x but not PfHsp70-1 or human Hsp70 (HsHsp70), suggesting a specific functional interaction. Also, PFA0660w produced a dose dependent suppression of rhodanese aggregation and cooperated with PfHsp70-1, PfHsp70-x and HsHsp70 to cause enhanced aggregation suppression. Its ability to independently suppress aggregation may help to maintain substrates in an unfolded conformation for eventual transfer to partner Hsp70s during refolding processes. Also, the *in vivo* characterisation using a PFA0660w peptide specific antibody confirmed that PFA0660w was exported into the cytosol of infected erythrocytes. Its lack of induction upon heat shock suggests that PFA0660w may not be involved in the response of the parasite to heat stress. Overall, this study has provided the first heterologous over-expression, purification and biochemical evidence for the possible functional role of PFA0660w, and has thereby provided the needed background for further exploration of this protein as a potential target for drug discovery.

DECLARATION

I, Michael Oluwatoyin DANIYAN, declare that this thesis is my work, submitted in fulfillment of the award of Doctor of Philosophy (Science) in Biochemistry of Rhodes University. This thesis has not been submitted for any other degree or examination in any other university

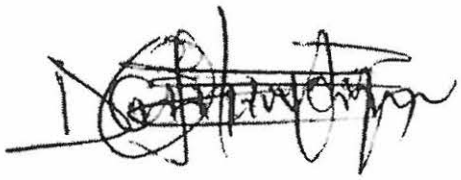

This 29th day of April, 2013.

TABLE OF CONTENTS

CHAPTER THREE:
BIOCHEMICAL CHARACTERISATION OF PFA0660w

CHAPTER FOUR:
IN VIVO CHARACTERISATION OF PFA0660w

LIST OF TABLES

LIST OF FIGURES

DEDICATION

This thesis is dedicated:

To my late Mother, Mrs Comfort Modamidola Ayinke Daniyan, who started this journey with me but was snatched away by the cold hand of death too soon to witness the glorious hour. Your prayers and love will forever be cherished. I LOVE YOU MOTHER

AND

To my Wife, Mojirade Oluwakemi, and my children, Oluwadunsin, Oore-ofe and Oluwatoyin (Temitope) for their love, perseverance, prayers and understanding throughout the thick and thin of this journey. I LOVE YOU ALL SO DEARLY.

ACKNOWLEDGEMENTS

*"Now unto him that is able to keep **me** from falling, and to present **me** faultless before the presence of his glory with exceeding joy, to the only wise God our Saviour, be glory and majesty, dominion and power, both now and ever. Amen" (Jude 1: 24, 25).*

I want to express my sincere appreciation to my supervisor, Professor G.L. Blatch, for his loving kindness, patience, understanding and genuine interest in my work. His advice and encouragements at all times make the seemingly difficult journey enjoyable. Thank you for the opportunity you granted to me to take from your wealth of experience.

I appreciate my co-supervisor, Dr. Aileen Boshoff, who is more to me a sister rather than a boss. Her interest in my wellbeing was demonstrated in her perseverance to ensure that I secure bursary and scholarship for my last year, without which this work may not have been completed. Thank you for being there when it was most needed.

I will not fail to appreciate Dr. Eva-Rachele Pesce, whose interest in my work was equally commendable. She taught me to be self dependent and always strive towards excellence. Thank you.

I would love to specially thank my able team leader, Dr. Adrienne Edkins, for her leadership, encouragement and interest in ensuring that all was provided to ensure the speedy completion of this project. Thank you.

My appreciation goes to Dr. Earl Prinsloo, who was always at hand to help with instrumentations and data interpretations. To Lola and Nana, who would not allow me to go hungry, to members of Lab 325, to James - my brother, my colleague, my help, a friend that stick closer than a brother -, to Fortunate, Mike, Dastin and Mugda (and her husband) for their help and gifts of love, and to other members of BioBRU, past and present for love and care. Thank you.

A special thank you goes to all my family friends in Grahamstown – Tshuma, Sibanda, Madgaza, Juma, Daniel and SDA Students' Movement family. To my Pastor, Donovan and his Wife, and members of Seventh Day Adventist (SDA) Church in Grahamstown for their moral and spiritual supports which were without equal. Keep the lamps burning bright, because it won't be long.

This acknowledgement would not be complete without recognizing the special love and care of the following: Members of Pharmacology department, Obafemi Awolowo University, Ile-Ife, Nigeria; Pastors Akanbi Joshua, Jimoh Samuel, Ogungbesan E.O, Afanga S and their families; Drs Opreh Peter and Jegede Akinlolu and their families. Others are Prof. E. O. Iwalewa, Dr and Pharm (Mrs) Adeloye O; Elder and Mrs Aworinde; Elder and Mrs Gbadeyan M.A, Elder and Mrs E.T. Onibiyo and Dr and Dr(Mrs) S. A. Daniyan and their families. Thank you for been there for me all the way. Your care, kindness, spiritual and moral supports are highly appreciated.

Many thanks to the love of my life, my dear Wife, and to my children, Oluwadunsin, Oore-ofe and Oluwatoyin (Temitope) for being there for me all the way. May you live long to enjoy with me the fruits of this glorious land.

"Finally, brethren, whatsoever things are true, whatsoever things are honest, whatsoever things are just, whatsoever things are pure, whatsoever things are lovely, whatsoever things are of good report; if there be any virtue, and if there be any praise, think on these things" (Philippians 4:8).

MARANATHA!!!

FUNDING ACKNOWLEDGEMENTS

I sincerely appreciate the funding supports from the following:

1. Education Trust Fund Academic Staff Training and Development (ETF AST&D) Scholarship of Obafemi Awolowo University, Ile-Ife, Nigeria.
2. National Research Foundation (NRF) of South Africa.
3. Rhodes University Council Research Scholarship.
4. Rhodes University International Sub-charge (RUIS) bursary.
5. Molecular Approaches to Malaria (MAM) 2012 travel award.

LIST OF RESEARCH OUTPUT

PUBLICATION (Peer review in progress)

Michael Oluwatoyin Daniyan, Aileen Boshoff, James Njunge, Eva-Rachele Pesce and Gregory L. Blatch (2013): The exported plasmodial heat shock protein 40, PFA0660w, is a potential co-chaperone of PfHsp70-x. Journal of Biochemical and Molecular Parasitology.

CONFERENCE PROCEEDINGS

Michael O. Daniyan, Aileen Boshoff, Eva-Rachele Pesce and Gregory L. Blatch (2012): Heterologous production and Functional assays of the exported Hsp40, PFA0660w. Molecular Approaches to Malaria (MAM) 2012 Conference, 19-23 February, Lorne, Victoria, Australia.

Michael O. Daniyan, Aileen Boshoff, Eva-Rachele Pesce, Earl Prinsloo, Gregory L. Blatch (2012): Functional interaction of PFA0660w, an exported Hsp40, with PfHsp70-x. 4th Interdisciplinary Post Graduate Conference (IPGC) 12 – 14 September, Rhodes University, Grahamstown, South Africa

LIST OF SYMBOLS AND ABBREVIATIONS

<	less than
>	greater than
α	alpha
β	beta
λ	lambda
°C	degrees Celsius
μ	micro
μg	microgram(s)
μl	microlitre(s)
M	molar
μM	micromolar
mol	mole(s)
μmol	micromole(s)
nmol	nanomole(s)
pmol	picomole(s)
μm	micrometre(s)
nm	nanometres
ml	millimetres
w/v	weight per volume
v/v	volume per volume
w/w	weight per weight
A	Absorbance
A_{600}	Absorbance at 600 nm
A_{850}	Absorbance at 850 nm
Amp^R	Ampicillin resistance (β-lactamase gene)
ADP	Adenosine Diphosphate
ATP	Adenosine Triphosphate
ATPase	Adenosine Triphosphatase
DnaJ	A family of proteins characterized by J domain
EEVD	Glutamate-Glutamate-Valine-Aspartate (Glu-Glu-Val-Asp) motif
EEVN	Glutamate-Glutamate-Valine-Asparagine (Glu-Glu-Val-Asn) motif
ER	Endoplasmic Reticulum
GF Domain	Glycine/Phenylalanine domain

HPD	Histidine-Proline-Aspartate (His-Pro-Asp) motif
Hsp	Heat Shock Protein
HsHsp	Human Hsp
Hsp40	40kDa Hsp
Hsp70	70kDa Hsp
J Domain	Conserved domain in DnaJ and DnaJ-like proteins which interact with Hsp70s
kDa	kiloDalton
PfHsp	*Plasmodium falciparum* Hsp

CHAPTER 0NE

LITERATURE REVIEW AND STUDY BACKGROUND

Malaria is one of the world's leading causes of death, especially among people living in sub-Sahara Africa and other tropical regions. Of the five species of the genus Plasmodium, the malaria protozoan parasites known to infect man, Plasmodium falciparum (P. falciparum) is responsible for the most virulent, severe and dangerous form of the disease. Over the years, chemotherapy has played a central role in the strategies towards the eradication of malaria. However, the ability of P. falciparum to develop resistance to effective and affordable drugs, coupled with the resistance of mosquitoes to pyrethroids, the active principle of the insecticide treated nets has made a constant search for new pharmacotherapy imperative. This review presents an overview of the life cycle of P. falciparum, the efforts at controlling the disease and the molecular and cellular basis of the infection with special emphasis on molecular chaperones of the heat shock protein family as critical components of the parasite intra-erythrocytic development and survival. The motivation for and the key objectives of the present work are also presented.

1.1 Introduction

Malaria is both preventable and curable, but yet it still impacts negatively on the health of millions of people and accounts for a high rate of mortality, especially among children in sub-Sahara Africa (Snow *et al.*, 2005; Rowe *et al.*, 2006). Five species of the genus *Plasmodium,* the protozoan parasites responsible for malaria infection are known to infect humans. They are *P. falciparum*, *P. vivax*, *P. malariae*, *P. ovale* and *P. knowlesi.* It has been proposed that *P. ovale* consists of two species (Cox-Singh, 2010) and that zoonosis is the medium through which *P. knowlesi* infects humans (White, 2008). Of these, *P. falciparum* and *P. vivax* are the most abundant and clinically most important, with the former responsible for the most virulent, severe and dangerous form of human malaria (Greenwood *et al.*, 2008).

The World Health Organization (WHO) 2012 Malaria report ("WHO | World Malaria Report," 2012) which updated the 2011 report, estimated a total of 219 million episodes of malaria in 2010 with at least 660 000 deaths, mostly in Africa and among children under the age of 5 years. Malaria was reported to be prevalent in 99 countries with an estimated 3.3 billion people at risk. Although support from international donors has led to a rapid decrease in malaria mortality, especially among adults in Africa, Murray *et al.*, (2012) contended that the malaria mortality burden may actually be larger than previously estimated and that for the necessary elimination and eradication to be achieved at larger scale, there is an urgent need for more supports. Factors such as lack of sanitation, malnutrition, lack of or reduced access to medications, poverty and the location of many of the poor countries affected by malaria in the tropical zones, combine together to create an enabling environment for the disease to thrive. Though preventive approaches such as good sanitation and distribution of insecticide treated nets (ITNs) (Curtis *et al.*, 2006) have been employed as a strategy towards the eradication of this disease, chemotherapy remains the most widely used approach. The ability of *P. falciparum* to develop resistance to effective and affordable drugs (Jambou *et al.*, 2005; Cheeseman *et al.*, 2012) and the resistance of mosquitoes to pyrethroids, the active principle of the ITNs (N'Guessan *et al.*, 2007; Fane *et al.*, 2012), have made a constant search for new pharmacotherapy imperative.

The life cycle of the malaria parasite is a complex mechanism involving two hosts, human and female *Anopheles* mosquitoes. However, the clinical symptoms of the disease are associated with the invasion of the erythrocytes by the parasite, its growth, division inside the host cell and the cyclic cell lysis and reinvasion of new erythrocytes (Cowman and Crabb, 2006; Goldberg and Cowman, 2010). The intra-erythrocytic survival and development of the parasite as well as the pathology of the infection are linked to structural and functional remodelling of the host cell

through the export of parasite-encoded proteins (Marti *et al.*, 2004; Haldar and Mohandas, 2007; Maier *et al.*, 2009). Meanwhile, attempts have been made to present an extensive description of the protein interaction network for *P. falciparum* (LaCount *et al.*, 2005) and about 300 parasite-encoded proteins were predicted to be exported (Hiller *et al.*, 2004; Marti *et al.*, 2004; Sargeant *et al.*, 2006). Among the exported proteins are molecular chaperones of the heat shock protein family (Maier *et al.*, 2008). Molecular chaperones are a family of proteins that function to stabilize proteins, facilitate their translocation across intracellular membranes, facilitate protein degradation, and ensure that proteins in a cell are properly folded and functional (Hartl, 1996; Hartl and Hayer-Hartl, 2002). Members of the 40 kDa heat shock protein family (PfHsp40), consisting of 49 proteins in total are part of the exportome in *P. falciparum* (Sargeant *et al.*, 2006; Njunge *et al.*, 2013). PFA0660w (PF3D7_0113700), a type II PfHsp40 protein, belongs to this extended Hsp40 family and has been shown to be transported by the parasite into the host cell (Külzer *et al.*, 2010). PFA0660w in complex with *P. falciparum* Hsp70-x (PfHsp70-x - PF3D7_0831700) is localized into structures in the infected erythrocyte called J-dots (Külzer *et al.*, 2010, 2012). Failure to obtain a viable *PFA0660w*-knocked-out parasite (Maier *et al.*, 2008), suggests that it may be essential for the survival of the parasite in the infected erythrocytes and therefore a potential drug target. This review endeavours to concisely present our current understanding of the *P. falciparum* chaperone complement, their importance in parasite survival and as target for drug action, with special focus on PFA0660w, being the basis of this research project.

1.2 Malaria Infection

1.2.1 Background information

Malaria remains a life-threatening disease that was prominent more than 4,000 years ago and continues to be responsible for millions of deaths. The World Health Organization (WHO) listed malaria among the most important infectious diseases of the tropics and form part of the sixth millennium development goal (MDG 6) ("WHO | MDG 6: combat HIV/AIDS, malaria and other diseases," 2012). An important target of MDG 6 is to bring malaria and other major diseases to a halt by 2015 and begin to reverse their incidences. With special focus on pregnant women and young children, the strategies advocated by WHO to combat malaria include prevention with the use of long-lasting ITNs, indoor residual spraying and rapid treatment with effective anti-malarial medicines. Also, relating to Nigeria, Olusegun *et al.*, (2012) identified prevention from mosquitoes and prompt treatment of malaria infection as an important intervention strategy in curbing maternal and child death. WHO "Roll Back Malaria" initiative further recommends that to control *P. falciparum* malaria during pregnancy, in addition to individual protection with ITNs and prompt management of anaemia and malaria using effective anti-malaria drugs, intermittent preventive treatment (IPTp) or chemoprophylaxis should be encouraged ("WHO | Malaria in pregnancy," 2012).

Malaria is transmitted to humans by female *Anopheles* mosquitoes during a blood meal. *P. falciparum* is the most dangerous of all the *Plasmodium* species affecting man and children under age 5 years are the most vulnerable (Breman, 2001; Rowe *et al.*, 2006). To date, chemotherapeutic drugs remains the most widely used approach at controlling the disease (Butler *et al.*, 2010; D'Alessandro, 2009), notwithstanding the success of preventive approaches such as the use of ITNs, IPTp and chemoprophylaxis with good sanitation (Curtis *et al.*, 2006; "WHO | Malaria in pregnancy," 2012). However, increase in incidences of resistant cases to effective and affordable drugs (Jambou *et al.*, 2005; Cheeseman *et al.*, 2012) by the parasite and mosquitoes' resistance to pyrethroids, the active principle of ITNs (N'Guessan *et al.*, 2007; Fane *et al.*, 2012), underscored the need for new pharmacotherapy. In addition efforts aimed at enhancing long lasting protective immunity through vaccination have also been intensified (Ballou, 2009; Casares *et al.*, 2010).

1.2.2 Life Cycle of Plasmodium falciparum

The malaria parasite completes its life cycle in two hosts, humans and female *Anopheles* mosquitoes (Figure 1.1). The survival of the parasite, during several stages of its development, depends on its ability to utilize specialized proteins for the purpose of invasion and development and for protection against the immune response of the host (Florens *et al.*, 2002; Greenwood *et al.*, 2008).

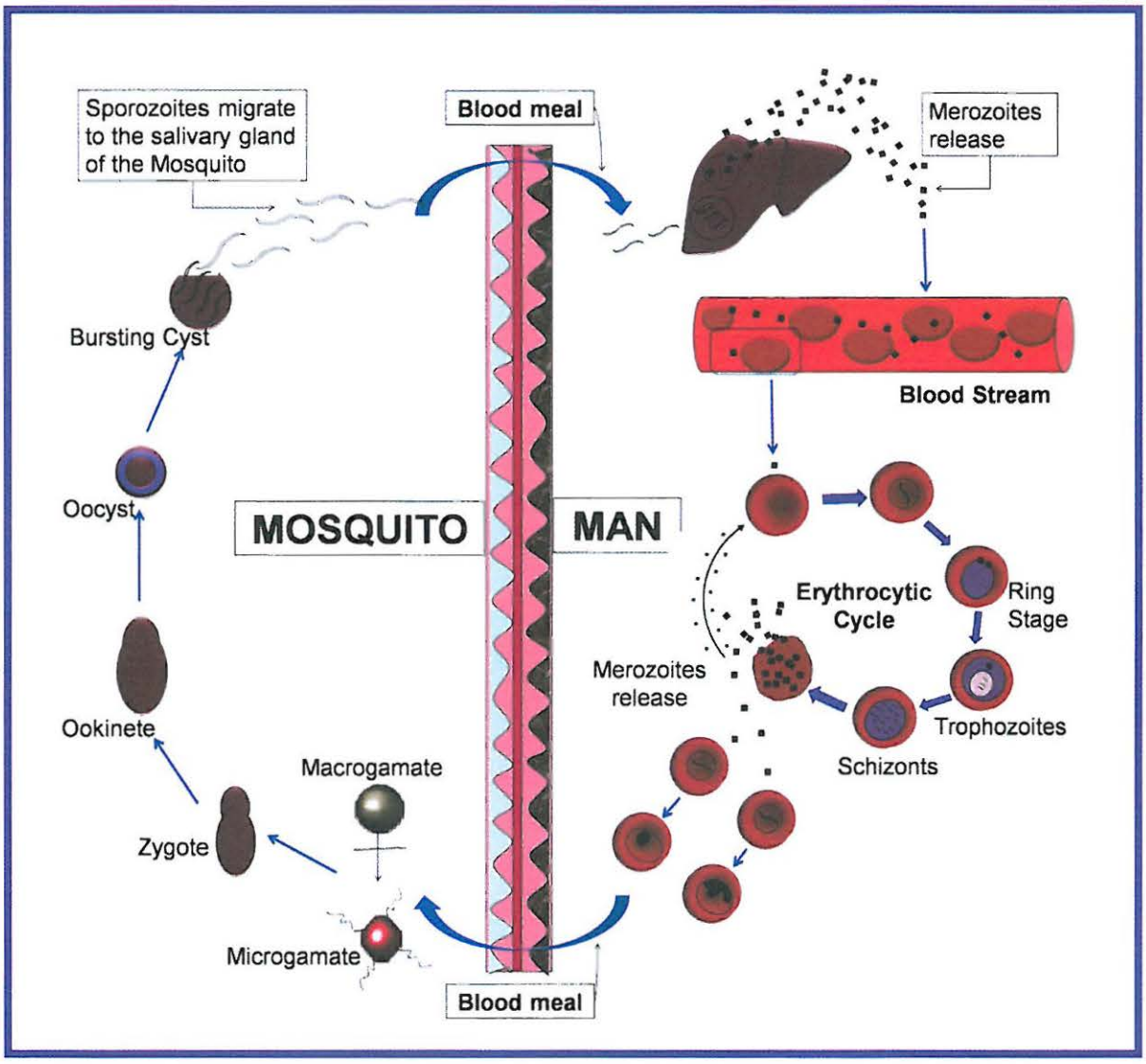

Figure 1.1: The life cycle of *Plasmodium falciparum*.
The parasite life cycle traverses two hosts (man and mosquito) with each stage involving complex cellular and molecular modifications. Sporozoite-infected saliva is deposited into the human host during blood meal by female Anopheles mosquitoes and the sporozoites make their way to the liver, develop over time into merozoites (that are released into blood stream to invade erythrocytes). The clinical symptoms of the disease are associated with the invasion of the erythrocytes by the parasite, its growth, division inside the host cell and the cyclic cell lysis and reinvasion of new erythrocytes. Some of the merozoites will eventually develop into gametocytes (male and female) which can be taken in by mosquitoes following another blood meal.

Sporozoites (infective stage), merozoites (erythrocytes invading stage), trophozoites (multiplying form in erythrocytes), and gametocytes (sexual stages) are stages involved in the development of the parasite (Figure 1.1). These stages are unique in shape, structure and protein profiles. The continuous changes in surface protein, as well as metabolic pathways during these stages help the parasites to survive the host immune response and create challenges for drug and vaccine development (Florens *et al.*, 2002). The sporogony or sexual phase occurs in mosquitoes, leading to the formation of numerous infective forms of the parasites. When a female *Anopheles* mosquito ingests blood from an individual infected with malaria, the parasite male and female gametocytes reach the mosquito gut where they initiate the sporogonic cycle (Figure 1.1). The fusion of male and female gametes produces a zygote, which subsequently develops into an active ookinete that pierces its way into the midgut wall of the mosquito to form an oocyst. Each oocyst divides to produce numerous active haploid forms called sporozoites which are subsequently released into the mosquito's body cavity following the burst of the oocyst. The sporozoites then invade the mosquito salivary glands, and are, together with the saliva, injected into the human bloodstream during another blood meal (Ferguson and Read, 2004; Barillas-Mury and Kumar, 2005; Hill, 2006).

The cycle in human is initiated from the liver by the sporozoites and later continues within the erythrocytes, resulting in the clinical manifestations of the malaria disease. The invasive sporozoites that were deposited into the skin after mosquito bite are either destroyed by macrophages or enter the lymphatics and drain into the lymph nodes from where they can develop into exoerythrocytic stages (Vaughan *et al.*, 2008) and prime the T cells as a way of mounting protective immune response (Good and Doolan, 2007) and/or blood vessel (Yamauchi *et al.*, 2007; Silvie *et al.*, 2008b; Vaughan *et al.*, 2008;), from where they make their way into the liver. While in the liver, sporozoites pierce through the sinusoids of the liver, enter into hepatocytes where they grow within parasitophorous vacuoles (PV) and multiply into schizonts, each of which contains thousands of merozoites (Amino *et al.*, 2006; Jones and Good, 2006; Kebaier *et al.*, 2009). The stick-and-slip motility prevents the parasite from been transported by the circulating blood into the kidneys where they can be destroyed and removed from the body. The sporozoites journey is propelled by a unique actin-myosin system, which allows extracellular migration, cell traversal and cell invasion (Kappe *et al.*, 2004). This is a single cycle phase with no clinical symptoms, unlike the intra-erythrocytic stage that is characterized by cyclic re-invasion accounting for the clinical manifestation of the disease.

The hepatocytic merozoites are stored in vesicles called merosomes where they are protected from the phagocytotic action of Kuppfer cells (Sturm *et al.*, 2006; Silvie *et al.*, 2008a). The release of

these merozoites into the blood stream via the lung capillaries initiates the blood stage of the infection (Silvie *et al.*, 2008b). The intra-erythrocytic development of the parasite occurs with precise cyclic accuracy with each repeated cycle producing hundreds of daughter cells that subsequently invade more red blood cells (RBCs). The clinical symptoms of the disease are associated with the invasion of the erythrocytes by the parasite, its growth, division inside the host cell and the cyclic cell lysis and reinvasion of new erythrocytes. The invasion of RBCs by the merozoites takes place within seconds and is made possible by a series of receptor–ligand interactions. The ability of the merozoites to quickly disappear from circulation into the RBCs protects its surface antigens from exposure to the host immune response (Cowman and Crabb, 2006; Greenwood *et al.*, 2008; Silvie *et al.*, 2008b). Micronemes, rhoptries, and dense granules are the unique apical secretory organelles of the merozoite with specialized functions including helping the merozoites to attach, invade, and establish itself in the RBC (Cowman and Crabb, 2006). The successful formation of a contact junction with the host cell is followed by entry into the cells (Cowman and Crabb, 2006) and subsequent formation of a PV, that isolates the intracellular ring parasite from the erythrocyte cytoplasm thereby creating a conducive environment for its development (Cowman and Crabb, 2006; Bosch *et al.*, 2007; Haldar and Mohandas, 2007). The intra-erythrocytic parasite is faced with the challenge of surviving in an environment devoid of organelles needed for normal biosynthetic and metabolic functions of the cells. This challenge is overcome by exporting several proteins for host cell remodelling (Sargeant *et al.*, 2006; Maier *et al.*, 2008; Crabb *et al.*, 2010; Goldberg and Cowman, 2010; Spielmann and Gilberger, 2010). Following the ingestion of the hemoglobin into the food vacuole, it is degraded to make available the amino acids for protein biosynthesis, while heme, a toxic free radical, is produced in the process of hemoglobin degradation and the parasite converts it to insoluble crystals called hemozoin (Francis *et al.*, 1997; Lew *et al.*, 2003; Robert *et al.*, 2005; Tekwani and Walker, 2005). Meanwhile, to reduce the high rate of mortality that is associated with malaria infection, preventive measures, chemoprophylaxis and vaccine development are essential components of approach for controlling the infection.

1.2.3 Control of malaria infection

1.2.3.1 Malaria Prevention

Preventive measures are a critical step towards the control and eradication of malaria. Preventive approach can broadly be divided into two – infection control and vector control. Infection control focuses on preventing the development of the disease as a result of occasional mosquito bite (Walsh

et al., 1999; Lell *et al.*, 2000). This involves the use of chemoprophylaxis. One important target group in the infection control using chemoprophylaxis are pregnant women. Intermittent preventive treatment for pregnant women (IPTp) is the globally acknowledged approach for prevention of malaria during pregnancy (Vallely *et al.*, 2007; "WHO | Malaria in pregnancy," 2012). Sulphadoxin-pyrimethamine (SP) has been used for this purpose and there are compelling arguments for the use of artesunate-SP (Jansen, 2011). To ensure long lasting prevention, this approach should be combined with vector control.

Vector control focuses on protecting against mosquitoes bites, thereby preventing the transmission of the parasite to man. Strategies for vector control include the use of residual spraying of insecticides, insect repellent cream or spray, sleeping under bed nets, especially, the insecticide impregnated bed nets (ITNs) and proper sanitation (Curtis *et al.*, 2006; Lavialle-Defaix *et al.*, 2011; "WHO | Insecticide-treated materials," 2012). WHO provides guideline for the production, preparation, distribution and the use of the ITNs ("WHO | Insecticide-treated materials," 2012). With the reported resistance to pyrathroids, an active principle of the ITNs (N'Guessan *et al.*, 2007; Fane *et al.*, 2012), all strategies involving the use of chemical agents, also face the global challenge of developing resistance. Personal and general hygiene which involve in-door and out-door cleaning, good refuse disposal practices, eradication of stagnant water, proper sewage disposal and clean, dry and uninterrupted drainages are examples of good sanitation practices that will not only prevent malaria infection, but also other killer diseases of the tropics. Sanitation is not only cheap and affordable; it is within the reach of everybody.

1.2.3.2 Malaria chemotherapy

Various approaches have been employed to identify new antimalarial agents with a view to reducing cost, ensuring availability and decreasing the incidences of resistance (Rosenthal, 2003). Many drugs in use today, including chloroquine, primaquine and mefloquine from quinine (Stocks *et al.*, 2001); 8-aminoquinoline and tafenoquine, from primaquine (Walsh *et al.*, 1999) and lumefantrine from halofantrine (van Vugt *et al.*, 2000) are produced through chemical modification approach. Another approach is the use of plant-derived compounds, with little or no chemical modification, that has led to the discovery of potent antimalarials such as artemisinins (Meshnick, 2001). Also, the use of other agents not originally designed for malaria, such as folate antagonists, tetracyclines and other antibiotics that were reported to be active against malaria parasites (Clough and Wilson, 2001) is another viable approach to drug discovery. Drugs involved in resistance reversals such as verapamil, desipramine and trifluoperazine (van Schalkwyk *et al.*, 2001) have also been used in combination with antimalarial drugs to improve therapy.

Table 1.1 present an overview of the common antimalarial drugs, their mode and mechanism of actions. These drugs are either schizonticidal (attacking and killing the schizonts at tissue level e.g. pyrimethamine or intra-erythrocytic level) or gametocidal (attacking and killing the gametes, thereby preventing man to mosquitoes transmission). Optimisation of therapy with these existing antimalarial agents, through combination therapy, is widely used as a productive approach towards improving treatments. However, for the combination to be ideal, it should improve antimalarial efficacy, provide additive or synergistic antiparasitic activity and slow the progression of parasite resistance. For example, combination of artesunate with sulfadoxine/pyrimethamine (von Seidlein *et al.*, 2000) or with amodiaquine (Adjuik *et al.*, 2002), if lacking in resistance to either of the partners which can lead to high rates of recrudescence (Dorsey *et al.*, 2002), may prove to be optimal antimalarial agents. Other combinations that have been effectively used include artesunate and mefloquine (Price *et al.*, 1997) and artemether and lumefantrine (Lefevre *et al.*, 2001). The combination of an analog of proguanil (chlorproguanil) with dihydropteroate synthase (DHPS) inhibitor (dapsone), originally produced to treat leprosy (Mutabingwa *et al.*, 2001) has opened up a new and effective approach to antimalarial drug therapy. Meanwhile, one important and innovative approach towards drug discovery in malaria chemotherapy is the search for new antimalarial drug targets. Such targets include parasite membrane (Vial and Calas, 2001), food vacuole (Banerjee *et al.*, 2002), mitochondria and apicoplast (Ralph *et al.*, 2001; Vaidya, 2001). The cytosol, which is the centre of metabolic (e.g. folate metabolism and glycolysis) and enzyme activities, has proven to be a valuable source of potential targets for drug action (Razakantoanina *et al.*, 2000; Plowe, 2001). Also, the export of proteins, including molecular chaperones of the heat shock protein family, by *P. falciparum* are the focus of many research works and are increasingly gaining ground as potential targets of drug action (Fewell *et al.*, 2004; Chang *et al.*, 2008a; Müller and Hyde, 2010).

Table 1.1: Classes and mechanism of some antimalarial drugs

Classes of drugs	Common drugs	Mode of actions	Mechanism of actions
4-Aminoquinolone[1]	Chloroquine	Schizonticidal Gametocidal	Accumulate at high concentrations in the parasite acid food vacuole, binding directly to heme, and inhibition of heme ferriprotoporphyrin-IX polymerase, vacuolar phospholipase and protein synthesis
	Amodiaquine	Schizonticidal	
8-Aminoquinoline[2]	Primaquine Tafenoquine	Schizonticidal Gametocidal	Possibly by interfering with mitochondrial function
Quinoline methanol[3]	*Quinine	Schizonticidal Gametocidal	Interacting with heme, and by inhibition of both heme polymerisation and activity of heme catalase.
	*Quinidine	Schizonticidal	
	**Mefloquine	Schizonticidal	May have effect on parasite acid vesicles similar to that of chloroquine. Mefloquine-binding proteins and plasmodial P-glycoprotein homolog-1, (Pgh-1) can also be a potential target of mefloquine action and resistance.
Folate antagonists[4]	*Sulfonamides, sulfones	Schizonticidal	Mimick PABA (para amino butyric acid) to compete for DHPS (dihydropteroate synthetase) active sites, thereby inhibiting the formation of dihydropteroate.
	**Pyrimethamine, biguanides (proguanil, cycloguanil), Trimethoprim	Schizonticidal	Mimick dihydrofolate to compete for DHFR (dihydro folate reductase) active sites, thereby inhibiting the reduction of di- to tetra-hydrofolate which is a cofactor for folic acid biosynthesis
Antibiotics[5]	Dexycycline, Tetracycline Clindamycin, Spiramycin	Schizonticidal	Possibly by acting against 70S ribosomes in the parasite mitochondrion.
Phenanthrene methanol[6]	Halofantrine	Schizonticidal	Act by binds to plasmepsin which is a haemoglobin degrading enzyme and to haematin.
Aryl alcohol[7]	Lumefantrine	Schizonticidal	May be connected with inhibition of the formation of ß-haematin through the formation of complex with haemin.
Sesquiterpene lactone endoperoxide[8]	Artemisinins and its derivatives	Schizonticidal	Interacts with reduced iron of heme moiety derived from hemoglobin digestion or free intracellular reduced iron species, leading to bioactivation of ART. They are also involved in heme alkylation, increased production of ROS and oxidative membrane damage by interacting with phospholipids.
Hydroxynaphthoquinone[9]	Atovaquone	Schizonticidal	Atovaquone acts on the mitochondrial electron transfer chain and interfere with mitochondrial membrane potential possibly by inhibition of dihydroorotate dehydrogenase (DHODase). Also, atovaquone may cause mitochondria depolarization or collapse of mitochondria membrane potential by inhibiting electron transfer from ubiquinol to cytochrome C.

[1](Bray *et al.*, 1999; Foster, 1994; O'Neill *et al.*, 1998; Pukrittayakamee *et al.*, 2000; Russelltt and Goldberg, 1996); [2](Beaudoin and Aikawa, 1968; Boulard *et al.*, 1983; Lell *et al.*, 2000; Walsh *et al.*, 1999); [3*](Chou and Fitch, 1993; Chou *et al.*, 1980; de Almeida Ribeiro *et al.*, 1997; Slater and Cerami, 1992); [3**](Cowman *et al.*, 1994; Desneves *et al.*, 1996; Krogstad *et al.*, 1985; Roos and Boron, 1981); [4*](Zhang and Meshnick, 1991); [4**](Brown, 1962; Futterman, 1957); [5](Divo *et al.*, 1985; Geary and Jensen, 1983); [6](Blauer and Akkawi, 1997; Lelièvrel *et al.*, 2012); [7](Lelièvrel *et al.*, 2012); [8](Golenser *et al.*, 2006; Hartwig *et al.*, 2009; O'Neill *et al.*, 2010; Robert *et al.*, 2005; Wang *et al.*, 2010) and [9](Fry and Pudney, 1992; Hudson, 1993; Krungkrai, 1995; Rottenberg, 1997; Vaidya, 2001; Vaidya *et al.*, 1993)

1.2.3.3 Malaria Vaccines

Efforts aimed at enhancing long lasting protective immunity through vaccination, of which RTS,S is emerging as the most promising vaccine formulation, have been intensified (Ballou, 2009; Casares *et al.*, 2010). The RTS,S vaccine candidate was engineered using a recombinant protein that is derived by the fusion of a part of *P. falciparum* circumsporozoite protein with the hepatitis B virus surface antigen and combined with an appropriate adjuvant system (Regules *et al.*, 2011; Wilby *et al.*, 2012). It was designed to prevent the *P. falciparum* parasite from entering the blood stream or prevent the development of the parasite in the liver. It is believed that the decrease in the ability of malaria parasite to infect, develop, and survive in the human liver is linked with the ability of RTS,S to induce the production of antibodies and T cells (Regules *et al.*, 2011; Wilby *et al.*, 2012). These attempts at producing an effective vaccine against malaria infection have, however, for many years proved unsuccessful (André, 2003; Artavanis-Tsakonas *et al.*, 2003). Having a vaccine that can completely block transmission from human to mosquito hosts and that can be developed in line with the model of naturally acquired immunity, may offer improved protection against morbidity and mortality and serve as a major leap towards global eradication of malaria (Struik and Riley, 2004).

Another approach that has gained some level of success in an attempt to produce a malaria vaccine is the use of the whole organism. Volunteers that were challenged by immunization through the bites from greater than 1,000 irradiated *P. falciparum*-infected mosquitoes were reported to have been protected from the infection (Hoffman *et al.*, 2002, 2010a). This led to the development of an approach that uses injection of metabolically active, non-replicating whole *P. falciparum* sporozoites (PfSPZ) thawed from long-term storage in liquid nitrogen (Hoffman *et al.*, 2002, 2010a). The manufacturer of this vaccine is Sanaria™. But there are challenges relating to product scale up; dose, dosage and clinically appropriate route of administration; and the logistics of delivering a vaccine that is cryopreserved in liquid nitrogen (Hoffman *et al.*, 2002, 2010a; Pinder *et al.*, 2010). Available data indicates that the PfSPZ vaccine can be administered successfully through clinically appropriate routes including the subcutaneous (SC), intradermal (ID), and intramuscular (IM) injections and that with well established final dose and dosage regimen, it is feasible to achieve sufficient quantities of the PfSPZ vaccine that will meet the anticipated requirements, thereby addressing some of these challenges (Hoffman *et al.*, 2010a, 2010b). However, to meet the regulatory requirement, the PfSPZ vaccine must be aseptic (free of contaminating pathogens), pure (significantly free of mosquito-derived material), attenuated (non-replicating) and potent (capable of eliciting a protective immune response) (Hoffman *et al.*, 2010a). Furthermore, the use of irradiated (Nussenzweig and Nussenzweig, 1984; Hoffman *et al.*, 2002) and genetically attenuated

(Douradinha *et al.*, 2011; Annoura *et al.*, 2012) sporozoites as vaccine candidates has been demonstrated to confer protection against malaria infection.

The development of natural immunity acquired after long term exposure to the infection, especially with people living in the endemic areas, has been reported (Hoffman *et al.*, 1987; Baird, 1995; Rogier *et al.*, 1996). The rate of acquired immunity in infants is faster than older children, but they also stand the chance of a higher risk of developing severe malaria infection and anaemia (Aponte *et al.*, 2007). Adults who have developed naturally acquired immunity and migrated to malaria-free zones stand the risk of contacting the diseases upon return to their endemic region. However evidences have revealed that their responses to such re-infection are very rapid and they tend to respond to treatment and recover faster than those who have not been previously exposed (Di Perri G *et al.*, 1994; Lepers *et al.*, 1988; Jelinek *et al.*, 2002). While this naturally acquired immunity is beneficial, it leaves the most vulnerable population (children and pregnant women – though the mother may be immune, the foetus is not) at risk, as they are yet to gain enough exposure for such immunity to take place. Aponte *et al.* (2007) showed that a reduced exposure to *P. falciparum* antigens through chemoprophylaxis early in life has the potential to delay immunity acquisition. Furthermore, it does not appear that naturally acquired immunity has any effect on transmission of malaria. This further explained the possibility of an evolving host-parasite relationship (Evans and Wellems, 2002), which might have been developed over a long time. Therefore, understanding the compromises that may have developed over time between the parasite and the host may be an important approach towards developing a much needed vaccine. Also, advances in molecular and cellular biology have improved our understanding of the disease conditions and is currently an important route, not just in drug discovery, but also in vaccine development.

1.3 Molecular and Cellular Basis of Malaria Infection

1.3.1 Development in the Mosquito

Following a blood meal by an *Anopheles* female mosquito on an infected human host, male and female gametocytes are ingested to start the schizogony stage of the parasite development. Every progenitor of a single erythrocytic schizont is committed to becoming a gametocyte (male or female) and the expression of Pfnek-4 (*Plasmodium falciparum,* Nima-related kinase-4) might help to identify the sexually committed gametocytes (Bruce *et al.*, 1990; Smith *et al.*, 2000). The expression of the first molecular markers (Pfs16 and Pfg27/25) of gametocytes within 24 hours of its development has been reported (Alonso *et al.*, 2011) and an earlier microarray analysis has identified an up-regulation of 11 genes in sexually committed *P. falciparum* parasite (Silvestrini *et al.*, 2005). *PfGECO*, a *P. falciparum*-encoded gametocytes type IV Hsp40 protein, was shown to be expressed in gametocyte stages I to IV and is exported to the erythrocyte cytoplasm (Morahan *et al.*, 2011). The mature male and female gametocytes possess secretory organelles called osmiophilic bodies that are involved in their escape from the erythrocytes during gametogenesis (Lal *et al.*, 2009; Ponzi *et al.*, 2009). Typically, the male gametocytes contain an axoneme to female gametes and zygotes, plasma membrane and nucleus with a much reduced network of ribosome and endoplasmic reticulum (Lal *et al.*, 2009; Ponzi *et al.*, 2009). On the other hand the female gametocytes have well-developed apicoplast, mitochondria and endoplasmic reticulum that are essential for their rapid development into zygotes (Thompson and Sinden, 1994).

To adjust itself to a drastic change in the environment (man to insect), gametocytes undergo a rapid molecular and cellular change which enables it to begin the sporogonic cycle. During gametogenesis, temperature and pH change, coupled with the release of xanthurenic acid (a molecule from mosquito) trigger the formation of exflagellation by male gamete (Billker *et al.*, 1997, 1998). Essential to this xanthurenic acid–mediated action on male gamete exflagellation is *P. falciparum* cGMP-dependent protein kinase (McRobert *et al.*, 2008). P48/45, a male-gamete-specific surface protein, and P230, both of which belong to the 6-cysteine repeat protein family, have been shown to be essential for fertilization. While P48/45 is uniquely expressed by male gametes and essential for its ability to fertilize (Van Dijk *et al.*, 2001), P230 is expressed by both (Eksi *et al.*, 2002) and showed to be important for fertilization (Eksi *et al.*, 2006). Other genes that have been implicated in gametogenesis and ookinetes formation include MDV-1 (male development gene-1) or Peg3, (Lal *et al.*, 2009), CDPK4 (*Plasmodium* calcium-dependent kinase

4), MAPK-2 (mitogen-activated protein kinase-2) (Billker *et al.*, 2004; Rangarajan *et al.*, 2005), and A NIMA (never in mitosis/*Aspergillus*)-related protein kinase (Nek-4) (Reininger *et al.*, 2005) as well as CDPK3 (a micronemal protein) (Ishino *et al.*, 2006) and circumsporozoite- and thrombospondin-related anonymous protein (TRAP)-related protein (CTRP) (Dessens *et al.*, 1999) that are also essential for the ookinetes motility in the mosquito gut. SOAP (secreted ookinete adhesive protein) (Dessens *et al.*, 2003) and CTRP (Limviroj *et al.*, 2002) are important to ookinetes transformation to oocyst while LAPs (lectin adhesive-like proteins), play a very important role in sporozoite formation from the oocyst (Pradel *et al.*, 2004). A micronemal protein, TRAP, and an actin–myosin motor, located underneath the plasma membrane, have been show to help sporozoites in its invasion of the salivary gland of mosquito vector and its subsequent continuous sequence of stick-and-slip motility in mammalian host (Kappe *et al.*, 1999; Baum *et al.*, 2006; Yamauchi *et al.*, 2007; Münter *et al.*, 2009). The sporozoite transversal to the liver constitutes an important and necessary process towards the establishment, survival and development of the parasite in human host.

1.3.2 Cell Transversal

Sporozoites possess the ability to transverse host cells by membrane disruption and SPECT1 (sporozoite microneme protein essential for cell traversal 1) and SPECT2 are proteins secreted by the micronemes that have been implicated in host cell traversal (Ishino *et al.*, 2004, 2005). The absence of *SPECT1* or *SPECT2* in mutant sporozoites does not prevent gliding (stick and slip) motility but prevents migration through host cells (Ishino *et al.*, 2004). Other proteins of importance to sporozoite cell traversal prior to hepatocyte infection, include TRAP-Like Protein (Moreira *et al.*, 2008), a sporozoite secreted phospholipase (Bhanot *et al.*, 2005), cell traversal protein for ookinete and sporozoite (Kariu *et al.*, 2006) and circumsporozoite protein (CSP) (Sinnis and Sim, 1997).

1.3.3 Liver stage development

Upon entering the bloodstream, infectious sporozoites head to the liver and the expression of circumsporozoite protein (CSP) is high at this stage. Frevert and colleagues (2005) showed that sporozoites migrate through several hepatocytes before finally settling to form a PV and begin the liver stage development (Frevert *et al.*, 2005). Another highly expressed protein in Kuppfer cells is LRP-1 (low-density lipoprotein receptor-related protein-1) and through its ability to mediate CSP, together, play an important role in inhibiting the generation of reactive oxygen species through the

stimulation of adenyl cyclase activity, thereby generating cyclic AMP (cAMP) (Usynin *et al.*, 2007). Ishino and co-workers reported that two parasite molecules - P36 and P52/P36p – are involved in the invasion of the hepatocytes with the formation of a PV membrane (PVM) (Ishino *et al.*, 2005). Also involve in hepatocyte invasion are microneme proteins such as sporozoite surface protein-2 (SSP2), or TRAP (thrombospondin-related adhesive protein) and their homologue, circumsporozoite- and TRAP-related protein. In the liver cells, the growth and development of the sporozoites are made possible by the circumsporozoite protein (CSP) of the parasite (Prudêncio *et al.*, 2006; Singh *et al.*, 2007). Apart from CSP, other gene products that has been implicated in liver stage development of the parasite include sporozoite low complexity asparagine-rich protein (SAP1) (Aly *et al.*, 2008) and sporozoite and liver stage asparagine-rich protein (SLARP) (Silvie *et al.*, 2008a).

1.3.4 Erythrocyte invasion

Erythrocyte invasion involves four steps, namely, initial merozoite binding, reorientation and erythrocyte deformation, specific interaction and junction formation, and parasite entry. Merozoite surface protein-1 (MSP-1) is a well characterized merozoite surface protein implicated in initial merozoite binding and inhibition of invasion can be attained with MSP-1 antibodies (Holder *et al.*, 1994). For the parasite to gain entry into the host erythrocytes, the initial contact is followed by reorientation and erythrocyte deformation. Apical membrane antigen-1 (AMA-1), a transmembrane protein localized at the apical end of the merozoite binding erythrocytes, has been implicated in this reorientation (Mitchell *et al.*, 2004). The inability of the antibodies against AMA-1 to prevent initial contact between merozoite and erythrocyte suggest that it is not involved in the attachment of the merozoites. However, the antibodies prevent reorientation and thus block merozoite invasion (Mitchell *et al.*, 2004). Content of the apical organelles (micronemes, rhoptries, and dense granules) also play important roles in invasion and establishment of the parasite within the host cells. Rhoptry neck proteins (RON2, RON4 and RON5) have been shown to interact with AMA-1 at the tight junction during invasion leading to the formation of AMA-1-RON complex (Alexander *et al.*, 2006; Richard *et al.*, 2010; Lamarque *et al.*, 2011). Recent report showed that by preventing the interaction of *P. falciparum* AMA-1 and RON, merozoites invasion can be inhibited (Richard *et al.*, 2010). Thus, it appears that the formation of this complex is essential for the secretion of the content of rhoptry, thereby encouraging successful invasion and establishment of parasite within the PV. Carruthers and Sibley (1997) showed that the release of the content of micronemes and rhoptries took place during initial contact with the host cell and the formation of the parasitophorous vacuole (PV) respectively. The dense granule contents may be involved in host cell

modification since its release takes place following complete parasite entry (Carruthers and Sibley, 1997). The transient nature of the process of invasion helps the parasite to evade the host immune system. Merozoite reorientation and microneme release lead to the formation of tight junction between the merozoite apical end and the host cell, thereby providing an avenue for the binding of microneme proteins with the receptors on the surface of the erythrocyte. EBA-175, a 175 kDa erythrocyte binding antigen and Duffy-binding protein (DBP) are among the micromene proteins that have been identified in *Plasmodium* species. However, unlike *P. vivax,* which invades the RBCs by binding to Duffy blood group, *P. falciparum* possesses several homologues of Duffy binding-like (DBL) proteins and the reticulocyte binding-like proteins that allows it to recognize and bind effectively to different RBC receptors (Weatherall *et al.*, 2002; Mayer *et al.*, 2009). The entrance of the parasite into the RBC is made possible with the aid of aldolase, TRAP proteins and the actin–myosin motor (Cowman and Crabb, 2006; Bosch *et al.*, 2007; Haldar and Mohandas, 2007). The invasion is followed by host cell remodelling needed for parasite survival and development.

1.3.5 Host cell remodelling

Host cell remodelling or modification provides an enabling environment for the intra-erythrocytic development and survival of the parasite. Host cell modification, such as cytoadherence of the infected erythrocytes to endothelial cells and subsequent sequestration of the mature parasites in capillaries provides a suitable microaerophilic environment for parasite metabolism, and protection from destruction by the spleen (Crabb *et al.*, 1997; Udomsangpetch *et al.*, 2002; Spielmann *et al.*, 2006). Another important structural alteration is knob formation, which is an electron dense protrusion on the infected erythrocytes containing several parasite proteins. One important protein that is localized to the knobs is a polymorphic protein, called *Pf*EMP1, and it translocation to the erythrocyte surface has been reported to depend in part on *Pf*EMP3 (Waterkeyn *et al.*, 2000). Also, it has been suggested that PfHsp70-x may play a role in this translocation (Külzer *et al.*, 2012), but this is yet to be validated. *Pf*EMP2 (erythrocyte membrane protein-2) or MESA and KAHRP (knob-associated histidine rich protein) are also said to be associated with the knobs (Deitsch and Wellems, 1996). In addition, reports have shown that knob formation and the ability to cytoadhere was lost following the disruption of KAHRP under flow conditions (Crabb *et al.* 1997; Horrocks *et al.*, 2005; Rug *et al.*, 2006).

During the intra-erythrocytic stage of the *P. falciparum* life cycle, the parasite's development and survival, in an environment devoid of the necessary cellular machinery for protein trafficking,

depends on its ability to structurally and functionally remodel the host cell (Przyborski and Lanzer, 2005; Botha *et al.*, 2007; Pesce and Blatch, 2009). This is made possible by exporting parasite proteins, termed the exportome, into the host cell (Figure 1.2). These proteins, especially those with hydrophobic N-terminal sequences, are routed through the endoplasmic reticulum (ER) to the Golgi apparatus, from where they are carried by vesicular transport and released into the lumen of the parasitophorous vacuole (PV) (Adisa *et al.*, 2003). The ER plays an important role in protein synthesis, modification and intracellular transport. The ER compartment is where newly-synthesized polypeptides fold, serves as assembly of multimeric proteins, and provide limited glycoproteins with the needed asparagine-linked glycans. Proteins are retained in the ER until they have acquired their correct conformation (Vitale *et al.*, 1993). The transport of the parasite proteins across the parasitophorous vacuolar membrane (PVM) into the host erythrocytes is mediated by a pentameric motif called *Plasmodium* export element (PEXEL) or host targeting signal (HT) (Hiller *et al.*, 2004; Marti *et al.*, 2004; Horrocks and Muhia, 2005).

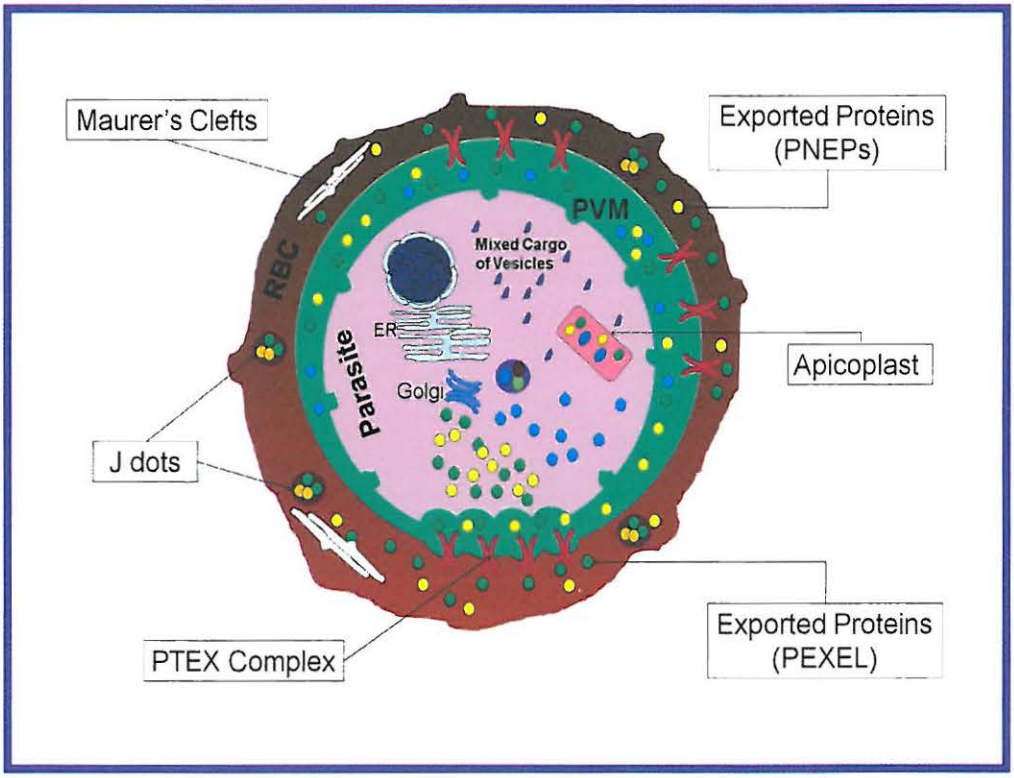

Figure 1.2: Export of parasite proteins into the cytosol of infected erythrocytes.
The parasite proteins meant for export are processed in the endoplasmic reticulum (ER) for onward movement into the plasma membrane by vesicular transport. The proteins to be exported are probably unfolded before they can be translocated by the *Plasmodium* translocon of exported proteins (PTEX) complex across the parasitophorous vacuole membrane (PVM) into the cytosol of the infected red blood cell (RBC). It has been suggested that there may be no need for a separate export mechanism for both PEXEL containing and PEXEL negative export proteins (PNEPs) (Spielmann and Gilberger, 2010). (The diagram was adapted from Crabb *et al.*, 2010).

However, the possibility that the parasite may be using more than one mode of export has been speculated since there are some exported proteins which lack a PEXEL or HT motif (Gormley *et*

al., 1992; Spielmann and Gilberger, 2010). The existence of several PEXEL-negative exported proteins (PNEPs) indicates that alternative export pathways might also exist and that an unknown number of proteins might be missing from the currently predicted exportome (Spielmann *et al.*, 2006). Among the PNEPs that has been identified and shown to be localized to Maurer's clefts are the skeleton binding protein 1 (SBP1) (Blisnick *et al.*, 2000) and the membrane associated histidine-rich protein 1 (MAHRP1) (Spycher *et al.*, 2003) both of which are required for the cytoadherence ligand PfEMP1 to reach the erythrocyte surface (Cooke *et al.*, 2006; Maier *et al.*, 2007; Spycher *et al.*, 2008). Also of importance are the ring-exported protein 1 and 2 (REX1 and 2) (Hawthorne *et al.*, 2004; Spielmann *et al.*, 2006; Spielmann and Gilberger, 2010). Meanwhile, Bhattacharjee *et al.* (2008) have reported that HT should be seen to function as a sorting signal that concentrates secretory parasite proteins destined to be exported into the cytosol of the infected erythrocyte into Maurer's clefts, rather than being regarded as a mediator of protein translocation across the PVM. Also de Koning-Ward *et al.* (2009) showed that a translocon of exported proteins, named PTEX, in *P. falciparum*, is an important requirement for the export of PEXEL-containing proteins. These PTEX proteins were identified on the basis of their restriction within the *Plasmodium* genus, likelihood of an ATPase powered source, PVM localisation, requirement for blood stage growth and binding specifically to their exported proteins. Among the identified proteins that appear to fulfil these criteria are PTEX150 (PF14_0344) and HSP101. These PTEX proteins were shown to bind specifically to PEXEL-motif containing exported proteins such as PF11_0037 and PF08_0137 (De Koning-Ward *et al.*, 2009). Also, the inability of the authors to generate gene knockouts of *P. falciparum* PTEX150 suggests that this protein may be essential for the intra-erythrocytic survival of the parasite. Thus, it was proposed that once the PEXEL-proteins are processed in the ER (Chang *et al.*, 2008b) and deposited in the PV, they are recognised by some members of the PTEX translocon for final translocation into the cytosol of infected erythrocytes (de Koning-Ward *et al.*, 2009). The processing involves the cleavage of the PEXEL motif which is preceded by the cleavage of the signal peptide by Plasmepsin V (Boddey *et al.*, 2009; Russo *et al.*, 2010). Plasmepsin V may also play a role in directing the protein into the desired export pathway (Boddey *et al.*, 2009, 2010).

Attempts have been made to present an extensive description of the protein interaction network for *P. falciparum* (LaCount *et al.*, 2005) and about 300 parasite-encoded proteins are predicted to be part of the exportome (Hiller *et al.*, 2004; Marti *et al.*, 2004; Sargeant *et al.*, 2006; van Ooij *et al.*, 2008). Among the exported proteins are the molecular chaperones of the 40 kDa heat shock protein family (Hsp40s) which also form a significant part of the PV proteome (Nyalwidhe and Lingelbach, 2006). Now we know that PfHsp70-x is also exported (Külzer *et al.*, 2012; Grover *et al.*, 2013).

1.4 Molecular Chaperones

1.4.1 Background information

To successfully produce functional proteins, it is important that the polypeptide chain is correctly folded into its native three-dimensional conformation, localized appropriately within or secreted from the cell, and properly assembled into multi-component complexes. Although the proper folding of a small protein into its native conformation is dictated by the amino acid sequence alone, given the highly concentrated and complex cellular environment, the proper folding of many polypeptides would only be made possible through the assistance of another type of machinery. This latter type of protein machinery involves the molecular chaperones (Hartl, 1996; Smith *et al.*, 1998; Hartl and Hayer-Hartl, 2002). Molecular chaperones are a family of proteins that function to stabilize proteins, facilitate their translocation across intracellular membranes or their degradation, and ensure that proteins in a cell are properly folded and functional (Hartl, 1996; Hartl and Hayer-Hartl, 2002). The capability of the molecular chaperones to perform their folding and refolding functions has been reviewed (Gräslund *et al.*, 2008). Heat and other forms of cellular stress can increase the expression of molecular chaperones (Baker *et al.*, 1984). However, many molecular chaperones are constitutively produced, (Craig *et al.*, 1993; Parsell and Lindquist, 1993; Hayes and Dice, 1996). Amongst the most important classes of molecular chaperones are the heat shock protein family of which Hsp40s (40 kDa heat shock proteins) and Hsp70s (70 kDa heat shock proteins) are two abundant families.

Table 1.2: Human heat shock protein nomenclature

New nomenclature	Traditional nomenclature
HSPA	Hsp70
HSPH	Hsp110
DNAJ	Hsp40
DNAJA	Hsp40 Type I
DNAJB	Hsp40 Type II
DNAJC	Hsp40 Type III
HSPB	Small Hsp
HSPC	Hsp90
HSPD	Hsp60; GroEL
HSPE	Hsp10; GroES

The table was adapted from Kampinga et al., (2009).

Guidelines for the nomenclature of human heat shock proteins have been presented (Kampinga *et al.*, 2009). Table 1.2 provides an overview of the new nomenclature for major classes and their traditional equivalents in humans.

1.4.2 Hsp70 molecular chaperones

The Hsp70 family constitutes an integral component of the network of molecular chaperones and folding catalysts. Hsp70 consists of a 45 kDa N-terminal ATPase domain and a 25 kDa C-terminal substrate binding domain (Figure 1.3). The functions of Hsp70s can be broadly categorized into two: first as house keeper, in which case they participate in folding, signal transduction pathways and assembling of newly synthesized proteins and their translocation across cell membranes (Fewell *et al.*, 2001). Second, as quality control manager, in which Hsp70s participate in controlling the activity of regulatory proteins and also screen proteins for any damage and repair the misfolded and aggregated proteins (Bukau *et al.*, 2000; Ryan and Pfanner, 2001; Hartl and Hayer-Hartl, 2002). Hsp70 proteins use energy generated by ATP binding and/or hydrolysis to unfold misfolded or aggregated proteins or maintain proteins in an unfolded state, thereby producing folding intermediates which then fold spontaneously (Rothman, 1989; Hubbard and Sander, 1991). It can be argued therefore that since all the information that any protein needs for folding to take place is embedded in its sequence and Hsp70 molecules do not impart any steric conformation that can influence the folding pathway of another protein, Hsp70, acts as an unfoldase (helping to maintain the proteins in their unfolded form), as a mechanism to suppress aggregation (Slepenkov and Witt, 2002; Sharma *et al.*, 2010). It has been proposed that in this unfoldase mechanism, Hsp70 makes use of the energy generated from ATP hydrolysis to recruit a force of entropy to locally unfold aggregates or pull proteins across membranes (De Los Rios *et al.*, 2006; Goloubinoff and De Los Rios, 2007). This mechanism is been explored as a potential approach to combat neurodegenerative disorder like Parkinsons (Hinault *et al.*, 2006, 2011).

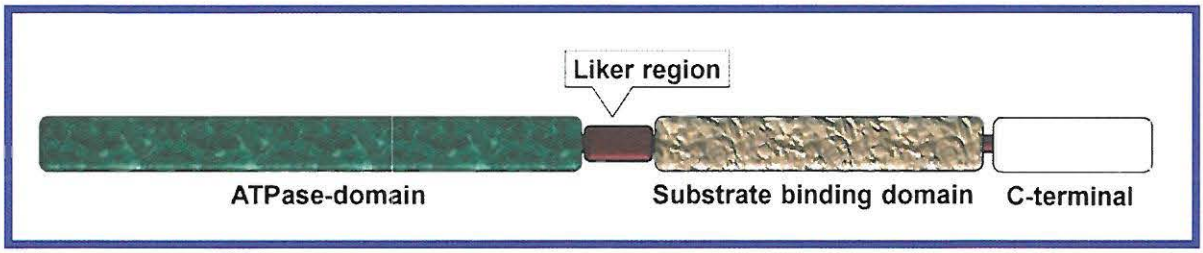

Figure 1.3: Schematic representation of the domains present in Hsp70
Hsp70 domain organization showing ATPase and substrate binding domains joined together by a linker region. The ATPase domain is important for its chaperone activity and interaction with Hsp40 co-chaperones.

Human heat shock proteins (HSPs), once regarded as stress-responsive proteins that are required to handle thermal and other related stresses, are now known to encode constitutively expressed members such as human Hsc70 (*HSPA8)*. Human Hsp70-1/2 (HSPA1A/B), Hsp40 (DNAJB1) and small Hsp (HSPB1) are among the most extensively studied of the HSPs and are heat inducible. The human genome encodes 13 members of the human Hsp70 (HSPA) family, apart from many pseudogenes (Kampinga *et al.*, 2009). The human Hsp70s (HSPA1A and HSPA1B), together with Hsp70B' (HSPA6) are known to be the most heat-inducible family members (Kampinga *et al.*, 2009). The fact that the human Hsp70-1 and Hsp70-2 only differ by two amino acids would suggest that they were very likely to be interchangeable (Kampinga *et al.*, 2009). The human genome also encodes four Hsp110 (*HSPH*) genes which constitute a family of HSPs that share high homology with Hsp70 members except that they have a longer linker domain that is located between the N-terminal ATPase domain and the C-terminal peptide binding domain. It has been shown that Hsp110 members are nucleotide exchange factors for the Hsp70 family (Dragovic *et al.*, 2006).

The Hsp70 proteins are known to be involved in protein folding by ATP-controlled cycles of substrate binding and release (Cheetham *et al.*, 1994; Suh *et al.*, 1998; Young *et al.*, 2003). The ATPase cycle of Hsp70 is characterized by alternating between a low affinity ATP bound state and a high affinity ADP bound state. The low affinity ATP bound state speeds up the rate of substrate exchange while the high affinity ADP bound state lowers the rate of substrate exchange (Mayer and Bukau, 2005). Also, genetic and biochemical evidence have shown that ATP hydrolysis is essential for the chaperone activity of Hsp70s (Ha *et al.*, 1999; Mayer & Bukau, 2005). It appears that the interaction of Hsp70s with the hydrophobic peptide portion of proteins in an ATP-controlled manner is responsible for its activities (Mayer and Bukau, 2005). However, in a thermodynamically coupled process, the rate of substrate stimulated ATP hydrolysis is very low for any functional Hsp70 cycle to take place. Thus, for a functional Hsp70 cycle to take place, co-chaperones are required to couple with substrate, thereby increasing the rate of ATP hydrolysis (Mayer and Bukau, 2005). Among the co-chaperones that have been implicated for this function are those belonging to the Hsp40 family (Laufen *et al.*, 1999).

1.4.3 Hsp40 molecular co-chaperones

Hsp40 proteins are defined by the presence of the J domain, an approximately 70 amino acid domain with similarity to the initial 73 amino acids of the *E. coli* Hsp40, DnaJ (Ohki *et al.*, 1986; Cyr *et al.*, 1994). They mainly function as co-chaperones of Hsp70s (Cheetham *et al.*, 1994; Kelley, 1998; Suh *et al.*, 1998; Young *et al.*, 2003). The J domain was first discovered to be present in *E.*

coli DnaJ with conserved HPD tripeptide that represents the signature motif of the Hsp40 protein family (Yochem *et al.*, 1978; Fan *et al.*, 2003). They facilitate the folding of nascent polypeptides through their interaction and regulation of partner Hsp70 proteins (Feldheim *et al.*, 1992). In addition, Hsp40 proteins have been implicated in protein translocation (Jubete *et al.*, 1996), protein degradation (Jiang *et al.*, 1997), clathrin uncoating (Campell *et al.*, 1997; Ma *et al.*, 2002), and viral infection (al-Herran and Ashraf, 1998).

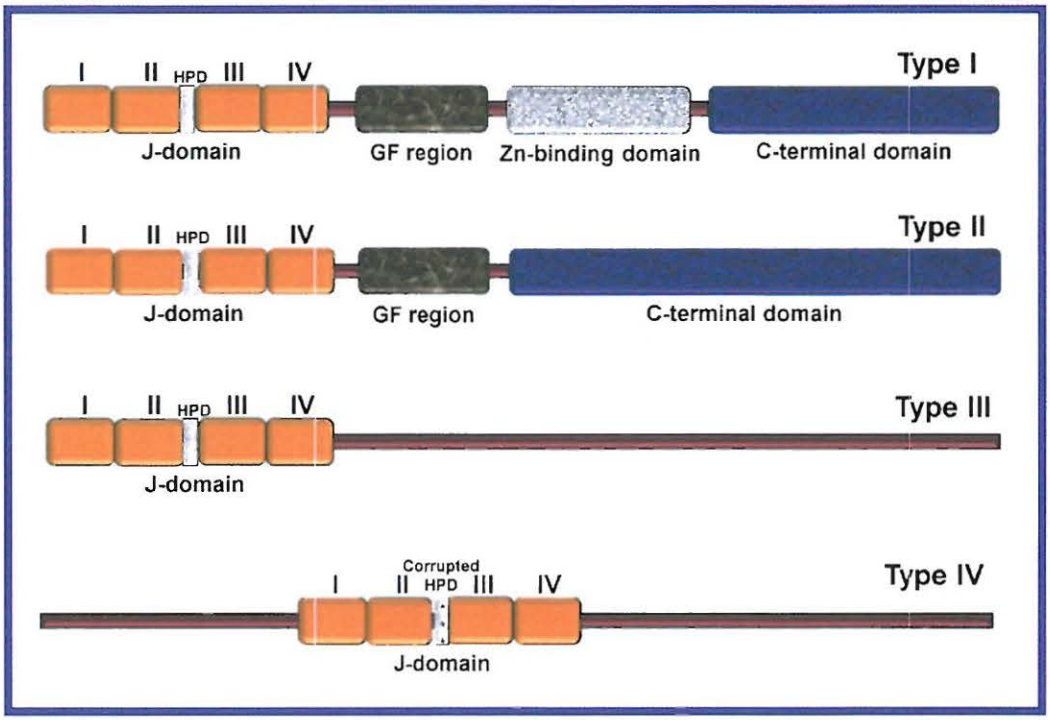

Figure 1.4: Schematic representation of the domains present in Hsp40
Schematic representation of Hsp40 type I to IV, showing the helix I to IV and the conserved HPD motif (corrupted in the case of type IV) of the J-domain. Via the J-domain, Hsp40 can interact with and stimulate the ATPase activity of Hsp70. Other domains in Hsp40 regulate and ensure stabilization of Hsp70-substrate binding (GF region); ensure stability of the Hsp40 tertiary structure (Zn-binding domain) and capturing of protein substrates and dimerisation (C-terminal domain). GF region = Gly/Phe-rich region (GF-domain), Zn-binding domain = cysteine-rich zinc binding domain.

Hsp40 possesses four canonical domains (Figure 1.4): a J-domain, with the highly conserved HPD (His-Pro-Asp) motif that is needed for the stimulation of the ATPase activity of Hsp70s (Cheetham and Caplan, 1998), a Gly/Phe-rich region (GF-domain), which regulates and ensures stabilization of Hsp70-substrate binding (Tsai and Douglas, 1996; Hennessy *et al.*, 2000); a cysteine-rich zinc binding domain, which possibly ensures stability of the Hsp40 tertiary structure (Martinez-Yamout *et al.*, 2000); and a C-terminal domain, which may be involved in protein substrates capturing and dimerisation (Borges *et al.*, 2005; Wu *et al.*, 2005). On the basis of these domains, Hsp40 proteins are classified as follows: type I Hsp40 proteins possess all the four canonical domains; type II Hsp40 proteins possess all but lack zinc binding domain; type III Hsp40 proteins only have the J–domain in common with other Hsp40s and type IV Hsp40 protein, have a J-like domain, in which

the tripeptide HPD is not conserved (Cheetham and Caplan, 1998; Botha *et al.*, 2007). The J-domain of type III and IV proteins may be at any place within the sequence unlike that of type I and II which always have its J-domain at the N-terminus of the mature protein.

The human genome encodes at least four type I (DNAJA) proteins, fourteen type II (DNAJB) proteins and 22 type III (DNAJC) proteins (Kampinga *et al.*, 2009). A number of other Hsp40 proteins including pseudogenes and 'J-like' proteins (Walsh *et al.* 2004) are scattered throughout the human genome (Kampinga *et al.*, 2009). The type II sub-family has the most widely expressed and heat-inducible human Hsp40 member (DNAJB1). They most likely function by recruiting human Hsp70 family members for specific functions (Kampinga and Craig, 2010). The mDj4 (DNAJB6) and mDj6 (DNAJB8), two closely related Hsp40 proteins, were identified as very potent inhibitors of aggregation and the associated toxicity of polyglutamine containing proteins and do not form dimers (Kazemi-Esfarjani and Benzer, 2000; Chuang *et al.*, 2002; Fayazi *et al.*, 2006; Hageman *et al.*, 2010). Hsj1 (DNAJB2) drives their clients toward degradation and antagonizes refolding of heat denatured luciferase mediated by human Hsp70-1 and Hsp40 (DNAJB1) (Michels *et al.*, 1997). Hsj1 is closely related to mDj4 and mDj6, and it has been reported that mDj6 could suppress the aggregation of heat denatured luciferase, but it could not support refolding. The inhibition of refolding is minimal when compared with Hsj1 (Hageman *et al.*, 2010). Thus it appears that the primary determinant of the fate of clients is the Hsp40 not the Hsp70 component of the core machinery, as the same clients may fold (by interacting with Hsp40) or be degraded (by interacting with Hsj1) (Kampinga and Craig, 2010). The type III human Hsp40 family are the most diverse containing some proteins that have additional but distinct motifs or domains such as transmembrane helices (Sec63 (DNAJC23)), tetratricopeptide repeats (Dnajc3 (DNAJC3) and mDj11 (DNAJC7)), and polypalmitoylated (cysteine string proteins) cysteine-rich regions (Kampinga and Craig, 2010).

Structurally, the J-domain of Hsp40 consists of four α-helices (helices I–IV) with a transhelix loop between helices II and III, where the highly conserved HPD tripeptide resides. Several reports have shown that the alteration of HPD residues will abolish the functional Hsp70-Hsp40 interaction (Tsai and Douglas, 1996; Laufen *et al.*, 1999; Mayer *et al.*, 1999; Genevaux *et al.*, 2003; Wittung-Stafshede *et al.*, 2003). Helix I possesses highly conserved hydrophobic residues, but in types II and III Hsp40 proteins, the tertiary structure is divergent. The helices II and III are conserved and are said to be important for the function of the J-domain (Pellecchia *et al.*, 1996). Though earlier proposed to be nonessential to the co-chaperone function of Hsp40 (Genevaux *et al.*, 2002), the identification of residues on helix IV that were important for the *in vivo* functions of the J-domain of *Agrobacterium tumefaciens* (Agt) DnaJ, suggest that helix IV may enhance the affinity or

specificity of Hsp40-Hsp70 interactions (Garimella *et al.*, 2006; Hennessy *et al.*, 2005a, 2005b). The interaction of Hsp40 proteins with substrates and how the substrate is delivered to Hsp70 partner proteins differ among the classes of Hsp40s. Type I and II Hsp40s can bind substrate and work with Hsp70s in protein folding, degradation and/or translocation processes and possess independent chaperone activity by suppressing aggregation of denatured protein (Langer *et al.*, 1992; Rüdiger *et al.*, 2001; Nicoll *et al.*, 2007). However the type III and IV proteins have more specialized roles. The type III Hsp40s are highly divergent in size, sequence and structure and can recruit an Hsp70 to a particular cellular location and stimulate its ATPase activity to drive a specialized function but are unable to function as chaperones (Nicoll *et al.*, 2007). Also, type III proteins may bind a restricted number of substrates or they may be positioned in close proximity to substrates. For example, Sec63 (DNAJC23) is placed in close proximity to the translocation pore of the endoplasmic reticulum and Tim14 (DNAJC19) is placed in close proximity to the translocase of the inner mitochondrial membrane (Mayer and Bukau, 2005).

1.4.4 Hsp70-Hsp40 interactions

The ability of the Hsp40 proteins to mediate the ATP hydrolysis-dependent locking of substrates into the cavity of Hsp70s is crucial for almost all the chaperone functions of Hsp70s. Hsp40s are a large family of chaperones with the ability to specify the actions of Hsp70 proteins (Cheetham and Caplan, 1998). By their interactions with Hsp70s, Hsp40s often perform specialized functions in which a single Hsp70 can interact with more than one Hsp40 to generate unique Hsp70-Hsp40 pairs that can facilitate specific processes at distinct locations within the cell (Horton *et al.*, 2001). A model of Hsp70-Hsp40 interaction is given in Figure 1.5. It involves the coupling of substrate with Hsp40s followed by subsequent attachment to the N-terminal ATPase domain of Hsp70s. The coupling of Hsp40s with substrates drives the ATP hydrolysis thereby increasing the affinity of Hsp70s for the substrates. With successful hydrolysis of ATP to a high substrate affinity ADP state, Hsp40 releases the substrate to Hsp70 and disengages. Nucleotide exchange factor (NEF) promotes the release of ADP from Hsp70 in exchange for ATP thereby ensuring substrate release and preparation of Hsp70 for the next cycle of substrate binding (Steel *et al.*, 2004; Dragovic *et al.*, 2006). The process of refolding by Hsp70 continues until the substrate bound Hsp70 attains another ATP bound state, a low affinity state. The cycle is repeated for as long as it is necessary for the substrate to be correctly folded. Furthermore, the functions of Hsp70s within a cellular compartment are multidimensional. It is therefore important to have substrate specific targeting of essential proteins for the survival of the cell. This regulatory activity is performed by the Hsp40 co-

chaperones by connecting Hsp70s with their specific proteins, including substrates and other chaperones (Fan *et al.*, 2003).

Generally, for effective functioning Hsp70s rarely work alone, but in complex with other proteins including the Hsp90 system and co-chaperone proteins. These chaperone substrate complexes have several features in common, including dependence of the formation of active complexes on the prior interaction of the substrate with Hsp70 during de novo synthesis and the sensitivity of the chaperone association to substrate-specific ligands or substrate phosphorylation (Pratt, 1997). The stimulation of ATPase activity is usually by Hsp40s, but reports have shown that synergistic stimulation by substrates and Hsp40s could also take place (Barouch *et al.*, 1997; Misselwitz *et al.*, 1998; Silberg and Vickery, 2000; Silberg *et al.*, 2004), indicating that the coupling mechanism of Hsp40 proteins may be conserved in some Hsp70 chaperones (Mayer and Bukau, 2005).

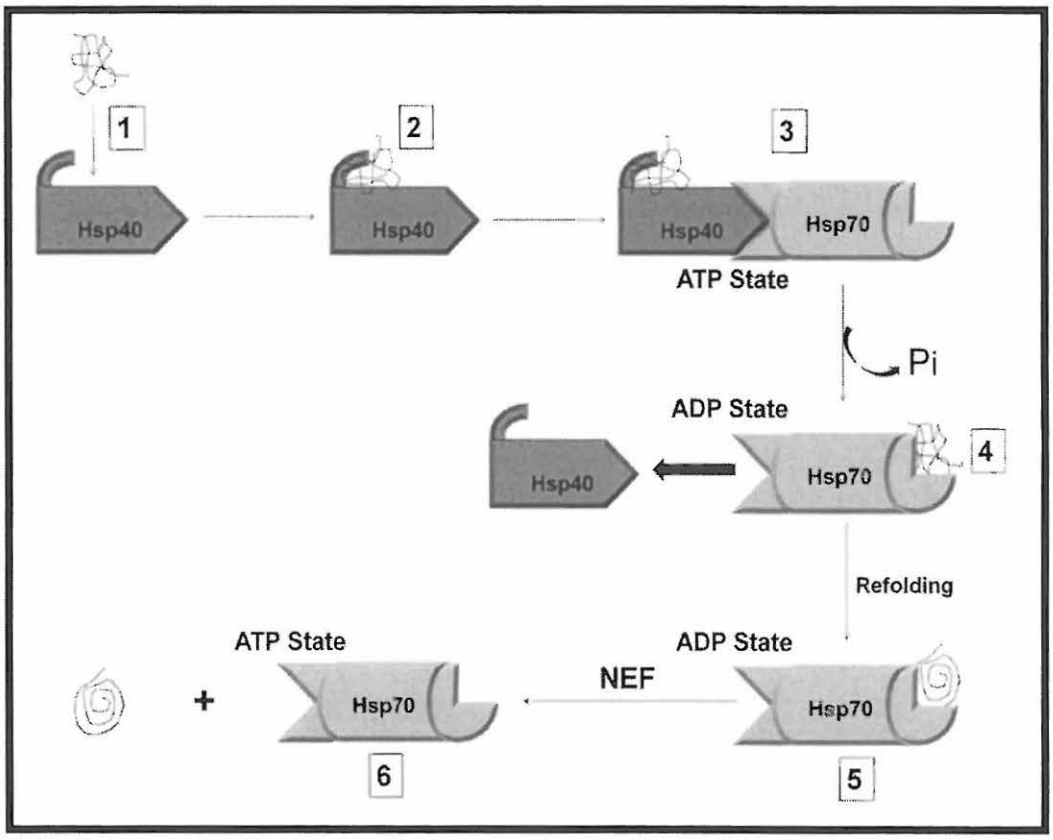

Figure 1.5: Model of Hsp70-Hsp40 interaction
Chaperone/co-chaperone interactions constitute an important mechanism in biochemical processes needed for the maintenance of proteins. The ATPase domain of Hsp70 and the J-domain of Hsp40 are essential components of these interactions. The interaction consists of the binding of substrate to Hsp40 (1 and 2), followed by interaction of substrate bound Hsp40 with the ATPase domain of Hsp70 (3), leading to the conversion of ATP to ADP. In the ADP bound state, the affinity of Hsp70-substrate interaction is high and very strong compared to the ATP bound state. Following the conversion to ADP bound state, Hsp40 dissociates and releases substrate to Hsp70 for refolding to take place (4 and 5). The nucleotide exchange factor (NEF) stimulates the exchange of ADP for ATP, leading to the release of the folded protein (6). This process is repeated until the substrate is completely folded. (Adapted from Pesce & Blatch, 2009)

1.4.5 Plasmodium falciparum Hsp70s (PfHsp70s)

In *P. falciparum*, six genes encoding Hsp70 proteins were identified. They are (PlasmoDB accession number in bracket) PfHsp70-1 (PF3D7_0818900), PfHsp70-2 (PF3D7_0917900), PfHsp70-3 (PF3D7_1134000), PfHsp70-x (PF3D7_0831700), PfHsp70-y (PF3D7_1344200) and PfHsp70-z (PF3D7_0708800) (Shonhai *et al.*, 2007). Table 1.3 summarizes their basic characteristic features. However, most research into this group of chaperones has focused only on investigating the chaperone properties of PfHsp70-1 (Matambo *et al.*, 2004; Ramya *et al.*, 2006; Botha *et al.*, 2011; Cockburn *et al.*, 2011; Stephens *et al.*, 2011) and its potential as a vaccine candidate as well as a target for drug development (Kumar *et al.*, 1990; Behr *et al.*, 1992; Chiang *et al.*, 2009; Cockburn *et al.*, 2011). PfHsp70-1 is a 70 kDa cytosolic/nuclear-localized Hsp70 (Kappes *et al.*, 1993) and is upregulated upon heat shock (Shonhai *et al.*, 2008; Botha *et al.*, 2011). Like other eukaryotic cytosolic Hsp70s, PfHsp70-1 has been shown to possess a characteristic C-terminal EEVD motif which binds to co-chaperones to facilitate its interaction with other partner proteins (Demand *et al.*, 1998). PfHsp70-1 has been successfully overexpressed in *E. coli* (Matambo *et al.*, 2004) and as co-expression partner in protein purification (Stephens *et al.*, 2011). Its expression during the blood stages of the parasite (Joshi *et al.*, 1992), solubility (Kappes *et al.*, 1993) and the detection of antibodies to PfHsp70-1 in malaria patients (Kumar *et al.*, 1990) may explain its importance in intra-erythrocytic survival. Other studies have reported that it is present in the PV (Nyalwidhe and Lingelbach, 2006) and Maurer's clefts (Vincensini *et al.*, 2005), raising the possibility of being exported into the erythrocyte. PfHsp70-x is a close homologue of PfHsp70-1 and shares a high level of sequence identity. PfHsp70-x has been reported to be exported into the PV and erythrocyte cytosol in *P. falciparum*-infected erythrocytes (Külzer *et al.*, 2012; Grover *et al.*, 2013). Therefore, it is possible that the study where PfHsp70-1 was detected in the Maurer's cleft (Vincensini *et al.*, 2005) may have been detecting PfHsp70-x. Meanwhile, the two reports on the export of PfHsp70-x into the erythrocyte cytosol (Külzer *et al.*, 2012; Grover *et al.*, 2013) gave two different localisations. While a report partially localised PfHsp70-x to the J-dots (highly mobile membrane structure within the cytosol of the infected erythrocytes (section 1.4.6)) (Külzer *et al.*, 2012), the other partially localised it to the Maurer's cleft (Grover *et al.*, 2013). Maurer's clefts, a parasite derived membranous structures that extend to the plasma membrane of the infected erythrocyte, have been shown to play a role in the export of parasite proteins (Lanzer *et al.*, 2006). Therefore, the partial localisation of PfHsp70-x to Maurer's clefts may suggest a role for this organelle in its translocation into the cytosol of infected erythrocyte. However, the controversial reports suggest that the localisation of PfHsp70-x may need further clarification. Compared to other heat shock proteins, PfHsp70-1 possesses an elongated C-terminal sub-domain, containing 60 residues, which is an important characteristic that PfHsp70-1 shares with some protozoan parasitic

Table 1.3: Characteristic features of *Plasmodium falciparum* Hsp70s

Protein	Homolog	Special Features	Localisation	Functional Characteristics
[1]PfHsp70-1		EEVD and GGMP motifs	cytosolic/ nuclear PV and MC	Export of *P. falciparum* proteins into the erythrocyte. It produces relatively high basal ATPase activity and an *in vitro* ATP-dependent chaperone activity. It could reverse the thermosensitivity of an *Escherichia coli dnaK* mutant strain. It could play a role in actin polymerization.
[2]PfHsp70-2 (73 kDa)	Grp78/ Bip	ER N-terminal leader sequence and a SDEL C-terminal ER retention signal	ER, MC	May associate with translational and transcriptional machinery, cytoskeletal and membrane proteins and enzymes including those involved in proteosome and proteolytic pathways, physiological and metabolic pathways, and DNA repair and replication. Interacts with PFI1830c, a *P. falciparum* erythrocyte membrane protein (Baruch *et al.* 1996).
[3]PfHsp70 -3 (73 kDa)	TcmtHsp70	Mitochondrial transit sequence	Mitochondrial	May associate with MAL13P.304 (a malaria antigen) and PF08_0060 and PF11_0111 (both of which are asparagines-rich antigen proteins that are exported into the erythrocytes). May be involved in mitochondrion protein import system as well as in Maurer's clefts protein export system. May be involved in facilitating the export of proteins into the infected erythrocyte.
[4]PfHsp70-y (100 kDa)	Hsp110/ Grp170	KDEL motif	ER	They display very low conservation in the peptide-binding domains (Shonhai *et al.*, 2007) and lack a conserved nuclear localisation signal found in others (Robbins *et al.* 1991). PfHsp70-z and PfHsp70-y also lack threonine residue and a distinct linker structure that are crucial for phosphorylation and allosteric control of Hsp70s respectively (McCarty and Walker 1991; Han and Christen 2001; Vogel *et al.* 2006b) suggesting a distinct role for these proteins. Also, there are indications that they could act as NEF.
[4]PfHsp70-z (108 kDa)	Hsp110/ Grp170		Cytoplasm	
[5]PfHsp70-x (76 kDa)		EEVN motif	Cytosolic, PV and J-dots	May functionally interact with other J-dots proteins and the complex may be involved in chaperoning parasite-encoded proteins, such as PfEMP1, through the human host cell, and aid their insertion into the erythrocyte plasma membrane.

[1](Kappes *et al.*, 1993; Matambo *et al.*, 2004; Nyalwidhe and Lingelbach, 2006; Ramya *et al.*, 2006; Sargeant *et al.*, 2006; Vincensini *et al.*, 2005).
[2](Kappes *et al.*, 1993; Kumar *et al.*, 1991; LaCount *et al.*, 2005; Pelham, 1989; Vincensini *et al.*, 2005) .
[3](Barale *et al.*, 1997; Botha *et al.*, 2007; Lanzer *et al.*, 2006; Sargeant *et al.*, 2006; Slapeta and Keithly, 2004; Vincensini *et al.*, 2005; Weber *et al.*, 1988).
[4](McCarty and Walker, 1991; Robbins *et al.*, 1991; Shonhai *et al.*, 2007).
[5](Külzer *et al.*, 2010, 2012; Marti *et al.*, 2004; Robbins *et al.*, 1991; Sargeant *et al.*, 2006; Shonhai *et al.*, 2007).
ER – Endoplasmic reticulum; PV – Parasitophorous vacuole; MC – Maurer cleft

Hsp70 homologs (Misra and Ramachandran, 2009). This extended region may be necessary for protein–protein interactions (Ramya *et al.*, 2006).

The identification and potential pharmacological uses of small molecules that specifically interact with and modulate the activities of Hsp70 have been reported (Fewell *et al.*, 2004; Chang *et al.*, 2008a; Cockburn *et al.*, 2011). Adenosine analogs (ATP mimics), spergualins, pyrimidinones, fatty acids and peptides have been identified as Hsp70 inhibitors (Evans *et al.*, 2010). Sulfogalactosyl ceramide, sulfogalactoglycerolipid and acyl benzamide family are examples of fatty acids with the ability to inhibit the chaperone activity of Hsp70 (Mamelak and Lingwood, 2001; Mamelak *et al.*, 2001a, 2001b). The cytotoxicity of ATP mimics on HCT116 (human colon cancer) cells was linked to the ability of this class of compounds to modulate Hsp70 (Williamson *et al.*, 2009). Pyrimidinone-peptoids and 15-deoxyspergualin (a structural analog of DSG) belonging to the pyrimidinones and spergualins respectively, have been shown to possess the ability to modulate Hsp70 chaperone activity (Brodsky, 1999; Ramya *et al.*, 2006). Their abilities to modulate the ATPase and aggregation suppression activity of Hsp70 have made the identification of inhibitors of basal and Hsp40-stimulated ATPase activity possible (Fewell *et al.*, 2004; Wright *et al.*, 2008). The structural assessment of pyrimidinones has revealed the importance of hydrophobic groups and the addition of steric bulk on its inhibitory activity (Wisén and Gestwicki, 2008), which might explain its possible mechanism of action. Chiang *et al.* (2009) reported the identification of nine pyrimidinone-amide compounds that showed significant inhibition of *P. falciparum* growth as well as the ATPase activity of PfHsp70-1, albeit at higher concentrations. These nine compounds shared a common ester pyrimidine core at position C-4 with eight of them having alkyl groups at position N-1 (Chiang *et al.*, 2009). They also have distinct features such as the morpholine moiety that is present on DMT3024 and MAL3-39 and tetrasubstituted pyrrole side chain on MAL2-215 and MAL2-213 (Chiang *et al.*, 2009), which might explain the differences in their inhibitory activities. Also, using malate dehydrogenase based aggregation suppression assays and growth inhibition assays on *P. falciparum* infected erythrocytes, five compounds belonging to two novel classes (malonganenone and naphthaquinones) of small molecule inhibitors of PfHsp70-1 have been identified (Cockburn *et al.*, 2011). The five identified compounds which include malonganenones A, B and C, lapachol and bromo-β-lapachona significantly inhibited PfHsp70-1 aggregation suppression activity, and except for malonganenone B, all were able to inhibit parasite growth to a level comparable to that earlier reported for MAL3-39 (Chiang *et al.*, 2009; Cockburn *et al.*, 2011). In this study, malonganenone A and malonganenone C produced the highest level of inhibition (Cockburn *et al.*, 2011), suggesting a possible emergence of malonganenones as a new class of antiplasmodial compounds.

1.4.6 Plasmodium falciparum Hsp40s

In *P. falciparum,* about 49 Hsp40s consisting of 2 type Is, 9 type IIs, 25 type IIIs and 13 type IVs have been identified (Njunge *et al.*, 2013). There is a high degree of conservation among the resident *P. falciparum* Hsp40 proteins and most of them have homologs in other *Plasmodium* species (Njunge *et al.*, 2013). Also, multiple protein sequence alignments have revealed a high level of sequence similarity and identity between each resident PfHsp40 protein and their orthologues across *Plasmodium* species, indicating a high level of structural and functional conservation (Njunge *et al.*, 2013). Also, comparative analysis revealed that *P. falciparum* possesses the highest number (*n = 19*) of exported Hsp40 proteins when compared with other *Plasmodium* species, an observation that was consistent with an expanded exportome in *P. falciparum* (Njunge *et al.*, 2013). These exported proteins consist of 3 type IIs, 5 type IIIs and 11 type IVs (Njunge *et al.*, 2013; Sargeant *et al.*, 2006). The structural features and the functional interaction of Hsp40s with Hsp70 chaperone have been discussed in sections 1.4.3 and 1.4.4 respectively.

Pfj1 and Pfj4 are type I and type II PfHsp40 proteins respectively and were first identified by Watanabe (Watanabe, 1997). The first functional characterisation of the interactions between Pfj1 and PfHsp70-1 was reported by Misra & Ramachandran (2009). Pfj1 was earlier proposed to be localized to the mitochondria (Watanabe, 1997), however, recent experimental data suggested the localisation of Pfj1 to the apicoplast with a potential role in DNA replication (Kumar *et al.*, 2010). Though an *in vitro* assay reported the interaction of Pfj1 with PfHsp70-1, in the light of Pfj1 localisation to the apicoplast, it is unlikely that such an association would occur *in vivo* (Misra and Ramachandran, 2009; Botha *et al.*, 2011). Also, Nicoll *et al.* (2007) showed that the J-domains of parasite Pfj1 and Pfj4 were able to functionally replace the J-domain of *Agrobacterium tumefaciens* DnaJ (Agt DnaJ) in a prokaryotic system. The Pfj4 J-domain functionality was confirmed in another study which also showed that the expression of Pfj4 increased upon heat shock (Pesce *et al.*, 2008). This could be an indication of distinct roles for Pfj1 and Pfj4 and that the G/F-rich and C-terminal regions of Pfj4 may retain important information needed for substrate specificity and for its interaction with partner Hsp70. Also, the localisation of both Pfj4 and PfHsp70-1 to the nucleus and cytoplasm, and the co-immunoprecipitation and co-fractionation of Pfj4 with PfHsp70-1 provides evidence that they may directly or indirectly interact (Pesce *et al.*, 2008). Such an interaction may have a role in cytoprotection, and by extension, parasite intra-erythrocytic survival and development. It is also possible that Pfj4 may collaborate with PfHsp70-1 in protein translocation across the cell membrane.

Another type I Hsp40 (PfHsp40) was recently investigated for its functional interaction with PfHsp70-1 (Botha *et al.*, 2011). PfHsp40 is expressed in all the stages of the intra-erythrocytic phase of parasite development in a similar pattern as PfHsp70-1 (Le Roch *et al.*, 2003; Botha *et al.*, 2011). PfHsp40 was localized to the parasite cytosol, implicating it as a potential interactor of PfHsp70-1. Also, PfHsp40 stimulated the ATP hydrolytic rates of PfHsp70-1 and human Hsp70, exhibited chaperone-dependent property and enhanced the aggregation suppression ability of PfHsp70-1 (Botha *et al.*, 2011). However, while MAL3-39 and DMT002264 were able to inhibit the Hdj2-stimulated ATPase activity of human Hsp70 under steady-state conditions, the inhibition of PfHsp40-stimulated ATPase activity of PfHsp70 was achieved with DMT002264 and only under single-turnover conditions, indicating selective inhibition (Botha *et al.*, 2011). However, the nature of this selectivity needs further investigation. Meanwhile, like MAL3-39, malonganenones A, C, lapachol and bromo-β-lapachona were reported to produce inhibition of parasite growth in addition to their ability to inhibit aggregation suppression activity of PfHsp70-1 (Cockburn *et al.*, 2011). Therefore, like MAL3-39, it is possible that these compounds might exercise some level of selective inhibition of co-chaperone-stimulated chaperone properties of PfHsp70-1 and human Hsp70. Such selective inhibition could be explored as potential target for drug development.

More so, the expanding nature of the exportome in *P. falciparum*, which now includes the export of PfHsp70-x (Külzer *et al.*, 2012), underscores the importance of Hsp70-Hsp40 malaria parasite protein interactions in the intra-erythrocytic survival and development of the parasite. Interestingly, PFA0660w, a type II Hsp40 protein, regarded to be essential for the intra-erythrocytic development and survival of the parasite (Maier *et al.*, 2008), together with PFB0090c and PFE0055c, have been shown to be exported into the cytosol of infected erythrocytes in complex with PfHsp70-x (Külzer *et al.*, 2010, 2012), suggesting a potential functional relationship among them. The three proteins are said to be homologous to human DnaJB4, a cytosolic type II Hsp40, known to interact with human Hsp70 to facilitate protein folding, transport and assembly (Sargeant *et al.*, 2006). Of all the *Plasmodium* species, *P. falciparum* has the highest number of Hsp40 proteins of which the type III Hsp40 class is the largest. Being more divergent, they may perform more specialized functions. Earlier, two type III proteins (PF11_0513 and PFB0920w) that were once predicted to be exported are now predicted to lack a PEXEL/HT motif (Sargeant *et al.*, 2006; Pesce and Blatch, 2009). Recently, another two type III Hsp40s (PFF1290c and PF10_0058) which were previously considered as typical Hsp40 proteins were found to display no J-domain and were therefore delisted (Njunge *et al.*, 2013). However, seven new Hsp40 proteins, which further enlarged the type III Hsp40 class, were added including PF14_0213, MAL13P1.162, MAL8P1.204, PF10_0057a, PF11_0433, and PF14_0111 and PFI0855w (Njunge *et al.*, 2013). Five type III Hsp40 proteins,

including PF11_0513, PF10_0378, PFB0920w, MAL8P1.204 and PFL0055c, are among the exportome.

Following the inclusion of PFF1010c into the group of Hsp40 proteins, 13 type IV Hsp40s are now encoded by the *P. falciparum* genome and 11 are predicted to be exported (Njunge *et al.*, 2013). Among this class are members of the ring-infected erythrocyte surface antigen (RESA) family that are probably the first set of proteins that are exported across the PV membrane (Maier *et al.*, 2008). RESA is produced during the final stages of the development of schizonts, stored in dense granules in each merozoite, secreted into the newly formed PV and exported to the erythrocyte where it can interacts with spectrin in the membrane skeleton (Cowman *et al.*, 1984; Aikawa *et al.*, 1990; Foley *et al.*, 1994; Rug *et al.*, 2004; Pei *et al.*, 2007; Maier *et al.*, 2009). While the disruption of the PFB0920w gene on the infected erythrocytes caused an increase in erythrocyte rigidity, a decrease in rigidity was observed following disruption RESA (Maier *et al.*, 2008). RESA may protect the red blood cell (RBC) against febrile shock resulting from rupture and cyclic re-invasion (Maier *et al.*, 2008, 2009). The ability of RESA and RESA-like proteins to interact with cytoskeletal proteins implicates them in erythrocyte remodelling. Though unable to achieve the disruption of PF11_0034 and PF11_0509 (Maier *et al.*, 2008), indicating that they may be essential for the intraerythrocytic development and survival of the parasite, the successful disruption of the genes of nine members of the RESA family (Maier *et al.*, 2008) shows some level of redundancy among the RESA family of protein or may indicate that their roles may be more crucial *in vivo* (Maier *et al.*, 2009). It has been shown that the absence of a type IV PEXEL-containing Hsp40 protein, PF10_0381, results in the loss of knobs (Maier *et al.*, 2008), indicating that it is essential for cytoadherence on the surface of the red blood cell. It is therefore evident that a number of the type IV Hsp40s are essential for the development and survival of the parasite and may be an important target of drug actions.

1.4.6 The J dots and PFA0660w

J-dots are highly mobile membrane structures within the cytosol of the infected erythrocytes and so far, three proteins were reported to be exported into these structures (Külzer *et al.*, 2010, 2012). Using transfected parasite expressing two type II Hsp40 proteins, PFE0055c (PF3D7_1133400) and PFA0660w (PF3D7_0113700) fused to GFP or to an HA-strep tag as a reporter, the localisation, expression and solubility characteristics of these proteins was studied (Külzer *et al.*, 2010). In this study the authors observed that both PFE0055c/PFA0660w–GFP were transported to the erythrocyte cytosol, where the chimeric proteins can be seen in previously uncharacterized 'dot-like' structures distributed within the host cell. The authors named these 'dot-like' structures 'J-

dots', as the defining characteristic was the presence of J-domain containing Hsp40s. The J-dots appear to be distinct from the Maurer's clefts as they are highly mobile and share none of the Maurer's clefts antigenic determinants (Külzer *et al.*, 2010). Also, upon staining with acridine orange, J-dots were discovered to be distinct from a previously described highly mobile 'vesicle like structures' in the *P. falciparum*-infected erythrocyte as their intra-erythrocytic velocity differed (Hibbs and Saul, 1994; Külzer *et al.*, 2010). Furthermore, using protease protection assays, Külzer *et al.* (2010) demonstrated that both PFE0055c and PFA0660w bind to the external face of J-dots, thereby indicating that the J-dots are of a membranous nature. Also, the binding was said to be dependent on cholesterol, thus implicating a role for cholesterol in the solubility properties of both PFE0055c and PFA0660w. Earlier reports have also shown that PFE0055c and PFA0660w have different expression profiles during intra-erythrocytic development and that for subcellular localisation of reporter constructs, there is a need for correct promoter control (Bozdech *et al.*, 2003; Le Roch *et al.*, 2003; Rug *et al.*, 2004; Llinás *et al.*, 2006). This difference in expression profile was confirmed by Külzer *et al.* (2010) who reported that the expression of PFA0660w was detected around 10 h post-invasion, and then dropped off during the remainder of the developmental cycle, in contrast to that of PFE0055c which appeared continuously during the parasite intra-erythrocytic 48 h life cycle, but contrary to earlier reports, showed that correct promoter control is not necessary for targeting these proteins to the J dots (Külzer *et al.*, 2010). PfHsp70-x has recently been added to the list of the J-dot proteins (Külzer *et al.*, 2012). Immunolocalisation analysis of PfHsp70-x with previously described PfHsp40 J-dot proteins (PFE0055c and PFA0660w) revealed a strong signal overlap, suggesting a possible functional interaction between them (Külzer *et al.*, 2012). However, the role of PFA0660w in intra-erythrocytic protein transport and parasite survival vis-à-vis its interaction with Hsp70 chaperones needs further elucidation.

1.5 Study Focus

1.5.1 Knowledge Gap

Külzer *et al.* (2010) reported that PFA0660w is localized in J-dots, a highly mobile structure, found to be different from any existing structures in the infected erythrocyte, thereby raising an important question as to how this protein will perform it functions. Also, Maier *et al.* (2008) reported their inability to obtain PFA0660w knock out parasites, thus indicating that PFA0660w may be essential for the intra-erythrocytic survival of the parasite. However, the chaperone properties of PFA0660w and possible interactions with potential chaperone partners of parasite and human origin, especially as a co-chaperone of PfHsp70-1, PfHsp70-x and human Hsp70 (HSPAIA) proteins are yet to be investigated. PfHsp70-x was reported to be exported in complex with PFA0660w and PFE0055c (Külzer *et al.*, 2012), suggesting a possible functional interaction. The experimental validation of a functional interaction between PfHsp70-x and PFA0660w may help to proffer a solution to the confusion surrounding the reported localisation of PfHsp70-x to J-dots (Külzer *et al.*, 2012) and Maurer's cleft (Grover *et al.*, 2013). Therefore, this study will attempt to characterize PFA0660w with a view to understand its functions and determine the nature of its involvement in the development and survival of the parasite in the infected erythrocytes. It is hoped that this study will advance our knowledge and understanding of the roles of PFA0660w at cellular and molecular levels and the identification of potential targets for drug development.

1.5.2 Hypothesis

The *Plasmodium falciparum* Hsp40 protein, PFA0660w, is a co-chaperone of PfHsp70-x.

1.5.3 Objectives

1.5.3.1 Broad Objective

The broad objective of this project is the biochemical and biological characterisation of PFA0660w with a view to gaining insight into its co-chaperone activity as a way to understand its role in the survival and development of the malaria parasite.

1.5.3.2 Specific Objectives

The specific objectives of this research work are as follows:

1. ***Heterologous production and purification of PFA0660w***

   The main focus of this study is the heterologous production and purification of hexahistidine-tagged *PFA0660w* ((His)$_6$-*PFA0660*w) from the PFA0660w codon-optimised coding region for expression in *E. coli* (a bacterial expression system), using nickel affinity chromatography. To achieve this, a codon-optimised coding region will be inserted into the pQE30 expression vector to produce plasmid pQE30-*PFA0660w* which will be used to express the recombinant 6xHis-PFA0660w using an *E. coli* expression system following induction of expression using isopropyl-1-thio-β-galactopyranoside (IPTG). Determination of the recombinant (His)$_6$-PFA0660w protein expression profiles and the solubility of the expressed protein will be conducted. Purified (His)$_6$-PFA0660w will be verified by SDS-PAGE and western analysis with appropriate antibodies and the assessment of its suitability for use in functional assays will be done using fast protein lipid chromatography (FPLC) and Fourier transformed infrared spectroscopy (FTIR).

2. ***Biochemical characterisation of PFA0660w***

   In this study, functional assays of PFA0660w, an exported *P. falciparum* type II Hsp40 protein, will be performed to gain better understanding of it functions alone and in combination with some selected possible Hsp70s chaperone partners. Three Hsp70s will be examined as potential chaperone partners of PFA0660w. They include a parasite resident Hsp70 protein, PfHsp70-1, a parasite exported Hsp70 protein, PfHsp70-x and human host cell resident Hsp70 protein, HsHsp70 (HSPAIA), which may be recruited by the parasite for use in maintaining its survival and development within the host cell. To do this, the ability of recombinant (His)$_6$-PFA0660w to suppress the aggregation of rhodanese alone and in combination with (His)$_6$-PfHsp70-1, (His)$_6$-PfHsp70-x and (His)$_6$-HsHsp70 and its ability to stimulate the ATP hydrolysis of these chaperones will be determined. Also chaperone co-chaperone interactions between (His)$_6$-PFA0660w and each chaperone using surface plasmon resonance spectroscopy (SPR) will be assessed.

3. ***In vivo localisation of PFA0660w***

   This study will further explore the *in vivo* characteristics of PFA0660w using a peptide specific antibody. The main aim is to explore its intra-erythrocytic function and complement the existing

knowledge. To do this, a peptide will be designed that will be used to raise peptide-specific antibodies against PFA0660w and the suitability of the antibody for *in vivo* characterisation will be examined using heterologously purified recombinant proteins, uninfected red blood cells and confirmation of the presence of PFA0660w protein in the *P. falciparum* parasite lysate. Protein expression profile of PFA0660w in the intra-erythrocytic stages of *P. falciparum* development will be determined in a time course experiment and the localisation of PFA0660w using fluorescence microscopy.

CHAPTER TWO

HETEROLOGOUS OVEREXPRESSION AND PURIFICATION OF PFA0660w

The heterologous overexpression and purification is a critical step for functional and structural determination of a protein. The use of expression systems, of which the bacterial system is the most widely employed, has made protein production on a large scale possible. In this report, the optimised coding sequence of PFA0660w was inserted into a pQE30 expression vector to generate the pQE30-PFA0660w plasmid. The plasmid was transformed into Escherichia coli M15[pREP4] cells and the protein was expressed following IPTG induction. A high expression level was attained within three hours following induction. The solubility assay revealed a high level of insolubility. Further analysis of the insoluble pellet revealed that it was composed of a high percentage of $(His)_6$-PFA0660w, characteristic of inclusion bodies. The $(His)_6$-PFA0660w was successfully purified from inclusion bodies using additive enhanced solubilisation and refolding methods. Size exclusion chromatography showed that the protein was monomeric in solution and Fourier transformed infrared spectroscopy confirmed the success of the refolding approach.

2.1 Introduction

Heterologous protein over-expression can be defined as a controlled synthesis of a high quantity of the desired proteins, which involves the introduction of foreign DNA into suitable host cells. An expression plasmid usually contains genetic elements such as origin of replication which controls plasmid copy number (del Solar *et al.*, 1998; Baneyx, 1999) and an antibiotic resistance marker which by conferring resistance to drugs such as ampicillin, chloramphenicol, kenamycin, and tetracycline ensures the selection of the organism carrying the plasmid (Connell *et al.*, 2003). Another genetic element of the plasmid is the transcriptional promoters for induction of expression. A commonly used inducer is isopropyl-beta-thiogalactopyranoside (IPTG) (Hannig and Makrides, 1998). Translation initiation regions (TIRs) and transcription and translational terminators are other important elements of the plasmid. Heterologous expression in prokaryotes is dependent on transcription efficiency with a direct correlation between mRNA levels and protein levels, such that any non-native sequence factors disrupting transcription or mRNA stability will limit the eventual yield of protein (Rai and Padh, 2001; Kimball and Jefferson, 2006).

A review on the approaches to the isolation and characterisation of molecular chaperones has been presented (Nicoll *et al.*, 2006). Purification of molecular chaperones can be achieved using both native and recombinant sources. Native source uses ER, which serves as reservoir of many new proteins, as the primary target (Görlich and Rapoport, 1993; Tyedmers *et al.*, 2000; Nicoll *et al.*, 2006). However, to obtain satisfactory yield of proteins, purification from recombinant sources using affinity tags is an alternative approach (Esposito and Chatterjee, 2006). Some of the available affinity tags used in protein purification includes large peptide tags such as calmodulin-binding peptide (Stofko-Hahn *et al.*, 1992), cellulose-binding domain (Xu *et al.*, 2002), glutathione S-transferase tag (Smith and Johnson, 1988), maltose-binding protein (Di Guan *et al.*, 1988) and streptavidin-binding peptide (SBP) tag (Wilson *et al.*, 2001). Others are the small peptide tags such as poly-Arg-tag (Sassenfeld and Brewer, 1984), FLAG-tag (Hopp *et al.*, 1988), poly-His-tag (Hochuli *et al.*, 1987), and Strep-tag (Schmidt and Skerra, 1993).

One of the most commonly used tags in protein purification is the poly-His-tag (Hochuli *et al.*, 1987) which can be located at the N- or the C-terminus of the target proteins (Hefti *et al.*, 2001). Utilizing an immobilised metal affinity chromatography (IMAC), small affinity-tags with poly-histidine residues have successfully been employed in recombinant protein purification in many expression systems such as bacteria, yeast, mammalian cells and baculovirus-infected insect cells (Hitzeman *et al.*, 1990; Levinson, 1990; Terpe, 2006; Campos-Sandoval *et al.*, 2007). While there

are evidences that suggest that the effects of His tag on protein structure and function is usually negligible and can therefore be retained (Derewenda, 2004; Ivey and Bruce, 2000; Vassiliev *et al.*, 2002; Carson *et al.*, 2007; Thielges *et al.*, 2011), there are reports of negative effects on protein structure and binding interactions, including enzyme assays (Amor-Mahjoub *et al.*, 2006; Song and Markley, 2007; Freydank *et al.*, 2008; Emoto *et al.*, 2009). For example, the formation of a dimer in human Hsc70 protein has been attributed to the presence of His-tag, indicating the need to remove the tag before structural characterisation of the protein (Amor-Mahjoub *et al.*, 2006). However, the availability of multiple expression vectors, scalable and high yield of pure product, easy purification under both native and denaturing conditions and easy immunoassay detection coupled with weak immunogenicity are some of the advantages of His-tags that made it the preferred choice (Young *et al.*, 2012). Table 2.1 shows some examples of proteins from selected organisms that are purified and used for further analysis such as functional characterisations, drug screening and antibodies purifications with their His-tag intact.

Table 2.1: Examples of His-tag proteins used for functional study

Organism/ Source	Proteins	Description	Applications	References
Escherichia coli	Hsp31	Co-Chaperone	Chaperone activity	Sastry *et al.*, 2009
	IbpA	Small heat shock proteins	Functional assay	Kitagawa *et al.*, 2002
	IbpB			
Clostridium acetobutylicum	DnaK	Chaperones and Co-chaperone	Functional characterisation	Rüngeling *et al.*, 1999
	DnaJ			
	GrpE			
Medicago sativa	MsHSP70-1	Chaperone	Functional characterisation	He *et al.*, 2008
Agrobacterium tumefaciens	DnaK	Chaperone	Functional characterisation	Boshoff *et al.*, 2004; Boshoff *et al.*, 2008.
Plasmodium falciparum	PfHsp70-1	Chaperone	Functional characterisation and drug screening	Cockburn *et al.*, 2011; Gitau *et al.*, 2012; Matambo *et al.*, 2004; Misra and Ramachandran, 2009.
	PfHsp40	Co-chaperones	Functional assay	Botha *et al.*, 2011
	KAHsp40			Acharya *et al.*, 2012
	PfGCHI			Stephens *et al.*, 2011
	PfDnaJA		Antibodies purification	Kumar *et al.*, 2010
Trypanosoma brucei	Tbj1	A novel Type III Hsp40	Functional characterisation	Louw *et al.*, 2010
Human	HSJ1a	Co-chaperone	Co-Chaperone activity	Gao *et al.*, 2011
	HsHsp70	Chaperone	Activity assay and Drug screening	Chiang *et al.*, 2009

Table 2.2: Common expression systems

Classes	Expression system	Advantages	Limitations
Prokaryotic	[1]Bacterial - *Escherichia coli*	Relative simplicity, inexpensiveness, easily grown to high density, better knowledge of its genetics, physiology and availability of complete genomic sequence. Lack of glycosylation may be an advantage in expressing *Plasmodium* proteins.	Subject to post-translational modifications problems such as glycosylation when used for eukaryotic protein purification. Insoluble protein aggregation and endotoxin release.
Eukaryotic	[2]Yeast - *Saccharomyces*	Unlike *E. coli,* lack toxic cell wall, can be grown relatively rapidly to high cell density in simple media and also possess advanced genetics, complete genomic sequence able to glycosylate.	Proteins of mammalian origin may not be correctly glycosated. Hypermannosylation (addition of high amount of mannose residues) may lead to improper folding and loss of activity.
	[3]Insect - Baculoviruses	Proteins modifications, transport systems and processing are similar to that of other higher eukaryotic cells. They are easily adaptable for growth in suspension cultures, and can be grown to relatively high density within a short time. Proteins are usually expressed into their proper cellular compartment (e.g. membrane proteins to the membrane) and are usually very soluble. Can be used to express potentially toxic proteins	Inefficient proteolytic cleavages at arginine- or lysine-rich sequences and lack of ability to process complex oligosaccharides (fructose, galactose and sialic acid) during glycosylation.
	[4]Mammalian	Best for all proteins requiring mammalian post-translational modifications and offers the greatest degree of product fidelity.	Glycosylation (e.g. oligosaccharide processing) is species- and cell type specific and required complex nutrient with low product concentration. It is also time consuming.
	[5]*Dictyostelium discoideum*	Like prokaryotes, it has circular plasmids and a life cycle that alternates between multicellular and single-celled stages. They can be grown to a high cell density without any need for serum factors and special aeration which are usually necessary in animal cell cultures. Like insect, proteins are expressed into appropriate compartment. They also carry out post-translational modification such as O- and N-glycosylation.	The ability to carry out post-translational modification may be a disadvantage for expressing *Plasmodium* proteins as the parasite only produced very limited glycosylation.

[1](Casadaban *et al.*, 1983; Shatzman and Rosenberg, 1987)
[2](Hitzeman *et al.*, 1990; Kukuruzinska *et al.*, 1987)
[3](Kitt and Possee, 1993; Matsuura *et al.*, 1987; O'Reilly *et al.*, 1992; Supyani *et al.*, 2007)
[4](Kaufman, 1990a, 1990b; Levinson, 1990)
[5](Dittrich *et al.*, 1994; DJ *et al.*, 1995; Fasel *et al.*, 1992; Jung and Williams, 1997)

Escherichia coli cells are relatively simple and inexpensive to use, providing high density growth within a short period of time. The availability of the *E. coli* complete genomic sequence coupled with an improved knowledge of its genetics and physiology have made it the most widely used expression system (Casadaban *et al.*, 1983; Shatzman and Rosenberg, 1987). The potential usefulness of other expression systems of bacterial origin such as *Bacillus brevis, Bacillus megaterium, Bacillus subtilis, Caulobacter crescentus* and other species has been reviewed (Terpe, 2006). Table 2.2 presents the commonly used expression systems for heterologous proteins purifications, their advantages and limitations. They are classified into two groups- prokaryotic (bacterial) or eukaryotic (yeast or mammalian or insect). The potential application of these and other expression systems such as *Toxoplasma gondii, Xenopus laevis,* plants and cell free protein expression systems in heterologous expression of plasmodial proteins for structural studies and functional annotation has been reviewed (Birkholtz *et al.*, 2008).

An important limitation associated with recombinant protein production using prokaryotic cells is the formation of insoluble aggregates or unfolded proteins called inclusion bodies. Inclusion bodies usually consist of tightly packed molecules of a single species of aggregated protein with partial secondary structure (Kopito, 2000; Markossian and Kurganov, 2004; García-Fruitós *et al.*, 2012). Isolation, solubilisation and renaturation are part of the strategies employed in making good use of inclusion bodies. Solubilisation can be achieved with denaturing agents like urea, guanidine HCl and mild detergents (Puri *et al.*, 1992; Patra *et al.*, 2000; Tsumoto *et al.*, 2003; Singh and Panda, 2005). Renaturation can be achieved using refolding buffers containing essential components that can promote the correct disulphide bond formation, encourage the formation of appropriate three-dimensional shape, reduce aggregation and promote solubility (Bondos and Bicknell, 2003; Dechavanne *et al.*, 2011). Another important obstacle to optimal expression of *P. falciparum* genes in *E. coli* is the drastic differences in their codons usage. The presence of rare codons within the target gene may adversely affect the expression level of the protein due to stalling of the translational processes (Gustafsson *et al.*, 2004). One way is to use plasmids which encode rare tRNAs in target expression organism, for example *E. coli* (Baca and Hol, 2000). Another approach is what is referred to as codon-optimisation (Gustafsson *et al.*, 2004; Zhou *et al.*, 2004). In codon optimisation, the rare codons in the target gene are altered to reflect the preferred codons usage of the host while maintaining the amino acid sequence of the protein encoded by the target gene (Gustafsson *et al.*, 2004). Codon harmonisation is another approach to improve protein expression which ensures that codons usage (low, intermediate or high) remains the same in the expression host as it is in the natural host, thereby allowing translational processes and the secondary and tertiary structures folding to occur as in the natural host (Thanaraj and Argos, 1996; Angov *et al.*,

2008, 2011). Though successful expression of many proteins has been achieved using any of these methods (Narum *et al.*, 2001; Zhou *et al.*, 2004; Tokuoka *et al.*, 2008; Tang *et al.*, 2011), better results may be obtained by combining them.

Therefore, it is clear that with good experimental design and protocol optimisation, high levels of protein expression can be achieved. However, co-purification of expression host (*E. coli*) resident proteins with the target protein is an important challenge to the purity of the protein of interest. Prominent among these resident proteins is DnaK, the bacterial Hsp70 molecular chaperone homolog, shown to be involved in protein folding (Hartl and Hayer-Hartl, 2002; Hartl, 1996). Co-purifying chaperones may strongly influence subsequent assays and downstream application of the target proteins. For example, antibody production with full length protein can be strongly influenced, as even small traces of DnaK may produce a strong antigenic response in rats and rabbits (Rial and Ceccarelli, 2002). Also, assays involving the determination of ATP hydrolysis activity may be affected, since DnaK, like other Hsp70 will hydrolyse ATP for chaperone function (Szabo *et al.*, 1994; Suh *et al.*, 1998; Chang *et al.*, 2008a). Various approaches have been reported to have potentially removed or drastically reduced DnaK contamination. They include washing the resin bound fusion protein with 20% glycerol (Guo *et al.*, 2007), or washing with ATP (Rial and Ceccarelli, 2002) or with MgATP plus soluble denatured *E. coli* proteins before elution (Rial and Ceccarelli, 2002) or construction of an *E. coli* DnaK-deletion mutant gene (Sugimoto *et al.*, 2008). It appears that there is no single universal approach to removing DnaK contamination. Therefore, optimisation and screening of the buffers using different approaches will help to identify the appropriate approach suitable for the protein of interest.

Using the codon-optimised coding region for the expression of PFA0660w (PF3D7_0113700) in *E. coli* cells, the main focus of this study was the heterologous production and purification of PFA0660w using nickel affinity chromatography, verification by SDS-PAGE and western analysis and the assessment of its suitability for use in functional assays using fast protein lipid chromatography (FPLC) and Fourier transformed infrared spectroscopy (FTIR).

The specific objectives of this study were to:

1. Construct pQE30-*PFA0660w* expression plasmid by insertion of the codon-optimised coding region into a pQE30 expression vector.
2. Express the recombinant $(His)_6$-PFA0660w from the pQE30-*PFA0660w* plasmid in an *E. coli* expression system following induction of expression using isopropyl-1-thio-β-galactopyranoside (IPTG)

3. Determine the $(His)_6$-PFA0660w protein expression profiles in *E. coli* and the solubility of the expressed protein.
4. Purify the recombinantly expressed $(His)_6$-PFA0660w using nickel affinity chromatography and verify by SDS-PAGE and Western analysis using anti-His antibodies.
5. Determine the suitability of the purified $(His)_6$-PFA0660w protein for functional assays by size exclusion chromatography using FPLC and secondary structure analysis using FTIR.

2.2 Materials and Methods

2.2.1 Materials

The nucleotides and amino acids letter codes as provided for by the Joint Commission of Biochemical Nomenclature (JBNC) of IUPAC (International Union of Pure and Applied Chemistry) and the IUBMB (International Union of Biochemistry and molecular Biology) are given in *Appendix A*. The optimised coding sequence of *PFA0660w* was synthesized by GenScript® (USA) and supplied as pUC57-PFA0660w (*Appendix B.1 and F.1*). The pQE30 (Qiagen, Germany), encoding N-terminally 6xHis-tag sequence and β-lactamase gene to confer ampicillin resistance was used as the expression vector. The restriction endonucleases that were used for restriction digest were *Bam*HI and *Kpn*I (Fermentas, Lithuania). λ *Pst*I DNA marker was prepared as given in *Appendix D2*. Helios Alpha UV-Vis spectrophotometer (Thermo Scientific, USA), ready-to-use Bradford reagent (Fermentas, USA), Snakeskin^{TM} Pleated dialysis tubing (Pierce – MWCO 10,000: Thermo Scientific, USA) and ABIPRISM 3100 Genetic Analyser for sequencing (Applied Biosystems, USA) were also used. Commercially available antibodies and assay kits and other standard grade chemicals and reagents are as given in *Appendix E*. 6xHis-PfDXR (*P. falciparum* 1-deoxy-D-xylulose 5-phosphate reductoisomerase), a 46.7 kDa recombinant protein, was a kind gift from Dr Jessica Goble, Rhodes University, 2011, and was used as positive control. Except otherwise indicated, *Escherichia coli* (*E. coli*) cells used are M15[p*REP4*] (NaIS, StrS, RifS, Thi–, Lac–, Ara+, Gal+, Mtl–, F–, RecA+, Uvr+, Lon+) and JM109 (*end*A1, *rec*A1, *gyr*A96, *thi, hsd*R17 (r_k^-, m_k^+), *rel*A1, *sup*E44, Δ(*lac-pro*AB), [F′ *tra*D36, *pro*AB, *lac*I^{q}ZΔM15].

2.2.2 Construction of expression construct

The *PFA0660w* coding sequence was optimised for expression in *E. coli* and the optimised sequence was synthesized and supplied as pUC57-PFA0660w by GenScript$^{(R)}$ with *Bam*HI and *Kpn*I restriction endonucleases incorporated at the 5' end and 3' end of the nucleotide sequence respectively. The pUC57-*PFA0660w* plasmid DNA and pQE30 expression vector were double digested (*Bam*HI/*Kpn*I) and the resultant *PFA0660w* DNA and digested pQE30 expression vector were subsequently gel purified using Zymoclean^{TM} Gel DNA Recovery Kit (ZYMO research, USA). The purified *PFA0660w* was ligated into the pQE30 expression vector, downstream of 6xHis-tag, transformed into competent *E. coli* JM109 cells (as per *Appendix D8 and D9*) and plated on 2xYT agar plate (1.5% (w/v) tryptone, 1% (w/v) yeast extract, 0.5% (w/v) NaCl and 1.5% (w/v) agar) supplemented with ampicillin to a final concentration of 100 µg/ml. *E. coli* colonies were

screened for successful transformants as follow: each selected colony was inoculated into 5 ml 2xYT broth (1.5% (w/v) tryptone, 1% (w/v) yeast extract and 0.5% (w/v) NaCl) and incubated at 37°C with shaking overnight. The cells were harvested by centrifugation at 10,000 x g for 2 minutes and the plasmids were extracted using the alkaline lysis methods (as per *Appendix D1*). Digestion with *Bam*HI and *Kpn*I was followed by agarose gel electrophoresis. Plasmid pQE30-PFA0660w DNA was isolated from the cells that produced expected digestion bands from the alkaline lysis method using QIAprep miniprep kit (Qiagen, USA) and confirmed by DNA sequencing (*Appendix D6*). The pQE30-PFA0660w DNA plasmid was propagated and stored in JM109 *E. coli* cells.

2.2.3 Analysis of expression and solubility of (His)$_6$-PFA0660w

Purified pQE30-*PFA0660w* plasmid DNA was transformed into competent *E. coli* M15[p*REP4*] cells (as per *Appendix D8 and D9*) and were plated onto 2xYT agar petri dishes supplemented with ampicillin and kanamycin to a final concentration of 100 µg/ml and 50 µg/ml respectively. A colony was picked and introduced into 25 ml 2xYT broth for overnight growth at 37°C with shaking. The overnight culture of the *E. coli* transformants was diluted to an A_{600} (absorbance at 600 nm) of 0.1 in 250 ml YT broth and incubated at 37°C with shaking until the A_{600} reached 0.6 – 0.8. Expression of protein was induced by the addition of IPTG to a final concentration of 0.4 mM and samples were taken at 0, 1, 2, 3, 4, 5 and 16 (overnight) hours following the determination of A_{600} of the culture at each time point. Each sample was harvested by centrifugation (13,000 × *g* for 2 minutes). The pellets were then resuspended in a volume of phosphate buffered saline (PBS - 137 mM NaCl, 2.7 mM KCl, 10 mM Na_2HPO_4 and 2 mM KH_2PO_4; pH 7.4) calculated as sample's A_{600} x 300 µL. The 5x SDS-PAGE (sodium dodecyl sulphate–polyacrylamide gel electrophoresis) sample buffers (10% glycerol, 2% SDS, 5% β-mercaptoethanol, 0.05% bromophenol blue, 0.0625 M Tris, pH 6.8) was added to the suspension in ratio 1:4 (buffer:sample), boiled for 5 minutes at 100°C and stored at -20°C for further analyses.

Also, to determine the level of solubility of the protein, the 250 ml culture was harvested by centrifugation (5,000 × *g* at 4°C for 20 minutes) 3 hours post induction and the pellet was resuspended in native lysis buffer (NLB - 2.5 ml; 10 mM Tris, pH 8.5, 300 mM NaCl, 50 mM imidazole, 1 mM PMSF and 1 mg/ml lysozyme) and frozen at -80°C overnight, followed by rapid thawing and sonication (5 times, 30 seconds each, at 30 second interval and 50 Hz) at 4°C. The suspension was clarified by centrifugation (16,000 × *g* for 30 minutes at 4°C). The supernatant (soluble fraction) was transferred to a new microcentrifuge tube and the pellet (insoluble fraction) was resuspended with 2.5 ml of native lysis buffer. Samples were taken (80 µl), into which 5x SDS-

PAGE sample buffers was added in ratio 1:4 (buffer:sample), boiled for 5 minutes at 100°C and stored at -20°C for further analysis. All samples (for expression and solubility studies) were analysed by SDS-PAGE and western analysis (as per *Appendix D11 and D12*) with mouse monoclonal anti-His primary antibody (1 in 5000) and HRP-conjugated anti-mouse IgG secondary antibody (1 in 10,000). Chemiluminescence-based protein detection was achieved using the ECL™ Western blotting kit (GE Healthcare, UK) as per the manufacturer's instructions, and captured with a Chemidoc chemiluminescence imaging system (Bio-Rad, USA).

2.2.4 Assessment of the nature of insoluble pellet

The nature of the insoluble pellet was assessed as follows: the insoluble pellet was obtained from 250 ml culture (as given in section 2.2.3) and resuspended in 2 ml of native lysis buffer and split equally into two pre-weighed microcentrifuge tubes. The pellets were recovered by centrifugation (16,000 × *g* for 30 minutes at 4°C) and the tube containing pellets were weighed. The weight of each pellet was determined by subtraction of the weight of the tube from that of the tube plus the pellet. One of the pellets was thoroughly washed thrice in pellet wash buffer (PWB - 50 mM Tris-HCl pH 8.5, 200 mM NaCl, 10 mM EDTA, 1% Triton X-100 and 1 mM PMSF) and finally twice in double distilled water as earlier described (Singh and Panda, 2005) and pellet was recovered by centrifugation (10,000 x g for 10 minutes at 4°C). As control the weight of the washed pellet was determined as before and compared with the initial weight prior to washing. The washed and the unwashed pellets were solubilised in 50 mM Tris-HCl pH 8.5, 200 mM NaCl and 8 M urea buffer and their concentrations were determined using Bradford reagent as per *Appendix D10* (Bradford, 1976). The percentages of washed relative to unwashed pellets were calculated. Samples were also taken for SDS-PAGE analyses and visualised by Coomassie brilliant blue staining (Laemmli, 1970) and confirmed by western analysis with mouse monoclonal anti-His antibody.

2.2.5 Purification of Recombinant $(His)_6$-PFA0660w

2.2.5.1 Isolation of Inclusion bodies

A 250 ml culture of pQE30-*PFA0660w* transformed competent *E. coli* M15[p*REP4*] cells in 2xYT broth were grown to an A_{600} (0.6 – 0.8) as described in section 2.2.3 and induced for expression by the addition of IPTG to a final concentration of 0.4 mM. Following incubation for further 3 hours, the culture was harvested by centrifugation (5,000 × *g* at 4°C for 20 minutes). The cell pellet was

resuspended in NLB and allowed to stand for 20 minutes at room temperature for lysis to take place. Lysozyme treated suspension was freezed at -80°C overnight followed by rapid thawing and sonication (5 times, 30 seconds each, at 30 second interval and 50 Hz) at 4°C. The insoluble cell pellet (inclusion bodies) was obtained by centrifugation (16,000 × *g* for 30 minutes at 4°C) with the supernatant discarded. The inclusion bodies were washed by thoroughly resuspending in pellet wash buffer (PWB - 50 mM Tris-HCl pH 8.5, 200 mM NaCl, 10 mM EDTA, 1% Triton X-100 and 1 mM PMSF) three times and finally twice in double distilled water to remove salts and detergent. The pellet was recovered after each washes following centrifugation (10,000 x g for 10 minutes at 4°C) and supernatant was discarded.

2.2.5.2 Optimisation of Solubilisation and Refolding conditions

Improvement of solubilisation and refolding conditions involves an initial pH optimisation as well as the selection and screening of refolding additives. The optimisation of pH with and without lower denaturant concentration was conducted using the adaptation of a previously described protocol (Singh and Panda, 2005). Briefly, inclusion bodies pellet were resuspended to a final concentration of 4 mg/ml in 100 mM Tris-Cl and 300 mM NaCl buffer with varying pH range of 3 – 12 with and without 2 M urea. The solubilisation was allowed to proceed for 1 hour with gentle agitation at 4°C and the samples were clarified by centrifugation (10,000 x g for 10 minutes at 4°C) to obtain the supernatant. The supernatant was analysed by SDS-PAGE (as per *Appendix D11*) and proteins were visualised by Coomassie brilliant blue staining (Laemmli, 1970).

For the optimisation of refolding condition, the additives were selected based on available experimental evidences of their ability to improve refolding and/or removal of contaminating DnaK (Cleland *et al.*, 1992; Cappel and Gilbert, 1988; Meng *et al.*, 2001; Vallejo and Rinas, 2004; Wang *et al.*, 2009b) and were screened using a modification of the previously reported protocols (Bondos and Bicknell, 2003; Churion and Bondos, 2012; Dechavanne *et al.*, 2011). The additives are dithiothreitol (DTT), ethenediaminetetraacetic acid (EDTA), glycerol (G), polyethylene glycol (PEG) and sucrose (S). The initial screening involved 32 different combinations of the additives in 100 mM Tris-Cl buffer, pH 8.5, and varying concentrations of NaCl (100, 200 and 300 mM). Table 2.2 presents the stock and the working concentrations of these additives and the layout of the screening model. The initial screening is as follows: clean inclusion bodies proteins were solubilised in 100 mM Tris-Cl buffer, pH 8.5 containing 8 M urea and centrifuged at 10,000 x g for 10 minutes at 4°C to obtain clear supernatant. Protein concentrations were determined by Bradford's assay as described in *Appendix D10* (Bradford, 1976), from where the initial mg amount was calculated. The supernatant was then pulse diluted into each of the additive containing buffer

(as in Table 2.2 layout) to a final concentration of 250 μg/ml. The refolding was allowed to proceed for 4 hours at 4°C with gentle agitation. Soluble protein was then separated from aggregated protein by centrifugation at 16,000 x g for 15 minutes and filtered through 0.45 μm filter. The final protein concentration in the filtrates was estimated using Bradford reagent (Bradford, 1976), from where the final mg amount was estimated. The results were expressed as percentage solubility (calculated as the fraction of the starting amount of solubilised protein).

Table 2.3: The selected additives, their concentrations and the screening layout

ADDITIVES	CONCENTRATION	
	STOCK	*WORKING*
D = Dithiothreitol (DTT)	100 mM	5 mM
E = Ethenediaminetetraacetic acid (EDTA)	10 mM	0.1 mM
P = Polyethylene glycol (PEG 2000)	10 % (w/v)	0.1 % (w/v)
S = Sucrose	50 % (w/v)	5 % (w/v)
G = Glycerol	100 %(v/v)	10 %(v/v)

96 WELL SCREENING LAYOUT FORMAT

Buffer	Salt	Additives combinations							
100 mM Tris-Cl (pH 8.5)	100 mM NaCl	D	E	G	P	S	DE	EG	GP
		PD	SE	DG	EP	GS	PS	SD	DEP
		EDS	GES	PSE	SDG	DEG	EGP	GDP	PSD
		SPG	DEPG	EDPS	GDES	PSGE	SPGD	DEGPS	Blank
100 mM Tris-Cl (pH 8.5)	200 mM NaCl	D	E	G	P	S	DE	EG	GP
		PD	SE	DG	EP	GS	PS	SD	DEP
		EDS	GES	PSE	SDG	DEG	EGP	GDP	PSD
		SPG	DEPG	EDPS	GDES	PSGE	SPGD	DEGPS	Blank
100 mM Tris-Cl (pH 8.5)	300 mM NaCl	D	E	G	P	S	DE	EG	GP
		PD	SE	DG	EP	GS	PS	SD	DEP
		EDS	GES	PSE	SDG	DEG	EGP	GDP	PSD
		SPG	DEPG	EDPS	GDES	PSGE	SPGD	DEGPS	Blank

The percentage solubility obtained was used to select buffer and additives combinations for the optimisation of solubilisation and refolding conditions as follows: Solubilising buffers were constituted with lower denaturant concentration (2 M urea) at pH 12 (Singh and Panda, 2005) and higher denaturant concentration (8 M Urea) at pH 8.5: Buffer A: 100 mM Tris-Cl, pH 8.5, 300 mM NaCl, 8 M Urea; Buffer B: Buffer A supplemented with 5 mM DTT and 0.1 mM EDTA; Buffer C: 100 mM Tris-Cl, pH 12.0, 300 mM NaCl, 2 M Urea and Buffer D: Buffer C supplemented with 5 mM DTT and 0.1 mM EDTA. Clean inclusion bodies proteins were solubilised in buffers A – D to a final concentration of 4 mg/ml and centrifuged at 10,000 x g for 10 minutes at 4°C to obtain the

supernatant. The supernatant was pulse diluted into the selected additives containing series of buffer conditions and refolded under the same experimental conditions as given above. The mg amount of the proteins (before and after refolding) were determined as given above and the results were expressed as percentage solubility and used to determine the most suitable solubilising and refolding condition.

2.2.5.3 Inclusion bodies Solubilisation

For subsequent protein purification, the clean inclusion bodies pellet was resuspended in optimised solubilising buffer (SB - 100 mM Tris-HCl pH 8.5, 300 mM NaCl, 8 M urea, 50 mM Imidazole, 5 mM DTT, 0.1 mM EDTA and 1 mM PMSF) and clarified by centrifugation at 16, 000 x g for 30 minutes at 4°C.

2.2.5.4 Protein refolding and Purification

To ensure proper refolding, refolding by dilution was followed by on-column refolding. The solubilised inclusion bodies proteins were diluted to a final concentration of 250 µg/ml with refolding buffer (RB - 100 mM Tris-HCl pH 8.5, 300 mM NaCl, 50 mM imidazole, 10% glycerol, 5% Sucrose, 1 mM DTT, 0.1 mM EDTA, 0.1% PEG 2000 and 1 mM PMSF) supplemented with 2 M urea and incubated with gentle stirring at 4°C for 2 hours. The diluted supernatant was filtered through 0.45 µm filters and loaded onto 5 ml HisTrap Column (GE Healthcare, Amersham Biosciences, UK) pre-equilibrated with RB supplemented with 2 M Urea. For on-column refolding, the column was subsequently washed with 5 column volume of refolding buffer, followed by another 5 column volume of refolding buffer without PEG 2000. Proteins bound to the resin were eluted with three column volumes of elution buffer (EB - 100 mM Tris-HCl pH 8.5, 300 mM NaCl, 0.5 M Imidazole, 10% Glycerol, 5% Sucrose, 1 mM DTT, 0.1 mM EDTA, and 1 mM PMSF) in 1 ml aliquots. All fractions collected were analysed by SDS–PAGE (as per *Appendix D11*) and proteins were visualised by Coomassie brilliant blue staining (Laemmli, 1970). Western analysis (as per *Appendix D12*) with mouse monoclonal anti-His antibody (1 in 5000) and mouse monoclonal anti-DnaK antibody (1 in 5000) was performed on the same sample to confirm the presence of target protein ($(His)_6$-PFA0660w) and rule out the presence of contaminating DnaK. The eluted proteins were subsequently stored at -80°C or dialysed using SnakeSkin dialysis membrane (10,000 MWCO) into dialysis buffer (DB - 50 mM Tris/HCl pH 8.5, 300 mM NaCl, 1 mM DTT, and 1 mM PMSF, except otherwise stated) for analysis. Protein concentrations were determined by Bradford's assay (Bradford, 1976) (as per *Appendix D10* using the standard curve – samples in *Appendix B.8*).

2.2.6 Size exclusion chromatography of PFA0660w

Size exclusion chromatography of purified $(His)_6$-PFA0660w was performed using an ÄKTAbasic FPLC system with a Superdex 200 HR 10/30 column (exclusion limit of about 2000 kDa) (Amersham Pharmacia Biotech) equilibrated with the buffer into which the $(His)_6$-PFA0660w was dialysed (50 mM Tris–HCl, pH 8.5, 0.15 M NaCl and 1 mM DTT). The calibration curve was generated using the following molecular mass standards: blue dextran (2000 kDa - void volume), catalase (240 kDa), bovine serum albumin (68 kDa), ovalbumin (45 kDa), carbonic anhydrase (29 kDa), RNase A (13.7 kDa) and lysozyme (14.3 kDa). The flow rate was maintained at 1 ml/minute and elutions were collected in 1 ml fractions for the duration of the analysis, while tracking protein by measuring absorbance at 280 nm. Fractions were analysed by SDS-PAGE and western blot with His-probe monoclonal antibody.

2.2.7 Secondary structure analysis of $(His)_6$-PFA0660w

Analysis of the structural elements and folding of $(His)_6$-PFA0660w were conducted with a PerkinElmer Spectrum 100 FTIR spectrometer (PerkinElmer Inc.) and data were acquired by Spectrum version 6.3.5 software. Solvent contribution was removed by subtraction of blanking buffer (50 mM Tris-HCl, pH 8.5, 300 mM NaCl, and 1 mM DTT) spectra recorded under the same scanning conditions as the sample. An aliquot of 10 µl of the protein sample in blanking buffer was used for each spectrum scan. Individual components of amide I band (1600 – 1700 cm^{-1}) were resolved by Fourier deconvolution procedure (Czarnecki and Ozaki, 1996; Kauppinen *et al.*, 1981; Mantsch *et al.*, 1988) by iterative adjustment of heights, widths, and position of the bands. The fractional area of the individual bands was quantified by Gaussian curve fitting of the amide I region using PeakFit ID (SySTAT Software Inc, USA). Bands were assigned to various secondary elements (α–helix, β–sheet and unordered motifs) as previously reported (Byler and Susi, 1986; Haris and Severcan, 1999; Kong and Yu, 2007).

2.2.8 Comparative protein modelling

Comparative protein modelling of the J domain and C-terminal domain (peptide binding and dimerisation domains) of PFA0660w was done using Swiss-Model automated server (Schwede, 2003; Bordoli *et al.*, 2009) with manual template selection. The SWISS-MODEL workspace template identification tool (Arnold *et al.*, 2006; Kiefer *et al.*, 2009) was used for template identification and was compared with a BLAST search of protein data bank (PDB) for template

retrieval using the amino acid sequence of each PFA0660w domains as query sequence. Three alignment approaches as provided for by the workplace template identification tool were employed to identify the best template. They include the use of a gapped BLAST (Altschul *et al.*, 1997) which performed a BLAST query against the template library; the iterative profile blast (Altschul *et al.*, 1997) which build an initial profile sequence by position specific iterative Blast (PSI-BLAST) (Altschul *et al.*, 1997; Schäffer *et al.*, 2001) search of the Non-redundant (NR) database (Wheeler, 2003; Wheeler *et al.*, 2004; Sayers *et al.*, 2007) and use the profile to search the template library; and lastly the hidden Markov models (HMM) based template library search which uses SAM-T2K (Hughey and Krogh, 1996) software (version 3.4) to create multiple sequence alignment from the iterative search of NR database to generate a library of hidden Markov models. Template selection was done by scoring the target sequence against the template search results or HMM library for the determination of the statistically significant matches. The alignment was manually refined using SwissPdbviewer software (Guex and Peitsch, 1997) and submitted for automated modelling using Swiss model server (Schwede, 2003; Arnold *et al.*, 2006; Bordoli *et al.*, 2009; Kiefer *et al.*, 2009). Model of the J-domain was generated using solution structure of J-domain from human DnaJ subfamily B member 12 as template while the crystal structure of dimerisation domain of HSP40 from *Cryptosporidium parvum* was used as template for C-terminal domain (*Appendix B.6*). The coordinates of the predicted secondary structures were rendered using Pymol software (open source 0.99rc6). The ribbon representations from Pymol were saved as image file. For the empirical correlation, the secondary structure content analysis of the C-terminal model was determined using an online server called ***2Struc: The Secondary Structure Server*** (Klose *et al.*, 2010). This server provided for eight different secondary structure assignment methods of which the defined secondary structure of proteins (DSSP) remains the golden standard for this analysis (Kabsch and Sander, 1983; Klose *et al.*, 2010). By using a single hydrogen bond energy term, DSSP can assign eight states of secondary structure elements (SSEs) to three-dimensional coordinates (Kabsch and Sander, 1983). Using this server, the DSSP analysis of the C-terminal model of PFA0660w was determined and the result was expressed in percentage secondary structure content.

2.3 Results

2.3.1 Construction of pQE30-PFA0660w expression vector

The optimised coding sequence (1038 bp) contained in the plasmid pUC57-PFA0660w (*Appendix B.1*) was synthesized with *Bam*HI (GGATCC), *Sph*I (GCATGC) and *Kpn*I (GGTACC) restriction sites at position 1, 7 and 1051 respectively to make a total of 1056 bp nucleotide sequence. Therefore, to release the coding sequence for cloning into expression vector, there are two possible enzyme combinations, namely, *Bam*HI/*Kpn*I and *Sph*I/*Kpn*I. It is noteworthy that only *Bam*HI/*Kpn*I can produce a non-complementary overhang, thereby making ligation to occur in only one direction (directional cloning). Directional cloning is an efficient approach to cloning involving the use of two different restriction enzymes that produces non-complementary overhangs, thereby making the ligation to occur in only one direction (Kaluz *et al.*, 1992; Wang *et al.*, 2009a).

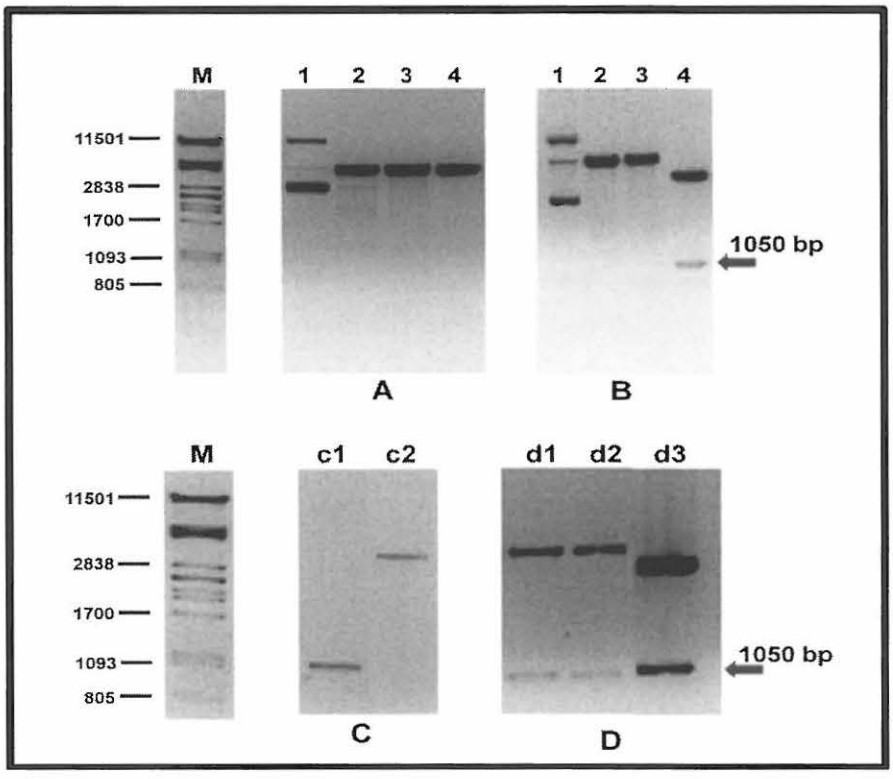

Figure 2.1: Agarose gel analysis of restriction digest and plasmid construct screening
A and **B** are agarose gels of the restriction digest of pQE30 expression vector and pUC57-*PFA0660w* plasmid respectively, where lane 1 is the uncut DNA, lane 2 and 3 is the *Bam*HI and *Kpn*I digested DNA respectively and lane 4 represents the double digestion with *Bam*HI/*Kpn*I. The digested fragments were gel purified using Zymoclean™ Gel DNA Recovery Kit (Zymo research). **C** is the agarose gel check of the purified *PFA0660w* DNA (lane c1) and linearized pQE30 vector (lane c2). **D** is the agarose gel analysis for screening for successful clones from ligation transformants. Lane d1 and d2 are successful clones, while lane d3 was pUC57-PFA0660w digest, serving as control. Gels are shown in inverted colours. The blue arrow showed the position of *PFA0660w* DNA and M is the DNA molecular marker.

To ensure the restriction of the desired *Bam*HI and *Kpn*I sites that will produce the correct coding gene, sequential stepwise approach was used to digest pUC57-PFA0660w plasmid. This involved an initial digestion with *Bam*HI to linearize the pUC57-PFA0660w plasmid, followed by fragment clean up using DNA clean and concentrate-5^{TM} kit (Zymo research, USA) to eliminate the smaller fragment. Digestion with *Kpn*I was then followed by agarose gel purification and ligation (section 2.2.2). The cloning strategy employed in this study is schematically presented in *Appendix B.3*. Figure 2.1 showed the agarose gel analysis of the restriction digest, agarose gel purification of the plasmid restriction fragments and construct screening. The analysis revealed that the inserted coding sequence was of the same size with the restricted insert from the pUC57-PFA0660w plasmid. The constructs obtained (*map shown in Appendix B.2*) were further confirmed by sequencing (*Appendix B.4*). Sequencing result showed the essential features of pQE30 expression vector including the promoter/Lac operator element and the 6xHis-tag with the inserted *PFA0660w* gene.

2.3.2 Expression and Solubility

The expression of $(His)_6$-PFA0660w was assessed in *E. coli* M15[pREP4] cells and a 46.7 kDa 6xHis-tag protein PfDXR (*P. falciparum* 1-deoxy-D-xylulose 5-phosphate reductoisomerase), was used as a positive control for western analysis. Analysis of the expression profile showed that a high level of expression was obtained within 3 hours post induction (Figure 2.2). Furthermore, no expression of the target protein was observed prior to induction (time 0) and western analysis with anti-His antibodies revealed a protein at the expected size of 41.3 kDa for each post induction time point, thereby confirming the presence of the protein of interest. The solubility profile revealed that the protein was largely found in the pellet fraction (Figure 2.2B), an indication of its insolubility. Attempts were made to improve the level of soluble protein through the optimisation of IPTG concentrations, different growth temperature, different *E. coli* strains (including BL21, XL1 Blue, BB1994 and M15[pREP4]), varying NaCl concentrations and addition of 0.1% PEI (polyethylenimine). Of all the *E. coli* strains used, protein expression was only detected in M15[pREP4] and BB1994 (a *dnaK* minus strain) . The expression level in *E. coli* BB1994 was drastically reduced compared to M15[pREP4]; and a change in IPTG concentration from 1 mM to 0.4 mM and lowering of the temperature to 20°C slightly decreased the level of protein expression in M15[pREP4]. The addition of PEI had no significant effect on the solubility of the $(His)_6$-PFA0660w protein (data not shown). But high salt concentrations, pH adjustment, addition of urea or combinations of extreme pH and low denaturant concentrations improved the solubility of the protein (section 2.3.3).

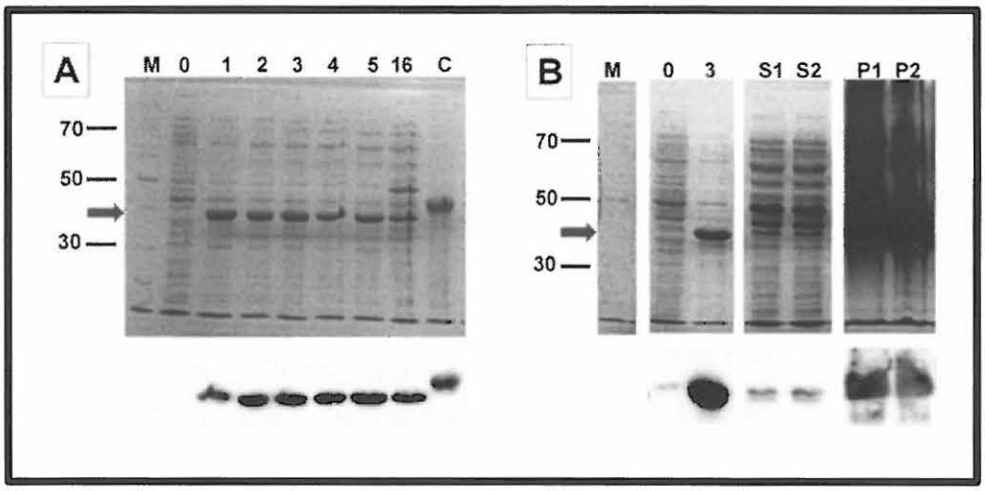

Figure 2.2: Analysis of expression and solubility of PFA0660w.
The 12 % SDS-PAGE gel (upper panel) and western analysis (lower panel) of **(A)** the expression and **(B)** the solubility profiles of PFA0660w in *E. coli* M15[pREP4] cells. Samples for the expression **(A)** were taken from the 250 ml cell culture at 0 (pre-induction), 1, 2, 3, 4, 5, and 16 hours post-induction, centrifuged and resuspended in denaturing SDS-PAGE loading buffer. The 6xHis-PfDXR was used as positive control (lane C). Total protein lysates were loaded in equal volume per lane. Solubility profile **(B)** of $(His)_6$-PFA0660w after 3 hour post induction. Lane 0 is the pre-induction sample and lane 3 is the 3 hours post induction samples of total protein lysate obtained as in **(A)**. For solubility study, the 3 hour post-induction cell pellet (from 250 ml culture) was resuspended in lysis buffer and centrifuged to obtain soluble (supernatant) and insoluble (pellet) fractions. The insoluble fraction was resuspended in equivalent volume of lysis buffer. 5x denaturing SDS-PAGE loading buffer was added to the fractions for loading. Lanes S1 and S2 as well as P1 and P2 are duplicate loading from the same sample for soluble and insoluble fractions respectively. Samples were loaded in equal volume. Western analysis (lower panels) using mouse anti-His monoclonal confirmed the presence of the proteins and the pellets consisted of mainly of $(His)_6$-PFA0660w. The blue arrows indicate the position of $(His)_6$-PFA0660w (41.3 kDa). M is the protein molecular mass marker (kDa).

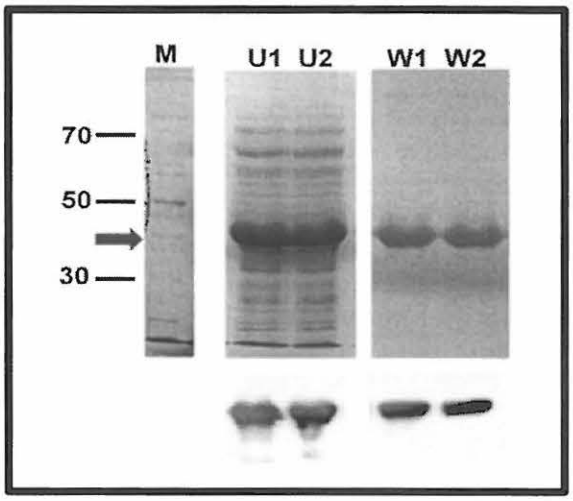

Figure 2.3: $(His)_6$-PFA0660w constitutes the bulk of the insoluble pellet
The assessment of the nature of the insoluble pellet using 12 % SDS-PAGE (upper panel) and western analysis (lower panel). Lane U1 and U2 are duplicate loading of the same sample of unwashed insoluble pellet fractions while lane W1 and W2 are duplicate loading of the same sample of washed insoluble pellet fractions, both of which are solubilised in 8 M urea buffer prior to loading. Higher percentage of the protein can be seen in the insoluble pellet fractions, indicating a high level of insolubility. The percentage of washed pellet relative to the unwashed pellet by weight and by concentration (Bradford assay) was 94.45 ± 1.03 %w/w and 96.05 ± 2.05 %w/w (expressed as mean ± standard error of mean). Western analysis (lower panels) using mouse anti-His monoclonal confirm the presence of the proteins and that the pellets consisted of mainly of $(His)_6$-PFA0660w. The blue arrows indicate the position of $(His)_6$-PFA0660w (41.3 kDa). M is the protein molecular mass (kDa).

2.3.3. PFA0660w constitutes the bulk of the insoluble pellet

A high level of expression of recombinant proteins in *E. coli* usually results in the deposition of insoluble pellets called inclusion bodies (Carrió and Villaverde, 2002; García-Fruitós *et al.*, 2012). Inclusion bodies have been described as amorphous aggregates, having amyloid-like properties such as binding to amyloid specific dyes (Thioflavin-T and Congo-Red) (Fink, 1998; Kopito, 2000; Wang *et al.*, 2008). Other characteristics include the presence of native-like structure, presence of biologically active proteins, resistance to proteases and consisting mostly of a single species of the recombinantly expressed protein (Tokatlidis *et al.*, 1991; Carrió and Villaverde, 2001; Peternel and Komel, 2010; García-Fruitós *et al.*, 2012). Following the removal of possible contaminants, the high level of homogeneity of the aggregated pellet is an essential distinguishing feature of the inclusion bodies (Singh and Panda, 2005; Upadhyay *et al.*, 2012). An attempt was made to perform a preliminary assessment of the nature of the insoluble pellet by determining the amount of $(His)_6$-PFA0660w that constitutes the pellet fraction. Pellet washes were done in PWB containing small amount of detergent to remove contaminating cellular fragment and co-aggregated proteins and in distilled water to remove contaminating salts and detergent. Following pellet washes, $(His)_6$-PFA0660w was virtually the only protein present in the washed samples (Lane W) as seen on the SDS-PAGE gel compared to many bands produced by the unwashed pellet (Lane U). The western analysis of the unwashed and washed pellet fractions (Lanes U and W of Figure 2.3) as well as the percentage of washed pellet relative to the unwashed pellet by weight and by Bradford assay (94.45 ± 1.03% w/w and 96.05 ± 2.05% w/w; expressed as mean ± standard error of mean) confirmed that $(His)_6$-PFA0660w constitutes the largest portion of the insoluble pellet, suggesting a high level of homogeneity, consistent with the nature of inclusion bodies (Kopito, 2000; Markossian and Kurganov, 2004; García-Fruitós *et al.*, 2012). Therefore, the result indicates that the insoluble pellet shares essential characteristics of inclusion bodies, suggesting that $(His)_6$-PFA0660w may have been deposited as inclusion bodies.

2.3.3. Purification

Several approaches were used to purify $(His)_6$-PFA0660w with a view to improve yield and purity. These included native or non-denaturing purification while optimizing for soluble expression or complete denaturing purification in urea with native or denaturing washes and elutions. Using *E. coli* M15[pREP4] cells, these approaches produced low yields and attempts at removing the DnaK contamination (e.g. by inclusion of an ATP wash step) were unsuccessful (Figure 2.4). Also, though the use of the *E. coli* BB1994 strain successfully resolved the DnaK contamination, the presence of

an unidentified contaminant at the same size as the DnaK and the low level of expression and yield, makes this system unsuitable for purifying $(His)_6$-PFA0660w (Figure 2.4).

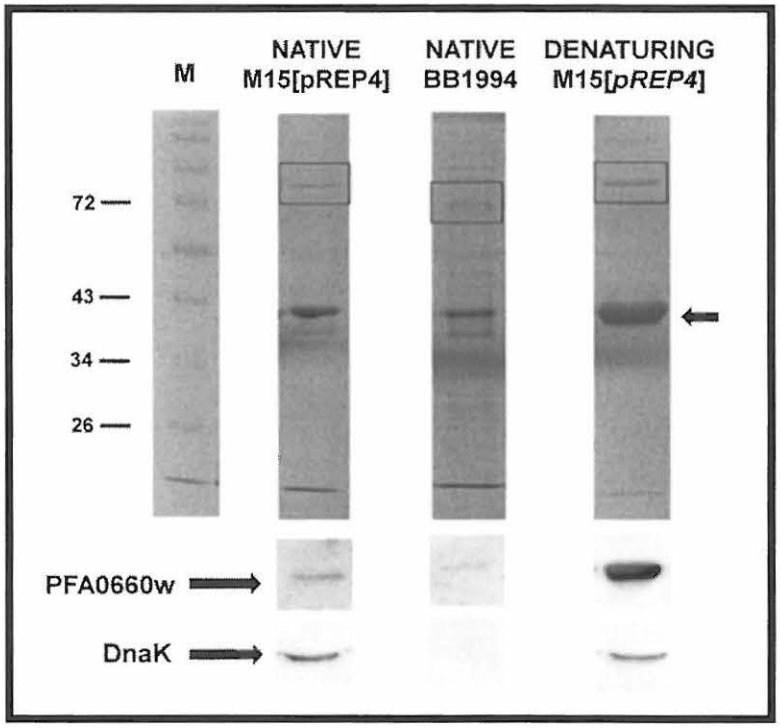

Figure 2.4: Purification of PFA0660w under native and denaturing conditions
The analysis of the elutions from nickel affinity chromatography purification with native and denaturing approaches using 12 % SDS-PAGE (upper panel) and western (middle and lower panels). The volume of the starting culture and elutions were the same and lanes were loaded with equivalent volumes of elution samples. Native and denaturing attempts at purifying $(His)_6$-PFA0660w did not produce a high enough yield of protein. DnaK contamination with *E. coli* M15[pREP4] cells and an unidentified contaminant with *E. coli* BB1994 cells are indicated as red boxes. Western analysis with mouse monoclonal anti-His antibody revealed protein expression in BB1994 and M15[p*REP4*] and mouse monoclonal anti DnaK antibody confirmed the presence of DnaK in M15[pREP4]. M is the protein molecular mass marker in kDa.

Experimental evidence has shown that with well designed experimental protocols consisting of suitable buffers and refolding additives, it is possible to purify functionally active proteins from the insoluble pellet called inclusion bodies (Middelberg, 2002; Bondos and Bicknell, 2003; Swietnicki, 2006; Dechavanne *et al.*, 2011; Churion and Bondos, 2012). The success of such purifications depends in part on the approach to solubilise the protein and it is possible to achieve improved solubility of inclusion body proteins at low denaturant concentrations with pH adjustment (Singh and Panda, 2005). Therefore, analysis of the effects of pH adjustment on the solubility of this protein with and without 2 M urea in buffers at pH ranges from 3 to 12 was conducted. The results showed an increase in solubility with an increase in pH and this was further enhanced in the presence of 2 M urea compared to no urea (Figure 2.5).

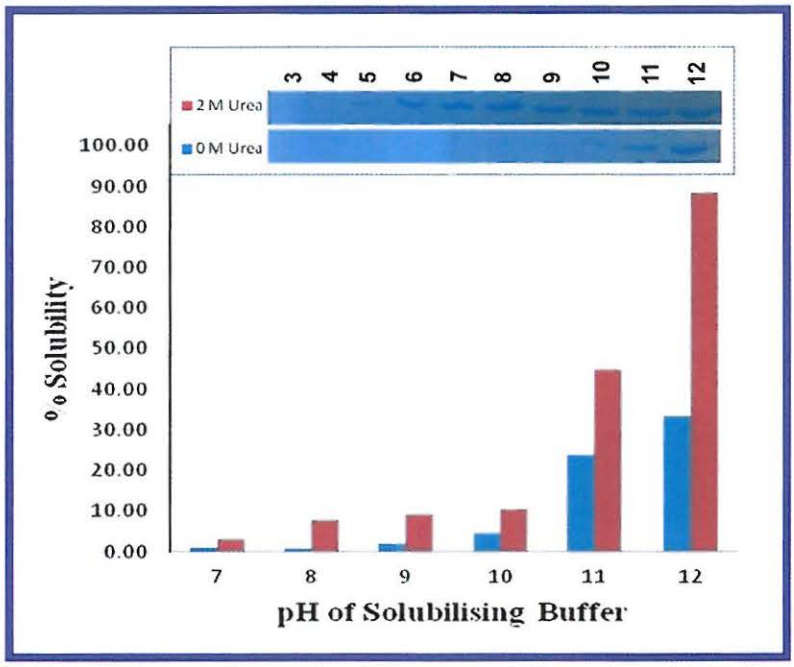

Figure 2.5: Effect of pH on solubility of inclusion bodies
The bar chart showing the effects of pH adjustment on solubility of the inclusion bodies conducted with (red coloured bars) and without (blue coloured bars) 2 M urea. Solubility was enhanced when 2 M urea was combined with pH adjustment and favoured the extreme alkaline pH (12.0). Lane 3 to 12 on the SDS-PAGE (upper panel) represents the pH ranges that were used. The concentration of solubilised protein was determined using Bradford's assay and expressed as percentage of initial mg amount of the protein to be refolded.

Therefore, apart from using high urea concentrations (8 M), a high level of solubilisation can also be achieved using lower denaturant concentrations (2 M) with pH adjustment (pH 12). In this light, four solubilisation buffers were constituted for use in determining an appropriate strategy to enhance solubility and improve renaturation. Using 16 additive combinations that produced promising results from the 96 well screening (section 2.2.5.2 and Table 2.3), the effects of these four solubilisation buffers on subsequent refolding was determined (Table 2.4). Table 2.4 showed that consistent with earlier reports (Fischer *et al.*, 1993), the addition of DTT and EDTA improved renaturation significantly. While solubilisation buffers supplemented with DTT and EDTA, showed that PEG/DTT and PEG/DTT/EDTA additive combinations for refolding provided better renaturation, other additive combinations used for refolding proteins solubilised in 8 M urea buffers also produced relatively high refolding yields, indicating that solubilisation in 8 M urea supplemented with DTT and EDTA would be a better alternative (Table 2.4). Furthermore, since any suitable additive combination must also aid the removal of DnaK and other contaminants, attempts were made to compare purifications using three denaturing approaches. They include a complete denaturing in 8 M urea lysis buffer (NLB in which lysozyme was replaced with 8 M urea) and inclusion bodies pellet denaturation in 2 M urea at pH 12 and in 8 M urea at pH 8.5 supplemented with DTT and EDTA. Though solubilisation was followed by additive enhanced refolding in all the approaches tested, the result (Figure 2.6) revealed a lack of DnaK contamination

when inclusion bodies pellet was denatured in either 2 M urea (pH 12) (Figure 2.6A) or 8 M urea (pH 8.5) (Figure 2.6B). This result suggests that pellet wash and inclusion of DTT and EDTA in inclusion bodies solubilisation buffers may play critical role in the removal of DnaK contamination.

Table 2.4: DTT and EDTA in solubilisation buffers enhanced renaturation

Additive combinations	% Refold following solubilisation in buffers		% Refold following solubilisation in buffers supplemented with 5 mM DTT and 0.1 mM EDTA	
	2 M urea (pH 12)	***8 M urea (pH 8.5)***	***2 M urea (pH 12)***	***8 M urea (pH 8.5)***
DE	29.15	33.73	40.44	47.36
EP	14.43	13.24	14.36	50.69
DP	26.89	36.48	47.88	57.95*
PED	28.01*	39.97*	50.34*	54.91
DES	21.76	34.16	46.50	47.18
EPS	10.29	12.96	12.02	49.10
DPS	17.44	30.45	36.92	49.45
PEDS	17.62	33.73	29.41	44.65
DEG	23.17	38.12	36.48	46.67
EPG	10.68	14.05	11.08	39.35
DPG	22.73	34.16	34.16	43.16
PEDG	25.69	35.60	32.20	47.70
DEGS	26.17	41.39	34.16	52.32
EPGS	10.07	13.75	10.91	46.50
DPGS	19.12	32.62	28.13	43.33
***PEDGS	18.84	29.15	27.14	43.33***
Buffer	9.97	11.51	10.91	35.31**

D = 5 mM Dithiothreitol (DTT), E = 0.1 mM Ethenediaminetetraacetic acid (EDTA), P = 0.1 %w/v Polyethylene glycol (PEG 2000), S = 5 %w/v Sucrose and G = 10 %v/v Glycerol. The additive combinations used were those selected following initial screening as per section 2.2.4.2. Each combination is given in column 1 with each alphabet representing the additive as denoted above. For example, DE stands for 5 mM DTT and 0.1 mM EDTA in the buffer which is made up of 50 mM Tris-Cl, pH 8.5 and 300 mM NaCl. Prior to refolding, solubilisation of clean inclusion bodies was achieved by either 2 M urea buffer at pH 12 or 8 M urea buffer at pH 8.5, with and without DTT and EDTA. Protein concentration was determined using Bradford methods (Fermentas ready-to-use Bradford reagent) and expressed as percentage of initial protein concentration in the refolding buffer or as percentage of initial mg amount of the protein to be refolded.

*Represents refolding effects that are regarded as outstanding per group.

**DTT and EDTA improved renaturation even when refolding in buffer without additives.

***Though, higher percentage could be achieved with other additives combination, other positive roles of these additives (e.g. ensure stability in storage and DnaK removal) informed the inclusion of all in the refolding buffer (column highlighted in gray) for subsequent uses.

Therefore, for subsequent purification of $(His)_6$-PFA0660w from inclusion bodies, solubilisation in 8 M urea buffer supplemented with DTT and EDTA and refolding in DTT/EDTA/glycerol/PEG /sucrose additive-containing buffers were used. Furthermore, refolding by dilution was followed by on-column refolding to enhance the efficiency of the refolding activity and by extension improve the quality of the purification.

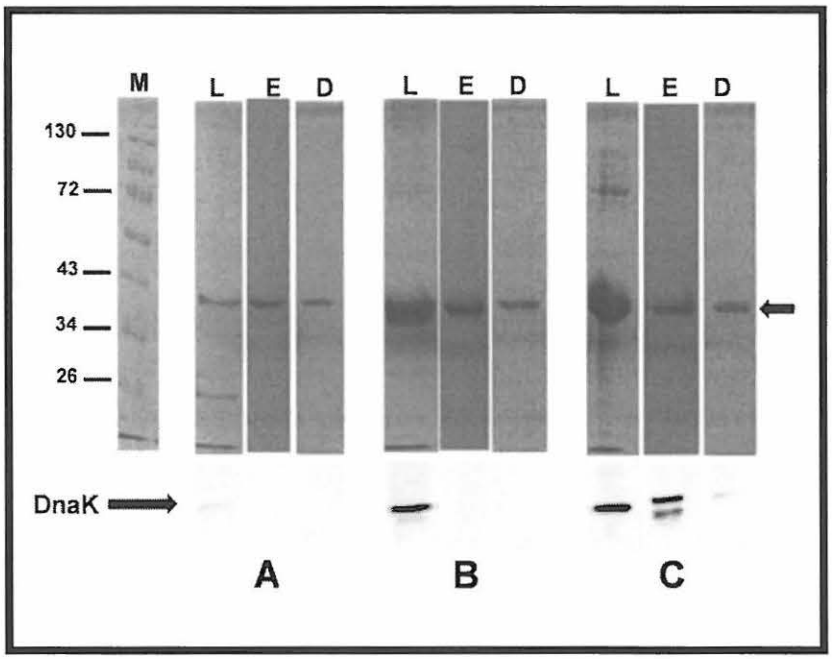

Figure 2.6: Removal of DnaK contamination using additive-enhanced buffers
The 12 % SDS-PAGE (upper panel) and western analyses (lower panel) of **(A)** the inclusion bodies purified from lysates solubilised with 2 M Urea (pH 12) and **(B)** the inclusion bodies purified from lysates solubilised with 8 M Urea (pH 8.5) and **(C)** purification using 8M Urea denaturing purification (pH 8.5). Solubilisation buffers in **(A)** and **(B)** were supplemented with DTT (5 mM) and EDTA (0.1 mM). Lanes L, E and D are lysate, elution and dialysis products respectively. All were refolded using additive-enhanced refolding buffers. $(His)_6$-PFA0660w (41.3 kDa) is indicated in blue arrow and M is the protein molecular mass marker in kDa.

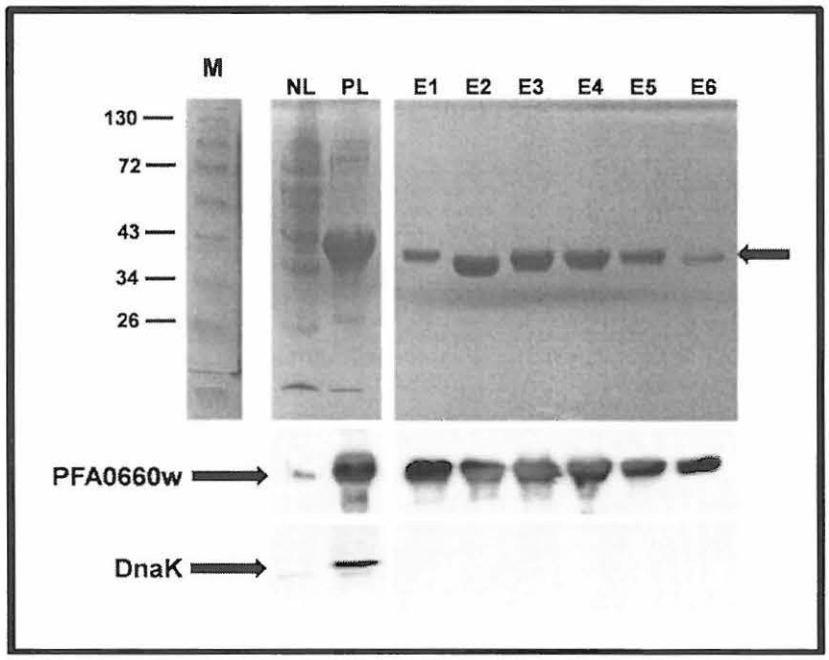

Figure 2.7: Purification of $(His)_6$-PFA0660w from inclusion bodies
SDS-PAGE (upper panel) and western analyses (lower panel) of recombinant $(His)_6$-PFA0660w purification from inclusion bodies using nickel affinity chromatography. NL is the supernatant obtained from whole cell lysis (by lysozyme lysis, freezed thawing and sonication of the harvested *E. coli* cells) and PL is the supernatant obtained from solubilised inclusion pellets (by solubility in 8 M urea solubilising buffer). E1 to E6 are elution fraction following purification of inclusion bodies supernatant (PL). Western analysis with mouse monoclonal anti-His (1 in 5000) and mouse monoclonal anti-DnaK antibodies (1 in 5000) confirm the presence of $(His)_6$-PFA0660w and lack of DnaK in eluted samples. The blue arrow indicates $(His)_6$-PFA0660w on the SDS-PAGE gel. M is the protein molecular mass marker in kDa.

A schematic representation of the inclusion bodies purification approach is presented in *Appendix B.5.* The results of the final purification are shown in Figure 2.7. Due to the high level of induction, solubilisation of inclusion bodies obtained from 1 L of starting culture usually produce an average of 212.04 ± 25.76 mg/L total protein (mean ± standard error of mean). Using 5 ml HisTrap column, the average elution yield was 30.04 ± 1.26 mg/L in 15 ml of eluted proteins, which further reduced to 17.18 ± 0.82 mg/L of protein after dialysis. Thus, an average of 57% refolding yield (calculated as dialyzed protein as percentage of eluted protein) was obtained with this approach.

2.3.4 Secondary structure and size exclusion analysis

The effectiveness of the refolding was assessed through the secondary structure and size exclusion chromatography of the purified $(His)_6$-PFA0660w. Secondary structure was determined using FTIR. The overlay of the spectra of native (black) and boiled (red) samples of $(His)_6$-PFA0660w with blank buffer (green) is given in Figure 2.8A while Figure 2.8B is an overlay of native and boiled spectra after normalisation with blank buffer. Boiling of the sample is expected to destroy both the secondary and tertiary structures and this was used as negative control while the buffer blank provides the baseline for data adjustment prior to subsequent analysis. Figure 2.8C represents the spectra range 900 – 1750 cm^{-1} of Figure 2.8B showing amide I band (1603.5 - 1695.5 cm^{-1}; peak at 1539.5 cm^{-1}), amide II band (1507.5 - 1596.5 cm^{-1}; peak at 1655.5 cm^{-1}), and an unidentified band (1110.5 - 971.5 cm^{-1}; peak at 1047.5 cm^{-1}). A major problem associated with measuring protein absorbance in aqueous solutions is the overlapping strong water absorption band with the protein vibration band (Arrondo *et al.*, 1993). The results of this study showed that the use of thin film, relatively high protein concentration (10 μM) and the subtraction of buffer spectra from that of the samples helped in minimizing such effects. The spectral overlay (Figure 2.8A) however, revealed that measurements taken in aqueous buffer can only be meaningful between 3000 and 1000 cm-1 as the solvent absorbance in other regions is too strong to allow for reasonable subtraction (Figure 2.8B).

Furthermore, while amide I and II were destroyed by boiling, the unidentified band was not. A comprehensive review of the assignment of infrared absorption band for amino acid side chains has been presented (Barth, 2000). Adapted from this review, Table 2.5 presents amino acids having some of their band assignment falling within the range of the unidentified band (1110.5 - 971.5 cm^{-1}). The table revealed that of the four amino acids identified, histidine, serine and tryptophan, are reported to produce strong band intensity within this range. Also, the amino acid analysis of $(His)_6$-

PFA0660w (*Appendix C.2*) showed 4.56% histidine, 2.41% proline, 6.17% serine and 0.86% tryptophan by weight. Therefore, since the boiled sample maintains the same primary structure (amino acid composition) found in the native sample, it is possible that the unidentified band may be a reflection of the stability of the protein primary structure and in the case of $(His)_6$-PFA0660w, the primary contributors to the band intensity of this region are histidine, proline, serine and tryptophan.

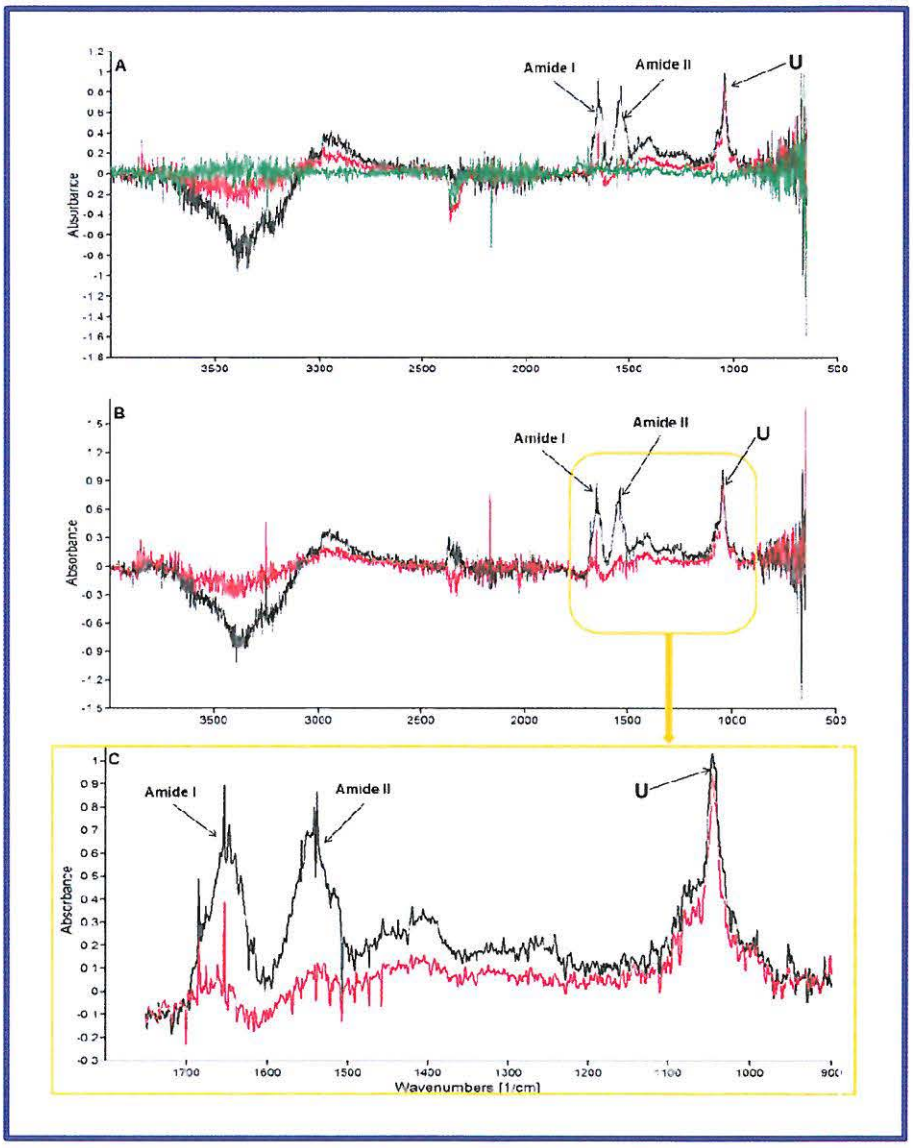

Figure 2.8: FTIR spectra of $(His)_6$-PFA0660w
The FTIR spectra for the assessment of the secondary structure formation following refolding of $(His)_6$-PFA0660w. (A) Spectra overlay of the native (black) and boiled (red) $(His)_6$-PFA0660w samples and the buffer blank (green). (B) Spectra overlay of the native (black) and boiled (red) $(His)_6$-PFA0660w samples following subtraction of the buffer blank. (C) Selected peaks from (B) showing amide I and II with peaks at 1539.5 cm^{-1} and 1655.5 cm^{-1} respectively and an unidentified peak (U, 1047.5 cm^{-1}). Boiled sample serves as control and boiling successfully destroyed amide I and II bands. The analysis was performed using Spekwin32 software for optical spectroscopy (version 1.71.5).

Table 2.5: Infrared absorption band for selected amino acid in the spectra range of 900 - 1110 cm-[1]

Amino acids	Infrared absorption spectra band		
	Assignment	*Vibration*	*in Protein*
Histidine[1]	1104s, 1090s, 1106s and 1094s	ν(CN), δ(CH)	1094–1114
Tryptophan[2]	1092vs	δ(CH), ν(NC)	
	1064s	ν(NC), δ(CH), ν(CC)	
	1012–1016 (1010s)	ν(CC), δ(CH)	
	970sh, 930w	$\nu(CC^b)$, $\delta(CH^b)$	
Serine[3]	1030s	$\nu(C\text{-}O)$, $\gamma(NH^{3+})$	1023
	983	$\nu(CO)$ or $\nu(CC)$, $\gamma a(NH^{3+})$	
Proline[4]	1083m	$\gamma a(CH_2)$	
	1051w, 1033m	$\gamma b(CH_2)$	
	979m, 945m, 911m	ν(CN), ν(CC)	

The table was adapted from Andreas Barth 2000 with the original articles given as [1](Noguchi *et al.* 1999), [2](Lautie' *et al.* 1980; Takeuchi and Harada, 1986), [3](Madec *et al.* 1978; Susi *et al.* 1983) and [4](Herlinger and Long, 1970; Rothschild *et al.*, 1989; Caswell and Spiro (1987). The band assignments for Histidine are for His, N^{1-}, N^{3-}protonated HisH and $HisH^{2+}$ respectively. The spectra bands of the amino acid in protein are given where available within the range of spectra region under consideration. ν: stretching vibration, δ: in plane bending vibration, γa: rocking vibration and γb: wagging vibration while b indicates vibration of the benzene moieties. The intensity of the vibration is described as very strong (vs), strong (s), shoulder (sh), medium (m) or weak (w).

The information on the protein secondary structure is contained in the amide bands that arise from the vibration of the peptide groups (Haris and Severcan, 1999; Kong and Yu, 2007). The vibrational frequency of the amide bands is generated by changes in the hydrogen bonding that is involved in the peptide linkages. The C=O stretching vibration of the peptide group principally gives rise to amide I band, while the N–H bending vibration coupled with some additional vibration from C–N stretching, gives rise to amide II band (Haris and Severcan, 1999). The bands mostly used for protein structural studies are amide I (1600 – 1700 cm^{-1}), amide II (1510 – 1580 cm^{-1}) and amide III (1200 – 1400 cm^{-1}). Other bands usually associated with proteins are amide V (610 – 710 cm^{-1}), amide A (~3300 cm^{-1}) and amide B (~3100 cm^{-1}) (Tamm and Tatulian, 1997). All amide frequencies are conformation-sensitive, however, amides I and II are two important components that provide information about the degree of folding of the proteins of which the most widely used vibrational mode for the determination of protein conformations is amide I (Haris and Severcan, 1999; Tamm and Tatulian, 1997). Therefore, the individual components of amide I band of protein in the spectral range 1600 – 1700 cm^{-1}, which consists of overlapping bands representing structural elements such as α–helices, β–sheets, turns and unordered structures were resolved by Fourier deconvolution procedure (Kauppinen *et al.*, 1981; Mantsch *et al.*, 1988; Czarnecki and Ozaki, 1996) thereby enhancing the separation of overlapping components within the band region (Figure 2.9) and the peaks were fitted with the Gaussian curve.

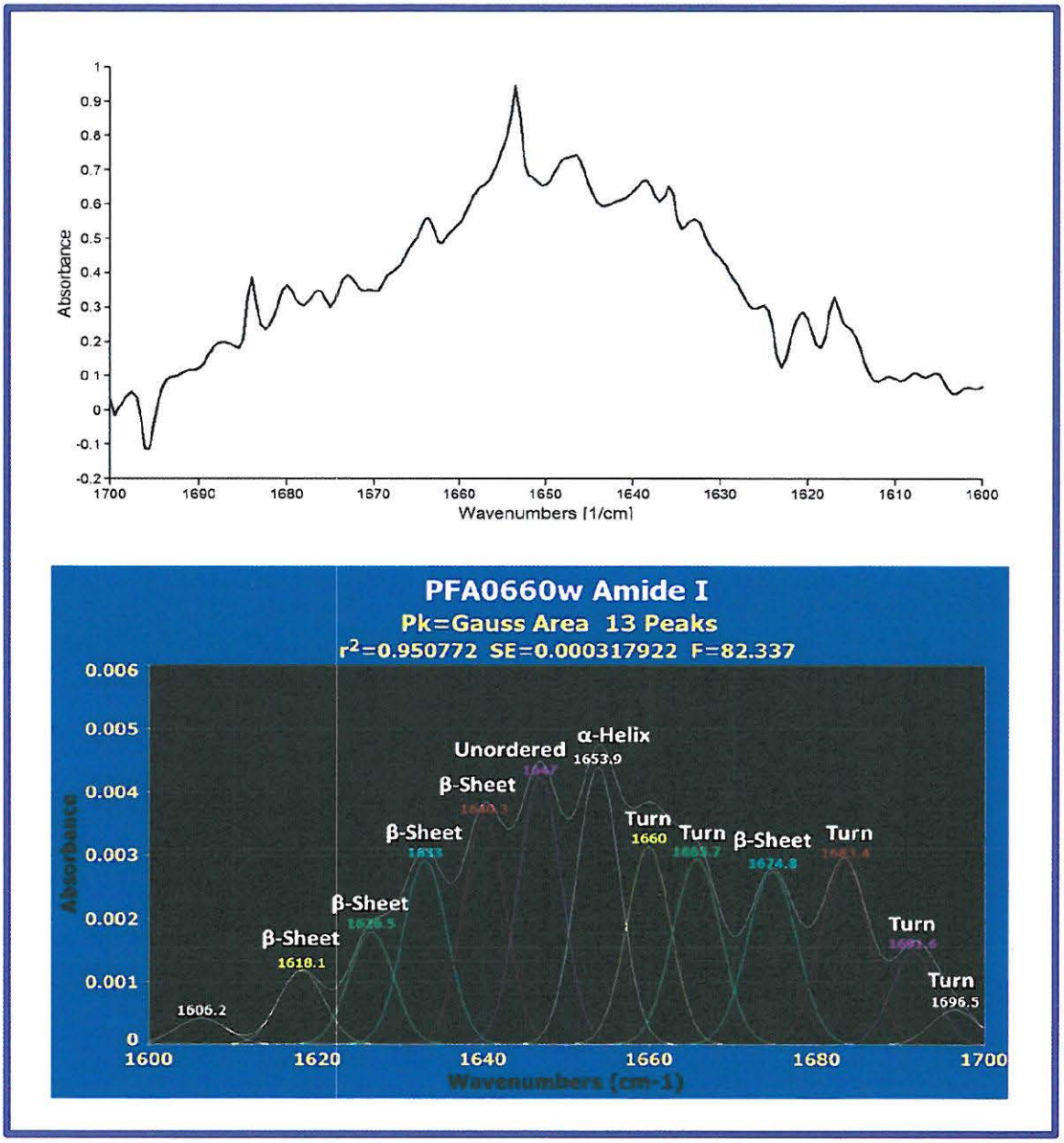

Figure 2.9: Secondary structure analysis of $(His)_6$-PFA0660w

Upper: The spectra of the amide I region (1600 - 1700 cm^{-1}) of normalized native $(His)_6$-PFA0660w samples. **Lower:** Secondary structure analysis using Peak fit software (version 4.12). The infrared spectra were deconvoluted and the peaks fitted with the Gaussian curve. Gaussian curves are shown as symmetrical peaks underneath the deconvolved IR spectra. The assigned secondary structures (Arrondo and Goñi, 1999; Byler and Susi, 1986; Kong and Yu, 2007) are shown at the top of each peak. Relative contents of the secondary structure calculated as the proportion of the peaks areas to the total area under the curve are 38.17% β-Sheets, 38.82% Turns, 13.03% α-Helix, 12.57% Unordered and 1.41% un-assigned.

The resolved bands (Figure 2.9) were used to identify various structures and detect conformational changes present in the protein by monitoring alterations in the frequency and intensity of these bands (Arrondo and Goñi, 1999; Arrondo *et al.*, 1993; Haris and Severcan, 1999). The secondary structure analysis revealed a high content of β-sheets (38.17%) and turns (38.82%), when compared to α-helices (13.03%) and others (9.98%). It is made up of anti-parallel β-sheets 1633 (1625 – 1640 cm^{-1}) and 1674.8 (1666 – 1684 cm^{-1}) with strong band intensity; parallel β-sheets 1618.1 (1610 –

1627 cm^{-1}), 1626.5 (1618 – 1636 cm^{-1}) and 1640.3 (1631 – 1649 cm^{-1}) which runs anti-parallel to turns 1660 (1652 – 1669 cm^{-1}), 1665.7 (1657 – 1675 cm^{-1}) and 1683.4 (1675 – 1693 cm^{-1}) and possessing weak, medium and strong band intensity respectively; unordered band 1647 (1638 – 1657 cm^{-1}) with very strong band intensity and running anti-parallel with Turn 1691.6 (1685 – 1700 cm^{-1}) having weak band intensity; and the α-Helix 1635.9 (1645 – 1663 cm^{-1}) with very strong band intensity.

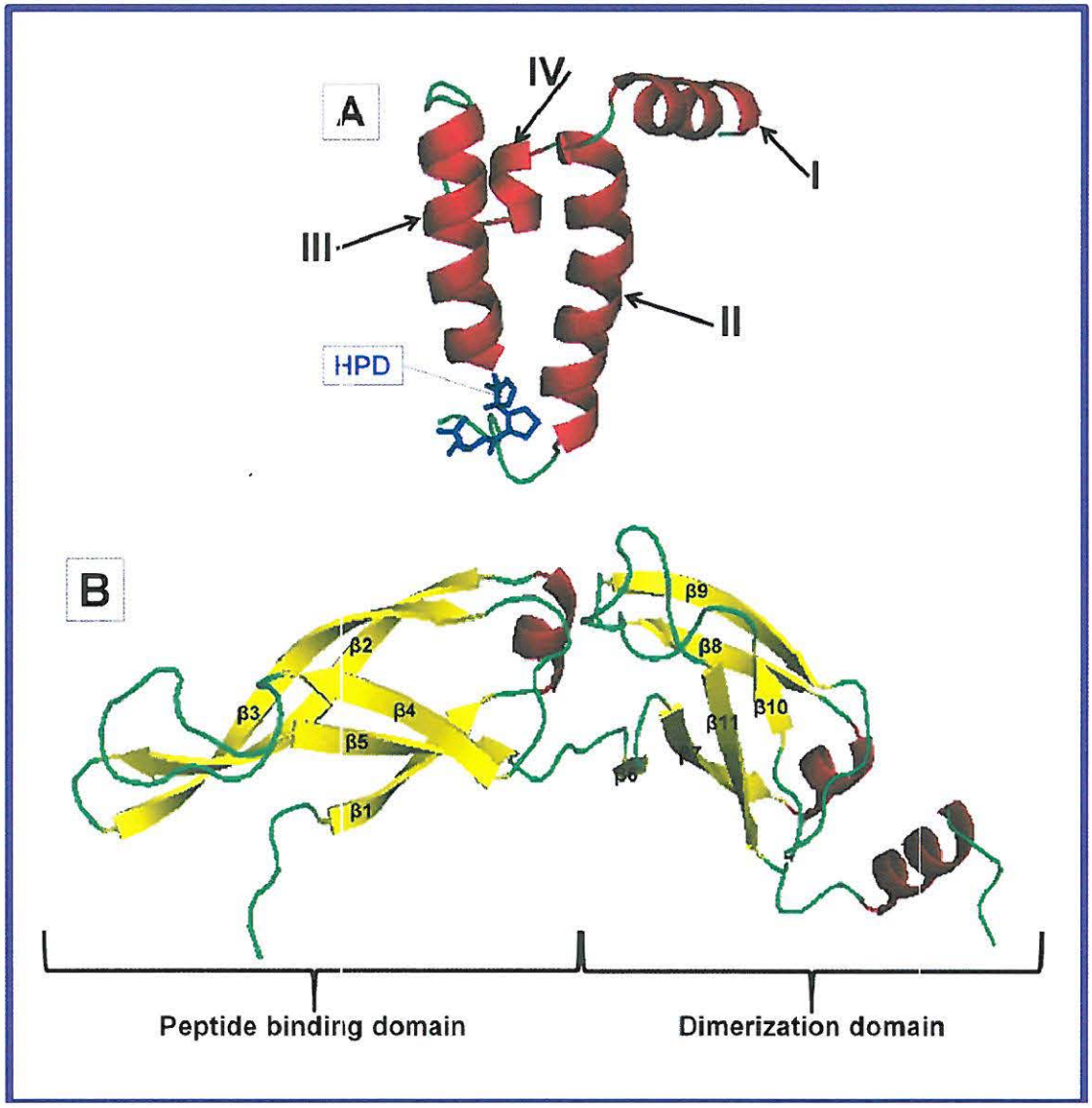

Figure 2.10: Ribbon representation of J-domain and C-terminal domain of PFA0660w
(A) The J-domain of PFA0660w consists of helices I - IV (red) joined together by loops (green) and the HPD motif (blue) located between helix II and III. (B) The anti-parallel β-Sheets of C-terminal domains (peptide binding domain and dimerisation domain) with repeated β-Sheet – Turns (Loop) - α-Helix (coloured as yellow-green-red) configuration at the beginning, centre and end. Models were generated from the solution structure of the J-domain from human DnaJ subfamily B member 12 (PDB # 2ctp) and the crystal structure of the dimerisation domain of Hsp40 from *Cryptosporidium parvum* (PDB # 2q2g) as template for (A) and (B) respectively using Swiss-Model server (Schwede *et al.*, 2003) (*Appendix B.6*). Pymol software (open source 0.99rc6) was used to render the coordinates of the predicted structures into ribbon images.

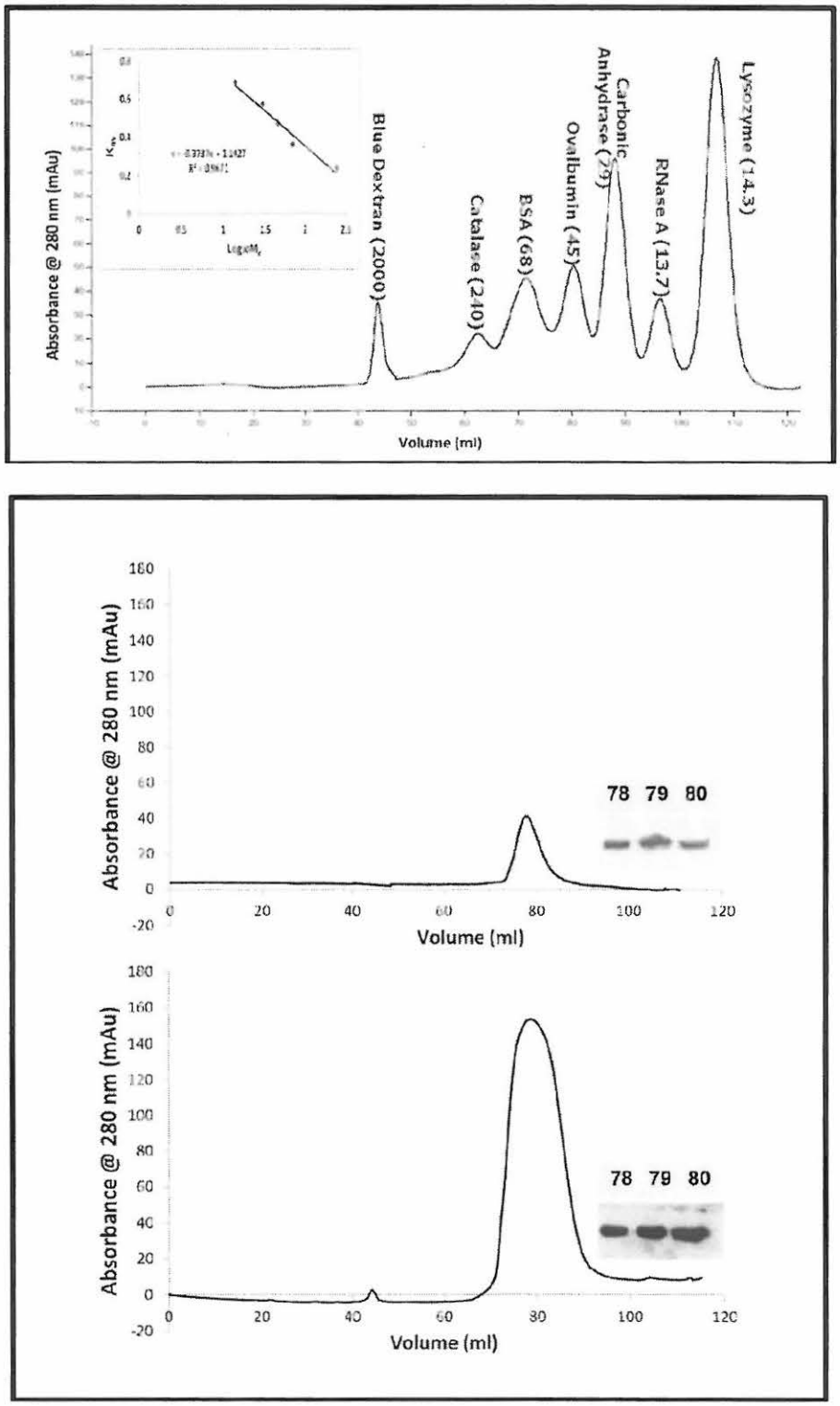

Figure 2.11: $(His)_6$-PFA0660w exists as a monomer in solution

Upper: FPLC calibration curves. Molecular masses in kDa are given in parenthesis and Blue dextran was used to determine the void volume. The elution volumes for standards used in the generation of the calibration curve were determined by peak integration and given as follows: 43.79 ml for blue dextran, 62.19 ml for catalase, 71.35 ml for BSA, 80.30 ml for ovalbumin, 87.99 ml for carbonic anhydrase and 96.25 for RNase A. ***Lower***: FPLC analysis of $(His)_6$-PFA0660w at two different concentrations of the proteins (0.105 mg/ml and 0.535 mg/ml) with an injection volume of 2 ml. At both concentrations, the protein eluted as a single peak at 78.55 ml, indicating a monomeric form in solution. Western analysis with mouse monoclonal anti-His antibody of elution volumes 78, 79 and 80 ml are inserted.

The empirical correlations between amide I frequencies and the secondary structures of proteins with solved X-ray crystallography structures had been proposed by several workers and these has been excellently reviewed (Byler and Susi, 1986; Arrondo *et al.*, 1993; Goormaghtigh *et al.*, 1994; Jackson and Mantsch, 1995). To date, the structure of PFA0660w or any of its domains have not been solved experimentally. Therefore, for the purpose of correlating the FTIR analysis with an expected structure, an attempt was made to perform a comparative protein modeling using Swiss-Model automated server (Schwede, 2003; Bordoli *et al.*, 2009) with a view to predicting the structure of the J-domain and C-terminal domain (peptide binding and dimerisation domains) of PFA0660w. No significant template matches were found for the full length and the GF region of the protein. Figure 2.10 shows the ribbon representation of the predicted structures. The C-terminal domains revealed a repeated β-Sheet – Turns (Loop) - α-Helix configuration at the beginning, centre and end, interspersed with anti-parallel β-sheets (β1/β7 and β2/β8) and parallel β-sheets (β3/β9, β4/β10 and β5/β11). The J-domain is highly conserved with predominant helical structure. For the empirical correlation, the secondary structure analysis was done using an online server called ***2Struc: The Secondary Structure Server*** (Klose *et al.*, 2010). Using this server, DSSP analysis of the C-terminal model of PFA0660w revealed a high content of β-sheets (44.3%) and low α-helices (12.0%). Others (turns, unordered, unassigned etc) were given as 43.7%. This result showed a high correlation between the model and the FTIR secondary structure analysis and further confirmed the success of the refolding activity.

In addition, size exclusion chromatographic analysis of the protein revealed a single peak for $(His)_6$-PFA0660w at both lower and higher concentrations (0.105 mg/ml and 0.535 mg/ml) with an injection volume of 2 ml. The $(His)_6$-PFA0660w eluted at 78.55 ml, close to ovalbumin (45 kDa) which eluted at 80.30 ml (Figure 2.11). Western analysis of the eluted fractions confirmed that the observed peak was $(His)_6$-PFA0660w. Using the calibration curve, PFA0660w was found to have a molecular mass of ~54 kDa. This was somewhat higher than the predicted molecular mass of a monomer (~41 kDa; from its protein sequence, and as observed by SDS-PAGE) but considerably lower than the predicted molecular mass of a dimer (~82 kDa). Therefore, this result suggests that PFA0660w is a monomer in solution; however, the shape and behaviour of the protein in solution under the chromatographic conditions used may have resulted in the observed higher apparent molecular mass.

2.4 Discussion

The purification of PFA0660w, a type II *P. falciparum* Hsp40 co-chaperone, is an essential step toward its functional characterisation. Recombinant $(His)_6$-PFA0660w was successfully expressed in *E. coli* M15[pREP4] cells to high density. However, the expressed protein was insoluble and constituted the largest percentage of the pellet, an important characteristic that is consistent with the nature of inclusion bodies. In addition to the lack of ability in bacteria to effectively perform post translational modification such as glycosylation and correct disulphide bond formation (Casadaban *et al.*, 1983; Shatzman and Rosenberg, 1987), another major factor that could have favoured the formation of inclusion bodies was a high level of protein expression in M15[pREP4] (Farabaugh, 1978; The QIAexpressionist™, 2003). It has been reported that protein expression at high concentrations (200 – 300 mg/ml) in the cytoplasm of *E. coli* may lead to macromolecular crowding of proteins which creates a highly unfavourable protein-folding environment, leading to the formation of insoluble pellets (Van Den Berg *et al.*, 1999). Also, the amino acid composition of $(His)_6$-PFA0660w may favour the formation of inclusion bodies. Consistent with the report that protein solubility favoured Asp, Glu, and Ser rather than the other hydrophilic amino acids (Trevino *et al.*, 2007), analysis of the amino acid composition of $(His)_6$-PFA0660w (*Appendix C.2*) appears to favour insolubility. This study has shown that the solubility of $(His)_6$-PFA0660w increases with increase in pH, indicating that pH may constitute an important determinant of its solubility.

Meanwhile, several reports have shown that using suitably optimised solubilisation and refolding buffers, functionally active proteins can be retrieved from the inclusion bodies (Middelberg, 2002; Bondos and Bicknell, 2003; Swietnicki, 2006; Dechavanne *et al.*, 2011). Purification from inclusion bodies requires optimisation of solubilisation and refolding conditions. In this study, solubilisation in 8 M urea buffer supplemented with DTT and EDTA was found to be optimal for subsequent refolding. Also refolding in buffers supplemented with glycerol, sucrose, PEG, DTT and EDTA improved yield and encouraged secondary structure formation. The additives have been shown to promote the correct disulphide bond formation, encourage the adoption of appropriate three-dimensional shape, reduce aggregation, promote solubility, aid refolding and remove contaminating DnaK (Cappel and Gilbert, 1988; Meng *et al.*, 2001; Bondos and Bicknell, 2003; Vallejo and Rinas, 2004; Guo *et al.*, 2007; Wang *et al.*, 2009b; Dechavanne *et al.*, 2011). Interestingly, experimental evidence revealed that imidazole, a common component of buffers in the purification of His-tagged protein, may serve as a catalyst in the *in vitro* protein refolding and suppress aggregation (Shi *et al.*, 2007). The result indicates that total unfolding or denaturation of the inclusion bodies may be essential for the optimum performance of DTT and EDTA in enhancing renaturation and the removal of DnaK contamination.

Recombinant $(His)_6$-PFA0660w was purified from inclusion bodies using nickel affinity chromatography. Other methods, including those described in *Appendix D15 and D16* or their modifications, have been used to successfully purify recombinant proteins (Matambo *et al.*, 2004; Nicoll *et al.*, 2007; Chiang *et al.*, 2009; Ramachandran, 2009; Louw *et al.*, 2010; Botha *et al.*, 2011; Misra and Stephens *et al.*, 2011). Enhanced levels of purity (made possible by the inclusion of a pellet wash step), drastic reduction in contaminating co-expressed proteins (Figure 2.3) leading to reduction in competitive binding to the purification matrix or binding to target proteins, successful removal of DnaK without additional steps and inclusion of refolding processes as part of the purification steps, are some of the advantages that make purification from inclusion bodies a better approach for proteins that are deposited as insoluble pellet. Though soluble proteins have been purified to high yield (usually > 10 mg/L) using a native approach, in this study (*Appendix B.7*) and by other investigators (Matambo *et al.*, 2004; Misra and Ramachandran, 2009; Cockburn *et al.*, 2011), such a high yield has not been successful when purifying insoluble proteins (Louw *et al.*, 2010), making the present approach (with improved yield) a better alternative. However, compared to other methods, it is more rigorous and could take more time than would be required for a denaturing approach. Also, the protocol has to be optimised for individual proteins and if insolubility of the protein is a factor of the amino acid composition, the high yield can only be maintained at dilute concentrations, making functional studies at higher concentrations difficult. Therefore, optimisation of coding sequence to produce soluble proteins that can be purified natively could be a better alternative to inclusion bodies purification. In this respect, harmonisation of the optimised coding sequence of PFA0660w may be considered. However codon optimisation and harmonisation approaches do not always guarantee soluble plasmodial proteins (Birkholtz *et al.*, 2008).

The formation of the secondary structure (as shown by FTIR analysis) and the existence of $(His)_6$-PFA0660w as a monomer in solution (as revealed by FPLC analysis), confirmed the success of the purification approach. The slightly higher molecular mass of $(His)_6$-PFA0660w calculated from the FPLC calibration curve (~54 kDa) as compared to the expected molecular mass of ~41 kDa for a monomer as observed by SDS-PAGE and predicted from its protein sequence, may be due to the fact that the size exclusion chromatography makes use of globular spherical-like proteins as molecular mass standards. Thus, if $(His)_6$-PFA0660w is not globular in shape, but rather in an extended conformation, it may have an apparent molecular mass that is higher when analysed using an approach that applies globular proteins as standards. However, the existence of a monomer was contrary to the in silico model of the C-terminal domain (Figure 2.10) which predicts dimer formation. With eight cysteine residues (*Appendix C.2*) the involvement of DTT, albeit at low

concentrations, at different stages of inclusion bodies protein purification may explain the lack of dimer formation. Also, as shown in Table 2.6, using structural determination approaches (MAD, X-ray crystallography or small angle X-ray scattering), analytical ultracentrifugation and size exclusion chromatography for gel filtration analysis, many Hsp40 proteins that have been characterized were shown to exist as homodimers (Sha *et al.*, 2000; Toutain *et al.*, 2003; Shi *et al.*, 2005; Wu *et al.*, 2005).

Table 2.6: Determination of dimer formation in selected Hsp40 proteins

Organism	Protein	Approach(es) used in determining dimer formation
E. coli	DnaJ	Structural determination by small angle x-ray scattering and size-exclusion chromatography
Yeast	Sis1	Structural determination by Multiwavelength anomalous diffraction (MAD) method and size-exclusion chromatography
	Ydj1	Structural determination by MAD method
Human	Hdj1	Structural determination by x-ray crystallography
	Hdj2	Structural determination by small angle x-ray scattering and analytical ultracentrifugation

Though the approach to secondary structural determination in these reports was different from the one used in this study (FTIR), the empirical correlations between these approaches has been proposed (Byler and Susi, 1986; Arrondo *et al.*, 1993; Goormaghtigh *et al.*, 1994; Jackson and Mantsch, 1995). Also the use of gel filtration was consistent and having been shown that dimerisation is very critical to the co-chaperone function of Hsp40 proteins (Shi *et al.*, 2005; Wu *et al.*, 2005; Li *et al.*, 2006), it is unclear what would be the effect of this monomeric state of $(His)_6$-PFA0660w on its role as a molecular chaperone. Since dimerisation can occur upon ligand binding (Schlessinger, 2002; Klein *et al.*, 2004), it may be suggested that PFA0660w is functionally different from other Hsp40 that form dimers and that for PFA0660w, dimer formation may not be needed to maintain the stability of the protein in solution, but rather it is a functional transformation needed to ensure proper co-chaperone function, that is, it is formed in response to functional necessities. However, to further explore this assumption, it is important to confirm the structural determination using more refined methods such as those employed in other related studies. Essentially, many structural studies have employed X-ray crystallography and nuclear magnetic resonance (NMR) spectroscopy. X-ray crystallography uses X-ray diffraction patterns arising from striking of pure protein crystal with a beam of X-ray (Cullity and Stock, 2001; Accordingly and Boxes, 2006; Thibault and Elser, 2010) to produce 2-dimensional (2D) map of electron density that can be transformed using Fourier Transform (James, 2002; Stein and Shakarchi, 2003) to 3-dimentional (3D) density which can be used to explore the chemical characteristics and thus the determination of their crystal structures with an acceptable resolution (Jelsch *et al.*, 2000). On the

other hand, NMR spectroscopy makes use of the interactions between proteins atomic nuclei and electrons which can be detected as magnetic shifts that are generated between magnetic fields and electromagnetic radiation (Osborne *et al.*, 1997; Model, 1998; Otting, 2010).

Meanwhile, dimer formation has been reported to play a critical role in chaperone activity of Hsp40s due to lack of chaperone functions following the disruption of the dimerisation motifs (Sha *et al.*, 2000; Li *et al.*, 2003, 2006; Wu *et al.*, 2005). The methods used for the determination of dimer formation in selected Hsp40 proteins are presented in Table 2.6. Though different approaches may be used, it appears that structural determination is the commonly used approach to determine dimer formation. Other methods include gel filtration/size exclusion chromatography and analytical ultracentrifugation. The importance of dimer formation to Hsp40 activity has been demonstrated using a number of Hsp40 proteins from different systems including yeast Sis1 and Ydj1, *E. coli* DnaJ and human Hdj1 and Hdj2 (Sha *et al.*, 2000; Li *et al.*, 2003; Shi *et al.*, 2005; Borges *et al.*, 2005; Wu *et al.*, 2005; Hu *et al.*, 2008). In a study on yeast type II Hsp40, Sis1, structural elucidation of the C-terminal fragment (171 – 352) revealed that Sis1 forms homodimer from two monomeric units (Sha *et al.*, 2000). Each monomeric unit consist of domains I and II. Sis1 dimer was able to enhance the refolding of denatured luciferase and stimulate the ATPase activity of Ssa1. However, when the residues that were responsible for dimer formation were deleted (338–352), the monomeric Sis1 (1–337) lost its ability to enhance luciferase refolding but was able to maintain its ability to stimulate the ATPase activity of Hsp70, indicating that the C-terminal is essential for dimer formation and chaperone activity. It appears that the existence of Sis1 as monomer or dimer is a function of its functional activities. Also, the C-terminal fragment of Ydj1, a yeast type I Hsp40 protein, was found to exist as dimer (Wu *et al.*, 2005). The structural elucidation revealed that Ydj1 dimer was different from Sis1 dimer. The modelled structure of the full length revealed the presence of a cleft between the two monomers that forms the dimer. This cleft may have a role to play in the specificity of Ydj1 for peptide substrate (Li *et al.*, 2003). However, each monomeric unit of Ydj1 dimer consist of domains I, II and III and a dimerisation motif as against the two domains in Sis1. It appears that in Sis1 and Ydj1 dimers, the cleft between the two monomers may be responsible for maintaining the substrate in a stabilised unfolded position, thereby preventing aggregation, and ensuring the formation of a stable complex between Sis1 or Ydj1 and the Hsp70 chaperone (SsaI). In addition, human type I Hsp40 proteins, Hdj1 and Hdj2, and *E. coli* DnaJ were reported to form homodimers, possibly by the interaction of the dimerisation domain of the two monomeric units (Borges *et al.*, 2005; Shi *et al.*, 2005; Hu *et al.*, 2008). While the monomeric truncated Hdj2 (DjA1-1–332) lost the ability to bind unfolded luciferase, the monomeric truncated DnaJ (1–330) was able to retain the thiol-disulfide oxidoreductase activity of the full length, but was unable to bind

peptide. These reports further confirm the importance of dimer formation to the chaperone activity of Hsp40 and that the C-terminal residues are essential for the formation of the dimer. Overall, the structural elucidation revealed that inter-domain interaction between monomeric units of the protein may be essential for the formation of dimers (Rüngeling *et al.*, 1999; Toutain *et al.*, 2003; Shi *et al.*, 2005; Wu *et al.*, 2005; Hu *et al.*, 2008). Also, like the C-terminal segments, the G/F-rich regions which are known to specify the functions of Hsp40s (Langer *et al.*, 1992; Sis *et al.*, 1999; Johnson and Craig, 2001; Sondheimer *et al.*, 2001; Lee *et al.*, 2002), has been implicated in the formation of dimers in type I and II Hsp40 proteins in solution (Langer *et al.*, 1992; Borges *et al.*, 2005; Ramos *et al.*, 2008). Furthermore, these reports also showed that though lack of dimer formation did affect chaperone functions, the ability of the proteins to stimulate ATPase activity of Hsp70s and thiol-disulfide oxidoreductase activity were not affected. This further confirmed the link between dimer formation and chaperone activity (maintenance of substrates in an unfolded state). It can therefore be assumed that the independent chaperone ability of $(His)_6$-PFA0660w may indicate that the formation of a dimer may not be essential to its functions. More so, many Hsp40 s do not dimerise and yet still appear to be active and in this study, the lack of dimer formation is consistent with a recent report on a novel type III Hsp40 from *Trypanosoma brucei* that occurred as a compact monomer in solution (Louw *et al.*, 2010).

In conclusion, these analyses showed that the refolding process in the purification of $(His)_6$-PFA0660w from inclusion bodies was effective and successful. High yields of protein, albeit in diluted concentrations, were obtained and both gel filtration and SDS-PAGE analysis of the purified $(His)_6$-PFA0660w revealed a high level of purity, with no DnaK contamination, and can therefore be used for subsequent assays. To our knowledge, this is the first attempt at purifying PFA0660w for functional characterisation and the first attempt at using inclusion bodies for purifying plasmodial co-chaperones to be used for subsequent functional assays.

CHAPTER THREE

BIOCHEMICAL CHARACTERISATION OF PFA0660w

The ability of PFA0660w to functionally interact with chaperones (PfHsp70-1, PfHsp70-x and HsHsp70) was determined using the rhodanese aggregation suppression assay, ATPase assay and surface plasmon resonance spectroscopy (SPR). $(His)_6$-PFA0660w significantly stimulated the ATPase activity of PfHsp70-x, while the ATPase activities of PfHsp70-1 and HsHsp70 were not significantly stimulated, suggesting a specific functional interaction with PfHsp70-x. The 6xHis-tagged PFA0660w as well as each Hsp70 individually produced a dose dependent suppression of rhodanese aggregation. Enhanced aggregation suppression was observed when $(His)_6$-PFA0660w was used together with each Hsp70. The kinetic analyses suggests a comparable effect of $(His)_6$-PFA0660w on the chaperone activities of each Hsp70. The preliminary SPR data revealed a high level of binding of $(His)_6$-PFA0660w to PfHsp70-x when compared to PfHsp70-1 and HsHsp70 and this interaction was enhanced in the presence of ATP, indicating a potential chaperone co-chaperone interaction. This work provides the first biochemical evidence for the possible functional role of $(His)_6$-PFA0660w, especially in association with PfHsp70-x,

3.1 Introduction

Molecular chaperones, like other proteins, are agents of biological functions and in *P. falciparum*, serves to maintain cellular activity on which the development and survival of the parasite depend. Functional and chaperone activities of heat shock proteins have been demonstrated using *in vitro* studies that access the ability to hydrolyse or stimulate the hydrolysis of ATP and suppression of aggregation (Szabo *et al.*, 1994; Fewell *et al.*, 2004; Chang *et al.*, 2008a; Cockburn *et al.*, 2011;) and only recently was the aggregation suppression assay employed in drug screening (Cockburn *et al.*, 2011). Hsp70-substrate binding and release depend on ATP hydrolysis which can be stimulated through the interaction of a partner Hsp40 (Cheetham *et al.*, 1994). Malate dehydrogenase has been employed by several workers to determine the ability of heat shock proteins to suppress heat induced aggregation (Basha *et al.*, 2004; Boshoff *et al.*, 2008; Louw *et al.*, 2010; Cockburn *et al.*, 2011; Sanz-Barrio *et al.*, 2011). Malate dehydrogenases are found in the tissues of both plants and animals and occur as tetramers (Noyes *et al.*, 2011). This method is, however, not suitable for chaperones or co-chaperones that aggregate at elevated temperature normally used for such studies. On the other hand, the rhodanese has been used by many investigators as a model system for the assessment of chaperone-assisted folding of denatured protein (Cyr, 1995; Ramsey *et al.*, 2000; Bhattacharyya and Horowitz, 2001; Allan *et al.*, 2006). Rhodanese is monomeric, folded into two domains with an interdomain interface which is strongly hydrophobic, resulting in strong interactions between domains and consequently, formation of large aggregates that can be monitored spectrophotometrically by light scattering (Bhattacharyya and Horowitz, 2001). The experiment is performed at room temperature which makes it suitable for all proteins. Furthermore, direct proportionality between the amount of aggregated protein and the absorbance has been experimentally validated (Finke *et al.*, 2000) and its applications have been reviewed (Kurganov, 2002), making it possible to kinetically analyse aggregation.

Another widely employed and well established method for measuring molecular interactions is through the use of surface plasmon resonance biosensors. The first attempt at using surface plasmon resonance spectroscopy (SPR) for biosensing experiments was demonstrated in 1983 by Liedberg *et al.*, (Liedberg *et al.*, 1995). SPR biosensor experiments typically involve immobilising or capturing one of the binding partners (ligand) on a surface (biosensor chip) and monitoring its interaction in real-time with a second binding partner (analyte) in solution. The complex formation or dissociation between the ligand and the analyte is measured as the change in refractive index of the solvent near the surface of the biosensor chip (Szabo *et al.*, 1995; Markey, 1999). Using a series of concentrations of the analyte, concentration dependent data can be generated, recorded in real-time

as sensorgrams and fitted into an appropriate kinetic model to estimate analyte association rate (*ka*) and dissociation rate (*kd*). The rate constants (*ka* and *kd*), are a measure of the degree of ligand-analyte complex formation and binding stability and the affinity constant K_D (*kd*/*ka*) is a measure of binding strength of the analyte for the ligand and serves as a link between protein function and structure (Rich and Myszka, 2000; Bronner *et al.*, 2006a; Abdiche *et al.*, 2008; Rich *et al.*, 2008). Thus, SPR biosensors made it possible to quantitatively (rate constants) and qualitatively (specificity of interaction) study the interactions of any biological system including proteins, lipids and cells among others (Rich and Myszka, 2000). When compared with other techniques, SPR biosensor techniques are very flexible, allowing for direct and rapid determination of kinetic constants and study of a large number of molecules at a time using small amount of samples with no need for labelling (Abdiche *et al.*, 2008). However, there are some limitations. For example there could be mass transport limitations which could negatively affect the kinetics of the interactions. Also, there are inherent limitations of immobilizing molecules, especially proteins that go through allosteric conformational changes for their functionality. Lack of needed conformational changes following immobilisation will result into loss of functions. More so, immobilisation conditions and buffer restrictions may limit the application of this system. For instance, it was reported that biotinylation impaired the chaperone function of DnaK but not DnaJ, making the use of biotin-streptavidin coupling process unsuitable for DnaK immobilisation (Mayer *et al.*, 1999). In addition, complete thermodynamic parameters cannot be determined using SPR. Despite these limitations, the ability of this system to provide information about the biomolecular interactions, possible mechanism and the kinetics of such interactions that are needed for understanding the biomolecular characteristic of the target proteins, makes SPR a widely employed system for biomolecular study (Rich *et al.*, 2008; Rich and Myszka, 2008, 2010, 2011)

Like other type II Hsp40 proteins identified in *P. falciparum*, PFA0660w (PF3D7_0113700) possesses domains that are essential for its co-chaperone activity (Figure 3.1). They include a J-domain which is essential for it interaction with the ATP domain and stimulation of the ATPase activity of partner Hsp70s (Cheetham and Caplan, 1998), a GF-domain, which may be involved in ensuring the stability of substrate release and capture by Hsp70 (Tsai and Douglas, 1996; Hennessy *et al.*, 2000) and a C-terminal domain, possibly used for substrate capturing and dimerisation (Borges *et al.*, 2005; Wu *et al.*, 2005). Other experimental evidence has shown that the stability of the Hsp40-Hsp70 interaction and the adequate release of substrate to Hsp70 is due in part to the interaction of Hsp40 with the C-terminal end of the Hsp70 (Qian *et al.*, 2002; Demand *et al.*, 1998) which may be made possible through dimer formation (Sha *et al.*, 2000; Qian *et al.*, 2002).

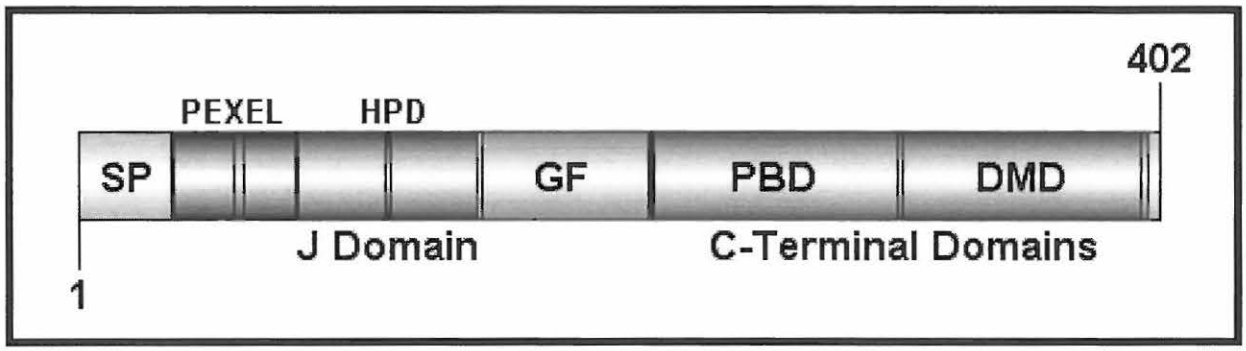

Figure 3.1: Schematic diagram of the domain organization of PFA0660w
SP is Signal peptide, PEXEL is *Plasmodium* export element, GF is Glycine-Phenylalanine rich region, PBD is peptide binding domain and DMD is dimerisation domain. The J-domain contains a highly conserved HPD motif. The diagram was generated using the amino acid sequences of PFA0660w with DOG 2.0 software (Ren *et al.*, 2009).

In this study, functional assays of $(His)_6$-PFA0660w were performed to gain better understanding of it functions alone and in combination with selected possible Hsp70 chaperone partners. Three Hsp70s were examined as potential chaperone partners of $(His)_6$-PFA0660w. They are *P. falciparum* Hsp70-1 and Hsp70-x (PfHsp70-1 (PF3D7_0818900) and PfHsp70-x (PF3D7_0831700) repectively) and human Hsp70 (HsHsp70 or HSPAIA). The parasite resident Hsp70 protein, PfHsp70-1, is the most studied of all the *P. falciparum* Hsp70s (Joshi *et al.*, 1992; Matambo *et al.*, 2004; Ramya *et al.*, 2006; Botha *et al.*, 2011; Cockburn *et al.*, 2011) and has been explored as potential target for vaccine and drug discovery (section 1.4.5). Also included are a parasite exported Hsp70 protein, PfHsp70-x, which has been shown to be exported in complex with PFA0660w into the J-dots (Külzer *et al.*, 2012), and human host cell resident Hsp70 protein, HsHsp70 (Alessandro *et al.*, 2010), which may be recruited by the parasite for use in maintaining its survival and development within the host cell.

PfHsp70-x is a close homolog of PfHsp70-1 and of all the PfHsp70s that have been identified, they share the highest (73%) sequence identity, consistent with the observed close phylogenetic link (Shonhai *et al.*, 2007). The alignment of the amino acid sequences of the three selected chaperones (Figure 3.2) revealed a high level of conservation. The PfHsp70-1 and PfHsp70-x share a high degree of sequence similarity and identity with HsHsp70. They share similar conserved residues including Y145, N147, D148, N170, and T173 that are necessary for their interaction with the J-domain of Hsp40 co-chaperones (Gässler *et al.*, 1998; Suh *et al.*, 1998) and T199, a DnaK phosphorylation site (Shonhai *et al.*, 2007). This may be an indication of their similar role as chaperones. It has been suggested that to facilitate efficient binding of protein substrates by Hsp70, the binding of the J domain of Hsp40 to Hsp70 may cause the SBD to shift away from the NBD (Jiang *et al.*, 2005; Awad *et al.*, 2008; Shonhai *et al.*, 2008).

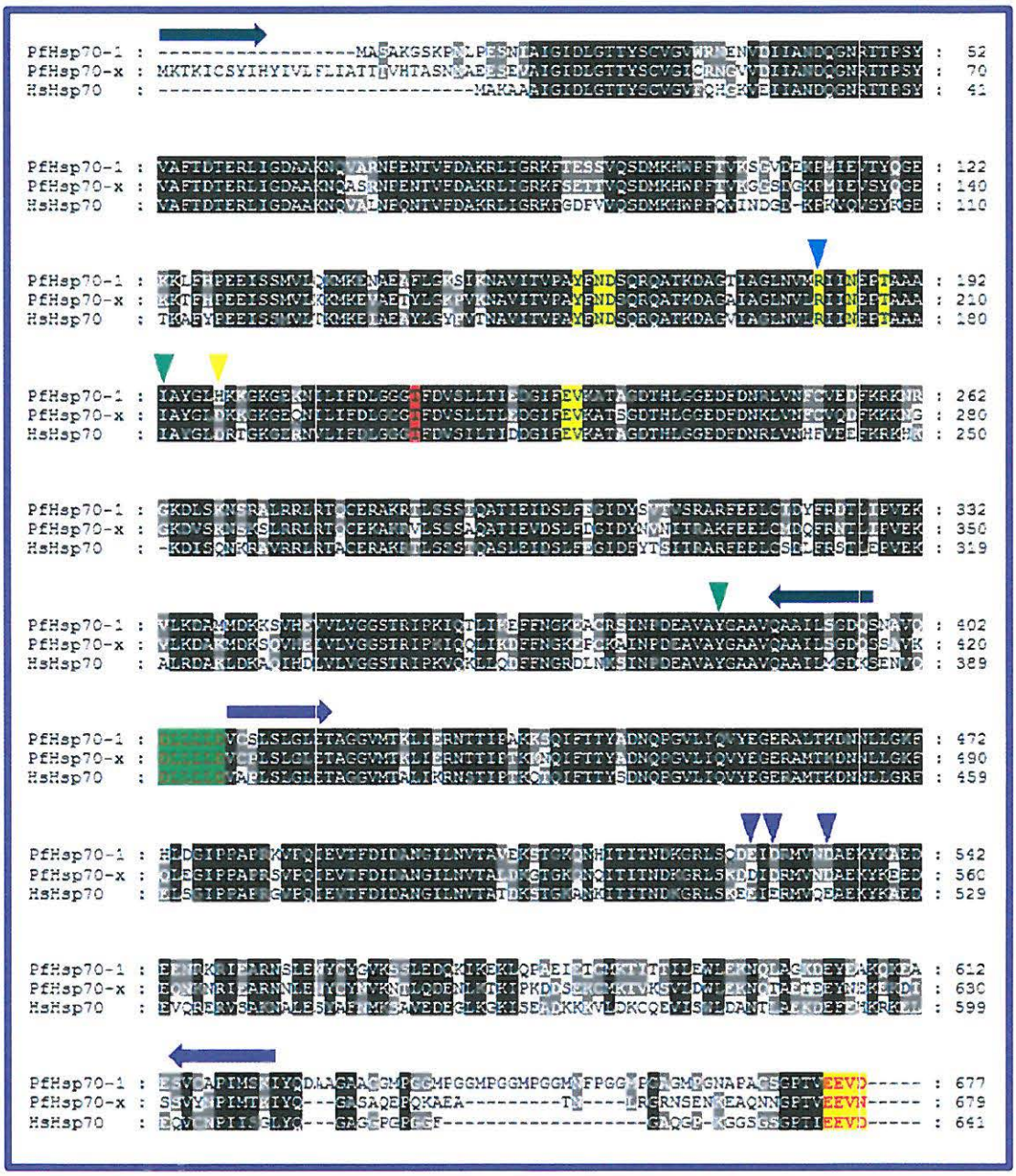

Figure 3.2: Amino acid sequence alignments of PfHsp70-1, PfHsp70-x and HsHsp70

The alignment of the amino acid sequences of the selected chaperones for the functional assays shows a high degree of sequence identity and similarity. The following key residues were identified as reported by (Shonhai *et al.*, 2007): The dark blue and pink arrows identify the amino acid sequences for ATPase domain and the substrate binding domain respectively. Yellow highlight with black letters are Y145, N147, D148, N170, and T173 residues which are said to interact with DnaJ (Gässler *et al.*, 1998; Suh *et al.*, 1998) while red highlight with black letters represents T199, a DnaK phosphorylation site (McCarty and Walker, 1991). Residues I181 and Y371 that may be involved in the relay of the chemical shift transmitted by the SBD through the linker to the NBD (Shonhai *et al.*, 2008) are indicated with green triangle. Indicated with blue triangle is R183 that has been proposed to form ionic interaction with negatively charged residues D536, E527 and D529 (purple triangles) to ensure close association between NBD and SBD (Moro *et al.*, 2004; Shonhai *et al.*, 2008; Worrall and Walkinshaw, 2007). Indicated with yellow triangle is the positively charged H198 residue in PfHsp70, as opposed to negatively charged D186 residue in human Hsp70 (Shonhai *et al.*, 2008). This could indicate that PfHsp70 may interact with Hsp40 partners through different residues compared to human Hsp70. The linker region is identified in red letters highlighted in green while the EEVD motifs are shown in red letter highlighted in yellow. The EEVD motif in PfHsp70-x was replaced with EEVN motif. It should be noted that the HsHsp70 used in these experiments lacked the EEVD motif. The numbers on the right-hand side represent the positions of residues in the respective proteins. The alignment was generated using ClustalW and GeneDoc multiple sequence alignment editor and shading utility (version 2.7.000) (Larkin *et al.*, 2007; Thompson *et al.*, 1994).

Meanwhile, residues I181 and Y371 that are conserved in PfHsp70 and human Hsp70 are said to be involved in the relay of the chemical shift transmitted by the substrate binding domain (SBD) through the linker to the nucleotide binding domain (NBD) (Shonhai *et al.*, 2008). Another residue of interest is R183 found in the NBD and in PfHsp70 is said to be in close proximity to the C-terminal helix A subdomain of the lid (Shonhai *et al.*, 2008) and may be involved in allosteric regulation and PfHsp70 conformational changes. It has been proposed that ionic interactions may exist between R183 and negatively charged residues D536, E527 and D529 that are also located at the lid subdomain of PfHsp70, thereby bringing NBD into close association with SBD (Moro *et al.*, 2004; Worrall and Walkinshaw, 2007; Shonhai *et al.*, 2008). This might be an indication of differences in conformational changes between PfHsp70 and human Hsp70. Also highly conserved in PfHsp70 and human Hsp70 are the Hsp40 binding sites (Jiang *et al.*, 2005). Generally, the positively charged J-domain tends to interact physically with the negatively charged residues of the Hsp70 chaperone. However, the presence of the positively charged H198 residue in PfHsp70, as opposed to the corresponding negatively charged D186 residue in human Hsp70, could be an indication of a unique difference in structural orientation needed for the interaction of Hsp70 with partner Hsp40 (Shonhai *et al.*, 2008). This could indicate that PfHsp70 may interact with Hsp40 partners through different residues compared to human Hsp70.

Furthermore, the cell biological characterisation of PfHsp70-x as an exported parasite-encoded Hsp70 has been presented (Külzer *et al.*, 2012; Grover *et al.*, 2013). PfHsp70-x was reported to be exported into the erythrocyte in complex with PFA0660w and other PfHsp40s that are contained in the J-dots (Külzer *et al.*, 2010, 2012). Though another recent report partially localizes PfHsp70-x to Maurer's cleft (Grover *et al.*, 2013), its association with PfEMP1, an important virulence factor that is largely responsible for cytoadherence of the infected erythrocytes (Baruch *et al.*, 1995; Su *et al.*, 1995; Miller *et al.*, 2002; Weatherall *et al.*, 2002), suggests that PfHsp70-x may be involved in the presentation of PfEMP1 on the surface of the infected erythrocyte. The export of PfHsp70-x in complex with J-dots proteins and possibly with PfEMP1 and localisation to the erythrocytes cytosol and PV may be an indication of its involvement in the efficient trafficking of proteins within the infected erythrocytes. It appears that the controlling factor for the intra-erythrocytic host-parasite interaction is a complex interplay of activities driven by parasite-encoded co-chaperones (such as PFA0660w), parasite-encoded chaperone Hsp70-x and possibly the host chaperones and co-chaperones. While this work provides evidence that PFA0660w potentially resides in a common complex with PfHsp70-x, there was no evidence for a direct interaction or any functional interaction. Therefore, in the light of the recent cell biological evidence indicating a potential interaction between PFA0660w and PfHsp70-x, it is timely to test their possible direct and

functional interaction using biochemical approaches. The main aim of this study is to gain insight into chaperone/co-chaperone functions of PFA0660w and its role in the survival and development of the parasite and as a potential target for drug development.

The specific objectives of this study were:

1. To recombinantly purify 6xHis-tagged PFA0660w, PfHsp70-1, PfHsp70-x and HsHsp70 using nickel affinity chromatography.
2. To determine the ability of $(His)_6$-PFA0660w to suppress the aggregation of rhodanese alone and in combination with recombinant PfHsp70-1, PfHsp70-x and HsHsp70.
3. To determine the ability of $(His)_6$-PFA0660w to stimulate the ATP hydrolysis of recombinant PfHsp70-1, PfHsp70-x and HsHsp70.
4. To determine the chaperone co-chaperone interactions between $(His)_6$-PFA0660w and each of recombinant PfHsp70-1, PfHsp70-x and HsHsp70 proteins using surface plasmon resonance spectroscopy (SPR).

3.2 Material and Methods

3.2.1 Materials

ProteOn XPR36 instrumentation, GLC biosensor chip and ProteOn Kits (amine coupling, deactivation and post maintenance kits) were obtained from Bio-Rad (Bio-Rad Laboratories, USA). ECL™ Western blotting kit (GE Healthcare, UK), Chemidoc chemiluminescence imaging system (Bio-Rad, USA), Helios Alpha UV-Vis spectrophotometer (Thermo Scientific, USA), ready-to-use Bradford reagent (Fermentas), Snakeskin™ Pleated dialysis tubing (Pierce – MWCO 10,000) and 96 well plates (Thermo Scientific, USA) were used in this study. Commercially available antibodies and standard grade chemicals and reagents are as given in *Appendix E*. Also used in this study are *E. coli* M15[pREP4], XL1 Blue and BL21 cells. The plasmid pQE30-Hsj1a was constructed by Ms. C. McNamara (Rhodes University, 2006), while pQE30-PfHsp70-1 was purchased from GenScript(R) (USA). The pQE30-PfHsp70-x expression construct was produced by Mr. R. Hatherley (Rhodes University, 2010). The pMSHsp70 plasmid encoding human HsHsp70 (HSPA1A) was a kind gift from Professor J. Brodsky, University of Pittsburgh, U.S.A. (Chiang *et al.*, 2009). Except otherwise indicated, statistical analysis was done using Microsoft® office excel statistical packages.

3.2.2 Protein purifications

3.2.2.1 Purification of $(His)_6$-PFA0660w from inclusion bodies

The purification of $(His)_6$-PFA0660w follows the procedure detailed in section 2.2.4. The eluted protein samples were dialysed into appropriate assay buffers for functional studies and protein concentrations was determined by Bradford's assay (Bradford, 1976) (as per *Appendix D10* using the standard curve samples in *Appendix B.8*). The eluted and dialysed proteins were analysed by SDS–PAGE and western analysis with mouse monoclonal anti-His (1 in 5000) and anti-DnaK (1 in 5000) antibodies (as per *Appendix D11 and D12*).

3.2.2.2 Purification of 6xHis-tagged Hsj1a and Hsp70s

The plasmid pQE30-Hsj1a (*Appendix B.2*) with 6xHis tag bearing the coding region for the expression of human Hsj1a (Hsj1a; Gene Bank accession number S37375.1) (*Appendix F.2*) and pQE30-PfHsp70-1 (*Appendix B.2*) with 6xHis tag bearing the optimised coding region for the

expression of *P. falciparum* Hsp70-1 (PfHsp70-1) (*Appendix F.4*) in *E. coli* were both transformed into XL1 Blue *E. coli* cells, while pQE30-PfHsp70-x and pMSHsp70 (*Appendix B.2*) with 6xHis tag and bearing respectively the optimised coding region for the expression of *P. falciparum* Hsp70-x (PfHsp70-x) (*Appendix F.4*) and the coding region for human Hsp70 (HsHsp70) (*Appendix F.4*) in *E. coli* were transformed into competent *E. coli* M15[pREP4] and BL21 cells for the purpose of purification respectively. PfHsp70-1, PfHsp70-x and Hsj1a were purified using the protocol detailed in *Appendix D15* while HsHsp70 was purified using the adaptation of the previously reported protocol (Chiang *et al.*, 2009) as contained in *Appendix D16*. All the eluted samples were analysed by SDS–PAGE (as per *Appendix D11*) and western analysis with mouse monoclonal anti-His antibody (1 in 5,000) and anti mouse horse-radish peroxidise (HRP)-conjugated secondary antibody (1:10,000) (as per *Appendix D12*). Samples were dialysed into native dialysis buffer (NDB: 200 mM NaCl, 10 mM Tris-HCl, pH 8.0) or into the appropriate assay buffers for functional studies. Protein concentrations were determined by Bradford's assay (Bradford, 1976) (as per *Appendix D10* using the standard curve – samples shown in *Appendix B.8*).

3.2.3 Functional assays

3.2.3.1 Stimulation of ATPase activities of Hsp70s

The protocol for the determination of the ability of $(His)_6$-PFA0660w to stimulate the ATP hydrolysis of Hsp70 molecular chaperones was adapted from previously reported protocols (Chamberlain and Burgoyne, 1997; Matambo *et al.*, 2004). The assay uses the ascorbate/molybdate colorimetric assay to detect the release of inorganic phosphate during the reaction. The purified proteins were dialyzed into ATPase buffer (50 mM Tris-HCl, pH 8.5; 2 mM $MgCl_2$; 100 mM KCl; 0.5 mM DTT). The chaperones (0.4 µM PfHsp70-1, PfHsp70-x or HsHsp70) were equilibrated at 37°C in ATPase buffer and the reaction was initiated with the addition of ATP (600 µM). Samples (50 µl) were removed at regular time intervals and added to an equal volume (50 µl) of 10% SDS in a 96-well microtitre plate. Sample that was taken immediately following initiation of reaction was considered as the zero time point and was used to normalize other samples. A standard curve (*Appendix B.9*) was prepared using potassium hydrogen phosphate and colorimetric detection of phosphate in samples and standard solutions was achieved by the addition of 50 µl 1% (w/v) ammonium molybdate in 1 M hydrochloric acid and 50 µl 6% (w/v) ascorbic acid in double distilled water. Colour development was allowed to proceed for 10 minutes at room temperature before the addition of 75 µl of the mixture of 4% (w/v) sodium citrate and 4% (v/v) acetic acid for colour stabilization. Following incubation at 37°C for 30 minutes, the absorbance was read at 850

nm (A_{850}). The ability of $(His)_6$-PFA0660w to stimulate the ATP hydrolysis of the chaperones were assessed by the addition of submolar (0.2 μM), equimolar (0.4 μM) and molar excess (0.8 μM) concentrations of the protein to 0.4 μM of the chaperones. All assays were corrected for spontaneous ATP breakdown and a boiled sample of the chaperones (boiled for 15 minutes at 100°C) was used as a non-enzymatic control. Assays were conducted in triplicate for each experiment, and at least three independent experiments were performed using independent batches of protein. Specific basal ATPase activity was expressed as nmol Pi released/min/mg Hsp70 protein and percent fold increase. Data are presented as mean ± standard error of mean (mean ± SEM).

3.2.3.2 Rhodanese aggregation suppression assay

The procedure for determining the ability of $(His)_6$-PFA0660w to suppress the aggregation of rhodanese either alone or in the presence of chaperones (0.4 μM PfHsp70-1, PfHsp70-x or HsHsp70) was adapted from previously published methods (Silberg *et al.*, 1998; Allan *et al.*, 2006; Rosser *et al.*, 2007). Briefly, 300 μM stock solution of bovine rhodanese (Sigma-Aldrich) was prepared in 50 mM Tris-HCl, pH 8.5 and stored in aliquots at -80°C until needed. Aliquots were denatured for 3 hours at 25 °C in denaturing buffer (6 M guanidine hydrochloride, 50 mM Tris-HCl, pH 8.5, 300 mM NaCl and 1 mM DTT) to a concentration of 25 μM. Denatured rhodanese was diluted in reaction buffer (50 mM Tris-HCl, pH 8.5, 300 mM NaCl, and 1 mM DTT) to 1.5 μM final concentrations in 400 μl assay cuvette and the rate of its aggregation was monitored at 320 nm for 20 minutes at room temperature. Where included, varying concentrations of proteins (individually or each chaperone in combination with $(His)_6$-PFA0660w) were added to assay buffer and pre-equilibrated to room temperature prior to the addition of denatured rhodanese. As a control, the aggregation of protein (PFA0660w or each chaperone) was monitored in the reaction buffer without rhodanese, while the preliminary assessment of the effect of residual denaturant concentration on the proteins was monitored by determining the ATPase activity (Hsp70s) or stimulation of ATPase activity (PFA0660w on PfHsp70-x) in the presence of equivalent residual concentration of the guanidine HCl. Assays were conducted in triplicate for each experiment, and at least three independent experiments were performed using independent batches of protein. Absorbance was plotted as percentage of rhodanese aggregation following normalisation against assays with rhodanese alone and expressed as mean ± SEM.

3.2.3.3 Kinetic analysis of Rhodanese aggregation suppression assay

Direct proportionality between the amount of aggregated protein and the absorbance has been experimentally validated (Finke *et al.*, 2000). Using the assumption of proportionality between

absorbance and aggregation, kinetic analysis of the terminal phase of aggregation was conducted as earlier described (Kurganov, 2002). The analysis of the terminal phase of aggregation has been shown to follow first order kinetics (Kurganov, 2002), described by the following equation:

$$\frac{dA}{dt} = \frac{nk[P]_0^{n-1}}{A_{lim}^{n-1}}(A_{lim} - A)^n$$ ---------- Equation 1 (Kurganov, 2002)

Where dA/dt is the change in absorbance per unit time, A is the absorbance, A_{lim} is the limiting value of absorbance, k is the aggregation rate constant, $[P]_0$ is the molar concentration of non-aggregated protein at time t equal 0, and n is the order of kinetic. Given that n is equal to 1 (first order kinetics in respect of aggregation), then the equation can be transformed into:

$$\frac{dA}{dt} = k_1(A_{lim} - A)$$ ---------- Equation 2

Also, the relationship between k_1A_{lim} and the ratio R (protein : rhodanese) can be expressed by the following equation:

$$k_1A_{lim} = k_c(R_{max} - R)$$ ---------- Equation 3

Where k_c is the protein (chaperone or co-chaperone) activity constant measured in absorbance unit per time ($nm.min^{-1}$) and R_{max} is the value of R where complete suppression of aggregation is expected to take place. In term of molar concentration, k_1A_{lim} can be expressed as k_1A_{lim} x $[P]_O/(k_1A_{lim})_{max}$, where $(k_1A_{lim})_{max}$ is the k_1A_{lim} value of rhodanese aggregation in the absence of protein. The equation 3 above can be transformed as follows:

$$k_1A_{lim} = \frac{(k_1A_{lim})_{max}}{[P]_0}k_c(R_{max} - R)$$ ---------- Equation 4

in which case the slope of the plot of k_1A_{lim} versus R will now produce $k_c(k_1A_{lim})_{max}/[P]_O$ and y-intercept $k_c(k_1A_{lim})_{max}$ x $R_{max}/[P]_O$ where k_c (now in molar concentration) and R_{max} can be derived.

To quantify the aggregation suppression ability of $(His)_6$-PFA0660w or the chaperones (PfHsp70-1, PfHsp70-x and HsHsp70) alone or in combination, each set of triplicate data obtained from three independent batches of protein were subjected to kinetic analyses. Applying equation 2, the dose response data were transformed to generate the plots of dA/dt versus A. The linear regression

analysis of the terminal phase of the plot was performed to produce a slope k_1 (rate constant for first order kinetic) and intercept on y-axis as k_1A_{lim} from where A_{lim} was calculated. Also, using equation 3, each set of k_1A_{lim} obtained were plotted against ratio R (protein: rhodanese) to generate a straight line graph from where k_c and R_{max} was deduced. Where $(His)_6$-PFA0660w was combined with fixed chaperone concentration, ratio R was based on $(His)_6$-PFA0660w concentrations ($(His)_6$-PFA0660w : rhodanese). The results (k_1, k_1A_{lim}, A_{lim}, k_c and R_{max}) were expressed as mean ± SEM. By applying equation 4, the value of k_c was transformed to molar concentration.

3.2.3.4 Protein interaction assay

3.2.3.4.1 Biosensor instrumentation and reagents

Surface plasmon resonance spectroscopy protein interaction studies were performed using ProteOn XPR36 (Bio-Rad Laboratories) optical biosensor. GLC biosensor chip, with a 2D surface monolayer for protein-protein interaction and < 8 kRU ligand binding density capacity was selected for use in this experiment. GLC biosensor chip, PBST (pH=7.4, 10 mM phosphate, 137 mM NaCl, 3 mM KCl, 0.005% Tween-20) running buffer and ProteOn Kits (amine coupling, deactivation and post maintenance kits) were obtained from Bio-Rad.

3.2.3.4.2 System and Chip Conditioning

The GLC chip was chosen based on its unique ability to immobilise His tagged proteins for protein-protein interactions (Bronner *et al.*, 2006). Conditioning was done using standard procedures as supplied. Briefly, the running buffer was set at a 30 µl/minutes flow rate for 60 seconds while the regeneration and ligand step injections were maintained at default quality with 0.5% SDS (Injection 1), 50 mM NaOH (Injection 2) and 100 mM HCl (Injection 3).

3.2.3.4.3 Ligand Immobilisation

Ligand channels on the chip were allocated as follows: channel 1 (L1) is $(His)_6$-PfHsp70-1 (PfHsp70-1), channel 2 (L2) is $(His)_6$-PfHsp70-x (PfHsp70-x), channel 3 (L3) is $(His)_6$-HsHsp70 (HsHsp70), channel 4 (L4) is blank channel, and channel 5 (L5) is $(His)_6$-PFA0660w. Ligands were immobilised onto GLC sensor chip surfaces docked into the ProteOn XPR36 instrument. The pH conditions for the buffer required for optimum ligands immobilisation were selected based on the pI of the proteins as follows: PfHsp70-1, pI = 5.5, pH 4.5; PfHsp70-x, pI = 5.0, pH 4.0; HsHsp70, pI = 5.34, pH 4.5; and $(His)_6$-PFA0660w, pI = 7.78, pH 5.5. Immobilisation of proteins on the chip in the ProteOnXPR36 biosensor system is an automated process of activation-coupling-deactivation

sequence. The ligand channels were activated with a 1:1 mixture of 40 mM EDC (N-ethyl-N-(dimethylaminopropyl) carbodiimide) and 10 mM sulfo-NHS (N-hydroxysuccinimide) prepared in double distilled water just before use. The activation step is made possible by the conversion of the carboxyl groups on the dextran to reactive N-hydroxysuccinimide esters by the interaction of sulfo-NHS and EDC. Activation of surfaces was followed immediately with the injection of 10 μg/ml of each ligand prepared in 10 mM sodium acetate buffer at their respective pre-determined immobilisation pH given above. The reference channel was injected with buffer alone. Finally, un-reacted sulfo-NHS groups were deactivated with 1 M ethanolamine HCl. All immobilisation steps were performed at an injection flow rate of 30 μl/min for 5 minutes each at 25°C using PBST as the running buffer.

3.2.3.4.4 Flow rate and Contact time optimisation and Controls

As part of the optimisation of the experimental procedures, contact time and flow rates were optimised using 1 μM concentration of the analytes ($(His)_6$-PFA0660w). In each case, all other parameters were kept constant while either contact time or the flow rate was varied. Two sets of controls were included in the study to be able to determine the specificity of the interaction. They include bovine serum albumin (BSA) (Promega, USA) and Hsj1a (Human Hsp40, 1 μM) with and without ATP (1 mM) as negative and positive controls respectively.

3.2.3.4.5 Analyte Interaction

Typically, protein interaction analysis cycle consisted of three main steps, namely, capturing of analyte proteins unto the surface of the chip immobilised with the protein ligand, interaction of the analytes with the ligand and regeneration of the surface. The protocols for interaction steps (involving flow rate, contact time, dissociation time and regeneration) were setup using the ProteOn software and analytes ($(His)_6$-PFA0660w) were diluted to desired concentrations in the running buffer (PBST) with or without ATP. Apart from blank channel, buffer blanks were also included either as part of the analyte (e.g A1) runs or as a separate analyte runs (A1 – A6). For interaction studies, a range of ($(His)_6$-PFA0660w concentrations (100, 200, 400, 600, 800 and 1000 nM) were injected on the immobilised chip surface at a flow rate of 60 μl/minute and a contact time of 90 seconds. Deactivation was allowed for 300 seconds. Referencing was done by channel referencing using the blank ligand channel and row or injection step referencing using buffer blank, thereby making double referencing by row or column possible. Each set of experiments were performed in triplicate using at least three independent batches of analyte protein {($(His)_6$-PFA0660w}. Sensogram of the mean of each set of overlapping triplicate data was constructed and compared to determine the level of data reproducibility.

3.3 Results

The 6xHis-tagged PFA0660w, Hsj1a and chaperones (PfHsp70-1, PfHsp70-x and HsHsp70) used in the functional assays were successfully purified to high purity. The *E. coli* cells used for each of Hsj1a and the Hsp70 chaperones were those found to be suitable for their expression, consistent with earlier reports (Matambo *et al.*, 2004; Shonhai *et al.*, 2008; Botha *et al.*, 2011). Previous reports have shown that high yields (usually > 10 mg/L) of HsHsp70 proteins were produced after nickel affinity chromatography (Matambo *et al.*, 2004; Misra and Ramachandran, 2009; Cockburn *et al.*, 2011). However, in this plasmid, the last six residues, including the EEVD motif of the HsHsp70 were replaced with the 6xHis-tag at the C-terminal end of the coding sequence. Therefore, the recombinant HsHsp70 produced does not possess the EEVD motif. Generally, the average purified protein yields, expressed as mean ± standard error of mean, were as given in Table 3.1. The SDS-PAGE and western analyses are presented in *Appendix B.7.*

Table 3.1: Average yields of the recombinantly purified proteins

Proteins	Average Yield
Hsj1a	14.48 ± 0.84 mg/L
PfHsp70-1	6.84 ± 0.26 mg/L
PfHsp70-x	19.38 ± 1.20 mg/L
HsHsp70	16.29 ± 1.05 mg/L

3.3.1 ATPase and aggregation suppression assays

The functional relationships between $(His)_6$-PFA0660w and the Hsp70 chaperones were examined by determining the ability of $(His)_6$-PFA0660w to stimulate the ATPase activities of the Hsp70s. ATP hydrolysis provides the energy to drive the substrate binding functions of the Hsp70 chaperones. In this cycle of substrate binding and release, the rate of ATP hydrolysis, which is thermodynamically weak, can be increased by the interaction of Hsp40 with the ATPase domain of the Hsp70s (Cheetham *et al.*, 1994; Tsai and Douglas, 1996; Cheetham and Caplan, 1998). The ability of $(His)_6$-PFA0660w to stimulate the ATP hydrolysis of PfHsp70-1, PfHsp70-x and HsHsp70 was investigated using submolar (0.2 μM), equimolar (0.4 μM) and molar excess (0.8 μM) concentration of the protein. Hsj1a and boiled samples of the chaperones were used as controls.

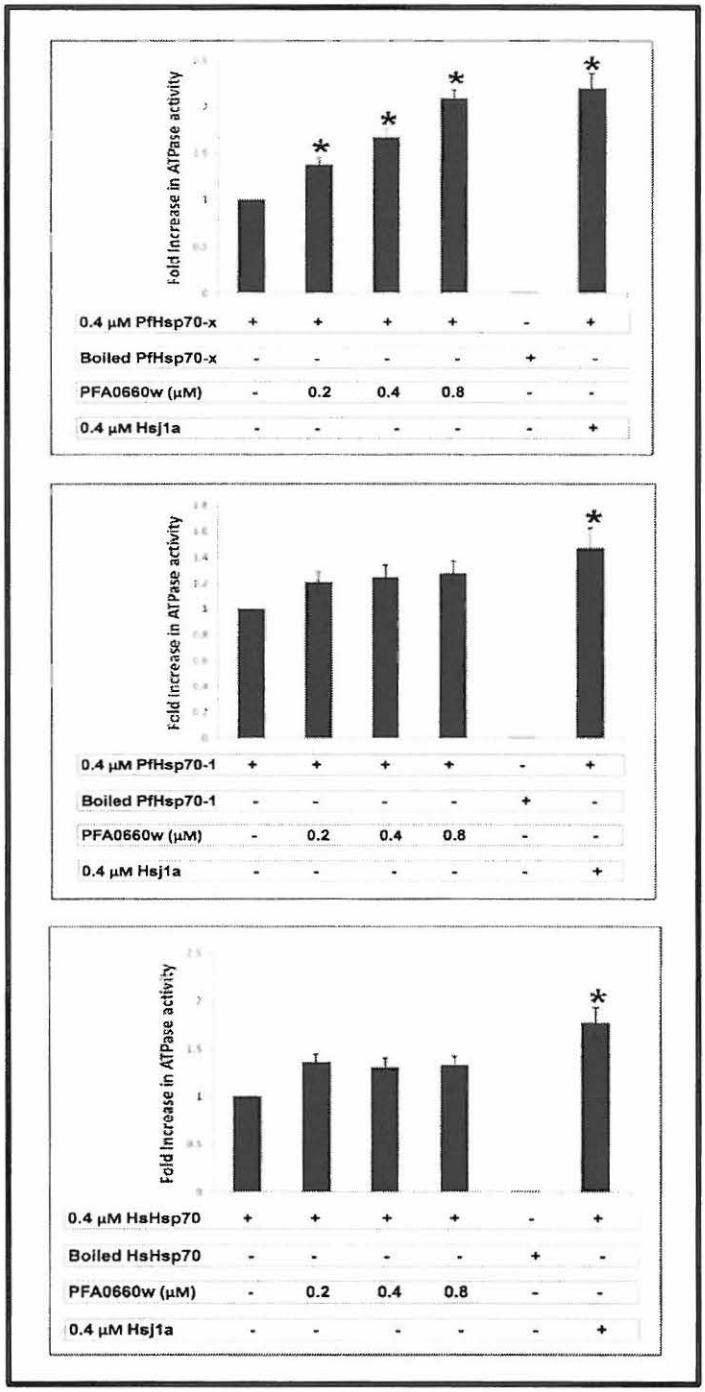

Figure 3.3: $(His)_6$-PFA0660w stimulates the ATPase activity of PfHsp70-x

The bar graphs showing the basal and $(His)_6$-PFA0660w-stimulated ATPase activities of PfHsp70-x (upper), PfHsp70-1 (middle) and HsHsp70 (lower) expressed as fold increase (calculated by dividing with respective basal ATPase value and given as mean ± SEM). Each set of bar graphs represents the fold increase in the ATPase activity of the Hsp70 chaperone alone (0.4 μM) or in combination with sub-molar (0.2 μM), equimolar (0.4 μM) and molar excess (0.8 μM) concentrations of $(His)_6$-PFA0660w or equimolar (0.4 μM) concentration of Hsj1a as indicated. The boiled samples of Hsp70s and native sample of Hsj1a serve as negative and positive controls respectively. All samples were corrected for spontaneous ATP hydrolysis before normalisation to obtain fold increase. Shown here is the aggregated data from three independent experiments performed in triplicate using at least three batches of independently purified proteins for each experiment. Error bars are as indicated on each bar (SEM) and * indicate statistical significance at $P<0.05$ relative to basal ATPase value for respective chaperone using paired Student T-test.

The basal ATP hydrolysis values for PfHsp70-x, PfHsp70-1 and HsHsp70 expressed as mean ± SEM (standard error of mean) are 12.788 ± 0.127, 9.151 ± 0.260 and 8.399 ± 0.159 nmol Pi/min/mg

respectively, indicating a comparative ATPase activity. Also, in the presence of $(His)_6$-PFA0660w, the results showed a dose dependent and statistically significant ($P<0.05$) increase in the stimulation of ATP hydrolysis of PfHsp70-x while the stimulation of PfHsp70-1 and HsHsp70 were neither dose dependent nor significant, indicating that $(His)_6$-PFA0660w possesses a preference for PfHsp70-x (Figure 3.3). Though the slight increase in the ATP hydrolysis of PfHsp70-1 and HsHsp70 may indicate some level of interaction with $(His)_6$-PFA0660w, the inability of $(His)_6$-PFA0660w to significantly and dose dependently stimulate their ATP hydrolysis suggests a lack of a specific functional interaction with these chaperones. Also, the controls (boiled proteins) did not produce any ATPase activity. Earlier reports have shown that Hsj1a was able to stimulate the ATPase activities of human and plasmodial Hsp70s (Cheetham *et al.*, 1994; Botha *et al.*, 2011), making it a good control for this study. Consistent with these reports, Hsj1a produced a relatively high and significant increase in the stimulation of the basal ATP hydrolytic activities of all the chaperones (PfHsp70-1, PfHsp70-x and HsHsp70). Also, not only was the Hsj1a stimulated ATP hydrolysis of PfHsp70-x the highest of the three chaperones, the fold increase in the stimulation of ATP hydrolysis of PfHsp70-x by Hsj1a (0.4 μM) was greater than the stimulation produced by equimolar (0.4 μM) and comparable to molar excess (0.8 μM) of $(His)_6$-PFA0660w stimulatory activity. However, while Hsj1a significantly interacted with the three chaperone, $(His)_6$-PFA0660w only significantly interacted with PfHsp70-x, suggesting possible selectivity in chaperone co-chaperone interaction.

The chaperone activity of $(His)_6$-PFA0660w and Hsp70 chaperone proteins were further assessed by determining the ability of $(His)_6$-PFA0660w to suppress the aggregation of chemically denatured rhodanese alone and in the presence of the PfHsp70-1, PfHsp70-x and HsHsp70. Following denaturation with guanidine hydrochloride (GnHCl), rhodanese aggregation was monitored spectrophotometrically at 320 nm for 20 minutes at a final concentration of 1.5 μM rhodanese. Both the $(His)_6$-PFA0660w and the Hsp70 chaperone proteins produced a dose dependent decrease in the aggregation of rhodanese (Figure 3.4). This result indicates that $(His)_6$-PFA0660w has independent chaperone activity. While 1.5 μM $(His)_6$-PFA0660w and PfHsp70-1 completely suppressed the aggregation of rhodanese, the same concentration of PfHsp70-x and HsHsp70 only produced 45.10 % and 45.99 % reduction in rhodanese aggregation respectively.

To assess the ability of $(His)_6$-PFA0660w to enhance the chaperone activities of the Hsp70s, the effect of $(His)_6$-PFA0660w on a range of concentrations of Hsp70s (0.25 μM PfHsp70-1, 1.0 μM PfHsp70-x and 1.0 μM HsHsp70) was determined.

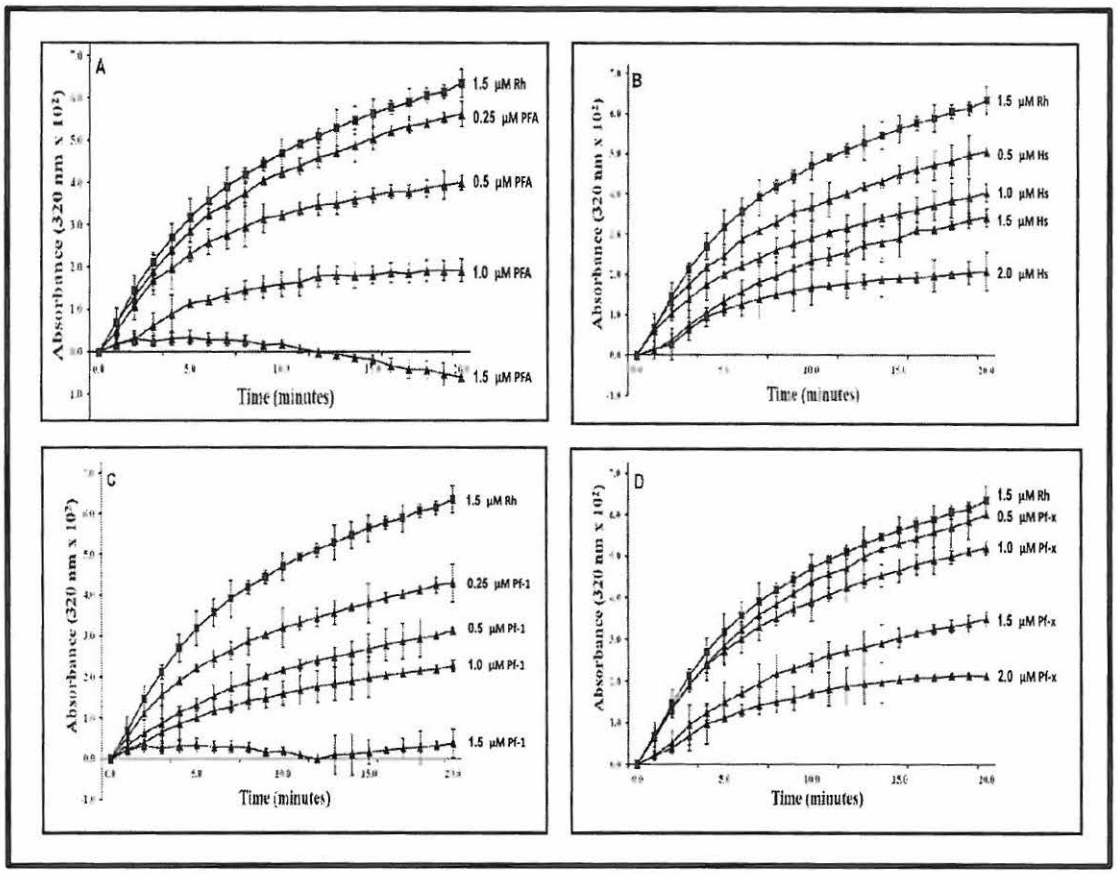

Figure 3.4: PFA0660w, HsHsp70, PfHsp70-1 and PfHsp70-x suppress rhodanese aggregation. Rhodanese aggregation suppression assays are essentially performed for 20 minutes at room temperature. The progress curves of absorbance (320 nm x 10^2) versus time (minutes) showing aggregation of rhodanese alone (1.5 μM Rh, *filled black squares*) or in the presence of a range of concentrations (*filled triangles*) of recombinant 6xHis tagged (**A**) PFA0660w (PFA), (**B**) HsHsp70 (Hs), (**C**) PfHsp70-1(Pf-1) and (**D**) PfHsp70-x (Pf-x). The concentrations used for each protein are shown at the end of their respective progress curves. The error bars (SEM) are as indicated for each plotted data. The absorbance was multiplied by 10^2, so that the calculated errors can be clearly seen on the graph. All proteins used showed dose dependent suppression of rhodanese aggregation and 1.5 μM of PFA0660w and PfHsp70-1 produced complete suppression of aggregation. Shown here is the aggregated data (mean ± SEM) of three independent experiments performed in triplicate using at least three batches of independently purified proteins for each experiment. 20 time points were used to plot the progress curves.

The selected concentrations of the Hsp70 proteins are those that resulted in greater than 50% rhodanese aggregation and which by the assumption of possible additivity of their individual chaperone activities with $(His)_6$-PFA0660w (Figure 3.4) will allow for higher $(His)_6$-PFA0660w concentrations to be tested before complete suppression of aggregation can be achieved. BSA (1.5 μM) was used as control and did not produce any effect on the aggregation of rhodanese. The results of the effects of varying concentrations of $(His)_6$-PFA0660w (0.25, 0.5 and 1.0 μM) on the chaperone activities of PfHsp70-1, PfHsp70-x and HsHsp70 are presented in Figure 3.5. For both PfHsp70-1 and PfHsp70-x, the suppression of rhodanese aggregation increased with an increase in the concentration of $(His)_6$-PFA0660w, suggesting a possible dose dependent interaction. On the other hand, an initial reduction in aggregation suppression was observed with HsHsp70 in the presence of 0.25 μM $(His)_6$-PFA0660w followed by a dose dependent increase suggesting that at

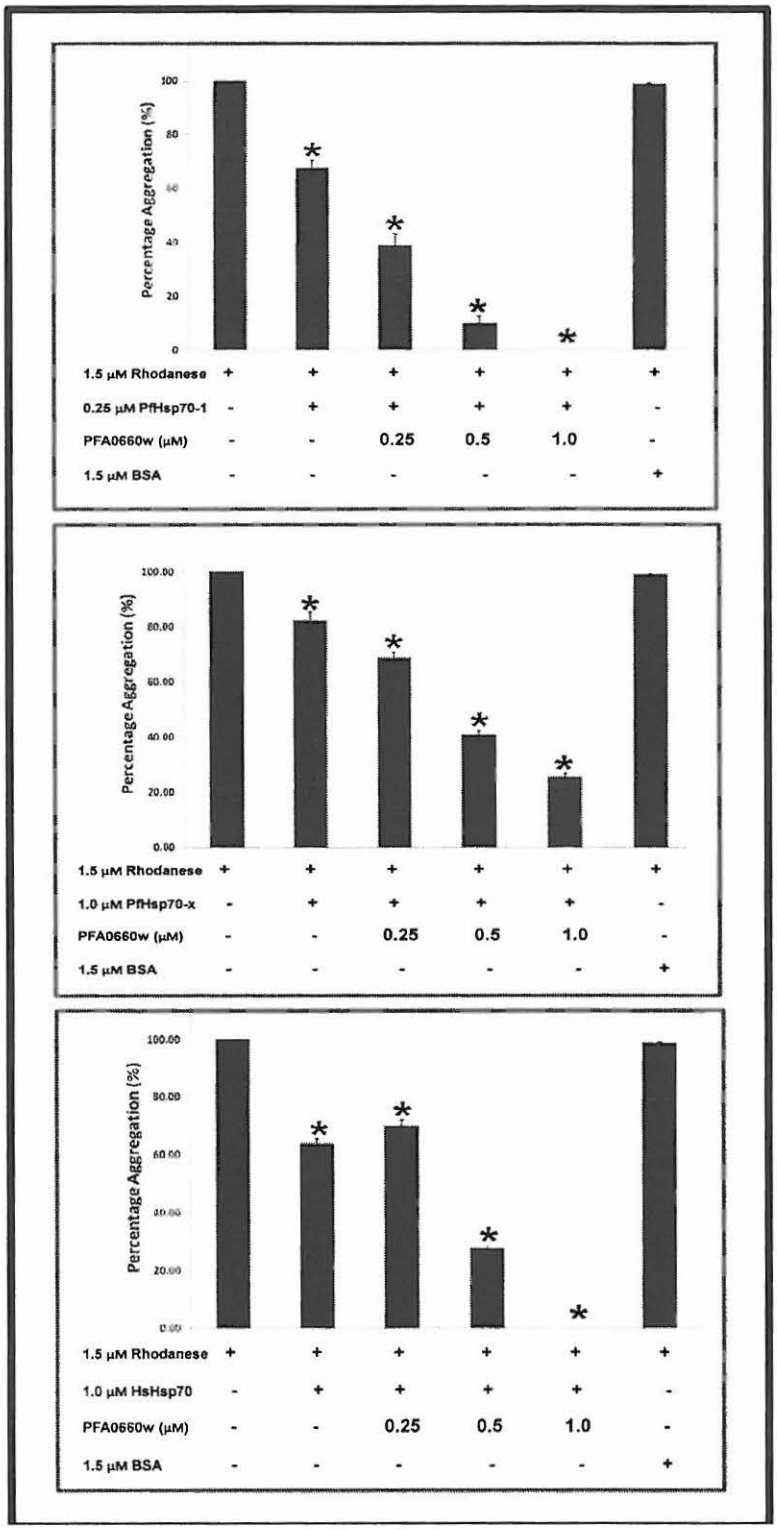

Figure 3.5: Rhodanese aggregation suppression assays using PFA0660w and Hsp70 molecular chaperones

The bar graphs showing the suppression of rhodanese aggregation by PfHsp70-1 (upper), PfHsp70-x (middle) and HsHsp70 (lower) alone or in the presence of a range of $(His)_6$-PFA0660w concentrations (0.25, 0.5 and 1.0 μM). Percentage aggregation was calculated relative to rhodanese alone and expressed as mean ± SEM. All assays were performed at room temperature (25°C) for 20 minutes. BSA was used as a control. The assays were performed in triplicate for at least three independent experiments using at least three independent batches of protein for each experiment. Shown here is the aggregated data of three independent experiments. Constituents that were either included or omitted from the reaction medium are indicated by (+) or (-) sign respectively. Error bars (SEM) are as indicated on each bar graph and * indicates statistical significance at $P<0.05$ relative to rhodanese alone using Student T-test.

lower concentrations, $(His)_6$-PFA0660w may exercise some level of preference for plasmodial chaperones compared to human Hsp70. Interestingly like PfHsp70-1 (0.25 μM), the result shows that HsHsp70 (1.0 μM) produced a complete suppression of aggregation in the presence of 1.0 μM $(His)_6$-PFA0660w (Figure 3.5), and though a similar result was not produced with 1 μM PfHsp70-x, there was significant suppression of aggregation. It is noteworthy that for each concentration of $(His)_6$-PFA0660w that enhanced the aggregation suppression activity of each chaperone, the effects were significant compared to reactions with Hsp70s alone.

Table 3.2: Assessment of the effects of PFA0660w on Hsp70s aggregation suppression

	PFA	0.25 μM	0.5 μM	1.0 μM	0.25 μM	0.5 μM	1.0 μM
		11.59	40.10	73.52	11.59	40.10	73.52
		BY ADDITION			BY ASSAYS		
0.25 μM PfHsp70-1	32.33	43.93	72.43	105.86	61.23	90.10	100.00
1.0 μM PfHsp70-x	17.63	29.22	57.73	91.16	31.27	59.17	74.57
1.0 μM HsHsp70	36.28	47.87	76.38	109.80	29.95	72.29	100.00

PFA represents $(His)_6$-PFA0660w. All values are percent reduction in rhodanese aggregation. Highlighted in grey are values obtained for individual protein concentrations as indicated. "By addition" values were obtained by adding the corresponding values of Hsp70s with each of PFA concentration. "By assays" values were experimentally determined.

The percentage reduction in aggregation in the presence of each concentration of $(His)_6$-PFA0660w was, however, more pronounced with PfHsp70-1 when compared to PfHsp70-x and HsHsp70. Also, when compared with the individual dose responses (Figure 3.4), the observed effects with HsHsp70 and PfHsp70-x appear additive while that of PfHsp70-1 appears stimulatory (Table 3.2). Given the respective fractions of Hsp70 relative to 0.25, 0.5 and 1 μM $(His)_6$-PFA0660w concentrations (calculated as Hsp70$(His)_6$/PFA0660w) to be 1, 0.5 and 0.25 for PfHsp70-1 and 4, 2 and 1 for each of PfHsp70-x and HsHsp70 respectively, it can be suggested that in the presence of $(His)_6$-PFA0660w a higher concentration of PfHsp70-x or HsHsp70 is needed to effect significant suppression of aggregation to levels similar to PfHsp70-1. For instance, in the presence of 1 μM $(His)_6$-PFA0660w, the result shows that a complete suppression of aggregation will require 0.25 μM PfHsp70-1 compared to 1 μM of HsHsp70 and a higher concentration for PfHsp70-x (since 1 μM could not produce complete aggregation suppression). However, it could also be argued that at higher concentrations of $(His)_6$-PFA0660w (1.0 μM), the effect produced when combined with PfHsp70-x is largely due to $(His)_6$-PFA0660w, since a similar effect was produced with the same concentration of $(His)_6$-PFA0660w alone (Figure 3.4). It should be noted that since $(His)_6$-PFA0660w showed high aggregation suppression activity at higher concentration when used alone, its effects on Hsp70s can only be distinguishable at the lower concentration. At 0.25 μM $(His)_6$-PFA0660w, its synergistic effect on PfHsp70-1 and additive effect on PfHsp70-x were statistically

significant when compared with respective Hsp70 alone. In addition, the preliminary kinetic analyses show that the effect of adding $(His)_6$-PFA0660w to PfHsp70-1 could be interpreted as stimulation of the PfHsp70-1's aggregation suppression activity by $(His)_6$-PFA0660w or stimulation of $(His)_6$-PFA0660w's aggregation suppression activity by PfHsp70-1 (*Appendix C.3 and C.4*). Therefore, it could be concluded that there is a synergistic effect between $(His)_6$-PFA0660w and PfHsp70-1, with further work being needed to ascertain the exact mechanism. Generally, the results revealed a significant enhancement of aggregation suppression of the Hsp70s (Figure 3.5) and to achieve the desired suppression of aggregation in the presence of $(His)_6$-PFA0660w, the molar ratio/fraction of Hsp70 relative to $(His)_6$-PFA0660w increases from PfHsp70-1, HsHsp70 to PfHsp70-x.

3.3.2 Analysis of Hsp70 – PFA0660w interaction

SPR studies were used to assess the co-chaperone interactions of $(His)_6$-PFA0660w with PfHsp70-1, PfHsp70-x and HsHsp70. The results of the rhodanese aggregation suppression and ATPase activity assays (detailed in section 3.3.1) provided the needed background information into this study. An example of the immobilisation sensogram is shown in *Appendix B.10*. Immobilisation of the chaperones on the GLC chip was achieved using 10 µg/ml of each Hsp70 (equivalent to ~135 nM PfHsp70-1, ~132 nM PfHsp70-x and 143 nM HsHsp70). The level of ligand immobilisation when viewed along the analyte channels were comparable and this is essential for reproducibility of results (*Appendix C.1*). Also change in the flow rate did not produce any observable impact on the kinetics of the interaction (*Appendix B.12 - B*). Binding rates appeared to have been affected with change in contact time and is more pronounced at 30 and 60 seconds (*Appendix B.12 - A*). From 90 seconds the differences are not significant across the ligands.

To explore the ability of ATP to cause enhanced chaperone co-chaperone interactions, the binding of ATP with Hsp70 ligands was determined with ATP concentrations ranging from 0 to 8 mM with and without 200 nM $(His)_6$-PFA0660w. The interaction with ATP with the ligands (Figure 3.6A) confirms that the immobilisation on the chip did not lead to loss of activity of the Hsp70 ligands. In the presence of 200 nM $(His)_6$-PFA0660w, the result shows that as ATP concentration increases, the interaction of the analyte with the ligands also increases (Figure 3.6 - L1-B, L2-B and L3-B). However, further analysis of the results by comparison (Figures 3.6 – A vs B by ligands), showed that the effects of the ATP can only be clearly deduced up to a maximum concentration of 2 mM for PfHsp70-1 and HsHsp70 and 4 mM for PfHsp70-x as the subtraction of ATP results after these values will produce no significant difference (data not shown).

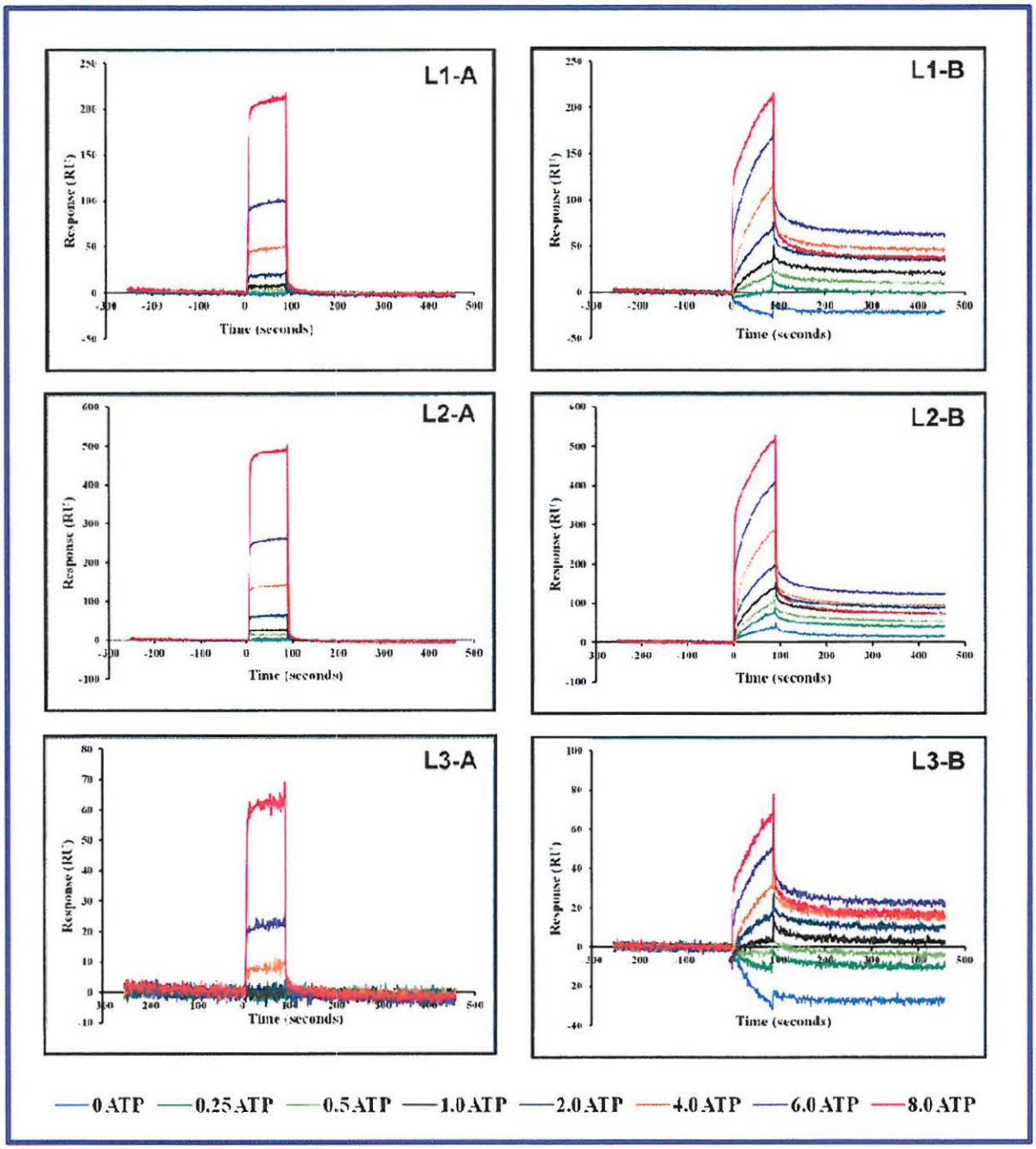

Figure 3.6: The effects of ATP on the interaction of $(His)_6$-PFA0660w with PfHsp70-1, PfHsp70-x and HsHsp70

The SPR analysis of the effect of ATP was done by passing a range of ATP concentrations (0 – 8 mM) over the immobilised chaperones (PfHsp70-1 on L1, PfHsp70-x on L2 and HsHsp70 on L3) in the absence (L1-A, L2-A and L3-A) or presence (L1-B, L2-B and L3-B) of 200 nM $(His)_6$-PFA0660w. Immobilisation of the chaperones on GLC chip was achieved using 10 µg/ml of each chaperone (equivalent to ~135 nM PfHsp70-1, ~132 nM PfHsp70-x and 143 nM HsHsp70). The interaction assay was performed in triplicate for each batch of $(His)_6$-PFA0660w protein (analyte) and similar results were obtained using at least three batches of analyte protein. ATP concentrations were prepared just prior to use. All data were double referenced using buffer blank and blank ligand. However, the triplicate data overlapped and shown here are representative sensograms generated using the mean of a triplicate data obtained from one batch of the analyte $(His)_6$-PFA0660w). RU is response unit. The legend showing the ATP concentrations are located below the sensograms.

Also, the interaction of $(His)_6$-PFA0660w (200 nM) with Hsp70 ligands in the absence of ATP (0 mM) showed that only PfHsp70-x produced some interaction (Figure 3.6-B), suggesting possible

preferential interaction of $(His)_6$-PFA0660w with PfHsp70-x. The enhancement of $(His)_6$-PFA0660w interaction with the Hsp70s in the presence of ATP further confirms the chaperone co-chaperone interaction as opposed to non-specific substrate binding. In addition, two sets of controls were introduced into the experiments to further confirm the observed specificity of the interactions. They are BSA (1 μM) and Hsj1a (1 μM) with and without ATP (1 mM) as negative and positive control respectively. BSA showed no interaction with the ligands either in the presence or absence of ATP while Hsj1a showed an increased interaction in the presence of ATP, thus confirming the earlier observation of an increase binding in the presence of ATP (Figure 3.7 and *Appendix B.11*).

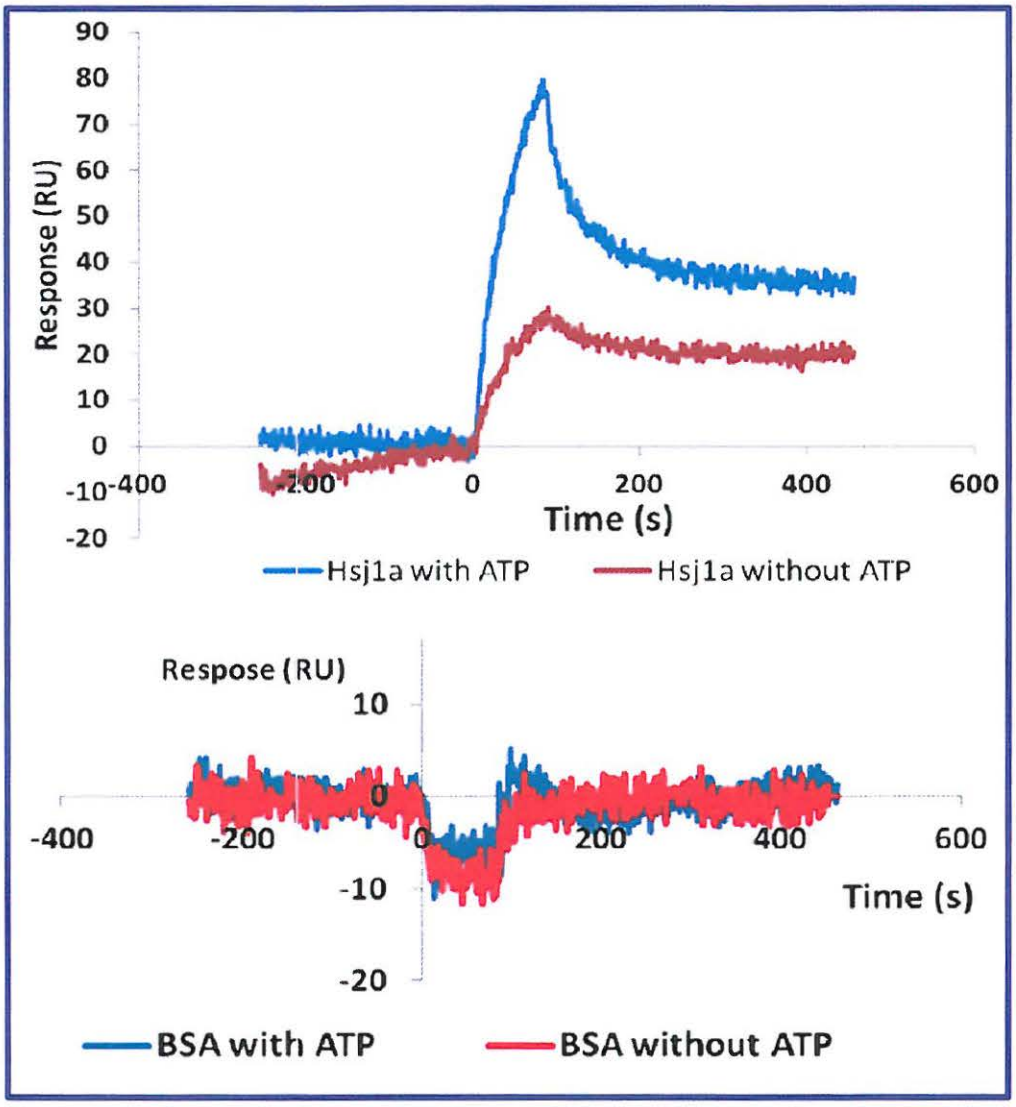

Figure 3.7: The interaction of Hsj1a and BSA with PfHsp70-x

SPR analysis of the interaction of Hsj1a and BSA with PfHsp70-x was performed by passing Hsj1a or BSA (1 μM; as analyte) over the immobilised PfHsp70-x on a GLC chip in the presence and absence of 1 mM ATP. The interactions of Hsj1a and BSA with the immobilised PfHsp70-x served as a control. The interaction assay was performed in triplicate and repeated at least three times. Hsj1a was freshly prepared for each set of triplicate runs while ATP and BSA concentrations were prepared just prior to use. All data were double referenced using buffer blanks (with or without ATP) and blank channel. All triplicate data overlapped and shown here is a representative sensograms for Hsj1a (upper panel) and BSA (lower panel), generated using the mean of a triplicate data obtained from one experiment. RU is response unit. Similar results were obtained for PfHsp70-1 and HsHsp70 (*Appendix B.11*).

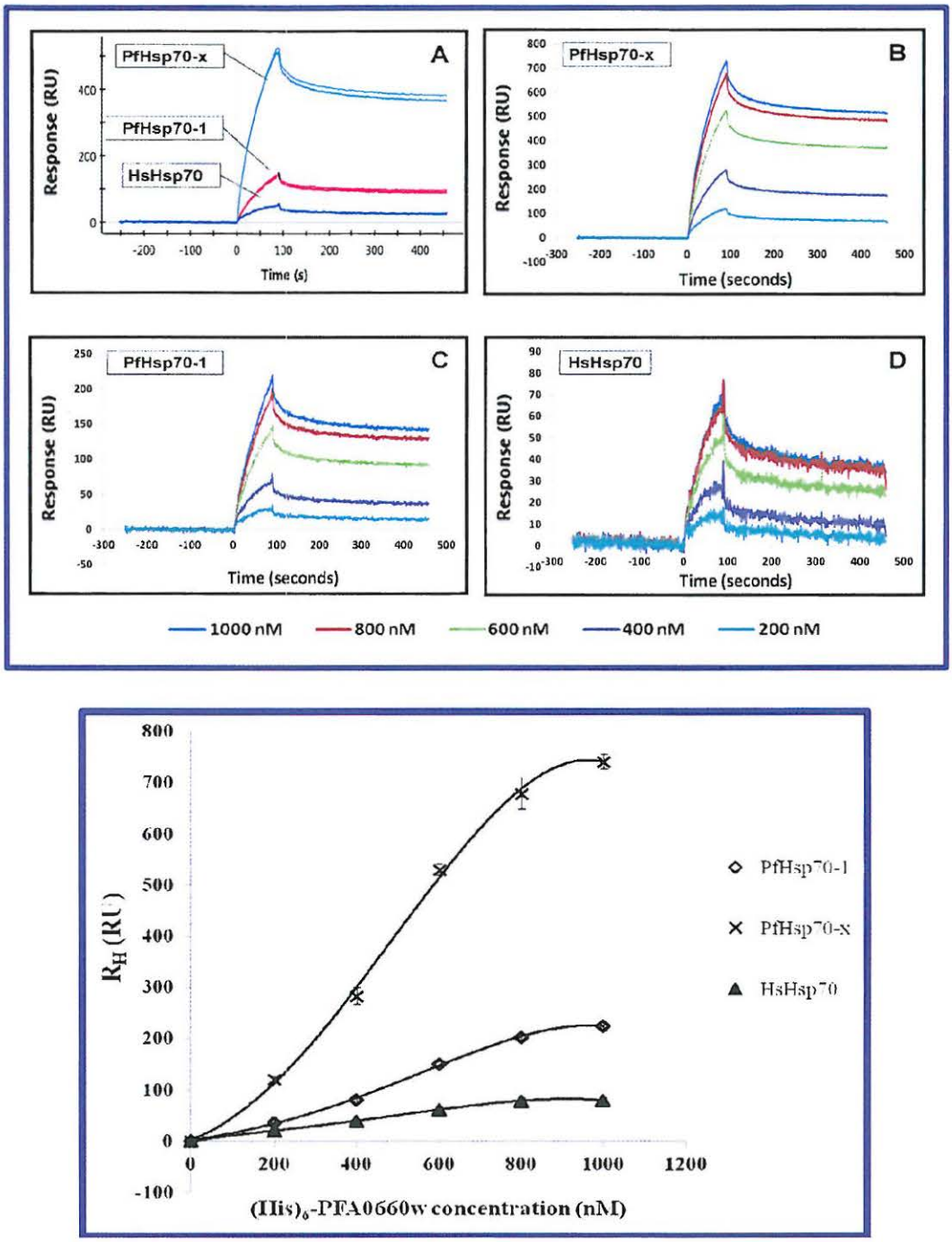

Figure 3.8: The association kinetics of (His)$_6$-PFA0660w with Hsp70 chaperones increases with increasing concentrations of (His)$_6$-PFA0660w, with reduced increases at the higher concentrations used, suggestive of saturation kinetics.

Upper: The SPR analysis of the interaction of (His)$_6$-PFA0660w with Hsp70 ligands (PfHsp70-1, PfHsp70-x and HsHsp70) was conducted by passing a range of (His)$_6$-PFA0660w concentrations (200, 400, 600, 800 and 1000 nM) over ligands immobilised on GLC chip in the presence of 1 mM ATP. The interaction assay was performed in triplicate for each concentration and repeated at least three times using different batches of (His)$_6$-PFA0660w (analyte). All data were double referenced using ATP buffer blank and blank channel. Shown here are example of sensograms for triplicates runs (A) generated using 600 nM of (His)$_6$-PFA0660w, and the representative sensorgrams generated from the mean of a triplicate data for the interaction of (His)$_6$-PFA0660w with PfHsp70-x (B), PfHsp70-1 (C) and HsHsp70 (D). RU is resonance unit. The legend showing the concentrations of the analyte in B-D is as indicated below the sensograms. ***Lower:*** The highest RUs observed in the association phase of the interaction curves (R_H) for each concentration of (His)$_6$-PFA0660w were obtained from the SPR data from three independent experiments performed in triplicate using at least three independent batches of proteins. The aggregated value of R_H was plotted against concentration and the curve fitted to the data by non-linear regression using Microsoft$^{(R)}$ excel package. Shown are the fitted curves for the interaction of (His)$_6$-PFA0660w with PfHsp70-1 (unfilled *square*), PfHsp70-x (*unfilled cross*) and HsHsp70 (*filled triangle*). The error bar (SEM) are as indicated.

Furthermore, dose dependent interaction of $(His)_6$-PFA0660w with the Hsp70s was determined in triplicate using concentrations ranging from 200 nM to 1000 nM. The triplicate runs were done for at least three independent batches of $(His)_6$-PFA0660w as analyte. A representative sensogram is presented in Figure 3.8A, showing overlapping of triplicate data from one of the experiments, thereby confirming the reproducibility of the experimental set up. Figure 3.8 (B – D) shows the sensorgrams of the mean of a triplicate per $(His)_6$-PFA0660w concentration while Figure 3.10 (lower panel) shows the fitted curve of the plot of the highest RUs observed in the association phase for each concentration (R_H) against the analyte concentration. These data revealed that with increasing concentration of $(His)_6$-PFA0660w, there is a corresponding increase in interaction with the Hsp70s ligands, with reduced increases at higher concentrations, suggesting that while the concentrations used were well below saturation, saturation kinetics were being approached. With comparable protein concentrations (10 µg/ml of each Hsp70 chaperone - equivalent to ~135 nM PfHsp70-1, ~132 nM PfHsp70-x and 143 nM HsHsp70) used to achieve comparable level of immobilisation along analyte channels (*Appendix C.1*), and as can be observed from Figure 3.8, it can be concluded that the interaction of $(His)_6$-PFA0660w with PfHsp70-x is potentially the strongest, followed by PfHsp70-1 and then HsHsp70.

3.4 Discussion

The determination of the functional characteristics of PFA0660w is essential for its use as a potential target of drug action. Lack of *PFA0660w* gene deletion (Maier *et al.*, 2008) and its export into the J-dots in complex with PfHsp70-x (Külzer *et al.*, 2010, 2012) suggests that it is essential for the intra-erythrocytic survival and development of the parasite, possibly through functional interactions with PfHsp70-x. Using the ATPase (stimulation of ATP hydrolysis), rhodanese aggregation suppression and SPR assays, the biochemical characterisation of PFA0660w was explored with a view to understanding its functions and functional relationships with selected Hsp70 chaperones. Three Hsp70 molecular chaperones were selected, with PfHsp70-1 being resident in the parasite, PfHsp70-x being exported and one human resident Hsp70 (HsHsp70). The human resident Hsp70 used was the Hsp70-1 (HSPA1A), whose purification has been established and has been used by other investigators (Chiang *et al.*, 2009; Botha *et al.*, 2011; Cockburn *et al.*, 2011). Following successful purification, the ATPase assays showed that Hsp70s were functional. The significant dose dependent stimulation of ATPase activity of PfHsp70-x by $(His)_6$-PFA0660w may be an indication of specificity of action and a reflection of a functional relationship between $(His)_6$-PFA0660w and PfHsp70-x. Such specificity is lacking in Hsj1a which shows significant functional interactions with all the Hsp70s, consistent with previous reports (Cheetham *et al.*, 1994; Botha *et al.*, 2011). Therefore Hsj1a is a good positive control to use when assessing the stimulation of the ATPase activity of a selected Hsp70.

The preliminary kinetic analyses of aggregation suppression of denatured rhodanese showed that $(His)_6$-PFA0660w possesses an independent ability to suppress aggregation and produced a comparable effect on the aggregation suppression activity of the Hsp70s. The data also suggests a possible bidirectional stimulatory chaperone-chaperone effect (stimulation of each other's chaperone activity), going by the quantitative analysis which revealed that a significant fold increase in $(His)_6$-PFA0660w aggregation suppression ability can be obtained in the presence of fixed Hsp70 concentrations. Bidirectional stimulation may be true for a protein such as $(His)_6$-PFA0660w which possesses an inherent ability to chaperone. The independent ability of $(His)_6$-PFA0660w to chaperone is consistent with other reports, which showed that apart from binding substrate and cooperating with Hsp70s for effective protein folding, degradation and/or translocation across membranes, type I and II Hsp40s possess independent chaperone activity, shown by their ability to suppress aggregation of denatured protein (Langer *et al.*, 1992; Rüdiger *et al.*, 2001; Nicoll *et al.*, 2007; Misra and Ramachandran, 2009; Botha *et al.*, 2011). Therefore, $(His)_6$-PFA0660w can function both as chaperone and co-chaperone. However, while the results of

the aggregation suppression assays revealed a potential synergistic interaction of $(His)_6$-PFA0660w with PfHsp70-1, the interaction with PfHsp70-x was potentially additive while there was no effect on HsHsp70. At the lower concentration of 0.25 μM $(His)_6$-PFA0660w, the synergistic as well as the additive effects were statistically significant when compared with respective Hsp70 alone. Though not included in this study, further evidence of functional chaperone co-chaperone relationships may be derived by the inclusion of ATP in the aggregation suppression assay (Muchowski and Clark, 1998). Meanwhile, the suppression of aggregation by $(His)_6$-PFA0660w appeared to be higher when compared to other reports of rhodanese aggregation suppression by other Hsp40 proteins. For instance, using rhodanese aggregation suppression assay, a near complete suppression of aggregation was only achieved using a molar ratio (rhodanese : protein) of 1:5 for Ydj1 (15% aggregation) (Cyr, 1995), and 1:8 for Hsc66 (<10% aggregation) (Silberg *et al.*, 1998), compared to $(His)_6$-PFA0660w, which caused a complete suppression of aggregation at a molar ratio of 1:1, suggesting that $(His)_6$-PFA0660w could be a better suppressor of aggregation.

Furthermore, SPR data showed increased binding of $(His)_6$-PFA0660w to the Hsp70 ligands in the presence of ATP (Figure 3.8), an indication that $(His)_6$-PFA0660w co-chaperone effects are enhanced in the presence of ATP. This is consistent with the observation of Mayer *et al.*, (1999), who showed that binding of DnaJ to DnaK requires ATP hydrolysis and that functionally defective DnaJ mutant protein, DnaJ259, produced no detectable interaction. Other workers have also shown that ATP hydrolysis is essential and serves as an indication of chaperone co-chaperone interaction as opposed to non-specific substrate binding (Yochem *et al.*, 1978; Gässler *et al.*, 1998; Suh *et al.*, 1998; Laufen *et al.*, 1999; Qian *et al.*, 2002). Also, genetic and biochemical evidence have shown that ATP hydrolysis is essential for the Hsp70s chaperone activity (Ha *et al.*, 1999; Mayer & Bukau, 2005). The assessment of the binding of a range of ATP concentrations with and without 200 nM $(His)_6$-PFA0660w (Figure 3.10) further confirmed this observation. In the work that determined the crystal structure of Sis1 peptide-binding fragment and Hsp70 Ssa1 C-terminal complex, it was shown that the residues involved include the EEVD motif (Li *et al.*, 2006). Earlier, the EEVD residues within the human Hsp70 had been shown to play a regulatory role in facilitating its chaperone activity (Freeman *et al.*, 1995). The human Hsp70 protein used in this study lacks an EEVD motif and this might explain its low level of interaction with $(His)_6$-PFA0660w. Therefore the SPR data revealed at a qualitative level that the interactions are that of a co-chaperone, and that the interaction with PfHsp70-x is potentially the strongest. This is however a preliminary assessment of the binding assay using SPR and more experiments will be required for quantitative analysis of the observed interaction.

Meanwhile, the complex nature of chaperone co-chaperone interaction has been reported (Suh *et al.*, 1998; Mayer *et al.*, 1999; Maeda *et al.*, 2007). In line with this observation, an anchoring and docking model of Hsp40 – Hsp70 interaction has been proposed (Qian *et al.*, 2002). It was observed that dimerisation would play an important role in the stability of the interaction complex. If this model is assumed to be physiologically relevant, then, the interaction of PFA0660w with Hsp70s will be a complex interplay of binding to ATPase domain and C-terminal subunit of Hsp70 and stabilised by binding together of the PFA0660w monomers to form dimers. Also, conformational changes that take place following stimulation of ATP hydrolysis may contribute to the ability of $(His)_6$-PFA0660w to form a stable complex, possibly by additional interactions with the C-terminal end of the Hsp70s as earlier suggested (Suh *et al.*, 1998, 1999; Mayer *et al.*, 1999). In addition, some experimental evidence has shown that the stability of the chaperone co-chaperone interaction may involve the interaction of the J domain of Hsp40 with the ATPase domain as well as some fragment of the C-terminal domain of Hsp70s (Demand *et al.*, 1998; Suh *et al.*, 1998, 1999; Mayer *et al.*, 1999; Qian *et al.*, 2002; Li *et al.*, 2006). Also, having been shown to exist as a monomer in solution (section 2.3.4), the stability of the interaction complex may be enhanced through the independent chaperone activity of $(His)_6$-PFA0660w.

The ability of $(His)_6$-PFA0660w to stimulate the ATPase activity of PfHsp70-x and to produce a more significant interaction compared to PfHsp70-1 and HsHsp70 pointed towards a specific functional interaction between these two proteins. The functional enhancement of chaperone activity of PfHsp70-x can aid the delivery of substrate in a stabilized interaction as earlier suggested. Also, the available evidence from this study indicates that PFA0660w could function both as chaperone and co-chaperone, displaying specificity for a functional interaction with PfHsp70-x. Thus, overall, this study has presented the first biochemical evidence for a direct and potentially specific interaction between PFA0660w and PfHsp70-x.

CHAPTER FOUR

IN VIVO CHARACTERISATION OF PFA0660w

Residing within the red blood cell, which lacks necessary organelles for the survival of any living organism, is a challenge for the survival and development of the malaria parasite. Export of parasite encoded proteins is a unique method that has been developed by the parasite to overcome this challenge. Advances in molecular and cellular biology have made it possible to gain a better understanding of the functions of some of these virulence factors. In this study, the in vivo cell biological analysis of PFA0660w was investigated to gain better understanding of it functions. This chapter presents the results of its expression profile, heat shock inducibility of its expression, solubility and localisation within the erythrocyte cytosol in 3D7 P. falciparum-infected erythrocytes.

4.1 Introduction

The survival and development of *P. falciparum* within an unusual environment of erythrocytes has been attributed to its ability to make use of specialized proteins, called chaperones, of which 70 kDa and 40 kDa heat shock proteins (Hsp70 and Hsp40) classes are critical components (Miller *et al.*, 2002; Przyborski and Lanzer, 2005; Maier *et al.*, 2008, 2009). Comparative analysis has shown that among the *Plasmodium* species, *P. falciparum* has the highest number of exported Hsp40 proteins (19 in total) consisting of 3 type IIs, 5 type IIIs and 11 type IVs, consistent with the existence of an expanded exportome observed in *P. falciparum* (Sargeant *et al.*, 2006; Njunge *et al.*, 2013). Also, only in *P. falciparum* has the export of an Hsp70 been established (PfHsp70-x), supporting the fact that the exported parasite-encoded proteins constitute an essential component of the intra-erythrocytic host-parasite interaction (Külzer *et al.*, 2012; Grover *et al.*, 2013). This high number of exported proteins may further help to understand its virulence and associated high rate of mortality. Also, the exported proteins play a central role in host cell remodelling (section 1.3.5) (Przyborski and Lanzer, 2005; Botha *et al.*, 2007; Pesce and Blatch, 2009). The entrance of the parasite into the erythrocytes causes the alteration of the biochemical characteristics of host chaperones which are recruited into membrane-bound, detergent-resistant complexes (Banumathy *et al.*, 2002; Evans and Wellems, 2002; Silvie *et al.*, 2008b; Rao *et al.*, 2010).

During the merozoite and ring stages of its development, several parasite Hsp40 proteins including type II - PFE0055c (PF3D7_0501100) and PFB0090c (PF3D7_0201800); type III - PFB0920w and PF11_0513; and type IV - PF11_0509, PFB0085c and PF14_0013 are said to have a relatively high expression level (Njunge *et al.*, 2013). Expression levels of some plasmodial chaperones, such as PfHsp70-1, PfHsp40 and Pfj4 have been shown to increase upon heat shock (Kumar *et al.*, 1991; Pesce *et al.*, 2008; Botha *et al.*, 2011), suggesting their involvement in cytoprotection and thereby ensuring parasite survival during its intra-erythrocytic life cycle. PFA0660w (PF3D7_0113700), an exported Hsp40 type II parasite encoded protein, together with PFE0055c, has been shown to be part of a membrane structure called J-dots within the cytosol of infected erythrocytes (Külzer *et al.*, 2010). Using gene expression profiles, PFA0660w was shown to be detectable around 10 h post-invasion, and then decreased during the remainder of the intra-erythrocytic developmental 48 hour life cycle (Bozdech *et al.*, 2003; Le Roch *et al.*, 2003; Llinás *et al.*, 2006; Külzer *et al.*, 2010). Interestingly, PfHsp70-x was found in complex with PFA0660w and PFE0055c in the J dots (Külzer *et al.*, 2012), though another report partially localized PfHsp70-x into the Maurer's cleft (Grover *et al.*, 2013). The export of PfHsp70-x in complex with PFA0660w may suggest a possible functional relationship. Also, the potential biochemical evidence for a direct and potentially specific

interaction between PFA0660w and PfHsp70-x has been demonstrated (Chapter 3), which further supports the potential functional interaction. However, while the localisation of PFA0660w has been established, the *in vivo* localisation using PFA0660w specific peptide antibody has not been demonstrated. Therefore, this study further explores the *in vivo* characteristics of PFA0660w using a peptide specific antibody. The main aim was to explore its intra-erythrocytic function, complement the existing knowledge and gain more insight into its potential as a target for drug development.

The specific objectives of the study were as follows:

1. To design a peptide that will be used to raise peptide specific antibodies against PFA0660w and to test the suitability of the antibody for *in vivo* characterisation.
2. To confirm the presence of PFA0660w protein in the *P. falciparum* parasite lysates.
3. To determine the protein expression profile of PFA0660w in the intra-erythrocytic stages of *P. falciparum* development.
4. To determine the localisation of PFA0660w using fluorescence microscopy.

4.2 Material and Methods

4.2.1 Material

Plasmodium falciparum 3D7 stains were used in this study. Human blood used in this experiment was obtained from a healthy volunteer following informed consent at the Ampath laboratories (Grahamstown, South Africa). The rabbit anti-PfHsp70-1 antibody was a kind gift from Dr. Addmore Shonhai, Rhodes University 2008. Anti-PFA0660w peptide antibody was ordered from Genscript®, USA. For fluorescence microscopy Dako mounting medium (Invitrogen, USA) for slide mounting and image capturing by AxioVert.A1 equipped with Zeiss efficient navigation (ZEN) imaging software (Zeiss, Jena, Germany) were used. A sample of $(His)_6$-PFB0595w protein was a kind gift from James Njunge, a fellow PhD student in Biomedical Biotechnology research unit (BioBRU). Recombinant 6xHis-tagged PFA0660w and Hsj1a were purified as in section 2.2.4 and 3.2.2.2 respectively. Other commercially available antibodies, materials and specialized reagents are given in *Appendix E*. Bioinformatics softwares used in this study are as indicated in the text. Sequences for multiple alignments and phylogenetic analysis were retrieved from PlasmoDB (where applicable accession numbers are shown in bracket at first mention).

4.2.2 Peptide design and antibodies production

Alignment of PFA0660w sequence with closely related proteins is an important step towards identification of potential regions for peptide selection. To identify proteins that share a high level of similarity and sequence conservation with PFA0660w, preliminary analysis of sequence similarity with related *P. falciparum* Hsp40 (PfHsp40) proteins using multiple sequence alignment, percentage similarity and phylogenetic analysis was conducted as follows: Multiple sequence alignments of the amino acid sequence of PFA0660w with other type II PfHsp40s was generated using ClustalW and shading was done using GeneDoc softwares (Thompson *et al.*, 1994; Larkin *et al.*, 2007). The local Blast search (Altschul *et al.*, 1997) of the amino acid sequence of PFA0660w against other type II PfHsp40s was done to determine the percentage similarity as provided for by BioEdit sequence alignment editor (version 7.0.9.0.) software (Hall, 1999). To further access the evolutionary relatedness of PFA0660w with other type II PfHsp40 and exported PfHsp40s, phylogenetic and molecular evolutionary analyses were conducted using *MEGA* version 5 (Tamura *et al.*, 2011) as follows: Using the multiple sequence alignments of PFA0660w with other type II PfHsp40s and exported PfHsp40s, phylogeny reconstruction was done using maximum likelihood

statistical method. Phylogeny test was by Boostrap method with a 5000 replicate and Jones-Taylor-Thornton (JTT) model was used as substitution model. Gap/missing data was treated with a partial deletion using a site coverage of 95% and close neighbour interchange was selected as the tree inference option. The multiple sequence alignment, percentage similarity and phylogenetic reconstruction were analysed and compared to determine the proteins with close identity to PFA0660w.

To identify the possible region of peptide selection, multiple sequence alignment of PFA0660w with three closely related type II PfHsp40s was generated as detailed above. PFB0090c, PFE0055c and PFB0595w (PF3D7_0213100) were selected based on the analysis of sequence similarity. Potential peptides for screening were selected from the region that showed lowest level of sequence conservation in the multiple sequence alignment. From the identified potential peptides, a PFA0660w specific peptide was then selected based on regions of high antigenicity. The epitopic region was selected using algorithms that were provided by Gene Runner software (version 3.05; Hastings Software Inc.). These included algorithms for surface probability (Emini *et al.*, 1985), hydropathy (Kyte and Doolittle., 1982), peptide antigenicity (Hopp and Woods., 1981; Jameson and Wolf., 1998), and chain flexibility (Karplus and Schulz., 1988). The identified peptide was confirmed for specificity to the target protein and avoidance of cross-reactivity of the antibody to be generated by BLAST search (Altschul *et al.*, 1997) against NCBI and PlasmoDB databases. Synthesis of the predicted peptide (DALKQSGFNSSNF) and production of antibodies in rabbit against the epitope was commercially performed by GenScript$^{(R)}$ (USA). The peptide was synthesized as (DALKQSGFNSSNFC) with an additional cysteine residue (C) and peptide-KLH conjugate. The antibody was supplied lyophilized. The specificity of the antibody was tested using heterologously produced 6xHis-tagged proteins (PFA0660w, PFB0565w and Hsj1a), uninfected erythrocytes and parasite lysate. The lysate preparations from infected and uninfected erythrocytes follow the procedure given in section 4.2.4.

4.2.3 Plasmodium falciparum parasite culture

Human blood was processed to obtain clean erythrocytes. To do this the serum and buffy coat were removed following initial centrifugation (3,200 x g for 5 min). The erythrocytes were then processed by washing them several times in incomplete RPMI 1640 medium (lacking AlbumaxII). Following the preparation of the erythrocytes, the propagation of *P. falciparum* parasite was performed as previously reported (Trager and Jensen, 1976; Pesce *et al.*, 2008; Botha *et al.*, 2011). *P. falciparum* strain 3D7 was cultured in human O^+ erythrocytes at a hematocrit level of 4% using

RPMI 1640 containing 50 mM glucose (Merck, USA), 200 μM hypoxanthine (Sigma-Aldrich, Germany), 25 mM Hepes and L-Glutamine (Whitehead scientific, South Africa) supplemented with 0.5% (w/v) AlbumaxII (Gibco, USA) and 50 μg/ml gentamicin (Sigma-Aldrich, Germany). The parasites were incubated at 37°C and maintained under an atmospheric composition of 5% (v/v) CO_2, 5%(v/v) O_2 and 90% (v/v) N_2. Synchronization of parasites to the ring stage was routinely performed through sorbitol lysis method as previously described (Biswas *et al.*, 1979; Lambros and Vanderberg, 1979).

4.2.4 Preparation of P. falciparum parasite lysate and detection of PFA0660w by western analysis

The protocol for the preparation of *P. falciparum* parasite lysate was adapted from previously reported saponin-permeabilisation method (Saliba, 1998; Alleva and Kirk, 2001) on ice (Tonkin *et al.*, 2004). It has been shown that through its ability to permeabilise the erythrocyte membrane, saponin can be used to isolate whole parasite-infected erythrocytes that are depleted of not less than 95% haemoglobin (Beaudoin and Aikawa, 1968; Kreier, 1977; Ansorgea *et al.*, 1997). Infected erythrocytes containing synchronized parasites at the trophozoite stage were harvested by centrifugation (800 g for 2 minutes at 4°C) and treated with 0.1% (w/v) saponin (Sigma-Aldrich, Germany) in phosphate-buffered saline (PBS; 137 mM NaCl, 2.7 mM KCl, 10.3 mM Na_2HPO_4, 1.8 mM KH_2PO_4, pH 7.4), on ice for 3-5 minutes and immediately centrifuged (2800 g for 5 minutes at 4°C), ensuring that total exposure to saponin is not more than 10 minutes. The supernatant containing majorly the released haemoglobin was aspirated and the pellet was washed twice with ice cold PBS and centrifuged (2,800 g for 5 minutes at 4°C) to remove residual haemoglobin and saponin. The washed parasite pellet was resuspended in reducing/denaturing sample buffer (Laemmli, 1970) and boiled for 5 minutes, followed by centrifugation (10,000 x g for 2 minutes) to remove the cell debris and obtain the soluble supernatant. Proteins were analyzed by SDS–PAGE and western analysis with rabbit anti-PFA0660w (1 in 4000) or rabbit anti-PfHsp70-1 (1 in 5000 dilution) primary antibody and Horseradish peroxidase (HRP)-conjugated goat anti-rabbit secondary antibody (1 in 5000 dilution) (Cell signaling technology, USA) in line with standard protocols (*Appendix D12*). However, for the western analysis, instead of blocking the membrane in 5% (w/v) fat-free milk powder in Tris-buffered saline, the membrane was blocked using 3% (w/v) bovine serum albumin (BSA) in Tris–buffered saline–Tween (TBST); (50 mM Tris, 150 mM NaCl, 0.1% (v/v) Tween-20, pH 7.5). The proteins were detected by using the enhanced chemiluminescence (ECL™) western blotting kit (GE Healthcare, UK) and images were acquired

using the Chemidoc imaging system equipped with Quantity one software version 4.4.1 (Bio-Rad, USA). The anti-PfHsp70-1 antibodies used here had been raised in rabbits and used as previously described (Pesce *et al.*, 2008; Botha *et al.*, 2011). These methods of erythrocyte membrane lysis and western analysis were maintained throughout the study unless otherwise stated.

4.2.5 Analysis of PFA0660w protein expression

Parasites were cultured as described above and synchronized using sorbitol at the ring stage. PFA0660w protein expression was determined in a time course experiment. For the time course experiment, the parasites were equally divided into eight flasks and incubated at 37°C. Parasite lysates were generated at 6 hour intervals over the 48 hour intra-erythrocytic parasite developmental life cycle and frozen at -80°C until use. The expression of PFA0660w was analyzed by SDS-PAGE and western blotting as described in section 4.2.4. Expression of PfHsp70-1 was also monitored as positive control and rabbit anti-glycophorin antibodies was used as a loading control (Thermo scientific, USA) (1:4000).

4.2.6 Determination of heat shock induction of PFA0660w

For the heat shock experiment, synchronized parasites were cultured as previously described and equally split into 6 flasks at the trophozoite stage. Heat shock was applied by incubating subcultures at 37°C (control), 41°C (heat shock) and 43°C (heat shock) for 1 and 2 hours. Parasite lysates were prepared as previously described and the expression of PFA0660w was analyzed by SDS-PAGE and western blotting as described in section 4.2.4. Glycophorin was used as a loading control as described in section 4.2.5.

4.2.7 Determination of solubility profile of PFA0660w

Parasite pellet (prepared as described in section 4.2.4) was resuspended in non-denaturing lysis buffer (50 mM Tris-Cl, pH 8.0, 300 mM NaCl, 1 mM PMSF, 1 mM EDTA, 0.1% NP-40, and 1µg/ml pepstatin). Following 3 cycles of freeze thawing in liquid nitrogen, the resultant suspension was clarified at 16, 000 x g for 1 hour to separate the supernatant from the pellet. 5x SDS-PAGE loading buffer was added to the supernatant (in ratio 1:4) and the pellet was resuspended in an equivalent volume of 1x SDS-PAGE loading buffer. The suspensions were boiled for 5 minutes, clarified by centrifugation at 16, 000 g for 5 minutes and loaded on the gel. Detection of PfHsp70-1

and glycophorin were used as positive and loading controls respectively. The western analysis was performed as described in section 4.2.4.

4.2.8 Indirect Immunofluorescence assays

For indirect immunofluorescence assays, the 3D7 parasite culture was maintained as previously described (section 4.2.3). The infected erythrocytes were harvested at the trophozoite stage from culture by centrifugation (800 x g for 2 minutes). The cell pellet was washed with PBS and fixed using the paraformaldehyde/glutaraldehyde method (Tonkin *et al.*, 2004). Briefly, infected erythrocytes were fixed by resuspending the cell pellet in PBS containing 4% (w/v) paraformaldehyde and 0.0075% (v/v) glutaraldehyde and incubated at 37°C for 30 minutes with gentle mixing. This was followed by washing for 10 minutes with 125 mM glycine in PBS, followed by centrifugation (1800 x g for 2 minutes) to obtain the pellet. Cell permeabilization was done by resuspending the cell pellet in 0.1% Triton X-100 followed by mixing and centrifugation (1,800 x g for 2 minutes). The cell pellet was incubated briefly with 125 mM glycine in PBS with gentle mixing, washed once with PBS and incubated in blocking buffer (3% (w/v) BSA in PBS) for 2 hours at room temperature, followed by overnight incubation with primary rabbit anti-PFA0660w (1:50) or rabbit anti-PfHsp70-1 (1: 500) antibodies diluted in the blocking buffer at 4°C on a gentle rocking platform. The cells were then washed three times with PBS for 10 minutes. The washed cells were incubated with anti-rabbit DyLight® 488 conjugated secondary antibody (Abcam$^{(R)}$) at 1: 250 dilution in blocking buffer in the dark for 1 hour at room temperature with gentle agitation and washed as earlier described. Hoechst 33258 (50 ng/ml) diluted in PBS was included in the last washing step to stain the nucleus. The cells were spotted onto a microscopy slide in the dark and mounted with glass cover slip using a small drop of Dako mounting medium (Invitrogen, USA). Images were captured using an AxioVert.A1 equipped with Zeiss efficient navigation (ZEN) imaging software (Zeiss, Jena, Germany) operated under the appropriate filter sets. Controls used in this experiment included incubating the fixed parasites with either the primary antibody alone or secondary antibody alone or no antibody. As an alternative, methanol fixation of parasitized erythrocytes (Wickham *et al.*, 2001) was also performed, in which case infected erythrocyte smears prepared on glass slides were fixed briefly with cold methanol. The slides were then blocked by incubation with the blocking buffer and treated with appropriate antibodies as described above. The captured images were processed using the ZEN imaging software and exported as TIF file. To create figures, the TIF files were imported into Microsoft PowerPoint where they were assembled and slides were exported as TIFs.

4.3 Results

4.3.1 Identification of PFA0660w specific peptide

Preliminary analysis of PFA0660w sequence similarity with related *P. falciparum* Hsp40 (PfHsp40) proteins using multiple sequence alignment, percentage similarity and phylogenetic analysis was done as an initial step towards identifying proteins that share high degree of sequence similarity and conservation with PFA0660w. The phylogenetic analysis (Figure 4.1) showed that type II PfHsp40s came from a common root and clustered together, indicating a high level of conservation among these proteins. It is noteworthy that PFA0660w clustered with other two type II PfHsp40 exported proteins, PFB0090c and PFE0055c, and a parasite resident type II PfHsp40 protein, PFB0595w, suggesting possible structural and functional relationships. The level of conservation was confirmed with a multiple sequence alignment (*Appendix G*) and sequence similarity (*Appendix C.5*) which revealed 48.0%, 46.3%, and 44.9% sequence similarity of PFA0660w to PFE0055c, PFB0090c and PFB0595w (PlasmoDB accession number PF3D7_0213100) respectively. More so, PFE0055c which showed the highest percentage of sequence similarity has been shown to be exported into the same J dot as PFA0660w (Külzer *et al.*, 2010). Therefore, the analysis of sequence similarity revealed that PFB0090c, PFE0055c and PFB0595w are closely related to and shared a high degree of sequence conservation with PFA0660w.

Figure 4.2 shows the multiple sequence alignment of PFA0660w with PFB0090c, PFE0055c and PFB0595w. The alignment was used to identify the unique antigenic regions of the amino acid sequence of PFA0660w. The alignment showed a high level of sequence conservation at the N-terminal J domain region and the C-terminal region. The GF-region appears less conserved, indicating a region where a possible peptide that will be specific to PFA0660w could be located. The peptide "DALKQSGFNSSNF" was selected following initial screening. The BLAST search (Altschul *et al.*, 1997) of the peptide "DALKQSGFNSSNF" against relevant data bases (NCBI, PlasmoDB) did not produce any hits, suggesting that the antibodies to be raised may not cross react with any other parasite or human host proteins. The results of the composite analysis as provided by Gene Runner software (version 3.05) (*Appendix B.13*), revealed that a high percentage of the peptide residues possess positive values, indicating a prediction of high antigenicity. These areas also corresponded with Hopp-Wood positive peak (high hydrophilicity), Kyte and Doolittle negative value (high hydrophilicity) and Emini regions of highest surface probability (significant at value > 20). In addition, the peptide generally showed positive values of Karplus-Schultz chain flexibility, indicating a high antigenic determinant.

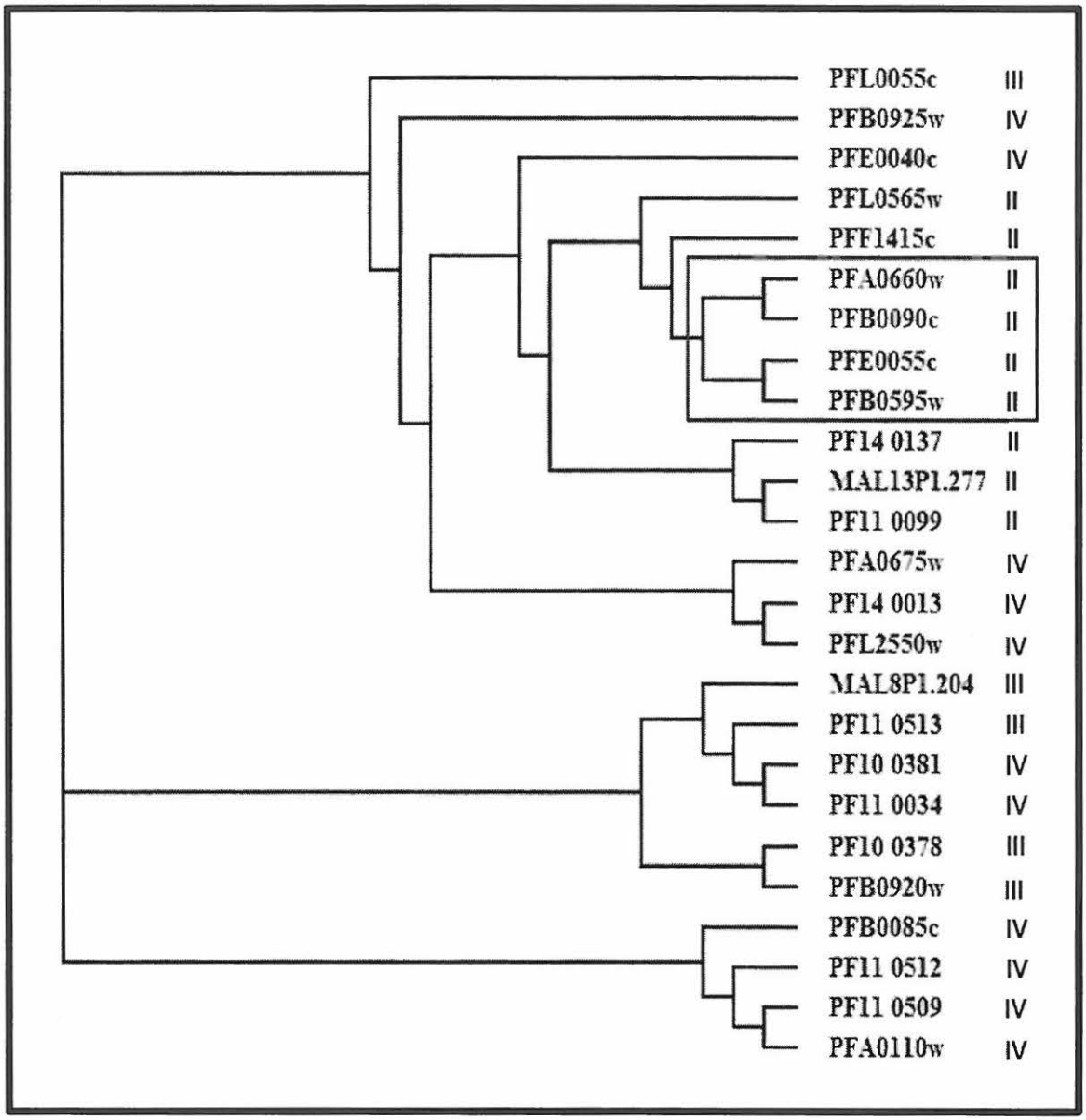

% similarity to PFA0660w	PFE0055c	PFB0090c	PFB0595w	PF11_0099	PFL0565w	PF14_0137	PFF1415c	MAL13P1.277
	48.0	46.3	44.9	43.1	40.3	31.5	27.9	27.7

Figure 4.1: Phylogenetic analysis of type II and other exported PfHsp40s

Multiple sequence alignment used for the reconstruction of the guide tree was generated using ClustalW (Larkin *et al.*, 2007; Thompson *et al.*, 1994). The phylogenetic and molecular evolutionary analyses were conducted using *MEGA* software (version 5) (Tamura *et al.*, 2011). Shown in the blue rectangle are the closely related proteins which clustered together with PFA0660w and showed a high degree of sequence similarity and conservation. The accompanying table shows the percent sequence similarity of PFA0660w with other type II PfHsp40s.

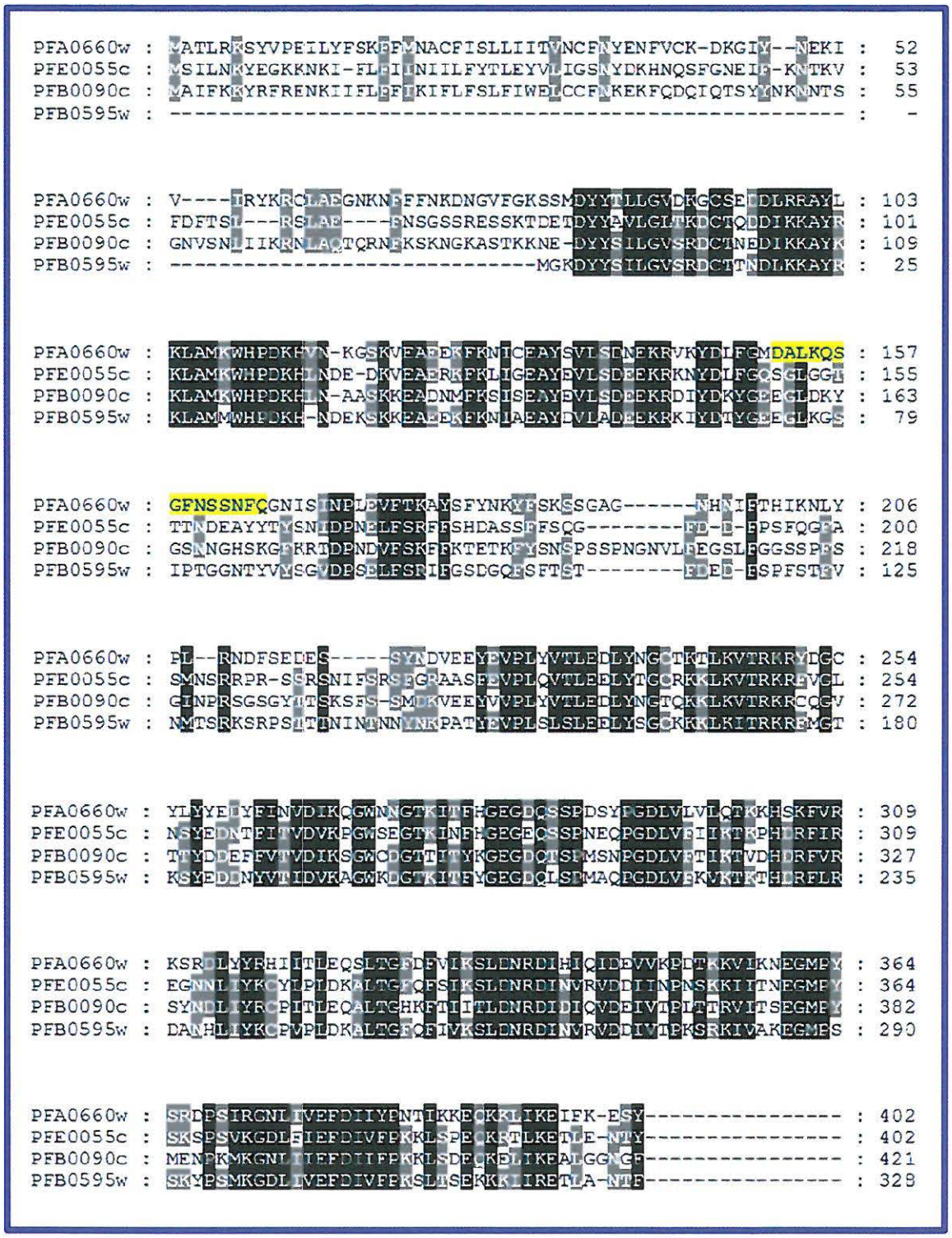

Figure 4.2: Multiple sequence alignment of PFA0660w with PFB0090c, PFE0055c and PFB0595w.

Multiple sequence alignment was generated using ClustalW (Larkin *et al.*, 2007; Thompson *et al.*, 1994) and shading was done using GeneDoc (Larkin *et al.*, 2007; Thompson *et al.*, 1994). The degrees of conservation are indicated by the shadings with the black shading being the sequences with highest degree of conservation. The regions of light shading were less conserved and less identical and these are the regions of potential peptide selection. The selected peptide is highlighted in yellow. The numbers on the right-hand side represent the positions of residues in the respective proteins.

4.3.2 The specificity of anti-PFA0660w peptide antibody

The anti-PFA0660w peptide antibody specificity was first tested using recombinantly expressed and purified His-tagged proteins (Figure 4.3 – Left panel). The 6xHis-tagged proteins used were PFB0595w (38.18 kDa), Hsj1a (31.87 kDa) and PFA0660w (41.3 kDa). Of these, only PFA0660w could be identified with anti-PFA0660w antibodies while reprobing with anti-His showed all of the proteins present (Figure 4.3 – Left panel). The other two exported and closely related proteins (PFB0090c and PFE0055c) could not be included in the study due to lack of availability. Also, no protein was detected when uninfected erythrocytes lysates were probed with anti-PFA0660w. The antibody also detected a single protein with western analysis of the parasite lysate (Figure 4.3 – Right panel), thereby confirming the specificity of the antibody. It can therefore be used for subsequent assays.

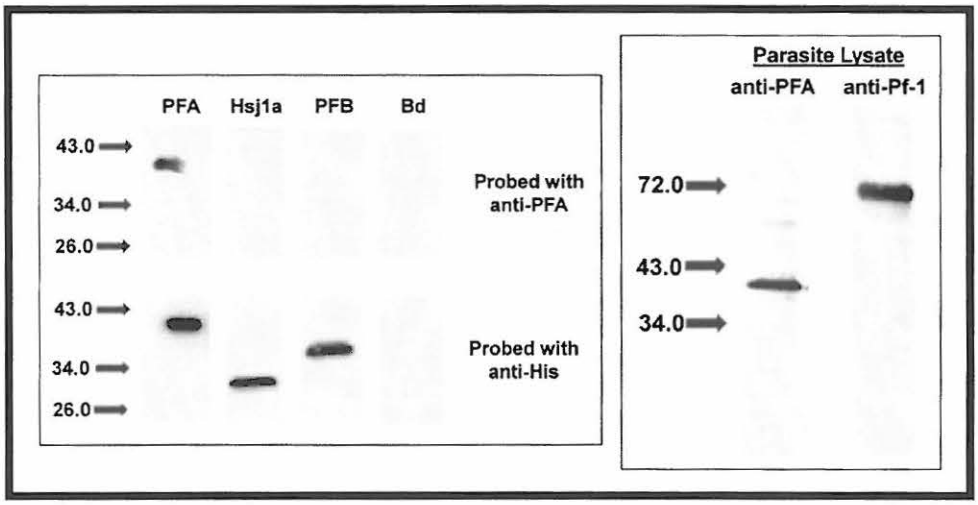

Figure 4.3: The specificity of anti-PFA0660w peptide antibody for PFA0660w
The anti-PFA0660w peptide (anti-PFA) antibody specificity was determined using purified recombinant proteins (PFA0660w (PFA), Hsj1a and PFB0595w (PFB)) as well as uninfected erythrocytes (Bd) and parasite lysate. Western analysis was performed with anti-PFA and anti-His as indicated. The anti-PFA was able to specifically detect only heterologously produced PFA0660w (Left panel) and a signal of high intensity in the parasite lysate (Right panel), suggesting a specificity of antibody. Also, neither of the antibodies produced any band in un-infected erythrocytes (Bd) lysate. Detection of PfHsp70-1 in the total lysate with anti-PfHsp70-1 (anti-Pf-1) was used as positive control. Protein molecular mass marker in kDa is indicated with blue arrows. This experiment was performed at least three times and shown here are the representative western blots.

4.3.3 PFA0660w shows highest expression level at the ring stage

The PFA0660w protein expression profile was studied in a time course experiment in which the detection of glycophorin and PfHsp70-1 served as loading and positive controls respectively. The asexual life cycle is characterized by cyclic re-invasion of new red blood cells (Holder *et al.*, 1994; Cowman and Crabb, 2006). Following sorbitol synchronization at ring stage, the culture was

maintained as detailed in section 4.2.3 and samples were taken 6 hourly over a period of 48 hours of the asexual life cycle of the *P. falciparum*. In this work, the first 6 hours coincided with early schizonts stage and was set as stage 1 in Figure 4.4. The results showed a gradual increase in protein expression, reaching maximum at late ring stage (24 hours – stage 4) and then decreasing to start increasing again after 6 hours (stage 5).

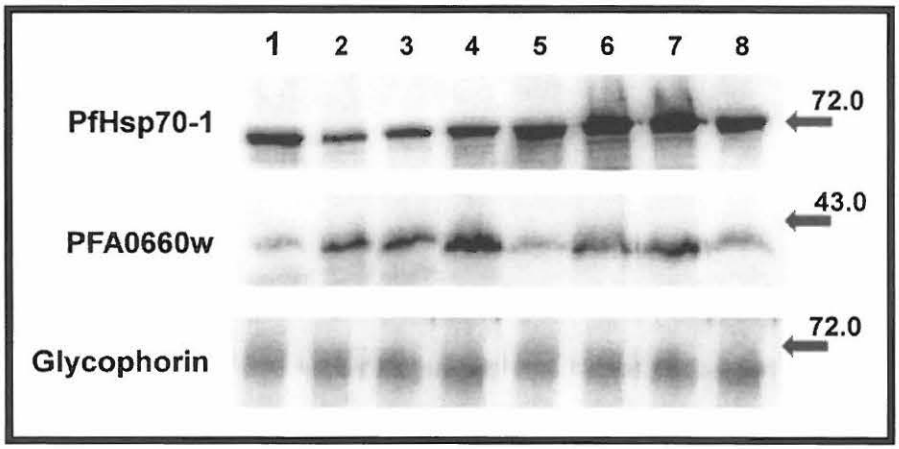

	1	2	3	4	5	6	7	8
PfHsp70-1	6.58	3.40	3.93	5.62	9.44	13.22	12.65	7.90
PFA0660w	1.01	2.23	3.16	6.03	1.33	1.86	3.95	1.89

Figure 4.4: Analysis of PFA0660w expression profile
Expression profile of PFA0660w was determined over a 48 hour intra-erythrocytic/asexual life cycle of the *P. falciparum*. The parasites (3D7) were synchronised at ring stage and the culture was maintained sub-divided in equal volume into 8 culture flasks with each culture representing a time point for sampling. Samples were taken six hourly for 48 hours and total protein lysate from the saponin-permeabilised 3D7 *P. falciparum*-infected erythrocytes was prepared as detailed in experimental section. Equal volume of total protein lysate from each sample was loaded on the gel. Detection of PfHsp70-1 and glycophorin with their respective primary antibodies (anti-PfHsp70-1 and anti-glycophorin) served as positive and loading controls respectively. PFA0660w was detected with anti-PFA0660w peptide antibody and the result showed a gradual increase in expression reaching maximum at late ring stage. Numbering represents parasite intra-erythrocytic developmental stages as follows: 1 and 2 = Early Rings, 3 and 4 = Late Rings, 5 = Early Trophozoites, 6 = Late Trophozoites, 7 = Early Schizonts, 8 = Late Schizonts. Protein molecular mass markers in kDa (blue arrows) are as indicated. The accompany table is the table of normalized values of relative band intensity obtained by dividing the values generated from densitometry analysis (using ImageJ software) of the western bands for PfHsp70-1 and PFA0660w by the corresponding values of glycophorin bands. The experiment was performed at least three times and the images shown are representative of series of western blots

In addition, densitometry analysis was performed (using ImageJ 1.43u software) on the western bands to normalize errors that may have arisen due to loading (Abràmoff *et al.*, 2004; Schneider *et al.*, 2012). The values of relative band intensity for the western lanes were normalized with glycophorin by dividing each sampling time value with the corresponding value of glycophorin (Figure 4.4 – accompany table). The densitometry analysis follows the same trend as the western analysis and appears to correlate well with the gene expression profile (*Appendix B.14*) from PlasmoDB (Le Roch *et al.*, 2003; Aurrecoechea *et al.*, 2009).

4.3.4 PFA0660w is insoluble and showed lack of upregulation upon heat shock

Temperature variation characterizes the life cycle of *P. falciparum*, ranging from 25°C or 26°C in the anopheles mosquito vector and 37°C in humans to 41°C in patients infected with malaria during febrile episodes. Heat shock proteins play important roles in parasite survival during this self induced elevated temperature.

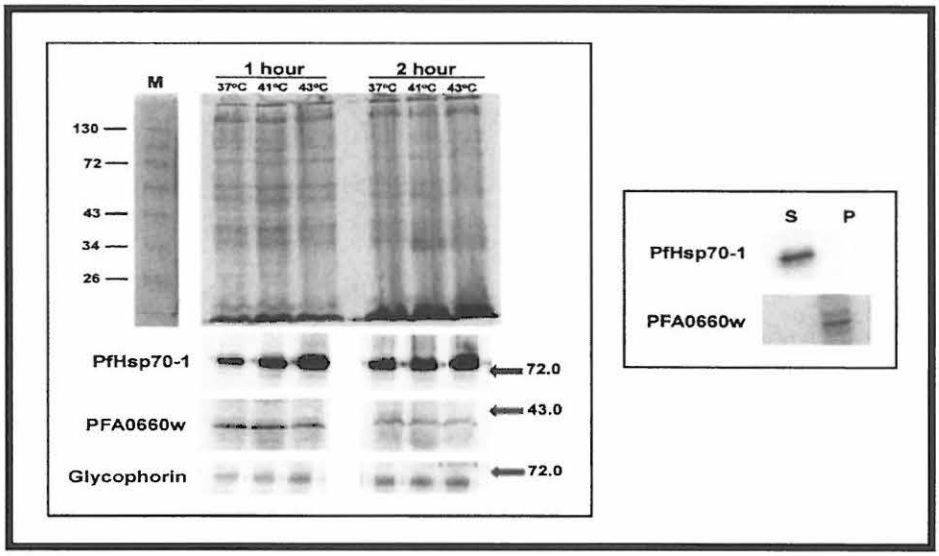

Figure 4.5: Heat shock and solubility analysis of PFA0660w
Left: The SDS-PAGE (upper panel) and western analysis (lower panel) of the heat shock experiment, performed at 41°C and 43°C for one and two hours. The lysis of 3D7 *P. falciparum*-infected erythrocytes was achieved using saponin-permeabilization method and total protein lysate from an equal number of cells was loaded on each lane. Western detection of PfHsp70-1, PFA0660w and glycophorin was done using anti-PfHsp70-1, anti-PFA0660w peptide and anti-glycophorin antibodies respectively. PfHsp70-1 showed an upregulation upon heat shock as expected while PFA0660w did not, indicating lack of response to heat induced stress. Also, a drastic reduction in PFA0660w protein expression at 2 hours compared to1 hour was observed. ***Right:*** The western analysis of the solubility assay using total protein lysate from the saponinpermeabilised 3D7 *P. falciparum*-infected erythrocytes. Equal volume of total protein from the same lysate was loaded on each lane. PFA0660w was seen in the pellet (P), indicating insolubility as opposed to PfHsp70-1 that was found in the supernatant (S), showing high level of solubility. Each experiment was performed at least three times and the images shown are representative of a series of SDS-PAGEs and western blots. Protein molecular mass markers in kDa are indicated with M and blue arrows. Glycophorin is the loading control.

In this study, the effect of heat shock, performed at 37°C, 41°C and 43°C for 1 and 2 hours, on the expression of PFA0660w was examined. At each time point, heat shock did not produce any significant difference in the expression of PFA0660w (Figure 4.5). This suggests that PFA0660w may not be involved in the parasite response to heat induced stress and that elevated temperature could impact negatively on its protein expression. Meanwhile, the result showed an upregulation of PfHsp70-1 upon heat shock consistent with earlier reports (Kumar *et al.*, 1991; Joshi *et al.*, 1992) while glycophorin remained the same. Also, the solubility study revealed that PFA0660w is in the pellet fraction, and this may explain its association with membranous structures (Figure 4.5 - right).

On the other hand, PfHsp70-1 was found in the soluble fraction, indicating a high level of solubility.

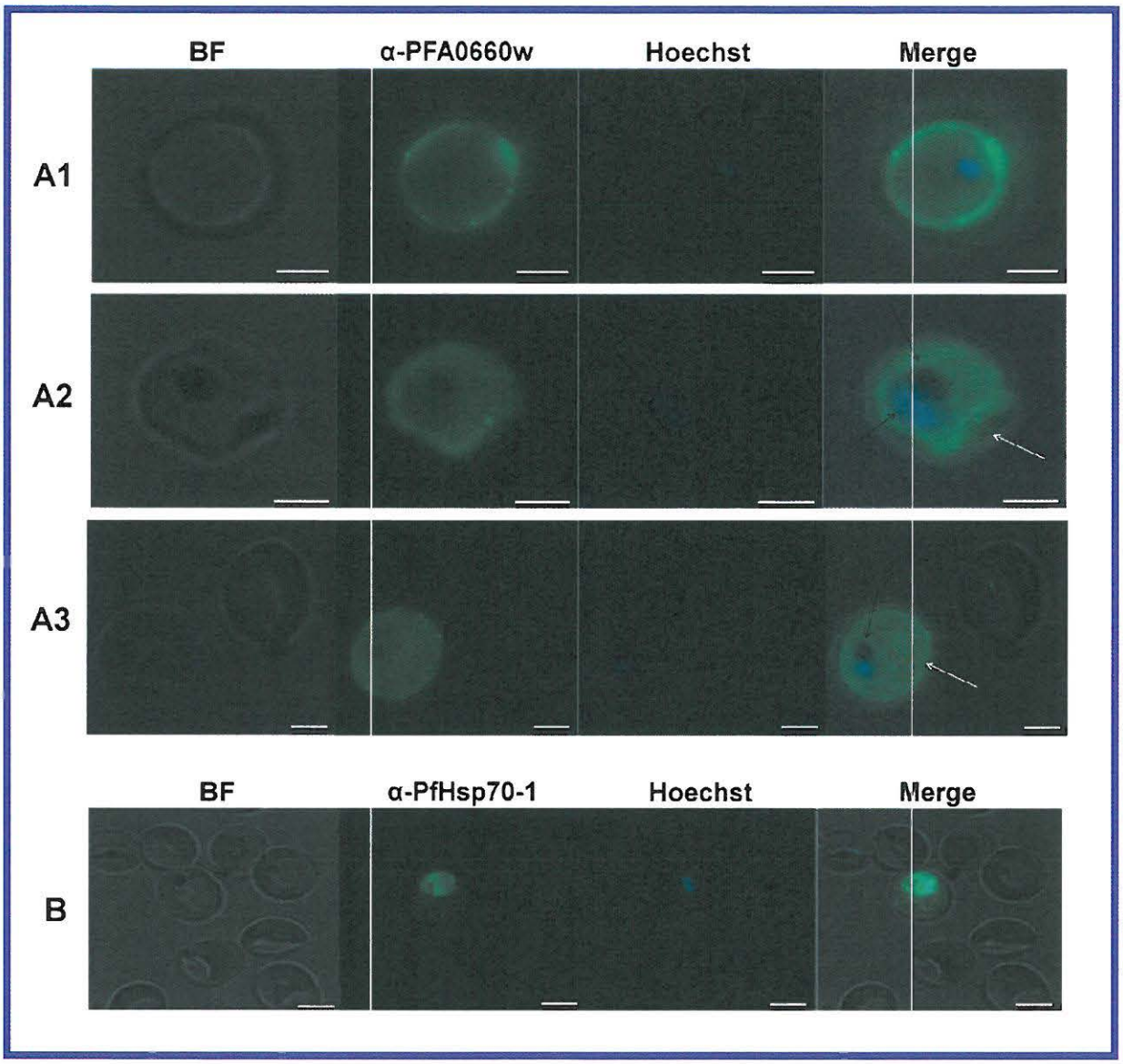

Figure 4.6: PFA0660w was exported to the erythrocyte cytosol in *P. falciparum*-infected erythrocytes

The assay was conducted using paraformaldehyde/glutaraldehyde fixation method on 3D7 *P. falciparum*-infected erythrocytes. A1 to A3 represent samples of images obtained for PFA0660w localisation study using rabbit anti-PFA0660w peptide antibody (1 in 50) and B represents sample of images obtained for PfHsp70-1 localisation study with rabbit anti-PfHsp70-1 antibodies (1 in 500). The detection of the proteins (indicated in green) were achieved following incubation with anti-rabbit DyLight® 488 conjugated secondary antibody (1: 250). Parasite nuclei were stained with Hoechst 33258 (50 ng/ml) (indicated in blue). The bright field (BF) showed the phase contrast images of the parasitized and normal erythrocytes. Merge represents the merged image, indicating PFA0660w (A1 – A3) or PfHsp70-1(B) localisation relative to the parasite nucleus and phase-contrast image. A fluorescence signal was absent in negative controls where primary or secondary antibody only was used. The white size bar in each frame indicates 5 µm. Black arrows indicate the parasite boundary and white arrows indicate the erythrocyte membrane. The detection of PfHsp70-1 was used as a control. PFA0660w showed localisation within the erythrocyte cytosol in the *P. falciparum*-infected erythrocytes and as expected, PfHsp70-1 was localized into the nucleus and cytoplasm of the parasite. This experiment was repeated at least three times, and shown here are representatives of a series of images.

4.3.5 PFA0660w is exported to the erythrocyte cytosol in P. falciparum-infected erythrocyte

Using paraformaldehyde/glutaraldehyde fixation technique and indirect immunofluorescence assays with rabbit anti-PFA0660w peptide antibody, the localisation of PFA0660w was investigated. The localisation of PfHsp70-1 with rabbit anti-PfHsp70-1 antibodies was used as positive control. The export of PFA0660w to the erythrocyte cytosol was determined at the trophozoite stage in *P. falciparum*-infected erythrocytes at an incidence of at least 85 %. Though staining within the parasite cytosol could be seen (especially in panel A3 of Figure 4.6), Figure 4.6 showed a predominantly smooth diffuse staining in the erythrocyte cytosol with some punctuate staining toward the erythrocyte membrane, suggesting the export of PFA0660w into the erythrocyte cytosol.

In comparison, PfHsp70-1 (Figure 4.6 - last panel) is seen localised to the cytosol and nucleus of the parasite as earlier reported (Kumar *et al.*, 1991; Kappes *et al.*, 1993; Pesce *et al.*, 2008; Botha *et al.*, 2011). Supplementary images are given in *Appendix B.15*. When methanol fixation was used (*Appendix B.16*), cytosolic and nuclear staining for PfHsp70-1 was observed as in paraformaldehyde/glutaraldehyde fixation method, the punctuate structures showing the localisation of PFA0660w into the erythrocyte cytosol were clearly distinguishable. However, although methanol fixation method is fast, allowing faster diffusion of the antibodies into the infected erythrocytes, and has the potential to produce good staining, the results showed that methanol appeared to produce artifacts and the erythrocytes appeared crushed, suggesting a harsh environment for both the parasites and the host cells.

4.4 Discussion

The trafficking of proteins into the cytosol of infected erythrocyte by *P. falciparum* is critical for the survival of the parasite in an environment devoid of necessary machinery that can support life. The study of these proteins has become an essential area in drug discovery. Rather than using existing secretory pathways in the host, the parasite has developed unique pathways for protein translocation into the host cytoplasm and assembly of virulence factors into a translocon at the PVM and membranous structures such as Maurer's cleft and the J-dots in the erythrocyte cytoplasm (Trelka *et al.*, 2000; Przyborski *et al.*, 2003; Lanzer *et al.*, 2006; Külzer *et al.*, 2010). PFA0660w and other type II PfHsp40 proteins that were predicted to be exported have been experimentally validated (Külzer *et al.*, 2010, 2012; Acharya *et al.*, 2012). To complement the existing body of knowledge, this study sought to further access the *in vivo* characteristics of PFA0660w using antibodies generated against a unique peptide of the protein. Properties such as surface probability, hydrophobicity and chain flexibility are important in determining the likely antigenic regions of the peptide of interest. In this regard, Jameson-Wolf antigenic index (Jameson and Wolf., 1998) is especially valuable as it combines these properties with secondary structure information to predict the regions of highest antigenicity. Of all the proteins used for the assessment of the specificity of the antibody, only PFA0660w was detected as recombinant protein and in the parasite lysate. Though, recombinant PFB0595w was probed and was not detected, the closeness of the expected molecular mass of PFB0090c (39.83 kDa), PFB0595w (37.36 kDa) and PFE0055c (38.82 kDa) to that of PFA0660w (39.59 kDa) in the parasite lysate makes it difficult to differentiate if the antibody does detect them. However, going by the specificity of the peptide used in the antibodies production for PFA0660w, it can be assumed that the antibody does not cross react with any other protein. Furthermore, uninfected erythrocyte lysates did not produce any band when probed with the anti-PFA0660w peptide specific antibody, thereby confirming lack of cross-reactivity of the antibody and was therefore used for subsequent assays.

It has been reported that PFA0660w expression was detectable around 10 h post-invasion and gradually decreased during the remainder of the developmental 48 h life cycle (Külzer *et al.*, 2010). The results of the expression study revealed a gradual increase in protein expression and it appeared that most of the expression occurred at the ring stage of the parasite development. This appears consistent with the mRNA expression profile (Le Roch *et al.*, 2003). Also, based on the reported expression profiles in PlasmoDB (version 9.2), gene expression profiles of PFA0660w and PfHsp70-x (PF3D7_0831700) (*Appendix B.14*) showed a high degree of correlation. PFA0660w has been shown to possess an inherent ability to suppress aggregation, cooperate with Hsp70s to enhance suppression of aggregation and stimulate the ATPase activity of PfHsp70-x (Section 3.3.1).

The presence of PfHsp70-x in the J-dot and its possible involvement in the transportation of other parasite proteins including PfEMP1 through the erythrocyte cytosol to the surface of the membrane (Külzer *et al.*, 2012), may indicate a partnership where PFA0660w functions to assist PfHsp70-x in ensuring proper delivery of its substrates. The chaperone activity and functional interactions with PfHsp70-x would support a role for PFA0660w in the trafficking of other exported parasite proteins to their final destination within the host erythrocyte. Thus, high correlation of their gene expression profiles may be an indication of this partnership especially since the protein expression profile of PFA0660w also correlated well with its gene expression. Another recent study also demonstrated the association of a parasite encoded knob associated protein (KAHsp40) with components of the knob, including KAHRP, PfEMP1 and PfEMP3 (Acharya *et al.*, 2012). KAHsp40 (PFB0090c), together with PFB0055c and PFB0595w shared a high sequence identity and conservation with PFA0660w (Figure 4.2) and clustered together in a phylogenetic analysis of all the type II and exported PfHsp40s (Figure 4.1). The clustering was consistent with the earlier report on the phylogram of all 44 PfHsp40s (Acharya *et al.*, 2007). Though there was no overlapping distribution of KAHsp40 with J-dots, its association with PfEMP1 which has been shown to be in complex with a J-dot protein, PfHsp70-x (Külzer *et al.*, 2012), does suggest possible complementary functions between KAHsp40 and the J-dot proteins. Such partnership could be a potential target for drug development.

Earlier studies, which exposed the parasite culture to a long duration of elevated temperature, have shown that ring stage parasites can resist high temperatures (up to 41°C) while trophozoites and developing schizonts could not (Anderson *et al.*, 1989; Long *et al.*, 2001). However, in studies that used elevated temperature to mimic febrile episodes, fever-induced cyto-adherence was observed in erythrocytes infected with rings and this was associated with enhanced expression of PfEMP-1 (Udomsangpetch *et al.*, 2002; Aunpad *et al.*, 2009). The expression of some other *P. falciparum* proteins, such as PfHsp40, Pfj4 and PfHsp70-1, has been shown to increase following heat shock (Kumar *et al.*, 1991; Pesce *et al.*, 2008; Misra and Ramachandran, 2009; Botha *et al.*, 2011). Moreover, prior heat shock has been reported to exact stimulatory effect on the development of parasites following subsequent heat shock exposure (Pavithra *et al.*, 2004), implying that repeated febrile episodes in malaria patients has the potential to enhance intra-erythrocytic development. In this study PFA0660w was not induced upon heat shock, suggesting the lack of a role in response to heat stress by the parasite. However, having being shown in a gene knock out study that *PFA0660w* may be essential for the parasite survival (Maier *et al.*, 2008), what the effect of a drastic reduction in expression with time at elevated temperatures (Figure 4.5) will have on its functions and functional relationship with other proteins of parasite and human origin is unclear. It may be

suggested that the reduction in expression is a protective mechanism to keep the gene from the adverse effects of the heat induced stress. The increase in expression of PfHsp70-1 was consistent with earlier reports (Kumar *et al.*, 1991; Pesce *et al.*, 2008; Botha *et al.*, 2011) and implicates a role for PfHsp70-1 in the survival of the parasite during elevated temperature in febrile episodes. Meanwhile, the solubility study revealed that PFA0660w is insoluble, indicating an association with membranous structure. It has been shown that the membrane association of PFA0660w is connected with cholesterol (Külzer *et al.*, 2010), suggesting that cholesterol may have a role to play in its solubility.

The export of parasite proteins takes place across multiple membranes, including endoplasmic reticulum membrane; parasite plasma membrane; parasitophorous vacuole membrane; and red blood cell plasma membrane (Crabb *et al.*, 2010). The roles of some of these soluble and membrane bound exported proteins, especially those that have been characterized, have been reviewed (Maier *et al.*, 2009). Using a transfectant parasite, earlier reports have shown that PFA0660w was localized into the J-dots (Külzer *et al.*, 2010). An attempt was made to access the localisation of PFA0660w using anti-PFA0660w peptide specific antibody in an indirect immunofluorescence assay. The result revealed that the protein was exported into the infected erythrocyte cytosol where it appeared predominantly as smooth diffuse staining with some punctuate staining toward the *P. falciparum*-infected erythrocyte membrane. However, the association of PFA0660w with the J-dots as earlier reported (Külzer *et al.*, 2010) was not determined in this study. Also, though the present study using anti-PFA0660w peptide specific antibody may have confirmed the export of PFA0660w into the erythrocyte cytosol, the predominantly diffuse staining was not consistent with the largely dot-like structures earlier reported (Külzer *et al.*, 2010). This might be due to differences in the approach used, though the use of methanol fixation (*Appendix B.16*) appeared to produce dominant punctuate structures closely related to the reported structure. Furthermore, though the detection of PfHsp70-1 could serve as a parasite-resident marker protein, to adequately assess the localisation of PFA0660w, and by extension the consistency of this study in the light of an earlier report (Külzer *et al.*, 2010), the use of erythrocyte cytosol-resident and membrane markers are inevitable. Such markers could include Maurer's clefts proteins such as STEVOR and MAHRP1 (Spycher *et al.*, 2003; Przyborski and Lanzer, 2005; Saridaki *et al.*, 2008), and membrane proteins such as KAHRP and PfEMP1, which also take residence in Maurer's cleft on their onward translocation to the membrane of the infected erythrocyte (Wickham *et al.*, 2001; Knuepfer *et al.*, 2005). Therefore, the indirect immunofluorescence assay should be regarded as a preliminary attempt at employing anti-PFA0660w peptide specific antibody for the characterisation of PFA0660w and further studies

using the antibodies will be needed to access PFA0660w localisation to the J-dots or other membrane structures and it potential co-localisation partners, especially PfHsp70-x.

Generally, this study has complemented the existing body of knowledge on the *in vivo* characteristics of PFA0660w, including it solubility, expression, and export into the erythrocyte cytosol. The study has provided evidence of the effect of elevated temperatures on the expression of PFA0660w and confirmed the export of PFA0660w into the erythrocyte cytosol of the *P. falciparum*-infected erythrocytes.

CHAPTER FIVE

CONCLUSION AND FUTURE PROSPECTS

In this work, the successful heterologous over-expression and purification of PFA0660w, its biochemical characterisation showing potential interaction with PfHsp70-x, its lack of induction following heat shock and confirmation of its localisation into the cytosol of infected erythrocytes have been presented. The prospects of further exploration of this protein for better understanding of its functions at biochemical and cellular levels and as a potential target for drug actions are here presented.

5.1 Conclusion

This study was aimed at characterizing PFA0660w (PF3D7_0113700) using biochemical and cell biological approaches, with a view to understanding its role in the survival and development of the parasite, and thus, explores it as potential target for drug action. Recombinant PFA0660w was successfully purified from inclusion bodies using *E. coli* M15[pREP4] cells. An unidentified band at the size of DnaK was however observed when *E. coli* BB1994 cells were used. This band can be identified using mass spectroscopy (MS). Various workers have purified proteins from inclusion bodies (Patra *et al.*, 2000; Singh and Panda, 2005), but to the best of our knowledge, this is the first report of an attempt at purifying a plasmodial chaperone from inclusion bodies. Though the main component of the inclusion bodies in recombinant *E. coli* cells is the target protein (Valax and Georgiou, 1993; Carrió and Villaverde, 2002; Vallejo and Rinas, 2004), minor amounts of other cell proteins, contaminants associated with the process of purification (Valax and Georgiou, 1993), co-precipitation of polypeptides that may be unrelated to the target protein (Rinas and Bailey, 1992) and folding assistant proteins such as small heat shock chaperone (IbpA and IbpB) (Kitagawa *et al.*, 2002) could be present in varying concentrations, making detailed assessment of the inclusion bodies essential. Inclusion of washing step ensures that these contaminants are removed. However, in this study, apart from determining the amount of target protein that constitutes the inclusion pellet, a detailed assessment of the inclusion bodies was not undertaken.

Furthermore, with new insights into protein folding, refolding and aggregation there are compelling evidences regarding the biological relevance and reversibility of inclusion bodies (Kazemi-Esfarjani and Benzer, 2000; Carrió and Villaverde, 2001; Hinault *et al.*, 2006; Tyedmers *et al.*, 2010). For instance, biological activity of enzyme-based inclusion bodies has been reported (Tokatlidis *et al.*, 1991; Worrall and Goss, 1989; Peternel and Komel, 2010), and coupled with a high level of secondary structure embodied within the inclusion bodies (Markossian and Kurganov, 2004; García-Fruitós, 2010; García-Fruitós *et al.*, 2012) indicates that properly folded molecules, having full access to the solvent are present in the inclusion bodies. Also, evidence has shown that in the absence of de novo protein synthesis *in vivo*, the disintegration of inclusion bodies resulted into an increase in soluble protein, leading to a corresponding rise in biological activity (Carrió and Villaverde, 2001), further supporting the reversibility of inclusion bodies and the presence of intact secondary structure. Therefore, in the light of these evidences, a more detailed investigation into the formation of inclusion bodies by the plasmodial chaperones expressed in bacterial or other expression systems from both structural and kinetic viewpoints may provide a better understanding of not just the mechanism of chaperone protein aggregation and de-aggregation, but also of the

nature and biological activity of the formed inclusion bodies and the roles of other chaperones in the process. Such assessment may also help to overcome the inherent limitation of having individualised protocols for each protein when purifying from the inclusion bodies. In addition, alternative approaches to expression and purification of PFA0660w may be explored with a view to enhancing its solubility, thereby creating the opportunity for biochemical characterisation at higher concentrations. Such approaches may include the use of an alternative expression system such as yeast, a mammalian or baculovirus/insect cell line, which has the ability to perform post-translational modification (Birkholtz *et al.*, 2008), provided such glycosylation mimics the conditions within the parasite. Others include the use of alternative vector systems that encode solubility fusion tags such as maltose binding protein (MBP) or glutathione S-transferase (GST) fusion tags; and PFA0660w domain based expression and purification which will involve the redesign of domain based coding regions and construction of expression constructs (Terpe, 2003). Domain based purification will make biochemical assessment of individual domains possible. Assessment of different domain functions may help to understand their overall involvement in PFA0660w functional activities. Secondary structure determination using techniques like X-ray crystallography or NMR can also provide information about the functions of PFA0660w. However, the insolubility of PFA0660w may not be unexpected as it has already been shown to be membrane-associated (Külzer *et al.*, 2010).

The biochemical characterisation of PFA0660w provided evidence for potential functional chaperone co-chaperone interactions between PfHsp70-x (PF3D7_0831700) and PFA0660w. However, though the ATPase data provides significant differences in the interaction of PFA0660w with the different Hsp70s and the qualitative analysis of SPR data showed that the interactions are that of a co-chaperone, and that the interaction with PfHsp70-x is potentially the strongest, further work will be needed to quantitatively assess the interaction. Also, though there are evidences that showed that His tag could be retained on protein for functional studies (Ivey and Bruce, 2000; Vassiliev *et al.*, 2002; Derewenda, 2004; Carson *et al.*, 2007; Thielges *et al.*, 2011; Table 2.1), to completely overrule the potential negative effects on protein functional assays as reported (Amor-Mahjoub *et al.*, 2006; Amor-Mahjoub *et al.*, 2006; Song and Markley, 2007; Freydank *et al.*, 2008; Emoto *et al.*, 2009), it may be essential to remove the His tag. Apart from SPR, using other *in vitro* or *in vivo* approaches to study the interaction of PFA0660w with chaperones will be an added advantage. For example, using Isothermal Titration Calorimetry (ITC) complete kinetics as well as thermodynamic parameters can be determined (Brown, 2009; Pagano *et al.*, 2009). The use of ITC is considered a gold standard for measuring biomolecular interactions and will help to overcome the limitations inherent in SPR, confirm the present report and enhance the quality of subsequent data

(Qian *et al.*, 2002). Apart from the advantages of SPR that can also be found in ITC, the added advantages of ITC include lack of buffer restrictions or weight limitation and importantly, there is no need of labeling or immobilisation as required by SPR, since both the ligand and the analyte are in solution, making it an approach of choice for many investigators (Qian *et al.*, 2002; Ball and Maechling, 2009; Brown, 2009; Magotti *et al.*, 2009). Also, *in vivo* approaches such as Green Fluorescent Protein (GFP) fragment reassembly trap system (Wilson *et al.*, 2004; Torrado *et al.*, 2008) and yeast two-hybrid analyses (LaCount *et al.*, 2005) can be employed to study the interaction of PFA0660w with potential chaperone partners.

Furthermore, the present study showed that PFA0660w can function both as chaperone and co-chaperone. Its chaperone activity was revealed by its dose dependent suppression of rhodanese aggregation. It has been reported that ATP enhanced molecular chaperone functions of the small heat shock protein (human αB crystalline) by causing an approximately two fold increase in its ability to reactivate citrate synthase (Muchowski and Clark, 1998). Thus, to further assess this function, chaperone activity can be assessed in the presence of ATP as the aggregation suppression assays are presumed to be in an ATP free environment. The presence of ATP has the potential to differentiate specific from non-specific interactions and enhance the chaperone co-chaperone interaction, thereby ensuring the determination of significant differences in the effect of PFA0660w on the aggregation suppression activity of the chaperones. Also, *in vivo* complementation assay can be considered to assess the ability of PFA0660w to functionally replace another type I Hsp40 in thermosensitive *S. cerevisiae* strain (Ydj1) or in thermosensitive *E. coli* strain (OD259). Importantly, the ability of PFA0660w to function both as chaperone and co-chaperone can be explored as a potential source of drug discovery by screening for potential inhibitors of PFA0660w chaperone activity and functional interaction with PfHsp70-x. However, in this report, the first biochemical evidence for potential interaction of PFA0660w with PfHsp70-x was presented, thereby allowing for further functional studies.

Meanwhile the monomeric nature of PFA0660w raised important questions relating to its functional role and mechanism of actions, relative to other Hsp40s that form dimers. Many investigators have reported that dimer formation is critical to chaperone activity of Hsp40s (Sha *et al.*, 2000; Li *et al.*, 2003, 2006; Wu *et al.*, 2005). For instance, structural elucidation revealed that dimer formation by human Hsp40 proteins (Hsj1 and Hdj1), *E. coli* DnaJ and yeast Hsp40 proteins (Sis1 and Ydj1) is essential for structural stability and chaperone functions (Rüngeling *et al.*, 1999; Toutain *et al.*, 2003; Shi *et al.*, 2005; Wu *et al.*, 2005; Hu *et al.*, 2008). In line with this observation, for the proposed anchoring and docking model of Hsp40 – Hsp70 interaction (Qian *et al.*, 2002) to be

applicable, dimerisation would play an important role in the stability of the interaction complex. Also, the involvement of G/F-rich regions in the formation of dimers in type I and II Hsp40 proteins in solution (Langer *et al.*, 1992; Borges *et al.*, 2005; Ramos *et al.*, 2008), further lend support to the importance of dimerisation to protein functions. Therefore, as a monomer, PFA0660w may possess a different mode of action from those chaperones that form dimers, though the effect of this monomeric state on its role as a molecular chaperone is unclear. However, some reports have shown that proteins can also function in their monomeric state (Or *et al.*, 2005; Hageman *et al.*, 2010; Louw *et al.*, 2010). For instance, a novel *Trypanosoma brucei* type III Hsp40, Tbj1, was reported to function as a monomer in solution (Louw *et al.*, 2010), while SecA, which is involved in the post-translational translocation of proteins in the bacterial inner membrane was reported to function both as monomer and dimer (Jilaveanu *et al.*, 2005; Or *et al.*, 2005). Also, mDj4 (DNAJB6) and mDj6 (DNAJB8) are identified as very potent inhibitors of aggregation and functions as monomers (Hageman *et al.*, 2010). Thus, for PFA0660w, dimer formation may not be important for its functions as a co-chaperone. More so, given the fact that dimer formation helps to maintain the substrate in an unfolded position, prevent aggregation and ensure timely and correct delivery of substrates to the chaperone, the chaperone ability of PFA0660w may compensate for these functions. That is, it may be suggested that since every protein possesses an inherent ability to refold, then like Hsp70s, PFA0660w may also be acting as an unfoldase, thereby maintaining the substrate in it correct conformation for refolding to take place. On the other hand, since dimerisation can occur upon ligand binding (Schlessinger, 2002; Klein *et al.*, 2004), and if anchoring is a necessary step in refolding, dimer formation by PFA0660w may be a functional modification that occurs at the point of substrate transfer to the chaperone. However, structural elucidation of PFA0660w may be needed to confirm these assumptions. Also, FPLC and/or native PAGE can be used to assess dimer formation following binding with partner Hsp70.

The detection of PFA0660w in the parasite lysates, the heat induction and solubility studies as well as localisation to the erythrocyte cytosol in *P. falciparum*-infected erythrocytes serves to complement the existing knowledge on the cellular biology of PFA0660w. Though not expected in this study that uses saponin-permeabilisation technique, the potential loss of protein following membrane disruption by saponin may influence the western results. Percoll-purified infected RBC may be an alternative approach to confirm the western results. Lack of inducibility upon heat shock revealed that PFA0660w might lack a functional role in the parasite's response to heat stress. However, considering that it may be essential to the survival and development of the parasite (Maier *et al.*, 2008), the effects of a drastic reduction in PFA0660w expression with time at elevated temperatures (Figure 4.5) on its functions needs further investigation. While the

immunofluorescence assays in this study confirmed the export of PFA0660w into the erythrocyte cytosol, its localisation into the J-dots as earlier reported (Külzer *et al.*, 2010) or to other membranous structures could not be ascertained due to lack of erythrocyte-resident and membrane proteins markers such as STEVOR, MAHRP1, KAHRP and PfEMP1. Also, in the light of recent reports that showed partial localisation of PfHsp70-x into the PV and erythrocyte cytosol (Külzer *et al.*, 2012; Grover *et al.*, 2013), co-localisation of PFA0660w with PfHsp70-x (a potential chaperone partner) needs to be elucidated. The establishment of co-localisation of PFA0660w with PfHsp70-x may help to address the seemingly contradictory reports on PfHsp70-x localisation, in which a report partially localises PfHsp70-x into the J-dots (Külzer *et al.*, 2012) while the other partially localizes it into the Maurer's cleft (Grover *et al.*, 2013) in the cytosol of the infected erythrocytes.

In general, the experimental validation of the export of the three type II PfHsp40s that were predicted to be exported (Külzer *et al.*, 2010; Acharya *et al.*, 2012), coupled with the export of PfHsp70-x (Külzer *et al.*, 2012; Grover *et al.*, 2013) into the erythrocyte cytosol in *P. falciparum*-infected erythrocytes, especially in complex with PFA0660w into the J-dots (Külzer *et al.*, 2012), make the discoveries detailed in this report very timely. Not only will the information contained in this report provide the much needed background for further study on PFA0660w, but also for its functional relationship with other type II Hsp40 exported proteins and PfHsp70-x, thereby creating impetus for exploring this essential protein in drug discovery.

5.2 Future prospects

The slip and stick gliding motility, Kuppfer cell incapacitation, parasitophorous vacuole (PV) formation in the liver, extremely fast entrance of the released merozoites into the erythrocytes, PV formation in the infected red blood cell and export of virulence factors including molecular chaperones are among the important strategies adopted by the *P. falciparum* parasite to survive and develop in human host (Struik and Riley, 2004; Maier *et al.*, 2008; Goldberg and Cowman, 2010; Montagna *et al.*, 2012). Despite recent advances in the understanding of the biology of *P. falciparum* and the molecular basis of protein trafficking or export systems including the discovery of the PEXEL export motif (Hiller *et al.*, 2004; Marti *et al.*, 2004) and *Plasmodium* translocon of exported proteins (PTEX) complex (De Koning-Ward *et al.*, 2009), both of which are critical for the transport of proteins from the point of production to their final destination, there are still many questions waiting to be addressed. Review articles have been written over the years with a view to direct attention to some of these issues and encourage further investigations (Cooke *et al.*, 2004; Crabb *et al.*, 2010; Deponte *et al.*, 2012). For instance, following the processing of PEXEL in the endoplasmic reticulum (ER), how are these proteins trafficked from the ER to be recognised specifically by the PTEX complex? Also, the discovery of PEXEL negative exported proteins (PNEPs) raised important questions as to how these proteins are processed by the ER (co-translationally or post-translationally), the exact pathways and sequences involved in their export and whether there are more than one export pathways in use by the organism, especially since there is still lack of identifiable consensus sequences needed for their export, and the fact that PEXEL-like sequences in some members of PNEPs do not behave like classical PEXEL motif (Crabb *et al.*, 2010; Deponte *et al.*, 2012). Therefore, understanding the export processes is crucial not only to better understand the biology of the infection, but also to explore the export system as an attractive target for pharmacotherapeutic intervention. Using PFA0660w and its potential interacting partner, PfHsp70-x, as templates, my future interest in the field of plasmodial chaperone will focus on attempting to provide answer(s) to some of these questions by focusing on the following:

5.2.1 Determination of the mechanism of proteins translocation through the plasma membrane and then the PVM to the erythrocyte cytosol.

The proteins destined for export have to overcome membrane barriers before getting to their final destinations. Many of the proteins predicted or validated to be exported contained a PEXEL/HT motif which is cleaved by Plasmepsin V (Boddey *et al.*, 2009; Russo *et al.*, 2010). The prevention

of export of identical mature proteins (whose PEXEL was cleaved by another protease) to the erythrocyte, suggests a role for Plasmepsin V in directing the protein into the desired export pathway (Boddey *et al.*, 2009, 2010). However, how the decision to export is taken and translated to the PVM is still largely a matter of speculation. Also, processed proteins from the ER are deposited into the PV from where those that are to be exported are recognized by the PTEX located on the parasitophorous vacuole membrane (PVM). It has been suggested that for the protein to cross the PVM it will be unfolded and then extruded through a pore across the (PVM) into the cytosol of the erythrocyte by the PTEX complex. While this model system may be suitable for soluble proteins, it does raise questions as to the fate of membrane bound proteins. Though it has been suggested that such proteins may be synthesized as soluble proteins and transported in that manner across the PVM to the host cytosol where they assume membrane-bound topology (Saridaki *et al.*, 2008, 2009), other reports showed that these proteins have already entered a membrane bound topology in the ER membrane (Günther *et al.*, 1991; Przyborski and Lanzer, 2005; Przyborski *et al.*, 2005). Therefore, how proteins with membrane bound topology manage to traverse the parasite plasma membrane, PVM and across to the cytosol of erythrocytes are still unclear. More so, as earlier stated, the lack of identifiable consensus sequences and lack of correlation of the activity between PEXEL-like sequences and the classical PEXEL motif in PNEPs (Crabb *et al.*, 2010; Deponte *et al.*, 2012) showed that there is more to be learnt on the mechanism of protein translocation. It will be interesting to discover the following:

i. If all exported proteins make use of the same pathways as they travel to the erythrocyte cytosol or if multiple pathways exist with each pathway dedicated to different categories of proteins.
ii. The 'Pexalase' protease that is said to be responsible for the cleavage of the PEXEL motif
iii. Consensus sequences for PNEPs and their mechanism of translocation across membranes. So far, no such sequence has been found and it appears that the secondary structure at the N-terminus may be the most important determinant of the protein export.
iv. Mechanism of PTEX functions and how it's able to specifically identify proteins destined for export.
v. The process of decision making on which protein is to be exported at any particular time and circumstances and how this is transmitted to the PTEX for appropriate actions
vi. Difference and/or similarities in the parasite handling of exported soluble and membrane bound proteins

vii. Possible involvement of host chaperones in the process of protein translocation across the PVM

5.2.2 Assessment of possible interaction of plasmodial and host chaperones or co-chaperone (Hsp40 or Hsp70) with the translocon

The discovery of *Plasmodium* translocon of exported proteins (PTEX) complex as an important structure in protein trafficking was recently reported (De Koning-Ward *et al.*, 2009). PTEX consists of a multimeric protein complex that are located in the PVM and found to be specific to genus *Plasmodium*, being the only PEXEL protein containing organisms (De Koning-Ward *et al.*, 2009; Crabb *et al.*, 2010;). It is made up of five proteins; EXP2, HSP101, PTEX150, PTEX88 and TRX2. HSP101 and PTEX150 are said to form homo-oligomeric complexes that can create connection with oligomeric EXP2 (De Koning-Ward *et al.*, 2009). EXP2 has been suggested to be responsible for pore formation in the PVM from where the exported proteins cross to the cytosol of the infected erythrocytes (De Koning-Ward *et al.*, 2009; Bullen *et al.*, 2012). PTEX88 and TRX2 are less abundant and may perform regulatory roles. While the PTEX complex has the capacity to specifically identify, and process proteins destined for export across the PVM, the component(s) of the complex that is/are responsible for such identification and possible binding of the proteins is(are) yet to be determined. Also, there is no evidence for an interaction of any Hsp40 or Hsp70 (host or parasite) with the translocon. The availability of such evidence will better our understanding of proteins trafficking process and could serve as potential target for drug action.

5.2.3 Structural elucidation of plasmodial chaperones and co-chaperones

The knowledge of the protein structure plays an important role in the determination of their functions. Proteins of different families, though diverged from a common ancestor, evolved with different domain combinations and organizations (Bork, 1991; Doolittle, 1995; Vogel *et al.*, 2004; Basu *et al.*, 2008). Domains in proteins are functional units with three-dimensional (3D) structures and through the mechanism of gene shuffling can move within and across biological systems (George and Heringa, 2002). Protein structures are essential for *in silico* drug design, experimental design to determine proteins functional mechanisms and for understanding disease conditions and mutations. Therefore, for structural determination aiming at gaining insight into the functions of the proteins, an understanding of their domain organization and structure are very essential. X-ray

crystallography and Nuclear magnetic resonance (NMR) spectroscopy have been used as experimental techniques for the determination of protein structures (Model, 1998; Jelsch *et al.*, 2000; Accordingly and Boxes, 2006; Otting, 2010; Thibault and Elser, 2010). The use of electron crystallography and single particle reconstruction has brought improvement to structural determination (Auer, 2000; Tao and Zhang, 2000; Ruprecht and Nield, 2001). Using these techniques, structural determinations of some chaperones from other organism like *E. coli* and yeast have been reported (Pellecchia *et al.*, 1996; Martinez-Yamout *et al.*, 2000; Li *et al.*, 2003; Jiang *et al.*, 2005; Shi *et al.*, 2005; Wu *et al.*, 2005). For example, the structural elucidation of the C-terminal fragment of *E. coli* DnaJ and yeast Hsp40 Ydj1 revealed the importance of these sequences for dimerisation and chaperone functional activity. Furthermore, though difficulties in experimental determinations of protein structures have made comparative or homology modeling an alternative approach to structural determination, homology modeling depends on the availability of a template with high percent of sequence similarity with the target proteins, and that being evolutionarily connected, will display similar structural features. Presently, homology modeling of plasmodial proteins depends largely on template proteins derived from other organisms, which is not always available. For instance, an attempt to model the GF region of PFA0660w in this study was not possible for lack of a suitable template. Therefore, the use of homology modeling will also be enhanced with the availability of plasmodial chaperones structures that have been experimentally validated. However, to date, there is no structural data for any plasmodial chaperone.

5.2.4 Trafficking of Proteins within and across the membrane of infected erythrocytes

Following successful export of proteins into the cytosol of the infected erythrocyte, proteins have to move to their final destinations where they are needed. Since the host cell lack necessary organelles for such trafficking, the parasite generates a series of membranous structures during the stages of its development. The structures that have been identified include the well characterized Maurer's cleft together with the tubovesicular network (TVN) (Lanzer *et al.*, 2006; Przyborski *et al.*, 2003; Bhattacharjee *et al.*, 2008), the electron dense vesicles (EDV) and vesicle-like structures (VLS) (Taraschi *et al.*, 2000; Trelka *et al.*, 2000; Wickert *et al.*, 2003) and the J-dots (Külzer *et al.*, 2010). Many proteins have been reported to localize or transiently localize into Maurer's cleft including KAHRP, PfEMP3 and PfEMP1 (Crabb *et al.*, 1997; Waterkeyn *et al.*, 2000; Knuepfer *et al.*, 2005). It appears that Maurer's cleft could serve as gate keeper and reservoir from where exported proteins are trafficked to their final destination. This might explain the seemingly contradictory localisation

of PfHsp70-x to Maurer's cleft and J-dots. For instance, it has been suggested that KAHRP, PfEMP3 and PfEMP1 may assemble at Maurer's cleft into a "cytoadherance complex" from where they are trafficked to the erythrocyte membrane (Wickham *et al.*, 2001). However, the exact sequence requirements for targeting these proteins to Maurer's cleft are yet to be determined. Vesicle-like structures (VLS) are numerous and could be found freely in the erythrocyte cytoplasm connected to Maurer's cleft (Bannister *et al.*, 2004; Hanssen *et al.*, 2008b). Proteins such as REX1 and SBP1 have been localized to this structure (Hanssen *et al.*, 2008a, 2008b). J-dots were recently discovered and PFE0055c, PfHsp70-x and PFA0660w (the focus of this research) have been localized to this structure (Külzer *et al.*, 2010, 2012). Going by its characteristic features, it is very unlikely that J-dots have any connection with Maurer's cleft. However, no trafficking motif for targeting of exported proteins to J-dots has been identified to date. Therefore, further studies aimed at understanding protein trafficking within the erythrocyte and to their final destination will help to shed light on their targeting requirements, determine their exact location, and improve our understanding of the potential multi-functional nature of these proteins.

REFERENCES

Abdiche, Y., Malashock, D., Pinkerton, A., and Pons, J. (2008): Determining kinetics and affinities of protein interactions using a parallel real-time label-free biosensor, the Octet. *Analytical Biochemistry*, *377*(2), 209–17.

Abràmoff, M. D., Hospitals, I., Magalhães, P. J., and Abràmoff, M. (2004): Image processing with ImageJ. *Biophotonics International*, *11*(7), 36–42.

Accordingly, V., and Boxes, I. (2006): Principles of X-ray diffraction. *Acta Physica Sinica*, *55*, 1–42.

Acharya, P., Chaubey, S., Grover, M., and Tatu, U. (2012): An exported heat shock protein 40 associates with pathogenesis-related Knobs in *Plasmodium falciparum* infected erythrocytes. *PloS one*, *7*(9), e44605 (1–11).

Acharya, P., Kumar, R., and Tatu, U. (2007): Chaperoning a cellular upheaval in malaria: Heat shock proteins in *Plasmodium falciparum*. *Molecular and Biochemical Parasitology*, *153*(2), 85–94.

Adisa, A., Rug, M., Klonis, N., Foley, M., Cowman, A. F., and Tilley, L. (2003): The signal sequence of exported protein-1 directs the green fluorescent protein to the parasitophorous vacuole of transfected malaria parasites. *The Journal of Biological Chemistry*, *278*(8), 6532–6542.

Adjuik, M., Agnamey, P., Babiker, A., Borrmann, S., Brasseur, P., Cisse, M., Cobelens, F., Diallo, S., Faucher, J. F., and Garner, P. *et al.* (2002): Amodiaquine-artesunate versus amodiaquine for uncomplicated *Plasmodium falciparum* malaria in African children: a randomised, multicentre trial. *Lancet*, *359*, 1365–1372.

Aikawa, M., Torii, M., Sjölander, A., Berzins, K., Perlmann, P., and Miller, L. H. (1990): Pf155/RESA antigen is localized in dense granules of *Plasmodium falciparum* merozoites. *Experimental Parasitology*, *71*(3), 326–9.

Alessandro, A. D., Righetti, P. G., and Zolla, L. (2010): The red blood cell proteome and interactome : An update. *Journal of Proteome Research*, *9*, 144–163.

Alexander, D. L., Arastu-Kapur, S., Dubremetz, J. F., and Boothroyd, J. C. (2006): *Plasmodium falciparum* AMA1 binds a rhoptry neck protein homologous to TgRON4, a component of the moving junction in Toxoplasma gondii. *Eukaryotic Cell*, *5*, 1169–1173.

al-Herran, S., and Ashraf, W. (1998): Physiological consequences of the over-production of *E. coli* truncated molecular chaperone DnaJ. *FEMS Microbiology Letters*, *162*(1), 117–122.

Allan, R. K., Mok, D., Ward, B. K., and Ratajczak, T. (2006): Modulation of chaperone function and cochaperone interaction by novobiocin in the C-terminal domain of Hsp90: evidence that

coumarin antibiotics disrupt Hsp90 dimerisation. *The Journal of Biological Chemistry*, *281*(11), 7161–71.

Alleva, L. M., and Kirk, K. (2001): Calcium regulation in the intraerythrocytic malaria parasite *Plasmodium falciparum*. *Molecular and Biochemical Parasitology*, *117*(2), 121–8.

Alonso, P. L., Brown, G., Arevalo-Herrera, M., Binka, F., Chitnis, C., Collins, F., Doumbo, O. K., Greenwood, B., Hall, B. F., Levine, M. M., Mendis, K., Newman, R. D., Plowe, C. V, Rodríguez, M. H., Sinden, R., Slutsker, L., and Tanner, M. (2011): A research agenda to underpin malaria eradication. *PLoS medicine*, *8*(1), 9.

Altschul, S. F., Madden, T. L., Schäffer, A. A., Zhang, J., Zhang, Z., Miller, W., and Lipman, D. J. (1997): Gapped BLAST and PSI-BLAST: a new generation of protein database search programs. *Nucleic Acids Research*, *25*(17), 3389–3402.

Aly, A. S. I., Mikolajczak, S. A., Rivera, H. S., Camargo, N., Jacobs-Lorena, V., Labaied, M., Coppens, I., and Kappe, S. H. I. (2008): Targeted deletion of SAP1 abolishes the expression of infectivity factors necessary for successful malaria parasite liver infection. *Molecular Microbiology*, *69*(1), 152–163.

Amino, R., Thiberge, S., Martin, B., Celli, S., Shorte, S., Frischknecht, F., and Ménard, R. (2006): Quantitative imaging of *Plasmodium* transmission from mosquito to mammal. *Nature medicine*, *12*(2), 220–224.

Amor-Mahjoub, M., Suppini, J.-P., Gomez-Vrielyunck, N., and Ladjimi, M. (2006): The effect of the hexahistidine-tag in the oligomerization of HSC70 constructs. *Journal of chromatography B*, *844*(2), 328–334.

Anderson, R. M., May, R., and Gupta, S. (1989): Non-linear phenomena in host-parasite interactions. *Parasitology*, *99*, S59–S79.

André, F. E. (2003): Vaccinology: past achievements, present roadblocks and future promises. *Vaccine*, *21*(7-8), 593–595.

Angov, E., Hillier, C. J., Kincaid, R. L., and Lyon, J. A. (2008): Heterologous protein expression is enhanced by harmonizing the codon usage frequencies of the target gene with those of the expression host. *PloS one*, *3*(5), e2189 (1–10).

Angov, E., Legler, P. M., and Mease, R. M. (2011): Adjustment of codon usage frequencies by codon harmonisation improves protein expression and folding. *Methods in molecular biology*, *705*, 1–13.

Annoura, T., Ploemen, I. H., van Schaijk, B. C., Sajid, M., Vos, M. W., van Gemert, G. J., Chevalley-Maurel, S., Franke-Fayard, B. M., Hermsen, C. C., Gego, A., Franetich, J. F., Mazier, D., Hoffman, S. L., Janse, C. J., Sauerwein, R. W., and Khan, S. M. (2012): Assessing

the adequacy of attenuation of genetically modified malaria parasite vaccine candidates. *Vaccine*, *30*(16), 2662–70.

Ansorgea, I., Paprotkaa, K., Bhakdib, S., and Lingelbacha, K. (1997): Permeabilization of the erythrocyte membrane with streptolysin O allows access to the vacuolar membrane of *Plasmodium falciparum* and a molecular analysis of membrane topology. *Molecular and Biochemical Parasitology*, *84*(2), 259–261.

Aponte, J. J., Menendez, C., Schellenberg, D., Kahigwa, E., Mshinda, H., Vountasou, P., Tanner, M., and Alonso, P. L. (2007): Age interactions in the development of naturally acquired immunity to *Plasmodium falciparum* and its clinical presentation. *PLoS medicine*, *4*(7), e242.

Arias, M., Quijano, J. C., Haridas, V., Gutterman, J. U., and Lemeshko, V. V. (2010): Red blood cell permeabilization by hypotonic treatments, saponin, and anticancer avicins. *Biochimica et biophysica acta*, *1798*(6), 1189–1196.

Arnold, K., Bordoli, L., Kopp, J., and Schwede, T. (2006): The SWISS-MODEL workspace: a web-based environment for protein structure homology modelling. *Bioinformatics*, *22*(2), 195–201.

Arrondo, J. L., and Goñi, F. M. (1999): Structure and dynamics of membrane proteins as studied by infrared spectroscopy. *Progress in Biophysics and Molecular Biology*, *72*(4), 367–405.

Arrondo, J. L., Muga, a, Castresana, J., and Goñi, F. M. (1993): Quantitative studies of the structure of proteins in solution by Fourier-transform infrared spectroscopy. *Progress in Biophysics and Molecular Biology*, *59*(1), 23–56.

Artavanis-Tsakonas, K., Tongren, J. E., and Riley, E. M. (2003): The war between the malaria parasite and the immune system: immunity, immunoregulation and immunopathology. *Clinical and experimental immunology*, *133*(2), 145–152.

Auer, M. (2000): Three-dimensional electron cryo-microscopy as a powerful structural tool in molecular medicine. *Journal of molecular medicine*, *78*(4), 191–202.

Aunpad, R., Somsri, S., Na-Bangchang, K., Udomsangpetch, R., Mungthin, M., Adisakwattana, P., and Chaijaroenkul, W. (2009): The effect of mimicking febrile temperature and drug stress on malarial development. *Annals of clinical microbiology and antimicrobials*, *8*, 19.

Aurrecoechea, C., Brestelli, J., Brunk, B. P., Dommer, J., Fischer, S., Gajria, B., Gao, X., Gingle, A., Grant, G., Harb, O. S., Heiges, M., Innamorato, F., Iodice, J., Kissinger, J. C., Kraemer, E., Li, W., Miller, J. A., Nayak, V., Pennington, C., Pinney, D. F., Roos, D. S., Ross, C., Stoeckert, C. J., Treatman, C., and Wang, H. (2009): PlasmoDB: a functional genomic database for malaria parasites. *Nucleic Acids Research*, *37*(Database issue), D539–D543.

Awad, W., Estrada, I., Shen, Y., and Hendershot, L. M. (2008): BiP mutants that are unable to interact with endoplasmic reticulum DnaJ proteins provide insights into interdomain

interactions in BiP. *Proceedings of the National Academy of Sciences, USA*, *105*(4), 1164–1169.

Baca, A. M., and Hol, W. G. (2000): Overcoming codon bias: a method for high-level overexpression of *Plasmodium* and other AT-rich parasite genes in *Escherichia coli*. *International journal for parasitology*, *30*(2), 113–8.

Baird, J. K. (1995): Host age as a determinant of naturally acquired immunity to *Plasmodium falciparum*. *Parasitology today*, *11*(3), 105–11.

Baker, T. A., Grossman, A. D., and Gross, C. A. (1984): A gene regulating the heat shock response in *Escherichia coli* also affects proteolysis. *Proceedings of the National Academy of Sciences, USA*, *81*(21), 6779–6783.

Ball, V., and Maechling, C. (2009): Isothermal microcalorimetry to investigate non specific interactions in biophysical chemistry. *International journal of molecular sciences*, *10*(8), 3283–3315.

Ballou, W. R. (2009): The development of the RTS,S malaria vaccine candidate: challenges and lessons. *Parasite immunology*, *31*(9), 492–500.

Banerjee, R., Liu, J., Beatty, W., Pelosof, L., Klemba, M., and E, G. D. (2002): Four plasmepsins are active in the *Plasmodium falciparum* food vacuole, including a protease with an active-site histidine. *Proceedings of the National Academy of Sciences, USA*, *99*, 990–995.

Baneyx, F. (1999): Recombinant protein expression in *Escherichia coli*. *Current opinion in biotechnology*, *10*, 411–421.

Bannister, L. H., Hopkins, J. M., Margos, G., Dluzewski, A. R., and Mitchell, G. H. (2004): Three-dimensional ultrastructure of the ring stage of *Plasmodium falciparum*: Evidence for export pathways. *Microscopy and microanalysis*, *10*(5), 551–562.

Banumathy, G., Singh, V., and Tatu, U. (2002): Host chaperones are recruited in membrane-bound complexes by *Plasmodium falciparum*. *The Journal of Biological Chemistry*, *277*(6), 3902–3912.

Barale, J. C., Candelle, D., Attal-Bonnefoy, G., Dehoux, P., Bonnefoy, S., Ridley, R., Pereira Da Silva, L., and Langsley, G. (1997): *Plasmodium falciparum* AARP1, a giant protein containing repeated motifs rich in asparagine and aspartate residues, is associated with the infected erythrocyte membrane. *Infection and Immunity*, *65*(8), 3003–3010.

Barillas-Mury, C., and Kumar, S. (2005): *Plasmodium*-mosquito interactions: a tale of dangerous liaisons. *Cellular microbiology*, *7*(11), 1539–45.

Barouch, W., Prasad, K., Greene, L., and Eisenberg, E. (1997): Auxilin-induced interaction of the molecular chaperone Hsc70 with clathrin baskets. *Biochemistry*, *36*(14), 4303–4308.

Barth, A. (2000): The infrared absorption of amino acid side chains. *Progress in Biophysics and Molecular Biology*, *74*, 141–173.

Baruch, D. I., Pasloske, B. L., Singh, H. B., Bi, X., Ma, X. C., Feldman, M., Taraschi, T. F., and Howard, R. J. (1995): Cloning the *P. falciparum* gene encoding PfEMP1, a malarial variant antigen and adherence receptor on the surface of parasitized human erythrocytes. *Cell*, *82*(1), 77–87.

Basha, E., Lee, G. J., Demeler, B., and Vierling, E. (2004): Chaperone activity of cytosolic small heat shock proteins from wheat. *The Federation of European Biochemical Societies Journal*, *271*(8), 1426–1436.

Basu, M. K., Carmel, L., Rogozin, I. B., and Koonin, E. V. (2008): Evolution of protein domain promiscuity in eukaryotes. *Genome Research*, *18*(3), 449–461.

Baum, J., Richard, D., Healer, J., Rug, M., Krnajski, Z., Gilberger, T.-W., Green, J. L., Holder, A. A., and Cowman, A. F. (2006): A conserved molecular motor drives cell invasion and gliding motility across malaria life cycle stages and other apicomplexan parasites. *The Journal of Biological Chemistry*, *281*(8), 5197–5208.

Beaudoin, R. L., and Aikawa, M. (1968): Primaquine-Induced Changes in Morphology of Exoerythrocytic Stages of Malaria. *Science*, *160*(3833), 1233–1234.

Behr, C., Sarthou, J. L., Rogier, C., Trape, J. F., Dat, M. H., Michel, J. C., Aribot, G., Dieye, A., Claverie, J. M., and Druihle, P. (1992): Antibodies and reactive T cells against the malaria heat-shock protein Pf72/Hsp70-1 and derived peptides in individuals continuously exposed to *Plasmodium falciparum*. *Journal of Immunology*, *149*(10), 3321–3330.

Bhanot, P., Schauer, K., Coppens, I., and Nussenzweig, V. (2005): A surface phospholipase is involved in the migration of *Plasmodium* sporozoites through cells. *The Journal of Biological Chemistry*, *280*(8), 6752–6760.

Bhattacharjee, S., Van Ooij, C., Balu, B., Adams, J. H., and Haldar, K. (2008): Maurer's clefts of *Plasmodium falciparum* are secretory organelles that concentrate virulence protein reporters for delivery to the host erythrocyte. *Blood*, *111*(4), 2418–26.

Bhattacharyya, a M., and Horowitz, P. M. (2001): The aggregation state of rhodanese during folding influences the ability of GroEL to assist reactivation. *The Journal of Biological Chemistry*, *276*(31), 28739–43.

Billker, O., Dechamps, S., Tewari, R., Wenig, G., Franke-Fayard, B., and Brinkmann, V. (2004): Calcium and a calcium-dependent protein kinase regulate gamete formation and mosquito transmission in a malaria parasite. *Cell*, *117*(4), 503–514.

Billker, O., Lindo, V., Panico, M., Etienne, A. E., Paxton, T., Dell, A., Rogers, M., Sinden, R. E., and Morris, H. R. (1998): Identification of xanthurenic acid as the putative inducer of malaria development in the mosquito. *Nature*, *392*(6673), 289–292.

Billker, O., Shaw, M. K., Margos, G., and Sinden, R. E. (1997): The roles of temperature, pH and mosquito factors as triggers of male and female gametogenesis of *Plasmodium berghei in vitro*. *Parasitology*, *115 (Pt 1*(Pt 1), 1–7.

Birkholtz, L.-M., Blatch, G., Coetzer, T. L., Hoppe, H. C., Human, E., Morris, E. J., Ngcete, Z., Oldfield, L., Roth, R., Shonhai, A., Stephens, L., and Louw, A. I. (2008): Heterologous expression of plasmodial proteins for structural studies and functional annotation. *Malaria Journal*, *7*(1), 197.

Biswas, S., Saxena, Q. B., Roy, A., Sharma, V. P., Lambros, C., and Vanderberg, J. P. (1979): Synchronization of *Plasmodium falciparum* erythrocytic stages in culture. *Journal of Parasitology*, *65*(3), 418–420.

Blauer, G., and Akkawi, M. (1997): Investigations of B- and beta-hematin. *Journal of Inorganic Biochemistry*, *66*, 145–152.

Blisnick, T., Morales Betoulle, M. E., Barale, J. C., Uzureau, P., Berry, L., Desroses, S., Fujioka, H., Mattei, D., and Braun Breton, C. (2000): Pfsbp1, a Maurer's cleft *Plasmodium falciparum* protein, is associated with the erythrocyte skeleton. *Molecular and Biochemical Parasitology*, *111*(1), 107–121.

Boddey, J. A., Hodder, A. N., Günther, S., Gilson, P. R., Patsiouras, H., Kapp, E. A., Pearce, J. A., De Koning-Ward, T. F., Simpson, R. J., Crabb, B. S., and Cowman, A. F. (2010): An aspartyl protease directs malaria effector proteins to the host cell. *Nature*, *463*(7281), 627–631.

Boddey, J. A., Moritz, R. L., Simpson, R. J., and Cowman, A. F. (2009): Role of the *Plasmodium* Export element in trafficking parasite proteins to the infected erythrocyte. *Traffic Copenhagen Denmark*, *10*(3), 285–299.

Bondos, S. E., and Bicknell, A. (2003): Detection and prevention of protein aggregation before, during, and after purification. *Analytical Biochemistry*, *316*(2), 223–231.

Bordoli, L., Kiefer, F., Arnold, K., Benkert, P., Battey, J., and Schwede, T. (2009): Protein structure homology modeling using SWISS-MODEL workspace. *Nature Protocols*, *4*(1), 1–13.

Borges, J. C., Fischer, H., Craievich, A. F., and Ramos, C. H. I. (2005): Low resolution structural study of two human HSP40 chaperones in solution. DJA1 from subfamily A and DJB4 from subfamily B have different quaternary structures. *The Journal of Biological Chemistry*, *280*(14), 13671–81.

Bork, P. (1991): Shuffled domains in extracellular proteins. *FEBS Letters*, *286*(1-2), 47–54.

Bosch, J., Buscaglia, C. A., Krumm, B., Ingason, B. P., Lucas, R., Roach, C., Cardozo, T., Nussenzweig, V., and Hol, W. G. J. (2007): Aldolase provides an unusual binding site for thrombospondin-related anonymous protein in the invasion machinery of the malaria parasite. *Proceedings of the National Academy of Sciences, USA*, *104*(17), 7015–7020.

Boshoff, A., Hennessy, F., and Blatch, G. L. (2004): The *in vivo* and *in vitro* characterisation of DnaK from *Agrobacterium tumefaciens* RUOR. *Protein Expression and Purification*, *38*(2), 161–9.

Boshoff, A., Stephens, L. L., and Blatch, G. L. (2008): The *Agrobacterium tumefaciens* DnaK: ATPase cycle, oligomeric state and chaperone properties. *The International Journal of Biochemistry and Cell Biology*, *40*(4), 804–12.

Botha, M., Chiang, A. N., Needham, P. G., Stephens, L. L., Hoppe, H. C., Külzer, S., Przyborski, J. M., Lingelbach, K., Wipf, P., Brodsky, J. L. J. L., Shonhai, A., and Blatch, G. L. (2011): *Plasmodium falciparum* encodes a single cytosolic type I Hsp40 that functionally interacts with Hsp70 and is upregulated by heat shock. *Cell Stress Chaperones*, *16*(4), 389 – 401.

Botha, M., Pesce, E.-R., and Blatch, G. L. (2007): The Hsp40 proteins of *Plasmodium falciparum* and other apicomplexa: regulating chaperone power in the parasite and the host. *The International Journal of Biochemistry and Cell Biology*, *39*(10), 1781–803.

Boulard, Y., Landau, I., Miltgen, F., Ellis, D. S., and Peters, W. (1983): The chemotherapy of rodent malaria, XXXIV. Causal prophylaxis Part III: ultrastructural changes induced in exoerythrocytic schizonts of *Plasmodium yoelii yoelii* by primaquine. *Annal of Tropical Medicine and Parasitology*, *77*, 555–568.

Bozdech, Z., Llinás, M., Pulliam, B. L., Wong, E. D., Zhu, J., and DeRisi, J. L. (2003): The transcriptome of the intraerythrocytic developmental cycle of *Plasmodium falciparum*. *PLoS Biology*, *1*(1), E5.

Bradford, M. M. (1976): A rapid and sensitive method for the quantitation of microgram quantities of protein utilizing the principle of protein-dye binding. *Analytical Biochemistry*, *72*, 248–54.

Bray, P. G., Janneh, O., Raynes, K. J., Mungthin, M., Ginsburg, H., and Ward, S. A. (1999): Cellular Uptake of Chloroquine Is Dependent on Binding to Ferriprotoporphyrin IX and Is Independent of NHE Activity in *Plasmodium falciparum*. *Cell*, *145*(2), 363–376.

Breman, J. G. (2001): The ears of the hippopotamus: manifestations, determinants, and estimates of the malaria burden. (Special issue: The intolerable burden of malaria: a new look at the numbers.). *American Journal of Tropical Medicine and Hygiene*, *64*(1/2 Suppl.), 1–11.

Brodsky, J. L. (1999): Selectivity of the molecular chaperone-specific immunosuppressive agent 15-deoxyspergualin: modulation of Hsc70 ATPase activity without compromising DnaJ chaperone interactions. *Biochemical Pharmacology*, *57*(8), 877–880.

Bronner V *et al.* (2006a): Rapid and efficient determination of kinetic rate constants using the ProteOn XPR36 protein interaction array system. *Bio-Rad Bulletin, 5368.*

Bronner V *et al.* (2006b): Rapid optimisation of immobilisation and binding conditions for kinetic analysis of protein-protein interactions using the ProteOn XPR36 protein interaction array system. *Bio-Rad Bulletin, 5367.*

Brown, A. (2009): Analysis of Cooperativity by Isothermal Titration Calorimetry. *International Journal of Molecular Sciences, 10*(8), 3457–3477.

Brown, G. M. (1962): The biosynthesis of folic acid. II. Inhibition by sulfonamides. *The Journal of Biological Chemistry, 237*, 536–40.

Bruce, M. C., Alano, P., Duthie, S., and Carter, R. (1990): Commitment of the malaria parasite *Plasmodium falciparum* to sexual and asexual development. *Parasitology, 100 Pt 2*, 191–200.

Bukau, B., Deuerling, E., Pfund, C., Craig, E. A., Str, H. H., and Freiburg, D. (2000): Getting newly synthesized proteins into shape. *Cell, 101*, 119–122.

Bullen, H. E., Charnaud, S. C., Kalanon, M., Riglar, D. T., Dekiwadia, C., Kangwanrangsan, N., Torii, M., Tsuboi, T., Baum, J., Ralph, S. A., Cowman, A. F., De Koning-Ward, T. F., Crabb, B. S., and Gilson, P. R. (2012): Biosynthesis, localisation, and macromolecular arrangement of the *Plasmodium falciparum* translocon of exported proteins (PTEX). *The Journal of Biological Chemistry, 287*(11), 7871–84.

Butler, A. R., Khan, S., and Ferguson, E. (2010): A brief history of malaria chemotherapy. *The Journal of the Royal College of Physicians of Edinburgh, 40*(2), 172–177.

Byler, D. M., and Susi, H. (1986): Examination of the secondary structure of proteins by deconvolved FTIR spectra. *Biopolymers, 25*(3), 469–87.

Campell, K., Mullane, K., Aksoy, I., Stubdal, H., Zalvide, J., Pipas, J., Silver, P., Roberts, T., Schaffhausen, B., and DeCaprio, J. (1997): DnaJ/Hsp40 chaperone domain of SV40 large T antigen promotes efficient viral DNA replication. *Genes Development, 11*, 1098–1110.

Campos-Sandoval, J. a, López de la Oliva, A. R., Lobo, C., Segura, J. a, Matés, J. M., Alonso, F. J., and Márquez, J. (2007): Expression of functional human glutaminase in baculovirus system: affinity purification, kinetic and molecular characterisation. *The International Journal of Biochemistry and Cell Biology, 39*(4), 765–73.

Cappel, R. E., and Gilbert, H. F. (1988): Thiol/disulfide exchange between 2-hdroxy-3-methylglutaryl.CoA reductase and glutathione. A thermodynamically facile dithiol oxidation. *Journal of Biological Chemistry, 263*, 12204 – 12212.

Carrió, M. M., and Villaverde, a. (2002): Construction and deconstruction of bacterial inclusion bodies. *Journal of Biotechnology, 96*(1), 3–12.

Carrió, M. M., and Villaverde, A. (2001): Protein aggregation as bacterial inclusion bodies is reversible. *FEBS Letters*, *489*(1), 29–33.

Carruthers, V. B., and Sibley, L. D. (1997): Sequential protein secretion from three distinct organelles of Toxoplasma gondii accompanies invasion of human fibroblasts. *European Journal of Cell Biology*, *73*(2), 114–123.

Carson, M., Johnson, D. H., McDonald, H., Brouillette, C., and Delucas, L. J. (2007): His-tag impact on structure. *Acta Crystallographica. Section D, Biological Crystallography*, *63*(Pt 3), 295–301.

Casadaban, M., Martinez-Arias, A., Shapira, S., and Chou, J. (1983): β-Galactosidase gene fusions for analysing gene expression in *Escherichia coli* and yeast. *Methods in Enzymology*, *100*, 293 – 308.

Casares, S., Brumeanu, T.-D., and Richie, T. L. (2010): The RTS,S malaria vaccine. *Vaccine*, *28*(31), 4880–4894.

Chamberlain, L. H., and Burgoyne, R. D. (1997): Activation of the ATPase activity of heat-shock proteins Hsc70/Hsp70 by cysteine-string protein. *The Biochemical Journal, 858*(Pt3), 853–858.

Chang, L., Bertelsen, E. B., Wisén, S., Larsen, E. M., Zuiderweg, E. R. P., and Gestwicki, J. E. (2008a): High-throughput screen for small molecules that modulate the ATPase activity of the molecular chaperone DnaK. *Analytical Biochemistry*, *372*(2), 167–76.

Chang, H. H., Falick, A. M., Carlton, P. M., Sedat, J. W., DeRisi, J. L., and Marletta, M. a. (2008b): N-terminal processing of proteins exported by malaria parasites. *Molecular and Biochemical Parasitology*, *160*(2), 107–15.

Cheeseman, I. H., Miller, B. A., Nair, S., Nkhoma, S., Tan, A., Tan, J. C., Al Saai, S., Phyo, A. P., Moo, C. L., Lwin, K. M., McGready, R., Ashley, E., Imwong, M., Stepniewska, K., Yi, P., Dondorp, A. M., Mayxay, M., Newton, P. N., White, N. J., Nosten, F., Ferdig, M. T., and Anderson, T. J. C. (2012): A major genome region underlying artemisinin resistance in malaria. *Science*, *336*(6077), 79–82.

Cheetham, M. E., and Caplan, A. J. (1998): Structure, function and evolution of DnaJ: Conservation and adaptation of chaperone function. *Cell Stress Chaperones,*, *3*, 28–36.

Cheetham, M. E., Jackson, A. P., and Anderton, B. H. (1994): Regulation of 70-kDa heat-shock-protein ATPase activity and substrate binding by human DnaJ-like proteins, HSJ1a and HSJ1b. *European Journal of Biochemistry FEBS*, *226*(1), 99–107.

Chiang, A. N., Valderramos, J.-C., Balachandran, R., Chovatiya, R. J., Mead, B. P., Schneider, C., Bell, S. L., Klein, M. G., Huryn, D. M., Chen, X. S., Day, B. W., Fidock, D. A., Wipf, P., and

Brodsky, J. L. (2009): Select pyrimidinones inhibit the propagation of the malarial parasite, *Plasmodium falciparum*. *Bioorganic and Medicinal Chemistry*, *17*(4), 1527–1533.

Chou, A. C., Chevli, R., and Fitch, C. D. (1980): Ferriprotoporphyrin IX fulfills the criteria for identification as the chloroquine receptor of malaria parasites. *Biochemistry*, *19*(8), 1543–9.

Chou, A. C., and Fitch, C. D. (1993): Control of heme polymerase by chloroquine and other quinoline derivatives. *Biochemical and Biophysical Research Communications*, *195*(1), 422–7.

Chuang, J.-Z., Zhou, H., Zhu, M., Li, S.-H., Li, X.-J., and Sung, C.-H. (2002): Characterisation of a brain-enriched chaperone, MRJ, that inhibits Huntingtin aggregation and toxicity independently. *The Journal of Biological Chemistry*, *277*(22), 19831–19838.

Churion, K. a, and Bondos, S. E. (2012): Identifying solubility-promoting buffers for intrinsically disordered proteins prior to purification. *In N. J. Clifton (Ed.), Methods in Molecular Biology*, *896*(9), 415–27.

Cleland, J. L., Hedgepeth, C., and Wang, D. I. C. (1992): Polyethylene glycol enhanced refolding of bovine carbonic anhydrase B. *Journal of Biological Chemistry*, *267*, 13327 – 13334.

Clough, B., and Wilson, R. J. M. (2001): Antibiotics and the plasmodial plastid organelle. *In P. J. Rosenthal (Ed.), Antimalarial chemotherapy: Mechanisms of action, resistance, and new directions in drug discovery* (pp. 265–286).

Cockburn, I. L., Pesce, E. R., Pryzborski, J. M., Davies-Coleman, M. T., Clark, P. G., Keyzers, R. A., Stephens, L. L., and Blatch, G. L. (2011): Screening for small molecule modulators of Hsp70 chaperone activity using protein aggregation suppression assays: inhibition of the plasmodial chaperone PfHsp70-1. *Biological Chemistry*, *392*, 431–438.

Connell, S. R., Tracz, D. M., Nierhaus, K. H., and Taylor, D. E. (2003): Ribosomal protection proteins and their mechanism of tetracycline resistance. *Antimicrobial Agents and Chemotherapy*, *47*, 3675 – 3681.

Cooke, B. M., Buckingham, D. W., Glenister, F. K., Fernandez, K. M., Bannister, L. H., Marti, M., Mohandas, N., and Coppel, R. L. (2006): A Maurer's cleft-associated protein is essential for expression of the major malaria virulence antigen on the surface of infected red blood cells. *The Journal of Cell Biology*, *172*(6), 899–908.

Cooke, B. M., Lingelbach, K., Bannister, L. H., and Tilley, L. (2004): Protein trafficking in *Plasmodium falciparum*-infected red blood cells. *Trends in Parasitology*, *20*(12), 581–9.

Cowman, A. F., Coppel, R. L., Saint, R. B., Favaloro, J., Crewther, P. E., Stahl, H. D., Bianco, A. E., Brown, G. V, Anders, R. F., and Kemp, D. J. (1984): The ring-infected erythrocyte surface antigen (RESA) polypeptide of *Plasmodium falciparum* contains two separate blocks of tandem repeats encoding antigenic epitopes that are naturally immunogenic in man. *Molecular Biology and Medicine*, *2*(3), 207–21.

Cowman, A. F., and Crabb, B. S. (2006): Invasion of red blood cells by malaria parasites. *Cell*, *124*(4), 755–766.

Cowman, A. F., Galatis, D., and Thompson, J. K. (1994): Selection for mefloquine resistance in *Plasmodium falciparum* is linked to amplification of the pfmdr1 gene and cross-resistance to halofantrine and quinine. *Proceedings of the National Academy of Sciences, USA*, *91*(3), 1143–1147.

Cox-Singh, J. (2010): Malaria: what can apes teach humans? *Future Microbiology*, *5*(8), 1157–1160.

Crabb, B. S., Cooke, B. M., Reeder, J. C., Waller, R. F., Caruana, S. R., Davern, K. M., Wickham, M. E., Brown, G. V, Coppel, R. L., and Cowman, A. F. (1997): Targeted gene disruption shows that knobs enable malaria-infected red cells to cytoadhere under physiological shear stress. *Cell*, *89*(2), 287–296.

Crabb, B. S., De Koning-Ward, T. F., and Gilson, P. R. (2010): Protein export in *Plasmodium* parasites: from the endoplasmic reticulum to the vacuolar export machine. *International Journal for Parasitology*, *40*(5), 509–513.

Craig, E. A., Gambill, B. D., and Nelson, R. J. (1993): Heat shock proteins: molecular chaperones of protein biogenesis. *Microbiological Reviews*, *57*(2), 402–414.

Cullity, B. D., and Stock, S. R. (2001): Elements of X-Ray Diffraction (M. Cohen, Ed.). *Prentice Hall publishing*, pages - 664.

Curtis, C. F., Maxwell, C. a, Magesa, S. M., Rwegoshora, R. T., and Wilkes, T. J. (2006): Insecticide-treated bed-nets for malaria mosquito control. *Journal of the American Mosquito Control Association*, *22*(3), 501–6.

Cyr, D. M. (1995): Cooperation of the molecular chaperone Ydj1 with specific Hsp70 homologs to suppress protein aggregation. *FEBS letters*, *359*(2-3), 129–32.

Cyr, D. M., Langer, T., and Douglas, M. G. (1994): DnaJ-like proteins: molecular chaperones and specific regulators of Hsp70. *Trends in Biochemical Sciences*, *19*(4), 176–181.

Czarnecki, M. a., and Ozaki, Y. (1996): Determination of integrated intensities of overlapped IR bands by curve-fitting, Fourier self-deconvolution and a combination of both methods. *Spectrochimica acta part A: Molecular and Biomolecular Spectroscopy*, *52*(12), 1593–1601.

D'Alessandro, U. (2009): Existing antimalarial agents and malaria-treatment strategies. *Expert Opinion on Pharmacotherapy*, *10*(8), 1291–1306.

De Almeida Ribeiro, M. C., Augusto, O., and Da Costa Ferreira, A. M. (1997): Influence of quinoline-containing antimalarials in the catalase activity of ferriprotoporphyrin IX. *Journal of Inorganic Biochemistry*, *65*(1), 15–23.

De Koning-Ward, T. F., Gilson, P. R., Boddey, J. A., Rug, M., Smith, B. J., Papenfuss, A. T., Sanders, P. R., Lundie, R. J., Maier, A. G., Cowman, A. F., and Crabb, B. S. (2009): A newly discovered protein export machine in malaria parasites. *Nature*, *459*(7249), 945–949.

De Los Rios, P., Ben-Zvi, A., Slutsky, O., Azem, A., and Goloubinoff, P. (2006): Hsp70 chaperones accelerate protein translocation and the unfolding of stable protein aggregates by entropic pulling. *Proceedings of the National Academy of Sciences, USA*, *103*(16), 6166–6171.

Dechavanne, V., Barrillat, N., Borlat, F., Hermant, A., Magnenat, L., Paquet, M., Antonsson, B., and Chevalet, L. (2011): A high-throughput protein refolding screen in 96-well format combined with design of experiments to optimize the refolding conditions. *Protein Expression and Purification*, *75*(2), 192–203.

Deitsch, K. W., and Wellems, T. E. (1996): Membrane modifications in erythrocytes parasitized by *Plasmodium falciparum*. *Molecular and Biochemical Parasitology*, *76*(1-2), 1–10.

Del Solar, G., Giraldo, R., Ruiz-Echevarria, M.J., Espinosa, M., and Diaz-Orejas R. (1998): Replication and control of circular bacterial plasmids. *Microbiology and Molecular Biology Review*, *62*, 434 – 464.

Demand, J., Lüders, J., Höhfeld, J., and Lu, J. (1998): The Carboxy-Terminal Domain of Hsc70 Provides Binding Sites for a Distinct Set of Chaperone Cofactors. *Molecular and Cellular Biology*, *18*(4), 2023 – 2028.

Deponte, M., Hoppe, H. C., Lee, M. C. S., Maier, A. G., Richard, D., Rug, M., Spielmann, T., and Przyborski, J. M. (2012): Wherever I may roam : Protein and membrane trafficking in *P. falciparum*-infected red blood cells. *Molecular and Biochemical Parasitology*, *186*(2), 95–116.

Derewenda, Z. S. (2004): The use of recombinant methods and molecular engineering in protein crystallization. *Methods San Diego Calif*, *34*(3), 354–363.

Desneves, J., Lfogy, P., Thorn, G., Bermanb, A., Galatis, D., Grecab, N. La, Sinding, J., Foleyb, M., Deady, L. W., Cowman, A. F., and Tilleyb, L. (1996): Photoaffinity labeling of mefloquine-binding proteins in human serum, uninfected erythrocytes and *Plasmodium falciparum*-infected erythrocytes. *Molecular and Biochemical Parasitology*, *6851*(96), 181–194.

Dessens, J. T., Beetsma, A. L., Dimopoulos, G., Wengelnik, K., Crisanti, A., Kafatos, F. C., and Sinden, R. E. (1999): CTRP is essential for mosquito infection by malaria ookinetes. *The European Molecular Biology Organization Journal*, *18*(22), 6221–6227.

Dessens, J. T., Sidén-Kiamos, I., Mendoza, J., Mahairaki, V., Khater, E., Vlachou, D., Xu, X.-J., Kafatos, F. C., Louis, C., Dimopoulos, G., and Sinden, R. E. (2003): SOAP, a novel malaria ookinete protein involved in mosquito midgut invasion and oocyst development. *Molecular Microbiology*, *49*(2), 319–329.

Di Guan, C., Li, P., Riggs, P. D., and Inouye, H. (1988): Vectors that facilitate the expression and purification of foreign peptides in *Escherichia coli* by fusion to maltose-binding protein. *Gene*, *67*, 21 – 30.

Di Perri G, Solbiati, M., Vento, S., De Checchi G, Luzzati, R., Bonora, S., Merighi, M., Marocco, S., Fibbia, G., and Concia, E. (1994): West African immigrants and new patterns of malaria imported to north eastern Italy. *Journal of Travel Medicine*, *1*(3), 147–151.

Dittrich, W., Williams, K. L., and Slade, M. B. (1994): Production and secretion of recombinant proteins in Dictyostelium discoideum. *Biotechnology (NY)*, *12*, 614 – 618.

Divo, A. A., Geary, T. G., and Jensen, J. B. (1985): Oxygen- and time-dependent effects of antibiotics and selected mitochondrial inhibitors on *Plasmodium falciparum* in culture. *Antimicrobial Agents and Chemotherapy*, *27*(1), 21–7.

DJ, M., H-P, S., P, M., and DM, H. (1995): Cloning vectors for the production of proteins in *Dictyostelium discoideum*. *Gene*, *162*, 129 – 134.

Doolittle, R. F. (1995): The multiplicity of domains in proteins. *Annual Review of Biochemistry*, *64*, 287–314.

Dorsey, G., Njama, D., Kamya, M. R., Cattamanchi, A., Kyabayinze, D., Staedke, S. G., Gasasira, A., and Rosenthal, P. J. (2002): Sulfadoxine/pyrimethamine alone or with amodiaquine or artesunate for treatment of uncomplicated malaria: a longitudinal randomised trial. *Lancet*, *360*, 2031–2038.

Douradinha, B., Dijk, M. Van, Gemert, G. Van, Khan, S. M., Janse, C. J., Waters, A. P., Sauerwein, R. W., Luty, A. J. F., Silva-santos, B., Mota, M. M., and Epiphanio, S. (2011): Immunization with genetically attenuated P52- deficient *Plasmodium berghei* sporozoites induces a long-lasting effector memory CD8 + T cell response in the liver. *Journal of Immune Based Therapy and Vaccines*, *9*(6), 2–6.

Dragovic, Z., Broadley, S. A., Shomura, Y., Bracher, A., and Hartl, F. U. (2006): Molecular chaperones of the Hsp110 family act as nucleotide exchange factors of Hsp70s. *EMBO J.*, *25*, 2519 – 2528.

Eksi, S., Czesny, B., Van Gemert, G.-J., Sauerwein, R. W., Eling, W., and Williamson, K. C. (2006): Malaria transmission-blocking antigen, Pfs230, mediates human red blood cell binding to exflagellating male parasites and oocyst production. *Molecular Microbiology*, *61*(4), 991–998.

Eksi, S., Stump, A., Fanning, S. L., Shenouda, M. I., Fujioka, H., and Williamson, K. C. (2002): Targeting and sequestration of truncated Pfs230 in an intraerythrocytic compartment during *Plasmodium falciparum* gametocytogenesis. *Molecular Microbiology*, *44*(6), 1507–1516.

Emini, E., Hughes, J. V., Perlow, D. S., and J., J. B. (1985): Induction of hepatitis A virus-neutralizing antibody by a virus-specific synthetic peptide. *Virology*, *55*, 836–839.

Emoto, C., Murayama, N., Wakiya, S., and Yamazaki, H. (2009): Effects of histidine-tag on recombinant human cytochrome P450 3A5 catalytic activity in reconstitution systems. *Drug Metabolism Letters*, *3*(4), 207–211.

Esposito, D., and Chatterjee, D. K. (2006): Enhancement of soluble protein expression through the use of fusion tags. *Current Opinion Biotechnology*, *17*, 353 – 358.

Evans, A. G., and Wellems, T. E. (2002): Coevolutionary genetics of *Plasmodium* malaria parasites and their human hosts. *Integrative and Comparative Biology*, *42*(2), 401–407.

Evans, C. G. C. G., Chang, L., and Gestwicki, J. E. J. E. (2010): Heat shock protein 70 (Hsp70) as an emerging drug target. *Journal of Medicinal Chemistry*, *53*(12), 4585 – 4602.

Fan, C.-Y., Lee, S., and Cyr, D. M. (2003): Mechanisms for regulation of Hsp70 function by Hsp40. *Cell Stress and Chaperones*, *8*(4), 309–316..

Fane, M., Cissé, O., Traore, C. S. F., and Sabatier, P. (2012): Anopheles gambiae resistance to pyrethroid-treated nets in cotton versus rice areas in Mali. *Acta Tropica*, *122*(1), 1–6.

Farabaugh, P. J. (1978): Sequence of the lacI gene. *Nature*, *274*(5673), 765–769.

Fasel, N., Begdadi-Rais, C., Bernard, M., Bron, C., Corradin, G., and Reymond, C. D. (1992): Dictyostelium discoideum as an expression host for the circumsporozoite protein of *Plasmodium falciparum*. *Gene*, *111*(2), 157 – 163.

Fayazi, Z., Ghosh, S., Marion, S., Bao, X., Shero, M., and Kazemi-Esfarjani, P. (2006): A Drosophila ortholog of the human MRJ modulates polyglutamine toxicity and aggregation. *Neurobiology of Disease*, *24*(2), 226–244.

Feldheim, D., Rothblatt, J., and Schekman, R. (1992): Topology and functional domains of Sec63p, an endoplasmic reticulum membrane protein required for secretory protein translocation. *Molecular and Cellular Biology*, *12*(7), 3288–96.

Ferguson, H. M., and Read, A. F. (2004): Mosquito appetite for blood is stimulated by *Plasmodium chabaudi* infections in themselves and their vertebrate hosts. *Malaria Journal*, *3*(1), 12.

Fewell, S. W., Day, B. W., and Brodsky, J. L. (2001): Identification of an inhibitor of hsc70-mediated protein translocation and ATP hydrolysis. *The Journal of Biological Chemistry*, *276*(2), 910–4.

Fewell, S. W., Smith, C. M., Lyon, M. a, Dumitrescu, T. P., Wipf, P., Day, B. W., and Brodsky, J. L. (2004): Small molecule modulators of endogenous and co-chaperone-stimulated Hsp70 ATPase activity. *The Journal of Biological Chemistry*, *279*(49), 51131–40.

Fink, A. L. (1998): Protein aggregation : folding aggregates , inclusion bodies and amyloid. *Folding and design*, *3*(1), R9 – R23.

Finke, J. M., Roy, M., Zimm, B. H., and Jennings, P. (2000): Aggregation events occur prior to stable intermediate formation during refolding of interleukin 1 β. *Biochemistry*, *39*, 575 – 583.

Fischer, B., Sumner, I., and Goodenough, P. (1993): Isolation, renaturation and formation of disulfide bonds of eukaryotic proteins expressed in *E. coli* as inclusion bodies. *Biotechnology and Bioengineering*, *41*, 3 – 13.

Florens, L., Washburn, M. P., Raine, J. D., Anthony, R. M., Grainger, M., Haynes, J. D., Moch, J. K., Muster, N., Sacci, J. B., Tabb, D. L., Witney, A. a, Wolters, D., Wu, Y., Gardner, M. J., Holder, A. a, Sinden, R. E., Yates, J. R., and Carucci, D. J. (2002): A proteomic view of the *Plasmodium falciparum* life cycle. *Nature*, *419*(6906), 520–526.

Foley, M., Corcoran, L., Tilley, L., and Anders, R. (1994): *Plasmodium falciparum*: mapping the membrane-binding domain in the ring-infected erythrocyte surface antigen. *Experimental Parasitology*, *79*(3), 340–350.

Foster, S. (1994): Economic prospects for a new antimalarial drug. *Transactions of the Royal Society of Tropical Medicine and Hygiene*, *88*, 55–56.

Francis, S. E., Sullivan, D. J., and Goldberg, D. E. (1997): Hemoglobin metabolism in the malaria parasite *Plasmodium falciparum*. *Annual Review of Microbiology*, *51*, 97–123.

Freeman, B. C., Myers, M. P., Schumacher, R., and Morimoto, R. I. (1995): Identification of a regulatory motif in Hsp70 that affects ATPase activity, substrate binding and interaction with Hdj-1. *EMBO J.*, *14*, 2281 – 2292.

Frevert, U., Engelmann, S., Zougbédé, S., Stange, J., Ng, B., Matuschewski, K., Liebes, L., and Yee, H. (2005): Intravital observation of *Plasmodium berghei* sporozoite infection of the liver. *PLoS Biology*, *3*(6), e192.

Freydank, A.-C., Brandt, W., and Dräger, B. (2008): Protein structure modeling indicates hexahistidine-tag interference with enzyme activity. *Proteins*, *72*(1), 173–183.

Fry, M., and Pudney, M. (1992): Site of action of the antimalarial hydroxynaphthoquinone, 2-[trans-4-(4'-chlorophenyl) cyclohexyl]-3- hydroxy-1,4-naphthoquinone (566C80). *Biochemical Pharmacology*, *43*(7), 1545–1553.

Futterman, S. (1957): Enzymatic reduction of folic acid and dihydrofolic acid to tetrahydrofolic acid. *Journal of Biological Chemistry*, *228*(2), 1031–1038.

Gao, X.-C., Zhou, C.-J., Zhou, Z.-R., Zhang, Y.-H., Zheng, X.-M., Song, A.-X., and Hu, H.-Y. (2011): Co-chaperone HSJ1a dually regulates the proteasomal degradation of ataxin-3. *PloS One*, *6*(5), e19763.

García-Fruitós, E. (2010): Inclusion bodies: a new concept. *Microbial Cell Factories*, *9*(1), 80-83.

García-Fruitós, E., Vázquez, E., Díez-Gil, C., Corchero, J. L., Seras-Franzoso, J., Ratera, I., Veciana, J., and Villaverde, A. (2012): Bacterial inclusion bodies: making gold from waste. *Trends in Biotechnology*, *30*(2), 65–70.

Garimella, R., Liu, X., Qiao, W., Liang, X., Zuiderweg, E. R. P., Riley, M. I., and Van Doren, S. R. (2006): Hsc70 contacts helix III of the J domain from polyomavirus T antigens: addressing a dilemma in the chaperone hypothesis of how they release E2F from pRb. *Biochemistry*, *45*(22), 6917–6929.

Gässler, C. S., Buchberger, A., Laufen, T., Mayer, M. P., Schröder, H., Valencia, A., and Bukau, B. (1998): Mutations in the DnaK chaperone affecting interaction with the DnaJ cochaperone. *Proceedings of the National Academy of Sciences, USA*, *95*(26), 15229–15234.

Geary, T. G., and Jensen, J. B. (1983): Effects of antibiotics on *Plasmodium falciparum in vitro*. *The American Journal of Tropical Medicine and Hygiene*, *32*(2), 221–225.

Genevaux, P., Lang, F., Schwager, F., Vartikar, J. V, Rundell, K., Pipas, J. M., Georgopoulos, C., and Kelley, W. L. (2003): Simian Virus 40 T Antigens and J Domains: Analysis of Hsp40 Cochaperone Functions in *Escherichia coli*. *Journal of virology*, *77*(19), 10706–10713.

Genevaux, P., Schwager, F., Georgopoulos, C., and Kelley, W. L. (2002): Scanning mutagenesis identifies amino acid residues essential for the *in vivo* activity of the *Escherichia coli* DnaJ (Hsp40) J-domain. *Genetics*, *162*(3), 1045–1053.

George, R. a, and Heringa, J. (2002): Protein domain identification and improved sequence similarity searching using PSI-BLAST. *Proteins*, *48*(4), 672–81.

Gitau, G. W., Mandal, P., Blatch, G. L., Przyborski, J., and Shonhai, A. (2012): Characterisation of the *Plasmodium falciparum* Hsp70-Hsp90 organising protein (PfHop). *Cell Stress and Chaperones*, *17*(2), 191–202.

Goldberg, D. E., and Cowman, A. F. (2010): Moving in and renovating: exporting proteins from *Plasmodium* into host erythrocytes. *Nature Reviews Microbiology*, *8*(9), 617–21.

Golenser, J., Waknine, J. ., Krugliak, M., Hunt, N. ., and Grau, G. . (2006): Current perspectives on the mechanism of action of artemisinins. *International Journal for Parasitology*, *36*(14), 1427–1441.

Goloubinoff, P., and De Los Rios, P. (2007): The mechanism of Hsp70 chaperones: (entropic) pulling the models together. *Trends in Biochemical Sciences* , *32*(8), 372–380.

Good, M. F., and Doolan, D. L. (2007): Malaria's journey through the lymph node. *Nature Medicine*, *13*(9), 1023–1024.

Goormaghtigh, E., Cabiaux, V., and Ruysschaert, J.-M. (1994): Determination of soluble and membrane protein structure by Fourier transform infrared spectroscopy. I. Assignments and model compounds. II. Experimental aspects, side chain structure, and H/D exchange. III.

Secondary structures. *In H. J. Hilderson and G. B. Ralston (Eds.), In Subcellular Biochemistry, f: Physicochemical Methods in the Study of Biomembranes*, pages 329 – 450.

Görlich, D., and Rapoport, T. A. (1993): Protein translocation into proteoliposomes reconstituted from purified components of the endoplasmic reticulum membrane. *Cell*, *75*(4), 615–630.

Gormley, J. A., Howard, R. J., and Taraschi, T. F. (1992): Trafficking of malarial proteins to the host cell cytoplasm and erythrocyte surface membrane involves multiple pathways. *The Journal of Cell Biology*, *119*(6), 1481–1495.

Gräslund, S., Nordlund, P., Weigelt, J., Hallberg, B. M., Bray, J., Gileadi, O., Knapp, S., Oppermann, U., Arrowsmith, C., Hui, R., Ming, J., dhe-Paganon, S., Park, H., Savchenko, A., Yee, A., Edwards, A., Vincentelli, R., Cambillau, C., Kim, R., Kim, S.-H., Rao, Z., Shi, Y., Terwilliger, T. C., Kim, C.-Y., Hung, L.-W., *et al.* (2008): Protein production and purification. *Nature Methods*, *5*(2), 135–46.

Greenwood, B. M., Fidock, D. A., Kyle, D. E., Kappe, S. H. I., Alonso, P. L., Collins, F. H., and Duffy, P. E. (2008): Malaria: progress, perils, and prospects for eradication. *The Journal of Clinical Investigation*, *118*(4), 1266–1276.

Grover, M., Chaubey, S., Ranade, S., and Tatu, U. (2013): Identification of an exported heat shock protein 70 in *Plasmodium falciparum*. *Parasite*, *20*(2), 1–9.

Günther, K., Tümmler, M., Arnold, H. H., Ridley, R., Goman, M., Scaife, J. G., and Lingelbach, K. (1991): An exported protein of *Plasmodium falciparum* is synthesized as an integral membrane protein. *Molecular and Biochemical Parasitology*, *46*(1), 149–157.

Guex, N., and Peitsch, M. C. (1997): SWISS-MODEL and the Swiss-PdbViewer: an environment for comparative protein modeling. *Electrophoresis*, *18*(15), 2714–2723.

Guo, L.-W., Assadi-Porter, F. M., Grant, J. E., Wu, H., Markley, J. L., and Ruoho, A. E. (2007): One-step purification of bacterially expressed recombinant transducin alpha-subunit and isotopically labeled PDE6 gamma-subunit for NMR analysis. *Protein Expression and Purification*, *51*(2), 187–97.

Gustafsson, C., Govindarajan, S., and Minshull, J. (2004): Codon bias and heterologous protein expression. *Trends in Biotechnology*, *22*(7), 346–353.

Ha J.-H., Johnson E. R., McKay D. B., Sousa M. C., T. S. and W. S. M. (1999): Structure and mechanism of Hsp70 proteins. *In B. Bukau (Ed.), Molecular chaperones and folding catalysts: regulation, cellular function and mechanism,* pages 573–607.

Hageman, J., Rujano, M. A., Van Waarde, M. A. W. H., Kakkar, V., Dirks, R. P., Govorukhina, N., Oosterveld-Hut, H. M. J., Lubsen, N. H., and Kampinga, H. H. (2010): A DNAJB chaperone subfamily with HDAC-dependent activities suppresses toxic protein aggregation. *Molecular Cell*, *37*(3), 355–369.

Haldar, K., and Mohandas, N. (2007): Erythrocyte remodeling by malaria parasites. *Current Opinion in Hematology*, *14*(3), 203–9.

Hall, T. A. (1999): BioEdit: a user-friendly biological sequence alignment editor and analysis program for Windows 95/98/NT. *Nucleic Acids Symposium Series*, *41*, 95–98.

Hannig, G., and Makrides, S. C. (1998): Strategies for optimizing heterologous protein expression in *Escherichia coli*. *Trends in Biotechnology*, *16*, 54 – 60.

Hanssen, E., Hawthorne, P., Dixon, M. W. A., Trenholme, K. R., McMillan, P. J., Spielmann, T., Gardiner, D. L., and Tilley, L. (2008a): Targeted mutagenesis of the ring-exported protein-1 of *Plasmodium falciparum* disrupts the architecture of Maurer's cleft organelles. *Molecular Microbiology*, *69*(4), 938–953.

Hanssen, E., Sougrat, R., Frankland, S., Deed, S., Klonis, N., Lippincott-Schwartz, J., and Tilley, L. (2008b): Electron tomography of the Maurer's cleft organelles of *Plasmodium falciparum*-infected erythrocytes reveals novel structural features. *Molecular Microbiology*, *67*(4), 703–718.

Haris, P. I., and Severcan, F. (1999): FTIR spectroscopic characterisation of protein structure in aqueous and non-aqueous media. *Journal of Molecular Catalysis B: Enzymatic*, *7*(1-4), 207–221.

Hartl, F. U. (1996): Molecular chaperones in cellular protein folding. *Nature*, *381*(6583), 571–580.

Hartl, F. U., and Hayer-Hartl, M. (2002): Molecular chaperones in the cytosol: from nascent chain to folded protein. *Science*, *295*(5561), 1852–1858.

Hartwig, C. L., Rosenthal, A. S., D'Angelo, J., Griffin, C. E., Posner, G. H., and Cooper, R. A. (2009): Accumulation of artemisinin trioxane derivatives within neutral lipids of *Plasmodium falciparum* malaria parasites is endoperoxidedependent. *Biochemical Pharmacology*, *77*(3), 322–336.

Hawthorne, P. L., Trenholme, K. R., Skinner-Adams, T. S., Spielmann, T., Fischer, K., Dixon, M. W. A., Ortega, M. R., Anderson, K. L., Kemp, D. J., and Gardiner, D. L. (2004): A novel *Plasmodium falciparum* ring stage protein, REX, is located in Maurer's clefts. *Molecular and Biochemical Parasitology*, *136*(2), 181–189.

Hayes, S. A., and Dice, J. F. (1996): Roles of molecular chaperones in protein degradation. *Cell*, *132*(3), 255–258.

He, Z., Xie, R., Wang, Y., Zou, H., Zhu, J., and Yu, G. (2008): Cloning and characterisation of a heat shock protein 70 gene, MsHSP70-1, in *Medicago sativa*. *Acta Biochimica et Biophysica Sinica*, *40*(3), 209–216.

Hefti, M. H., Caroline, J. G., Der Toorn, V., Dixon, R., and Vervoort, J. (2001): A novel purificationmethod for histidine-tagged proteins containing a thrombin cleavage site. *Analytical Biochemistry*, *295*, 180 – 185.

Hennessy, F., Boshoff, A., and Blatch, G. L. (2005a): Rational mutagenesis of a 40 kDa heat shock protein from *Agrobacterium tumefaciens* identifies amino acid residues critical to its *in vivo* function. *The International Journal of Biochemistry and Cell Biology*, *37*(1), 177–91.

Hennessy, F., Cheetham, M. E., Dirr, H. W., and Blatch, G. L. (2000): Analysis of the levels of conservation of the J domain among the various types of DnaJ-like proteins. *Cell Stress Chaperones*, *5*(4), 347–358.

Hennessy, F., Nicoll, W. S., Zimmermann, R., Cheetham, M. E., and Blatch, G. L. (2005b): Not all J domains are created equal : Implications for the specificity of Hsp40 – Hsp70 interactions. *Society*, 1697–1709.

Hibbs, A. R., and Saul, A. J. (1994): *Plasmodium falciparum*: highly mobile small vesicles in the malaria-infected red blood cell cytoplasm. *Experimental Parasitology*, *79*(3), 260–269.

Hill, A. V. S. (2006): Pre-erythrocytic malaria vaccines: towards greater efficacy. *Nature Reviews Immunology*, *6*(1), 21–32.

Hiller, N. L., Bhattacharjee, S., Van Ooij, C., Liolios, K., Harrison, T., Lopez-Estraño, C., and Haldar, K. (2004): A host-targeting signal in virulence proteins reveals a secretome in malarial infection. *Science*, *306*(5703), 1934–7.

Hinault, M.-P., Ben-Zvi, A., and Goloubinoff, P. (2006): Chaperones and proteases: cellular fold-controlling factors of proteins in neurodegenerative diseases and aging. *Journal of Molecular Neuroscience MN*, *30*(3), 249–265.

Hinault, M.-P., Farina-Henriquez-Cuendet, A., and Goloubinoff, P. (2011): Molecular chaperones and associated cellular clearance mechanisms against toxic protein conformers in Parkinson's disease. *Neurodegenerative Diseases*, *8*(6), 397–412.

Hitzeman, R. A., Chen, C. Y., Dowbenko, D. J., Renz, M. E., Liu, C., Pai, R., Simpson, N. J., Kohr, W. J., Singh, A., Chisholm, V., Hamilton, R., and Chang, C. N. (1990): Use of heterologous and homologous signal sequences for secretion of heterologous proteins from yeast. *Methods in Enzymology*, *185*, 421 – 440.

Hochuli, E., D_beli, H., and Schacher, A. (1987): New metal chelate adsorbent selective for proteins and peptide containing neighbouring histidine residues. *Journal of Chromatography*, *411*, 177 – 184.

Hoffman, S. L., Billingsley, P. F., James, E., Richman, A., Loyevsky, M., Li, T., Chakravarty, S., Gunasekera, A., Chattopadhyay, R., Li, M., Stafford, R., Ahumada, A., Epstein, J. E., Sedegah, M., Reyes, S., Richie, T. L., Lyke, K. E., Edelman, R., Laurens, M. B., Plowe, C. V, and Sim,

B. K. L. (2010a): Development of a metabolically active , non-replicating sporozoite vaccine to prevent *Plasmodium falciparum* malaria. *Human Vaccines*, *6*(1), 97–106.

Hoffman, S. L., Goh, L. M. L., Luke, T. C., Schneider, I., Le, T. P., Doolan, D. L., Sacci, J., Vega, P. De, Dowler, M., Paul, C., Gordon, D. M., Stoute, J. A., Church, L. W. P., Sedegah, M., Heppner, D. G., Ballou, W. R., Richie, T. L., and De La Vega, P. (2002): Protection of humans against malaria by immunization with radiation-attenuated *Plasmodium falciparum* sporozoites. *The Journal of Infectious Diseases*, 185(8), 1155–1164.

Hoffman, S. L., Sim, B. K. L., Richman, A., Pizon-Charry, A., Good, M. F., and McCarthy, J. (2010b): Pre-erythrocytic and asexual erythrocytic stage whole-organism malaria vaccines. *In Michael Levine, Gordon Dougan, Michael F. Good, Margaret Liu, Gary Nabel (Ed.), New generation vaccines,* 4th ed., pages 783–789.

Hoffman, S. L., Wistar, R., Ballou, W. R., Hollingdale, M. R., Wirtz, R. A., Schneider, I., Marwoto, H. A., and Hockmeyer, W. T. (1987): Immunity to malaria and naturally acquired antibodies to the circumsporozoite protein of *Plasmodium falciparum. The new England Journal of Medicine,* 316:415.

Holder, A., Blackman, M., Borre, M., Burghaus, P., Chappel, J., Keen, J., Ling, I., Ogun, S., Owen, C., and Sinha, K. (1994): Malaria parasites and erythrocyte invasion. *Biochemical Society Transactions* , *22*(2), 291–295.

Hopp, T. P., Pricket, K. S., Price, V. L., Libby, R. T., March, C. J., Ceretti, D. P., Urdal, D. L., and Conlon, P. J. (1988): A short polypeptide marker sequence useful for recombinant protein identification and purification. *Biotechnology*, *6*, 1204 – 1210.

Hopp, T. P., and Woods., K. R. (1981): Prediction of protein antigenic determinants from amino acid sequences. *Proceedings of the National Academy of Science, USA*, *78*, 3824–3828.

Horrocks, P., and Muhia, D. (2005): Pexel/VTS: a protein-export motif in erythrocytes infected with malaria parasites. *Trends in Parasitology*, *21*(9), 396–9.

Horrocks, P., Pinches, R. a, Chakravorty, S. J., Papakrivos, J., Christodoulou, Z., Kyes, S. a, Urban, B. C., Ferguson, D. J. P., and Newbold, C. I. (2005): PfEMP1 expression is reduced on the surface of knobless *Plasmodium falciparum* infected erythrocytes. *Journal of Cell Science*, *118*(Pt 11), 2507–18.

Horton, L. E., James, P., Craig, E. A., and Hensold, J. O. (2001): The yeast hsp70 homologue Ssa is required for translation and interacts with Sis1 and Pab1 on translating ribosomes. *The Journal of Biological Chemistry*, *276*(17), 14426–14433.

Hu, J., Wu, Y., Li, J., Qian, X., Fu, Z., and Sha, B. (2008): The crystal structure of the putative peptide-binding fragment from the human Hsp40 protein Hdj1. *BMC Structural Biology*, *8*, 3.

Hubbard, T. J., and Sander, C. (1991): The role of heat-shock and chaperone proteins in protein folding: possible molecular mechanisms. *Protein Engineering*, *4*(7), 711–7.

Hudson, A. T. (1993): Atovaquone - a novel broad-spectrum anti-infective drug. *Parasitology Today*, *9*(2), 66–8.

Hughey, R., and Krogh, A. (1996): Hidden Markov models for sequence analysis: extension and analysis of the basic method. *Computer Applications in the Biosciences*, *12*(2), 95–107.

Ishino, T., Chinzei, Y., and Yuda, M. (2005): Two proteins with 6-cys motifs are required for malarial parasites to commit to infection of the hepatocyte. *Molecular Microbiology*, *58*(5), 1264–1275.

Ishino, T., Orito, Y., Chinzei, Y., and Yuda, M. (2006): A calcium-dependent protein kinase regulates *Plasmodium* ookinete access to the midgut epithelial cell. *Molecular Microbiology*, *59*(4), 1175–1184.

Ishino, T., Yano, K., Chinzei, Y., and Yuda, M. (2004): Cell-Passage Activity Is Required for the Malarial Parasite to Cross the Liver Sinusoidal Cell Layer. *PLoS Biology*, *2*(1), E4.

Ivey, R. A., and Bruce, B. D. (2000): *In vivo* and *in vitro* interaction of DnaK and a chloroplast transit peptide. *Cell Stress Chaperones*, *5*(1), 62–71.

Jackson, M., and Mantsch, H. H. (1995): The use and misuse of FTIR spectroscopy in the determination of protein structure. *Critical Review Biochemistry and Molecular Biology*, *30*, 95 – 120.

Jambou, R., Legrand, E., Niang, M., Khim, N., Lim, P., Volney, B., Ekala, M. T., Bouchier, C., Esterre, P., Fandeur, T., and Mercereau-Puijalon, O. (2005): Resistance of *Plasmodium falciparum* field isolates to in-vitro artemether and point mutations of the SERCA-type PfATPase6. *Lancet*, *366*(9501), 1960–3.

James, J. F. (2002): A Student's Guide to Fourier Transforms. *Science,* 147.

Jameson, B. A., and Wolf., H. (1998): The antigenic index: a novel algorithm for predicting antigenic determinants. *Computer Applications in the Biosciences*, *4*, 181–186.

Jansen, F. H. (2011): Intermittent preventive therapy for malaria: arguments in favour of artesunate and sulphamethoxypyrazine - pyrimethamine combination. *Malaria Journal*, *10*(1), 70.

Jelinek, T., Schulte, C., Behrens, R., Grobusch, M. P., Coulaud, J. P., Bisoffi, Z., Matteelli, A., Clerinx, J., Corachán, M., Puente, S., Gjørup, I., Harms, G., Kollaritsch, H., Kotlowski, A., Björkmann, A., Delmont, J. P., Knobloch, J., Nielsen, L. N., Cuadros, J., Hatz, C., Beran, J., Schmid, M. L., Schulze, M., Lopez-Velez, R., Fleischer, K., *et al.* (2002): Imported *Falciparum* malaria in Europe: sentinel surveillance data from the European network on surveillance of imported infectious diseases. *Clinical Infectious Diseases*, *34*(5), 572–576.

Jelsch, C., Teeter, M. M., Lamzin, V., Pichon-Pesme, V., Blessing, R. H., and Lecomte, C. (2000): Accurate protein crystallography at ultra-high resolution: valence electron distribution in crambin. *Proceedings of the National Academy of Sciences, USA*, *97*(7), 3171–3176.

Jiang, J., Prasad, K., Lafer, E. M., and Sousa, R. (2005): Structural basis of interdomain communication in the Hsc70 chaperone. *Molecular Cell*, *20*(4), 513–524.

Jiang, R. F., Greener, T., Barouch, W., Greene, L., and Eisenberg, E. (1997): Interaction of auxilin with the molecular chaperone, Hsc70. *The Journal of Biological Chemistry*, *272*(10), 6141–6145.

Jilaveanu, L. B., Zito, C. R., and Oliver, D. (2005): Dimeric SecA is essential for protein translocation. *Proceedings of the National Academy of Sciences, USA*, *102*(21), 7511–7516.

Johnson, J. L., and Craig, E. A. (2001): An essential role for the substrate-binding region of Hsp40s in Saccharomyces cerevisiae. *The Journal of Cell Biology*, *152*(4), 851–6.

Jones, M. K., and Good, M. F. (2006): Malaria parasites up close. *Nature Medicine*, *12*(2), 170–171.

Joshi, B., Biswas, S., and Sharma, Y. D. (1992): Effect of heat-shock on *Plasmodium falciparum* viability, growth and expression of the heat-shock protein "PFHSP70-I" gene. *FEBS Letters*, *312*(1), 91–4.

Jubete, Y., Maurizi, M. R., and Gottesman, S. (1996): Role of the heat shock protein DnaJ in the lon-dependent degradation of naturally unstable proteins. *The Journal of Biological Chemistry*, *271*(48), 30798–30803.

Jung, E., and Williams, K. L. (1997): The production of glycoproteins with soecial reference to simple eukaryotes including *Dictyostelium discoideum*. *Biotechnology and Applied Biochemistry*, *25*, 3 – 8.

Kabsch, W., and Sander, C. (1983): Protein Secondary Structure: Pattern Recognition of Hydrogen-Bonded and Geometrical Features. *Biopolymers*, *22*(12), 2577–2637.

Kaluz, S., Kolble, K., and Reid, K. B. M. (1992): Directional cloning of PCR products using exonuclease Ill. *Nucleic Acids Research*, *20*(16), 4369–4370.

Kampinga, H. H., and Craig, E. A. (2010): The Hsp70 chaperone machinery: J-proteins as drivers of functional specificity. *Molecular Cell*, *11*(8), 579–592.

Kampinga, H. H., Hageman, J., Vos, M. J., Kubota, H., Tanguay, R. M., Bruford, E. A., Cheetham, M. E., Chen, B., and Hightower, L. E. (2009): Guidelines for the nomenclature of the human heat shock proteins. *Cell Stress and Chaperones*, *14*, 105–111.

Kappe, S., Bruderer, T., Gantt, S., Fujioka, H., Nussenzweig, V., and Ménard, R. (1999): Conservation of a gliding motility and cell invasion machinery in apicomplexan parasites. *The Journal of Cell Biology*, *147*(5), 937–944.

Kappe, S. H. I., Buscaglia, C. A., and Nussenzweig, V. (2004): *Plasmodium* sporozoite molecular cell biology. *Annual Review of Cell and Developmental Biology*, *20*, 29–59.

Kappes, B., Suetterlin, B. W., Hofer-Warbinek, R., Humar, R., and Franklin, R. M. (1993): Two major phosphoproteins of *Plasmodium falciparum* are heat shock proteins. *Molecular and Biochemical Parasitology*, *59*(1), 83–94.

Kariu, T., Ishino, T., Yano, K., Chinzei, Y., and Yuda, M. (2006): CelTOS, a novel malarial protein that mediates transmission to mosquito and vertebrate hosts. *Molecular Microbiology*, *59*(5), 1369–1379.

Karplus, P. A., and Schulz., G. E. (1988): Pediction of chain flexibility in proteins. *Naturwissenschaften*, *72*, 212–213.

Kaufman, R. J. (1990a): Selection and coamplification of heterologous genes in mammalian cells. *Methods in Enzymology*, *185*, 537 – 566.

Kaufman, R. J. (1990b): Vectors used for expression in mammalian cells. *Methods in Enzymology*, *185*, 487 – 511.

Kauppinen, J. K. ., Moffatt, D. J. ., Mantsch, H. H., and Cameron, D. G. (1981): Fourier Self-Deconvolution: A method for resolving intrinsically overlapped bands. *Applied Spectroscopy*, *35*(3), 271 – 276.

Kazemi-Esfarjani, P., and Benzer, S. (2000): Genetic suppression of polyglutamine toxicity in Drosophila. *Science*, *287*(5459), 1837–1840.

Kebaier, C., Voza, T., and Vanderberg, J. (2009): Kinetics of mosquito-injected *Plasmodium* sporozoites in mice: Fewer sporozoites are injected into sporozoite-immunized mice. *PLoS Pathogens*, *5*(4), 10.

Kelley, W. L. (1998): The J-domain family and the recruitment of chaperone power. *Trends in Biochemical Sciences*, *23*(6), 222–7.

Kiefer, F., Arnold, K., Künzli, M., Bordoli, L., and Schwede, T. (2009): The SWISS-MODEL repository and associated resources. *Nucleic Acids Research*, *37*(Database issue), D387–92.

Kimball, S. R., and Jefferson, L. S. (2006): New functions for amino acids: effects on gene transcription and translation. *The American Journal of Clinical Nutrition*, *83*(2), 500S–507S.

Kitagawa, M., Miyakawa, M., Matsumura, Y., and Tsuchido, T. (2002): *Escherichia coli* small heat shock proteins, IbpA and IbpB, protect enzymes from inactivation by heat and oxidants. *The Federation of European Biochemical Societies Journal*, *269*(12), 2907–2917.

Kitt, P. A., and Possee, R. D. (1993): A method for producing recombinant baculovirus expression vectors at high frequency. *BioTechniques*, *14*, 810 – 817.

Klein, P., Mattoon, D., Lemmon, M. A., and Schlessinger, J. (2004): A structure-based model for ligand binding and dimerisation of EGF receptors. *Proceedings of the National Academy of Sciences, USA*, *101*(4), 929–34.

Klose, D. P., Wallace, B. A., and Janes, R. W. (2010): 2Struc: the secondary structure server. *Bioinformatics*, *26*(20), 2624–5.

Knuepfer, E., Rug, M., Klonis, N., Tilley, L., and Cowman, A. F. (2005): Trafficking of the major virulence factor to the surface of transfected *P. falciparum*–infected erythrocytes. *Blood*, *105*(10), 4078–4087.

Kong, J., and Yu, S. (2007): Fourier transform infrared spectroscopic analysis (FTIR) of protein secondary structures protein, data analysis and band assignment. *Biochemistry*, *39*(8), 549–559.

Kopito, R. R. (2000): Aggresomes, inclusion bodies and protein aggregation. *Trends in Cell Biology*, *10*(12), 524–530.

Kreier, J. P. (1977): The isolation and fractionation of malaria-infected cells. *Bulletin of the World Health Organization*, *55*(2-3), 317–331.

Krogstad, D. J., Schlesinger, P. H., and Gluzman, I. Y. (1985): Antimalarials increase vesicle pH in *Plasmodium falciparum*. *The Journal of Cell Biology*, 101:2302 - 2309.

Krungkrai, J. (1995): Purification, characterisation and localisation of mitochondrial dihydroorotate dehydrogenase in *Plasmodium falciparum*, human malaria parasite. *Biochimica et Biophysica Acta*, *1243*(3), 351–60.

Külzer, S., Charnaud, S., Dagan, T., Riedel, J., Mandal, P., Pesce, E. R., Blatch, G. L., Crabb, B. S., Gilson, P. R., and Przyborski, J. M. (2012): *Plasmodium falciparum*-encoded exported hsp70/hsp40 chaperone/co-chaperone complexes within the host erythrocyte. *Cellular Microbiology*, *14*(11):1784-95.

Külzer, S., Rug, M., Brinkmann, K., Cannon, P., Cowman, A., Lingelbach, K., Blatch, G. L., Maier, A. G., and Przyborski, J. M. (2010): Parasite-encoded Hsp40 proteins define novel mobile structures in the cytosol of the *P. falciparum*-infected erythrocyte. *Cellular Microbiology*, *12*(10), 1398–420.

Kukuruzinska, M. A., Bergh, M. L. E., and Jackson, B. L. (1987): Protein glycosylation in yeast. *Annual Review Biochemistry*, *56*, 915–944.

Kumar, A., Tanveer, A., Biswas, S., Ram, E. E. V. S. R., Gupta, A., Kumar, B., and Habib, S. (2010): Nuclear-encoded DnaJ homologue of *Plasmodium falciparum* interacts with replication ori of the apicoplast genome. *Molecular Microbiology*, *75*(4), 942–56.

Kumar, N., Koski, G., Harada, M., Aikawa, M., and Zheng, H. (1991): Induction and localisation of *Plasmodium falciparum* stress proteins related to the heat shock protein 70 family. *Molecular and Biochemical Parasitology*, *48*(1), 47–58.

Kumar, N., Zhao, Y., Graves, P., Perez Folgar, J., Maloy, L., and Zheng, H. (1990): Human immune response directed against *Plasmodium falciparum* heat shock-related proteins. *Infection and Immunity*, *58*(5), 1408–1414.

Kurganov, B. I. (2002): Kinetics of protein aggregation. Quantitative estimation of the chaperone-like activity in test-systems based on suppression of protein aggregation. *Biochemistry*, *67*(4), 409–22.

Kyte, J., and Doolittle., R. F. (1982): A simple method for displaying the hydropathic character of a protein. *Journal of Molecular Biology*, *157*, 105 – 132.

LaCount, D. J., Vignali, M., Chettier, R., Phansalkar, A., Bell, R., Hesselberth, J. R., Schoenfeld, L. W., Ota, I., Sahasrabudhe, S., Kurschner, C., Fields, S., and Hughes, R. E. (2005): A protein interaction network of the malaria parasite *Plasmodium falciparum*. *Nature*, *438*(7064), 103–107.

Lal, K., Delves, M. J., Bromley, E., Wastling, J. M., Tomley, F. M., and Sinden, R. E. (2009): *Plasmodium* male development gene-1 (mdv-1) is important for female sexual development and identifies a polarised plasma membrane during zygote development. *International Journal for Parasitology*, *39*(7), 755–61.

Lamarque, M., Besteiro, S., Papoin, J., Roques, M., Normand, B. V.-L., Morlon-Guyot, J., Dubremetz, J. F., Fauquenoy, S., Tomavo, S., and Faber, B. W. *et al.* (2011): The RON2-AMA1 interaction is a critical step in moving junction-dependent invasion by apicomplexan parasites. *PLoS Pathogens*, *7*, e1001276.

Lambros, C., and Vanderberg, J. P. (1979): Synchronization of *Plasmodium falciparum* erythrocytic stages in culture. *Journal of Parasitology*, *65*(3), 418–420.

Langer, T., Lu, C., Echols, H., Flanagan, J., Hayer, M. K., and Hartl, F. U. (1992): Successive action of DnaK, DnaJ and GroEL along the pathway of chaperone-mediated protein folding. *Nature*, *356*(6371), 683–689.

Lanzer, M., Wickert, H., Krohne, G., Vincensini, L., and Braun Breton, C. (2006): Maurer's clefts: a novel multi-functional organelle in the cytoplasm of *Plasmodium falciparum*-infected erythrocytes. *International Journal for Parasitology*, *36*(1), 23–36.

Larkin, M. a, Blackshields, G., Brown, N. P., Chenna, R., Mcgettigan, P. a, McWilliam, H., Valentin, F., Wallace, I. M., Wilm, A., Lopez, R., Thompson, J. D., Gibson, T. J., and Higgins, D. G. (2007): Clustal W and Clustal X version 2.0. *Bioinformatics*, *23*(21), 2947–8.

Laufen, T., Mayer, M. P., Beisel, C., Klostermeier, D., Mogk, A., Reinstein, J., and Bukau, B. (1999): Mechanism of regulation of hsp70 chaperones by DnaJ cochaperones. *Proceedings of the National Academy of Sciences, USA*, *96*(10), 5452–7.

Lavialle-Defaix, C., Apaire-Marchais, V., Legros, C., Pennetier, C., Mohamed, A., Licznar, P., Corbel, V., and Lapied, B. (2011): Anopheles gambiae mosquito isolated neurons: A new biological model for optimizing insecticide/repellent efficacy. *Journal of Neuroscience Methods*, *200*(1), 68–73.

Le Roch, K. G., Zhou, Y., Blair, P. L., Grainger, M., Moch, J. K., Haynes, J. D., De La Vega, P., Holder, A. a, Batalov, S., Carucci, D. J., and Winzeler, E. a. (2003): Discovery of gene function by expression profiling of the malaria parasite life cycle. *Science*, *301*(5639), 1503–8.

Lee, S., Fan, C. Y., Younger, J. M., Ren, H., and Cyr, D. M. (2002): Identification of essential residues in the type II Hsp40 Sis1 that function in polypeptide binding. *The Journal of Biological Chemistry*, *277*(24), 21675–82.

Lefevre, G., Looareesuwan, S., Treeprasertsuk, S., Krudsood, S., Silachamroon, U., Gathmann, I., Mull, R., and Bakshi, R. (2001): A clinical and pharmacokinetic trial of six doses of artemether- lumefantrine for multidrug-resistant *Plasmodium falciparum* malaria in Thailand. *American Journal of Tropical Medicine and Hygiene*, *64*, 247–256.

Lelièvre1, J., Almela, M. J., Lozano, S., Miguel, C., Franco, V., Leroy, D., and Herreros, E. (2012): Activity of clinically relevant antimalarial drugs on *Plasmodium falciparum* mature gametocytes in an atp bioluminescence "transmission blocking" assay. *PLoS One*, *7*(4), 1–8.

Lell, B., Faucher, J. F., Missinou, M. A., Borrmann, S., Dangelmaier, O., Horton, J., and Kremsner, P. G. (2000): Malaria chemoprophylaxis with tafenoquine: a randomised study. *Lancet*, *355*(9220), 2041–5.

Lepers, J. P., Deloron, P., Fontenille, D., and Coulanges, P. (1988): Reappearance of falciparum malaria in central highland plateaux of Madagascar. *Lancet*, *1*(8585), 586.

Levinson, A. D. (1990): Expression of heterologous genes in mammalian cells. *Methods in Enzymology*, *185*, 485 – 487.

Lew, V. L., Tiffert, T., and Ginsburg, H. (2003): Excess hemoglobin digestion and the osmotic stability of *Plasmodium falciparum*-infected red blood cells. *Blood*, *101*(10), 4189–4194.

Li, J., Qian, X., and Sha, B. (2003): The crystal structure of the yeast Hsp40 Ydj1 complexed with its peptide substrate. *Structure*, *11*(12), 1475–83.

Li, J., Wu, Y., Qian, X., and Sha, B. (2006): Crystal structure of yeast Sis1 peptide-binding fragment and Hsp70 Ssa1 C-terminal complex. *Biochemical Journal*, *398*, 353 – 360.

Liedberg, B., Nylander, C., and Lundstrm, I. (1995): Biosensing with surface plasmon resonance---how it all started. *Biosensor and Bioelectronics*, *10*, i – ix.

Limviroj, W., Yano, K., Yuda, M., Ando, K., and Chinzei, Y. (2002): Immuno-electron microscopic observation of *Plasmodium berghei* CTRP localisation in the midgut of the vector mosquito Anopheles stephensi. *The Journal of Parasitology*, *88*(4), 664–672.

Llinás, M., Bozdech, Z., Wong, E. D., Adai, A. T., and DeRisi, J. L. (2006): Comparative whole genome transcriptome analysis of three *Plasmodium falciparum* strains. *Nucleic Acids Research*, *34*(4), 1166–73.

Long, H. Y., Lell, B., Dietz, K., and Kremsner, P. G. (2001): *Plasmodium falciparum*: *in vitro* growth inhibition by febrile temperature. *Parasitology Research*, *87*, 553–555.

Longshaw, B. V. M., Nicoll, W. S., Botha, M., Ludewig, M. H., Shonhai, A., Stephens, L. L., and Blatch, G. L. (2006): Getting practical with molecular chaperone. *Biotechnology International*, *18*, 24–27.

Louw, C. A., Ludewig, M. H., and Blatch, G. L. (2010): Overproduction , purification and characterisation of Tbj1 , a novel Type III Hsp40 from *Trypanosoma brucei* , the African sleeping sickness parasite. *Protein Expression and Purification*, *69*(2), 168–177.

Ma, Y., Greener, T., Pacold, M. E., Kaushal, S., Greene, L. E., and Eisenberg, E. (2002): Identification of domain required for catalytic activity of auxilin in supporting clathrin uncoating by Hsc70. *The Journal of Biological Chemistry*, *277*(51), 49267–49274.

Maeda, H., Sahara, H., Mori, Y., Torigo, T., Kamiguchi, K., Tamura, Y., Tamura, Y., Hirata, K., and Sato, N. (2007): Biological heterogeneity of the peptide-binding motif of the 70-kDa heat shock protein by surface plasmon resonance analysis. *Journal of Biological Chemistry*, *282*(37), 26956 – 26962.

Magotti, P., Ricklin, D., Qu, H., Wu, Y.-Q., Kaznessis, Y. N., and Lambris, J. D. (2009): Structure-kinetic relationship analysis of the therapeutic complement inhibitor compstatin. *Journal of Molecular Recognition : JMR*, *22*(6), 495–505.

Maier, A. G., Cooke, B. M., Cowman, A. F., and Tilley, L. (2009): Malaria parasite proteins that remodel the host erythrocyte. *Nature Reviews Microbiology*, *7*(5), 341–54.

Maier, A. G., Rug, M., O'Neill, M. T., Beeson, J. G., Marti, M., Reeder, J., and Cowman, A. F. (2007): Skeleton-binding protein 1 functions at the parasitophorous vacuole membrane to traffic PfEMP1 to the *Plasmodium falciparum*-infected erythrocyte surface. *Blood*, *109*(3), 1289–1297.

Maier, A. G., Rug, M., O'Neill, M. T., Brown, M., Chakravorty, S., Szestak, T., Chesson, J., Wu, Y., Hughes, K., Coppel, R. L., Newbold, C., Beeson, J. G., Craig, A., Crabb, B. S., and Cowman, A. F. (2008): Exported proteins required for virulence and rigidity of *Plasmodium falciparum*-infected human erythrocytes. *Cell*, *134*(1), 48–61.

Mamelak, D., and Lingwood, C. (2001): The ATPase domain of hsp70 possesses a unique binding specificity for 3'-sulfogalactolipids. *The Journal of Biological Chemistry*, *276*(1), 449–456.

Mamelak, D., Mylvaganam, M., Tanahashi, E., Ito, H., Ishida, H., Kiso, M., and Lingwood, C. (2001a): The aglycone of sulfogalactolipids can alter the sulfate ester substitution position required for hsc70 recognition. *Carbohydrate research*, *335*(2), 91–100.

Mamelak, D., Mylvaganam, M., Whetstone, H., Hartmann, E., Lennarz, W., Wyrick, P. B., Raulston, J., Han, H., Hoffman, P., and Lingwood, C. A. (2001b): Hsp70s contain a specific sulfogalactolipid binding site: Differential aglycone influence on sulfogalactosyl ceramide binding by recombinant prokaryotic and eukaryotic hsp70 family members. *Biochemistry*, *40*(12), 3572–3582.

Mantsch, H. H., Moffatt, D. J., and Casal, H. L. (1988): Fourier Transform methods for spectral resolution enhancement. *Journal of Molecular Structure*, *173*, 285–298.

Markey, F. (1999): What is SPR anyway? *BIA J*, *6*, 14–17.

Markossian, K. a, and Kurganov, B. I. (2004): Protein folding, misfolding, and aggregation: Formation of inclusion bodies and aggresomes. *Biochemistry*, *69*(9), 971–84.

Marti, M., Good, R. T., Rug, M., Knuepfer, E., and Cowman, A. F. (2004): Targeting malaria virulence and remodeling proteins to the host erythrocyte. *Science*, *306*(5703), 1930–3.

Martinez-Yamout, M., Legge, G. B., Zhang, O., Wright, P. E., and Dyson, H. J. (2000): Solution structure of the cysteine-rich domain of the *Escherichia coli* chaperone protein DnaJ. *Journal of Molecular Biology*, *300*(4), 805–818.

Matambo, T. S., Odunuga, O. O., Boshoff, A., and Blatch, G. L. (2004): Overproduction, purification, and characterisation of the *Plasmodium falciparum* heat shock protein 70. *Protein Expression and Purification*, *33*(2), 214–222.

Matsuura, Y., Possee, R. D., Overton, H., and Bishop, D. H. L., J. (1987): Baculovirus expression vectors: the requirement for high level expression of proteins, including glycoproteins. *Gene virology*, *68*, 1233–1250.

Mayer, D. C. G., Cofie, J., Jiang, L., Hartl, D. L., Tracy, E., Kabat, J., Mendoza, L. H., and Miller, L. H. (2009): Glycophorin B is the erythrocyte receptor of *Plasmodium falciparum* erythrocyte-binding ligand, EBL-1. *Proceedings of the National Academy of Sciences, USA*, *106*(13), 5348–5352.

Mayer, M. P., and Bukau, B. (2005): Hsp70 chaperones: Cellular functions and molecular mechanism. *Cellular and Molecular Life Sciences*, *62*(6), 670–684.

Mayer, M. P., Laufen, T., Paal, K., McCarty, J. S., and Bukau, B. (1999): Investigation of the interaction between DnaK and DnaJ by surface plasmon resonance spectroscopy. *Journal of Molecular Biology*, *289*, 1131 – 1144.

McCarty, J. S., and Walker, G. C. (1991): DnaK as a thermometer: threonine-199 is site of autophosphorylation and is critical for ATPase activity. *Proceedings of the National Academy of Sciences, USA*, *88*(21), 9513–9517.

McRobert, L., Taylor, C. J., Deng, W., Fivelman, Q. L., Cummings, R. M., Polley, S. D., Billker, O., and Baker, D. A. (2008): Gametogenesis in Malaria Parasites Is Mediated by the cGMP-Dependent Protein Kinase. *PLoS Biology*, *6*(6), 10.

Meng, F., Park, Y., and Zhou, H. (2001): Role of proline, glycerol, and heparin as protein folding aids during refolding of rabbit muscle creatine kinase. *The International Journal of Biochemistry and Cell Biology*, *33*(7), 701–9.

Meshnick, S. R. (2001): Artemisinin and its derivatives. *In P. J. Rosenthal (Ed.), Antimalarial Chemotherapy: Mechanisms of action, resistance, and new directions in drug discovery,* pages 191–201.

Michels, A. A., Kanon, B., Konings, A. W. T., Ohtsuka, K., Bensaude, O., and Kampinga, H. H. (1997): Hsp70 and Hsp40 chaperone activities in the cytoplasm and the nucleus of mammalian cells. *The Journal of Biological Chemistry*, *272*(52), 33283–33289.

Middelberg, A. (2002): Preparative protein refolding. *Trends in Biotechnology*, *20*, 437 – 443.

Miller, L. H., Baruch, D. I., Marsh, K., and Doumbo, O. K. (2002): The pathogenic basis of malaria. *Nature*, *415*(6872), 673–679.

Misra, G., and Ramachandran, R. (2009): Hsp70-1 from *Plasmodium falciparum*: protein stability, domain analysis and chaperone activity. *Biophysical chemistry*, *142*(1-3), 55–64.

Misselwitz, B., Staeck, O., and Rapoport, T. A. (1998): J proteins catalytically activate Hsp70 molecules to trap a wide range of peptide sequences. *Molecular Cell*, *2*(5), 593–603.

Mitchell, G. H., Thomas, A. W., Margos, G., Dluzewski, A. R., and Bannister, L. H. (2004): Apical Membrane Antigen 1, a Major Malaria Vaccine Candidate, Mediates the Close Attachment of Invasive Merozoites to Host Red Blood Cells. *Infection and Immunity*, *72*(1), 154–158.

Model, T. C. (1998): Fundamentals of NMR. *Nucleus*, 1–38.

Montagna, G. N., Matuschewski, K., and Buscaglia, C. A. (2012): *Plasmodium* sporozoite motility: an update. *Frontier Bioscience*, *17*, 726–744.

Morahan, B. J., Strobel, C., Hasan, U., Czesny, B., Mantel, P.-Y., Marti, M., Eksi, S., and Williamson, K. C. (2011): Functional analysis of the exported type IV HSP40 protein PfGECO in *Plasmodium falciparum* gametocytes. *Eukaryotic Cell*, *10*(11), 1492–503.

Moreira, C. K., Templeton, T. J., Lavazec, C., Hayward, R. E., Hobbs, C. V, Kroeze, H., Janse, C. J., Waters, A. P., Sinnis, P., and Coppi, A. (2008): The *Plasmodium* TRAP / MIC2 family member , TRAP-Like Protein (TLP), is involved in tissue traversal by sporozoites. *Cellular Microbiology*, *10*(7), 1505–1516.

Moro, F., Fernández-Sáiz, V., and Muga, A. (2004): The lid subdomain of DnaK is required for the stabilization of the substrate-binding site. *The Journal of Biological Chemistry*, *279*(19), 19600–19606.

Muchowski, J. ., and Clark, J. . (1998): ATP-enhanced molecular chaperone functions of the small heat shock protein human αB crystallin. *Proceedings of the National Academy of Sciences, USA*, *95*, 1004–1009.

Müller, I. B., and Hyde, J. E. (2010): Antimalarial drugs: modes of action and mechanisms of parasite resistance. *Future Microbiology*, *5*(12), 1857–73.

Münter, S., Sabass, B., Selhuber-Unkel, C., Kudryashev, M., Hegge, S., Engel, U., Spatz, J. P., Matuschewski, K., Schwarz, U. S., and Frischknecht, F. (2009): *Plasmodium* sporozoite motility is modulated by the turnover of discrete adhesion sites. *Cell Host Microbe*, *6*(6), 551–562.

Murray, C. J. L., Rosenfeld, L. C., Lim, S. S., Andrews, K. G., Foreman, K. J., Haring, D., Fullman, N., Naghavi, M., Lozano, R., and Lopez, A. D. (2012): Global malaria mortality between 1980 and 2010: a systematic analysis. *Lancet*, *379*(9814), 413–31.

Mutabingwa, T., Nzila, A., Mberu, E., Nduati, E., Winstanley, P., Hills, E., and Watkins, W. (2001): Chlorproguanil-dapsone for treatment of drugresistant *Plasmodium falciparum* malaria in Tanzania. *Lancet*, *358*, 1218–1223.

N'Guessan, R., Corbel, V., Akogbéto, M., and Rowland, M. (2007): Reduced Efficacy of Insecticide-treated Nets and Indoor Residual Spraying for Malaria Control in Pyrethroid Resistance Area, Benin. *Emerging Infectious Diseases*, *13*(2), 199–206.

Narum, D. L., Kumar, S., Rogers, W. O., Steven, R., Liang, H., Oakley, M., Taye, A., Kim, B., Sim, L., Hoffman, S. L., Fuhrmann, S. R., and Sim, B. K. I. M. L. E. E. (2001): Codon optimisation of gene fragments encoding *Plasmodium falciparum* merzoite proteins enhances DNA vaccine protein expression and immunogenicity in mice. *Infection and Immunity*, *69*(12), 7250 – 7253.

Nicoll, W. S., Boshoff, A., Ludewig, M. H., Hennessy, F., Jung, M., and Blatch, G. L. (2006): Approaches to the isolation and characterisation of molecular chaperones. *Protein Expression and Purification*, *46*(1), 1–15.

Nicoll, W. S., Botha, M., McNamara, C., Schlange, M., Pesce, E. R., Boshoff, A., Ludewig, M. H., Zimmermann, R., Cheetham, M. E., Chapple, J. P., and Blatch, G. L. (2007): Cytosolic and ER J-domains of mammalian and parasitic origin can functionally interact with DnaK. *The International Journal of Biochemistry and Cell Biology*, *39*(4), 736–751.

Njunge, J. M., Ludewig, M. H., Boshoff, A., Pesce, E., and Blatch, G. L. (2013): Hsp70s and J proteins of *Plasmodium* parasites infecting rodents and primates : Structure , function , clinical relevance , and drug targets. *Current Pharmaceutical Design, 19*(3):387-403.

Noyes, B. E., Glatthaar, B. E., Garavelli, J. S., Bradshaw, R. A., and Apr, N. (2011): Structural and functional similarities between mitochondrial malate dehydrogenase and L-3- Hydroxyacyl CoA dehydrogenase. *Sciences*, *71*(4), 1334–1338.

Nussenzweig, R. S., and Nussenzweig, V. (1984): Development of sporozoite vaccines. *Philosophical transactions of the Royal Society of London.*, *307*, 117–128.

Nyalwidhe, J., and Lingelbach, K. (2006): Proteases and chaperones are the most abundant proteins in the parasitophorous vacuole of *Plasmodium falciparum*-infected erythrocytes. *Proteomics*, *6*(5), 1563–1573.

O'Neill, P. M., Barton, V. ., and Ward, S. . (2010): The molecular mechanism of action of artemisinin – the debatecontinues. *Molecules*, *15*(3), 1705–1721.

O'Neill, P. M., Bray, P. G., Hawley, S. R., Ward, S. A., and Park, B. K. (1998): 4-Aminoquinolines—Past, present, and future; A chemical perspective. *Pharmacology and Therapeutics*, *77*(1), 29–58.

O'Reilly, D. R., Miller, L. K., and Lucknow, V. A. (1992): *Baculovirus Expression System – A Laboratory Manual*, pages 216. Oxford University Press, USA.

Ohki, M., Tamura, F., Nishimura, S., and Uchidag, H. (1986): Nucleotide Sequence of the. *Society*, 1778–1781.

Olusegun, O. L., Thomas, R., and Micheal, I. M. (2012): Curbing maternal and child mortality: The Nigerian experience. *International Journal of Nursing and Midwifery*, *4*(3), 33–39.

Or, E., Boyd, D., Gon, S., Beckwith, J., and Rapoport, T. (2005): The bacterial ATPase SecA functions as a monomer in protein translocation. *The Journal of Biological Chemistry*, *280*(10), 9097–9105.

Osborne, M. J., Crowe, D., Davy, S. L., Macdonald, C., and Moore, G. R. (1997): NMR of paramagnetic proteins. *Methods in Molecular Biology (Clifton NJ, Ed)*, *60*, 233–269.

Otting, G. (2010): Protein NMR using paramagnetic ions. *Annual Review of Biophysics*, *39*, 387–405.

Pagano, B., Mattia, C. A., and Giancola, C. (2009): Applications of isothermal titration calorimetry in biophysical studies of G-quadruplexes. *International Journal of Molecular Sciences*, *10*(7), 2935–2957.

Parsell, D. A., and Lindquist, S. (1993): The function of heat-shock proteins in stress tolerance: degradation and reactivation of damaged proteins. *Annual Review of Genetics*, *27*(1), 437–496.

Patra, a K., Mukhopadhyay, R., Mukhija, R., Krishnan, a, Garg, L. C., and Panda, a K. (2000): Optimisation of inclusion body solubilisation and renaturation of recombinant human growth hormone from *Escherichia coli*. *Protein Expression and Purification*, *18*(2), 182–92.

Pavithra, S. R., Banumathy, G., Joy, O., Singh, V., and Tatu, U. (2004): Recurrent fever promotes *Plasmodim falciparum* development in human erythrocytes. *Journal of Biological Chemistry*, *279*(45), 46692 – 46699.

Pei, X., Guo, X., Coppel, R., Bhattacharjee, S., Haldar, K., Gratzer, W., Mohandas, N., and An, X. (2007): The ring-infected erythrocyte surface antigen (RESA) of *Plasmodium falciparum* stabilizes spectrin tetramers and suppresses further invasion. *Blood*, *110*(3), 1036–42.

Pelham, H. R. (1989): Heat shock and the sorting of luminal ER proteins. *The EMBO Journal*, *8*(11), 3171–6.

Pellecchia, M., Szyperski, T., Wall, D., Georgopoulos, C., and Wüthrich, K. (1996): NMR structure of the J-domain and the Gly/Phe-rich region of the *Escherichia coli* DnaJ chaperone. *Journal of Molecular Biology*, *260*(2), 236–250.

Pesce, E., and Blatch, G. L. (2009): The Hsp40-Hsp70 chaperone machinery of *Plasmodium falciparum*. *Journal of Biochemistry*, *3*(5), 154–163.

Pesce, E.-R., Acharya, P., Tatu, U., Nicoll, W. S., Shonhai, A., Hoppe, H. C., and Blatch, G. L. (2008): The *Plasmodium falciparum* heat shock protein 40, Pfj4, associates with heat shock protein 70 and shows similar heat induction and localisation patterns. *The International Journal of Biochemistry and Cell Biology*, *40*(12), 2914–26.

Peternel, Š., and Komel, R. (2010): Isolation of biologically active nanomaterial (inclusion bodies) from bacterial cells. *Microbial Cell Factories*, *9*(1), 66. .

Pinder, M., Moorthy, V. S., Akanmori, B. D., Genton, B., and Brown, G. V. (2010): MALVAC 2009: progress and challenges in development of whole organism malaria vaccines for endemic countries, 3-4 June 2009, Dakar, Senegal. *Vaccine*, *28*(30), 4695–702.

Plowe, C. (2001): Folate antagonists and mechanisms of resistance. *In P. J. Rosenthal (Ed.), Antimalarial chemotherapy: Mechanisms of action, resistance, and new directions in drug discovery,* pages 173–190.

Ponzi, M., Sidén-Kiamos, I., Bertuccini, L., Currà, C., Kroeze, H., Camarda, G., Pace, T., Franke-Fayard, B., Laurentino, E. C., Louis, C., Waters, A. P., Janse, C. J., and Alano, P. (2009): Egress of *Plasmodium berghei* gametes from their host erythrocyte is mediated by the MDV-1/PEG3 protein. *Cellular Microbiology*, *11*(8), 1272–1288.

Pradel, G., Hayton, K., Aravind, L., Iyer, L. M., Abrahamsen, M. S., Bonawitz, A., Mejia, C., and Templeton, T. J. (2004): A multidomain adhesion protein family expressed in *Plasmodium*

falciparum is essential for transmission to the mosquito. *The Journal of Experimental Medicine*, *199*(11), 1533–1544.

Pratt, W. B. (1997): The role of the hsp90-based chaperone system in signal transduction by nuclear receptors and receptors signaling via MAP kinase. *Annual Review of Pharmacology and Toxicology*, *37*, 297–326.

Price, R. N., Nosten, F., Luxemburger, C., Van Vugt, M., Phaipun, L., Chongsuphajaisiddhi, T., and White, N. J. (1997): Artesunate/mefloquine 3744 treatment of multi-drug resistant falciparum malaria. *Transactions of the Royal Society of Tropical Medicine and Hygiene*, *91*, 574–577.

Prudêncio, M., Rodriguez, A., and Mota, M. M. (2006): The silent path to thousands of merozoites: the *Plasmodium* liver stage. *Nature Reviews Microbiology*, *4*(11), 849–856.

Przyborski, J. M., and Lanzer, M. (2005): Protein transport and trafficking in *Plasmodium falciparum*-infected erythrocytes. *Parasitology*, *130*(Pt 4), 373–388.

Przyborski, J. M., Miller, S. K., Pfahler, J. M., Henrich, P. P., Rohrbach, P., Crabb, B. S., and Lanzer, M. (2005): Trafficking of STEVOR to the Maurer's clefts in *Plasmodium falciparum*-infected erythrocytes. *The European Molecular Biology Organization Journal*, *24*(13), 2306–2317.

Przyborski, J. M., Wickert, H., Krohne, G., and Lanzer, M. (2003): Maurer's clefts--a novel secretory organelle? *Molecular and Biochemical Parasitology*, *132*(1), 17–26.

Pukrittayakamee, S., Chantra, A., Clemens, R., Looareesuwan, S., White, N. J., and Vanijanonta, S. (2000): Therapeutic responses to quinine and clindamycin in multidrug-resistant *falciparum* malaria. *Society*, 5–9.

Puri, N. K., Crivelli, E., Cardamone, M., Fiddes, R., Bertolini, J., Ninham, B., and Brandon, M. R. (1992): Solubilisation of growth hormone and other recombinant proteins from *Escherichia coli* inclusion bodies by using a cationic surfactant. *Biochemical Journal*, *285*, 871 – 879.

Qian, X., Hou, W., Zhengang, L., and Sha, B. (2002): Direct interactions between molecular chaperones heat-shock protein (Hsp) 70 and Hsp40 : yeast Hsp70 Ssa1 binds the extreme C-terminal region of yeast Hsp40 Sis1. *Biochemical Journal*, *34*(361), 27–34.

Rai, M., and Padh, H. (2001): Expression systems for production of heterologous proteins. *Current Science*, *80*(9), 1121–1128.

Ralph, S. A., D'Ombrain, M. C., and McFadden, G. I. (2001): The apicoplast as an antimalarial drug target. *Drug Resistance Update*, *4*, 145–151.

Ramos, C. H. I., Oliveira, C. L. P., Fan, C.-Y., Torriani, I. L., and Cyr, D. M. (2008): Conserved central domains control the quaternary structure of type I and type II Hsp40 molecular chaperones. *Journal of Molecular Biology*, *383*(1), 155–66.

Ramsey, a J., Russell, L. C., Whitt, S. R., and Chinkers, M. (2000): Overlapping sites of tetratricopeptide repeat protein binding and chaperone activity in heat shock protein 90. *The Journal of Biological Chemistry*, *275*(23), 17857–62.

Ramya, T. N. C., Surolia, N., and Surolia, A. (2006): 15-Deoxyspergualin modulates *Plasmodium falciparum* heat shock protein function. *Biochemical and Biophysical Research Communications*, *348*(2), 585–592.

Rangarajan, R., Bei, A. K., Jethwaney, D., Maldonado, P., Dorin, D., Sultan, A. A., and Doerig, C. (2005): A mitogen-activated protein kinase regulates male gametogenesis and transmission of the malaria parasite *Plasmodium berghei*. *EMBO Reports*, *6*(5), 464–469.

Rao, A., Kumar, M. K., Joseph, T., and Bulusu, G. (2010): Cerebral malaria : insights from host-parasite protein-protein interactions. *Malaria Journal*, 1–7.

Razakantoanina, V., Nguyen Kim, P. P., and Jaureguiberry, G. (2000): Antimalarial activity of new gossypol derivatives. *Parasitology Research*, *86*, 665–668.

Regules, J. A., Cummings, J. F., and Ockenhouse, C. F. (2011): The RTS,S vaccine candidate for malaria. *Expert Review of Vaccines*, *10*(5), 589–599.

Reininger, L., Billker, O., Tewari, R., Mukhopadhyay, A., Fennell, C., Dorin-Semblat, D., Doerig, C., Goldring, D., Harmse, L., Ranford-Cartwright, L., Packer, J., and Doerig, C. (2005): A NIMA-related protein kinase is essential for completion of the sexual cycle of malaria parasites. *The Journal of Biological Chemistry*, *280*(36), 31957–31964.

Ren, J., Wen, L., Gao, X., Jin, C., Xue, Y., and Yao, X. (2009): DOG 1.0: Illustrator of protein domain structures. *Cell Research*, *19*(2), 271–3.

Rial, D. V, and Ceccarelli, E. a. (2002): Removal of DnaK contamination during fusion protein purifications. *Protein Expression and Purification*, *25*(3), 503–7.

Rich, R. L., Cannon, M. J., Jenkins, J., Pandian, P., Sundaram, S., Magyar, R., Brockman, J., Lambert, J., and Myszka, D. G. (2008): Extracting kinetic rate constants from surface plasmon resonance array systems. *Analytical Biochemistry*, *373*(1), 112–20.

Rich, R. L., and Myszka, D. G. (2000): Advances in surface plasmon resonance biosensor analysis. *Current Opinion in Biotechnology*, *11*(1), 54–61.

Rich, R. L., and Myszka, D. G. (2008): Survey of the year 2007 commercial optical biosensor literature. *Journal of Molecular Recognition*, *21*(6), 355–400.

Rich, R. L., and Myszka, D. G. (2010): Grading the commercial optical biosensor literature-Class of 2008: "The Mighty Binders". *Journal of Molecular Recognition*, *23*(1), 1–64.

Rich, R. L., and Myszka, D. G. (2011): Survey of the 2009 commercial optical biosensor literature. *Journal of Molecular Recognition*, *24*(6), 892–914.

Richard, D., MacRaild, C. a, Riglar, D. T., Chan, J.-A., Foley, M., Baum, J., Ralph, S. a, Norton, R. S., and Cowman, A. F. (2010): Interaction between *Plasmodium falciparum* apical membrane antigen 1 and the rhoptry neck protein complex defines a key step in the erythrocyte invasion process of malaria parasites. *The Journal of Biological Chemistry*, *285*(19), 14815–22.

Rinas, U., and Bailey, J. E. (1992): Protein compositional analysis of inclusion bodies produced in recombinant *Escherichia coli*. *Applied Microbiology and Biotechnology*, *37*(5), 609–614.

Robbins, J., Dilworth, S. M., Laskey, R. A., and Dingwall, C. (1991): Two interdependent basic domains in nucleoplasmin nuclear targeting sequence: identification of a class of bipartite nuclear targeting sequence. *Cell*, *64*(3), 615–623.

Robert, A., Benoit-Vical, F., Claparols, C., and Meunier, B. (2005): The antimalarial drug artemisinin alkylates heme in infected mice. *Proceedings of the National Academy of Sciences, USA*, *102*(38), 13676–13680.

Rogier, C., Commenges, D., and Trape, J. F. (1996): Evidence for an age-dependent pyrogenic threshold of *Plasmodium falciparum* parasitemia in highly endemic populations. *The American Journal of Tropical Medicine and Hygiene*, *54*(6), 613–619.

Roos, A., and Boron, W. F. (1981): Intracellular pH. . *Physiological Reviews* , *61* (2), 296–434.

Rosenthal, P. J. (2003): Antimalarial drug discovery: old and new approaches. *Journal of Experimental Biology*, *206*(21), 3735–3744.

Rosser, M. F. N., Washburn, E., Muchowski, P. J., Patterson, C., and Cyr, D. M. (2007): Chaperone functions of the E3 ubiquitin ligase CHIP. *The Journal of Biological Chemistry*, *282*(31), 22267–77.

Rothman, J. E. (1989): Polypeptide chain binding proteins: catalysts of protein folding and related processes in cells. *Cell*, *59*(4), 591–601.

Rottenberg, H. (1997): Atovaquone, a broad spectrum antiparasitic drug, collapses mitochondrial membrane potential in a malarial parasite. *Journal of Biological Chemistry*, *272*(7), 3961–3966.

Rowe, A. K., Rowe, S. Y., Snow, R. W., Korenromp, E. L., Schellenberg, J. R. A., Stein, C., Nahlen, B. L., Bryce, J., Black, R. E., and Steketee, R. W. (2006): The burden of malaria mortality among African children in the year 2000. *International Journal of Epidemiology*, *35*(3), 691–704.

Rüdiger, S., Schneider-Mergener, J., and Bukau, B. (2001): Its substrate specificity characterizes the DnaJ co-chaperone as a scanning factor for the DnaK chaperone. *The European Molecular Biology Organization Journal*, *20*(5), 1042–1050.

Rüngeling, E., Laufen, T., and Bahl, H. (1999): Functional characterisation of the chaperones DnaK, DnaJ, and GrpE from Clostridium acetobutylicum. *FEMS Microbiology Letters*, *170*(1), 119–23.

Rug, M., Prescott, S. W., Fernandez, K. M., Cooke, B. M., and Cowman, A. F. (2006): The role of KAHRP domains in knob formation and cytoadherence of *P. falciparum*-infected human erythrocytes. *Blood*, *108*(1), 370–8.

Rug, M., Wickham, M. E., Foley, M., Cowman, A. F., and Tilley, L. (2004): Correct promoter control is needed for trafficking of the ring-infected erythrocyte surface antigen to the host cytosol in transfected malaria parasites. *Infection and Immunity*, *72*(10), 6095–6105.

Ruprecht, J., and Nield, J. (2001): Determining the structure of biological macromolecules by transmission electron microscopy, single particle analysis and 3D reconstruction. *Progress in Biophysics and Molecular Biology*, *75*(3), 121–164.

Russelltt, D. G., and Goldberg, D. E. (1996): On the molecular mechanism of chloroquine's antimalarial action. *Sciences*, *93*, 11865–11870.

Russo, I., Babbitt, S., Muralidharan, V., Butler, T., Oksman, A., and Goldberg, D. E. (2010): Plasmepsin V licenses *Plasmodium* proteins for export into the host erythrocyte. *Nature*, *463*(7281), 632–636.

Ryan, M. T., and Pfanner, N. (2001): Protein folding in the cell. *Advances in Protein Chemistry*, *59*, 223–242.

Saliba, K. J. (1998): Transport and metabolism of the essential vitamin pantothenic acid in human erythrocytes infected with the malaria parasite *Plasmodium falciparum*. *Journal of Biological Chemistry*, *273*(17), 10190–10195.

Sanz-Barrio, R., Fernández-San Millán, A., Carballeda, J., Corral-Martínez, P., Seguí-Simarro, J. M., and Farran, I. (2011): Chaperone-like properties of tobacco plastid thioredoxins f and m. *Journal of Experimental Botany*, *63*(1), 365–79.

Sargeant, T. J., Marti, M., Caler, E., Carlton, J. M., Simpson, K., Speed, T. P., and Cowman, A. F. (2006): Lineage-specific expansion of proteins exported to erythrocytes in malaria parasites. *Genome Biology*, *7*(2), R12.

Saridaki, T., Fröhlich, K. S., Braun-Breton, C., and Lanzer, M. (2009): Export of PfSBP1 to the *Plasmodium falciparum* Maurer's clefts. *Traffic Copenhagen Denmark*, *10*(2), 137–152.

Saridaki, T., Sanchez, C. P., Pfahler, J., and Lanzer, M. (2008): A conditional export system provides new insights into protein export in *Plasmodium falciparum*-infected erythrocytes. *Cellular Microbiology*, *10*(12), 2483–95.

Sassenfeld, H. M., and Brewer, S. J. (1984): A polypeptide fusion designed for purification of recombinant proteins. *Nature Biotechnology*, *2*, 76 – 81.

Sastry, M. S. R., Zhou, W., and Baneyx, F. (2009): Integrity of N- and C-termini is important for *E. coli* Hsp31 chaperone activity. *Protein Science*, *18*(7), 1439–1447.

Sayers, E. W., Barrett, T., Benson, D. A., Bolton, E., Bryant, S. H., Canese, K., Chetvernin, V., Church, D. M., DiCuccio, M., Federhen, S., Feolo, M., Geer, L. Y., Helmberg, W., Kapustin, Y., Landsman, D., Lipman, D. J., Lu, Z., Madden, T. L., Madej, T., Maglott, D. R., Marchler-Bauer, A., Miller, V., Mizrachi, I., Ostell, J., Panchenko, A., *et al.* (2007): Database resources of the national center for biotechnology information. *Nucleic Acids Research*, *35*, 3124.

Schäffer, A. A., Aravind, L., Madden, T. L., Shavirin, S., Spouge, J. L., Wolf, Y. I., Koonin, E. V, and Altschul, S. F. (2001): Improving the accuracy of PSI-BLAST protein database searches with composition-based statistics and other refinements. *Nucleic Acids Research*, *29*(14), 2994–3005.

Schlessinger, J. (2002): Ligand-induced, receptor-mediated dimerisation and activation of EGF receptor. *Cell*, *110*(6), 669–72.

Schmidt, T. G. M., and Skerra, A. (1993): The random peptide libraryassisted engineering of a C-terminal affinity peptide, useful for the detection and purification of a functional Ig Fv fragment. *Protein Engineering*, *6*, 109 – 122.

Schneider, C. A., Rasband, W. S., and Eliceiri, K. W. (2012): NIH Image to ImageJ: 25 years of image analysis. *Nature Methods*, *9*(7), 671–675.

Schwede, T. (2003): SWISS-MODEL: an automated protein homology-modeling server. *Nucleic Acids Research*, *31*(13), 3381–3385.

Sha, B., Lee, S., and Cyr, D. M. (2000): The crystal structure of the peptide-binding fragment from the yeast Hsp40 protein Sis1. *Structure*, *8*(8), 799–807.

Sharma, S. K., De Los Rios, P., Christen, P., Lustig, A., and Goloubinoff, P. (2010): The kinetic parameters and energy cost of the Hsp70 chaperone as a polypeptide unfoldase. *Nature Chemical Biology*, *6*(12), 914–920.

Shatzman, A. R., and Rosenberg, M. (1987): Expression, identification, and characterisation of recombinant gene producs in *Escherichia coli*. *Methods in Enzymology*, *152*, 661 – 673.

Shi, R., Pan, Q., Guan, Y., Hua, Z., Huang, Y., Zhao, M., and Li, Y. (2007): Imidazole as a catalyst for *in vitro* refolding of enhanced green fluorescent protein. *Archives of Biochemistry and Biophysics*, *459*, 122–128.

Shi, Y., Hong, X., and Wang, C. (2005): The C-terminal (331–376) Sequence of *Escherichia coli* DnaJ is essential for dimerisation and chaperone activity. *Journal of Biological Chemistry*, *280*(24), 22761–22768.

Shonhai, A., Boshoff, A., and Blatch, G. L. (2007): The structural and functional diversity of Hsp70 proteins from *Plasmodium falciparum*. *Protein Science*, *16*(9), 1803–18.

Shonhai, A., Botha, M., De Beer, T., Boshoff, A., and Blatch, G. (2008): Structure-function study of *Plasmodium falciparum* heat shock protein 70 using three dimensional modeling and *in vitro* analysis. *Protein and Peptide Letters*, *15*, 1117–1125.

Silberg, J. J., Hoff, K. G., and Vickery, L. E. (1998): The Hsc66-Hsc20 chaperone system in *Escherichia coli*: chaperone activity and interactions with the DnaK-DnaJ-grpE system. *Journal of Bacteriology*, *180*(24), 6617–24.

Silberg, J. J., Tapley, T. L., Hoff, K. G., and Vickery, L. E. (2004): Regulation of the HscA ATPase reaction cycle by the co-chaperone HscB and the iron-sulfur cluster assembly protein IscU. *The Journal of Biological Chemistry*, *279*(52), 53924–53931.

Silberg, J. J., and Vickery, L. E. (2000): Kinetic Characterisation of the ATPase Cycle of the molecular chaperone Hsc66 from *Escherichia coli*. *Biochemistry*, *275*(11), 7779–7786.

Silvestrini, F., Bozdech, Z., Lanfrancotti, A., Di Giulio, E., Bultrini, E., Picci, L., Derisi, J. L., Pizzi, E., and Alano, P. (2005): Genome-wide identification of genes upregulated at the onset of gametocytogenesis in *Plasmodium falciparum*. *Molecular and Biochemical Parasitology*, *143*(1), 100–110.

Silvie, O., Goetz, K., and Matuschewski, K. (2008a): A sporozoite asparagine-rich protein controls initiation of *Plasmodium* liver stage development.*PLoS Pathogens*, *4*(6), 12.

Silvie, O., Mota, M. M., Matuschewski, K., and Prudêncio, M. (2008b): Interactions of the malaria parasite and its mammalian host. *Current Opinion in Microbiology*, *11*(4), 352–359.

Singh, A. P., Buscaglia, C. A., Wang, Q., Levay, A., Nussenzweig, D. R., Walker, J. R., Winzeler, E. A., Fujii, H., Fontoura, B. M. A., and Nussenzweig, V. (2007): *Plasmodium* circumsporozoite protein promotes the development of the liver stages of the parasite. *Cell*, *131*(3), 492–504.

Singh, S. M., and Panda, A. K. (2005): Solubilisation and refolding of bacterial inclusion body proteins. *Journal of Bioscience and Bioengineering*, *99*(4), 303–10.

Sinnis, P., and Sim, B. K. (1997): Cell invasion by the vertebrate stages of *Plasmodium*. *Trends in Microbiology*, *5*(2), 52–58.

Sis, H., Yan, W., and Craig, E. A. (1999): The glycine-phenylalanine-rich region determines the specificity of the yeast Hsp40 Sis1. *Society*, *19*(11).

Slapeta, J., and Keithly, J. S. (2004): Cryptosporidium parvum mitochondrial-type HSP70 targets homologous and heterologous mitochondria. *Eukaryotic Cell*, *3*(2), 483–494.

Slater, A. F., and Cerami, A. (1992): Inhibition by chloroquine of a novel haem polymerase enzyme activity in malaria trophozoites. *Nature*, *355*(6356), 167–169.

Slepenkov, S. V, and Witt, S. N. (2002): The unfolding story of the *Escherichia coli* Hsp70 DnaK: is DnaK a holdase or an unfoldase? *Molecular Microbiology*, *45*(5), 1197–1206.

Smith, D. B., and Johnson, K. S. (1988): Single-step purification of polypeptides expressed in *Escherichia coli* as fusions with glutathione S-transferase. *Gene*, *67*, 31 – 40.

Smith, D. F., Whitesell, L., and Katsanis, E. (1998): Molecular chaperones: biology and prospects for pharmacological intervention. *Pharmacological Reviews*, *50*(4), 493–514.

Smith, T. G., Lourenço, P., Carter, R., Walliker, D., and Ranford-Cartwright, L. C. (2000): Commitment to sexual differentiation in the human malaria parasite, *Plasmodium falciparum*. *Parasitology*, *121 (Pt 2*, 127–133.

Snow, R. W., Guerra, C. A., Noor, A. M., Myint, H. Y., and Hay, S. I. (2005): The global distribution of clinical episodes of *Plasmodium falciparum* malaria. *Nature*, *434*(7030), 214–217.

Sondheimer, N., Lopez, N., Craig, E. A., and Lindquist, S. (2001): The role of Sis1 in the maintenance of the [RNQ+] prion. *The EMBO Journal*, *20*(10), 2435–42.

Song, J., and Markley, J. L. (2007): Cautionary tail: the presence of an N-terminal tag on dynein light-chain Roadblock/LC7 affects its interaction with a functional partner. *Protein and Peptide Letters*, *14*(3), 265–268.

Sowunmi, A., Oduola, A. M., Ogundahunsi, O. A., Falade, C. O., Gbotosho, G. O., and Salako, L. A. (1997): Enhanced efficacy of chloroquine-chlorpheniramine combination in acute uncomplicated falciparum malaria in children. *Transactions of the Royal Society of Tropical Medicine and Hygiene*, *91*, 63–67.

Spielmann, T., and Gilberger, T.-W. (2010): Protein export in malaria parasites: do multiple export motifs add up to multiple export pathways? *Trends in Parasitology*, *26*(1), 6–10.

Spielmann, T., Hawthorne, P. L., Dixon, M. W. A., Hannemann, M., Klotz, K., Kemp, D. J., Klonis, N., Tilley, L., Trenholme, K. R., and Gardiner, D. L. (2006): A cluster of ring stage–specific genes linked to a locus implicated in cytoadherence in *Plasmodium falciparum* codes for PEXEL-negative and PEXEL-positive proteins exported into the host cell. *Molecular Biology of the Cell*, *17*(8), 3613–3624.

Spycher, C., Klonis, N., Spielmann, T., Kump, E., Steiger, S., Tilley, L., and Beck, H.-P. (2003): MAHRP-1, a novel *Plasmodium falciparum* histidine-rich protein, binds ferriprotoporphyrin IX and localizes to the Maurer's clefts. *The Journal of Biological Chemistry*, *278*(37), 35373–35383.

Spycher, C., Rug, M., Pachlatko, E., Hanssen, E., Ferguson, D., Cowman, A. F., Tilley, L., and Beck, H.-P. (2008): The Maurer's cleft protein MAHRP1 is essential for trafficking of PfEMP1 to the surface of *Plasmodium falciparum*-infected erythrocytes. *Molecular Microbiology*, *68*(5), 1300–1314.

Steel, G. J., Fullerton, D. M., Tyson, J. R., and Stirling, C. J. (2004): Coordinated activation of Hsp70 chaperones. *Science*, *303*, 98 – 101.

Stein, E. M., and Shakarchi, R. (2003): Fourier Analysis: An Introduction. *ReCALL*, pages 1–7.

Stephens, L. L., Shonhai, A., and Blatch, G. L. (2011): Co-expression of the *Plasmodium falciparum* molecular chaperone, PfHsp70, improves the heterologous production of the antimalarial drug target GTP cyclohydrolase I, PfGCHI. *Protein Expression and Purification*, *77*(2), 159–65.

Stocks, P. A., Raynes, K. J., and Ward, S. A. (2001): Novel quinoline antimalarials. *In P. J. Rosenthal (Ed.), Antimalarial chemotherapy: Mechanisms of action, resistance, and new directions in drug discovery,* pages 235–253.

Stofko-Hahn, R. E., Carr, D. W., and Scott, J. D. (1992): A single step purification for recombinant proteins. *FEBS Letters*, *302*, 274–278.

Sturm, A., Amino, R., van de Sand, C., Regen, T., Retzlaff, S., Rennenberg, A., Krueger, A., Pollok, J.-M., Menard, R., and Heussler, V. T. (2006): Manipulation of host hepatocytes by the malaria parasite for delivery into liver sinusoids. *Science*, *313*(5791), 1287–90.

Struik, S. S., and Riley, E. M. (2004): Does malaria suffer from lack of memory? *Immunological Reviews*, *201*, 268–90.

Su, X. Z., Heatwole, V. M., Wertheimer, S. P., Guinet, F., Herrfeldt, J. A., Peterson, D. S., Ravetch, J. A., and Wellems, T. E. (1995): The large diverse gene family var encodes proteins involved in cytoadherence and antigenic variation of *Plasmodium falciparum*-infected erythrocytes. *Cell*, *82*(1), 89–100.

Sugimoto, S., Higashi, C., Yoshida, H., and Sonomoto, K. (2008): Construction of *Escherichia coli* DnaK-deletion mutant infected by lambda-DE3 for overexpression and purification of recombinant GrpE proteins. *Protein Expression and Purification*, *60*(1), 31–6.

Suh, W.-C. C., Burkholder, W. F., Lu, C. Z., Zhao, X., Gottesman, M. E., and Gross, C. A. (1998): Interaction of the Hsp70 molecular chaperone, DnaK, with its cochaperone DnaJ. *Proceedings of the National Academy of Sciences, USA*, *95*(26), 15223–8.

Suh, W.-C., Lu, C. Z., and Gross, C. A. (1999): Structural features required for the interaction of the hsp70 molecular chaperone DnaK with its Cochaperone DnaJ. *The Journal of Biological Chemistry*, *274*(43), 30534 – 30539.

Supyani, S., Hillman, B. I., and Suzuki, N. (2007): Baculovirus expression of the 11 mycoreovirus-1 genome segments and identification of the guanylyltransferase-encoding segment. *Proteins*, 342–350.

Swietnicki, W. (2006): Folding aggregated proteins into functionally active forms. *Current Opinion in Biotechnology*, *17*, 367 – 372.

Szabo, a, Stolz, L., and Granzow, R. (1995): Surface plasmon resonance and its use in biomolecular interaction analysis (BIA). *Current Opinion in Structural Biology*, *5*(5), 699–705.

Szabo, A., Langer, T., Schröder, H., Flanagan, J., Bukau, B., and Hartl, F. U. (1994): The ATP hydrolysis-dependent reaction cycle of the *Escherichia coli* Hsp70 system DnaK, DnaJ, and GrpE. *Proceedings of the National Academy of Sciences, USA*, *91*(22), 10345–9.

Tamm, L. K., and Tatulian, S. a. (1997): Infrared spectroscopy of proteins and peptides in lipid bilayers. *Quarterly Reviews of Biophysics*, *30*(4), 365–429.

Tamura, K., Peterson, D., Peterson, N., Stecher, G., Nei, M., and Kumar, S. (2011): MEGA5: molecular evolutionary genetics analysis using maximum likelihood, evolutionary distance, and maximum parsimony methods. *Molecular Biology*, *28*(10), 1530–4.

Tang, L., Yu, J., Dai, D., and Fang, B. (2011): Expression of glycerol dehydrogenase gene in *Escherichia coli* by codon optimisation. *Acta Microbiologica Sinica*, *51*(4), 504–509.

Tao, Y., and Zhang, W. (2000): Recent developments in cryo-electron microscopy reconstruction of single particles. *Current Opinion in Structural Biology*, *10*(5), 616–622.

Taraschi, T. F., Trelka, D., Martinez, S., Schneider, T., and O'Donnell, M. E. (2000): Vesicle-mediated trafficking of parasite proteins to the host cell cytosol and erythrocyte surface membrane in *Plasmodium falciparum* infected erythrocytes. *Molecular and Biochemical Parasitology*, *31*(1), 1381–1391.

Tekwani, B. L., and Walker, L. a. (2005): Targeting the hemozoin synthesis pathway for new antimalarial drug discovery: technologies for *in vitro* beta-hematin formation assay. *Combinatorial Chemistry and High Throughput Screening*, *8*(1), 63–79.

Terpe, K. (2003): Overview of tag protein fusions: from molecular and biochemical fundamentals to commercial systems. *Applied Microbiology and Biotechnology*, *60*(5), 523–33.

Terpe, K. (2006): Overview of bacterial expression systems for heterologous protein production: from molecular and biochemical fundamentals to commercial systems. *Applied Microbiology and Biotechnology*, *72*(2), 211–22.

Thanaraj, T. A., and Argos, P. (1996): Ribosome-mediated translational pause and protein domain organization. *Protein Science*, *5*(8), 1594–612.

The QIAexpressionist™. (2003): A handbook for high-level expression and purification of 6xHis-tagged proteins, Fifth edition, pages 1 – 128.

Thibault, P., and Elser, V. (2010): X-Ray diffraction microscopy. *Annual Review of Condensed Matter Physics*, *1*(1), 237–255.

Thielges, M. C., Chung, J. K., Axup, J. Y., and Fayer, M. D. (2011): Influence of histidine tag attachment on picosecond protein dynamics. *Biochemistry*, *50*(25), 5799–5805.

Thompson, J. D., Higgins, D. G., and Gibson, T. J. (1994): CLUSTAL W: improving the sensitivity of progressive multiple sequence alignment through sequence weighting, position specific gap penalties and weight matrix choice. *Nucleic Acids Research*, *22*, 4673–4680.

Thompson, J., and Sinden, R. E. (1994): In situ detection of Pbs21 mRNA during sexual development of *Plasmodium berghei*. *Molecular and Biochemical Parasitology*, *68*(2), 189–196.

Tokatlidis, K., Dhurjati, P., Millet, J., Béguin, P., and Aubert, J. P. (1991): High activity of inclusion bodies formed in *Escherichia coli* overproducing *Clostridium thermocellum* endoglucanase D. *FEBS Letters*, *282*(1), 205–208.

Tokuoka, M., Tanaka, M., Ono, K., Takagi, S., Shintani, T., and Gomi, K. (2008): Codon optimisation increases steady-state mRNA levels in *Aspergillus oryzae* heterologous gene expression. *Applied and Environmental Microbiology*, *74*(21), 6538–6546.

Tonkin, C. J., Dooren, G. G. Van, Spurck, T. P., Struck, N. S., Good, R. T., Handman, E., Cowman, A. F., and Mcfadden, G. I. (2004): Localisation of organellar proteins in *Plasmodium falciparum* using a novel set of transfection vectors and a new immunofluorescence fixation method. *Molecular and Biochemical Parasitology*, *137*, 13–21.

Torrado, M., Iglesias, R., and Mikhailov, A. T. (2008): Detection of protein interactions based on GFP fragment complementation by fluorescence microscopy and spectrofluorometry. *Biotechniques*, *44*(1), 70, 72, 74.

Toutain, C. M., Clarke, D. J., Leeds, J. A., Kuhn, J., Beckwith, J., Holland, I. B., and Jacq, A. (2003): The transmembrane domain of the DnaJ-like protein DjlA is a dimerisation domain. *Molecular Genetics and Genomics MGG*, *268*(6), 761–770.

Trager, W., and Jensen, J. B. (1976): Human malaria parasites in continuous culture. *Science*, *193*, 673–675.

Trelka, D. P., Schneider, T. G., Reeder, J. C., and Taraschi, T. F. (2000): Evidence for vesicle-mediated trafficking of parasite proteins to the host cell cytosol and erythrocyte surface membrane in *Plasmodium falciparum* infected erythrocytes. *Molecular and Biochemical Parasitology*, *106*(1), 131–45.

Trevino, S. R., Scholtz, J. M., and Pace, C. N. (2007): Amino acid contribution to protein solubility: Asp, Glu, and Ser contribute more favorably than the other hydrophilic amino acids in RNase Sa. *Journal of Molecular Biology*, *366*(2), 449–460.

Tsai, J., and Douglas, M. G. (1996): A conserved HPD sequence of the J-domain is necessary for YDJ1 stimulation of Hsp70 ATPase activity at a site distinct from substrate binding. *The Journal of Biological Chemistry*, *271*(16), 9347–54.

Tsumoto, K., Umetsu, M., Kumagai, I., Ejima, D., and Arakawa, T. (2003): Solubilisation of active green fluorescent protein from insoluble particles by guanidine and arginine. *Biochemical and Biophysical Research Communications*, *312*, 1383–1386.

Tyedmers, J., Lerner, M., Bies, C., Dudek, J., Skowronek, M. H., Haas, I. G., Heim, N., Nastainczyk, W., Volkmer, J., and Zimmermann, R. (2000): Homologs of the yeast Sec complex subunits Sec62p and Sec63p are abundant proteins in dog pancreas microsomes. *Proceedings of the National Academy of Sciences, USA*, *97*(13), 7214–7219.

Tyedmers, J., Mogk, A., and Bukau, B. (2010): Cellular strategies for controlling protein aggregation. *Nature Reviews Molecular Cell Biology*, *11*(11), 777–788.

Udomsangpetch, R., Pipitaporn, B., Silamut, K., Pinches, R., Kyes, S., Looareesuwan, S., Newbold, C., and White, N. J. (2002): Febrile temperatures induce cytoadherence of ring-stage *Plasmodium falciparum*-infected erythrocytes. *Proceedings of the National Academy of Sciences, USA*, *99*, 11825–11829.

Upadhyay, A. K., Murmu, A., Singh, A., and Panda, A. K. (2012): Kinetics of inclusion body formation and its correlation with the characteristics of protein aggregates in *Escherichia coli*. *PLoS ONE*, *7*(3), e33951 (1–11).

Usynin, I., Klotz, C., and Frevert, U. (2007): Malaria circumsporozoite protein inhibits the respiratory burst in Kuppfer cells. *Cellular Microbiology*, *9*(11), 2610–2628.

Vaidya, A. B. (2001): Atovaquone-proguanil combination. *In P. J. Rosenthal (Ed.), Antimalarial chemotherapy: Mechanisms of action, resistance, and new directions in drug discovery* (pp. 203–218).

Vaidya, A. B., Lashgari, M. S., Pologe, L. G., and Morrisey, J. (1993): Structural features of *Plasmodium* cytochrome b that may underlie susceptibility to 8-aminoquinolines and hydroxynaphthoquinones. *Molecular and Biochemical Parasitology*, *58*(1), 33–42.

Valax, P., and Georgiou, G. (1993): Molecular characterisation of 8-lactamase inclusion bodies produced in *Escherichia coli*. *Biotechnology Programme*, *9*(5),539–547.

Vallejo, L. F., and Rinas, U. (2004): Strategies for the recovery of active proteins through refolding of bacterial inclusion body proteins. *Microbial Cell Factories*, *3*, 11.

Vallely, A., Vallely, L., Changalucha, J., Greenwood, B., and Chandramohan, D. (2007): Intermittent preventive treatment for malaria in pregnancy in Africa: what's new, what's needed? *Malaria Journal*, *6*, 1-13.

Van Den Berg, B., Ellis, R. J., and Dobson, C. M. (1999): Effects of macromolecular crowding on protein folding and aggregation. *The European Molecular Biology Organization Journal*, *18*(24), 6927–6933.

Van Dijk, M. R., Janse, C. J., Thompson, J., Waters, A. P., Braks, J. A., Dodemont, H. J., Stunnenberg, H. G., Van Gemert, G. J., Sauerwein, R. W., and Eling, W. (2001): A central role for P48/45 in malaria parasite male gamete fertility. *Cell*, *104*(1), 153–64.

Van Ooij, C., Tamez, P., Bhattacharjee, S., Hiller, N. L., Harrison, T., Liolios, K., Kooij, T., Ramesar, J., Balu, B., Adams, J., Waters, A. P., Waters, A., Janse, C. J., Janse, C., and Haldar, K. (2008): The malaria secretome: from algorithms to essential function in blood stage infection. *PLoS Pathogens*, *4*(6), e1000084.

Van Schalkwyk, D. A., Walden, J. C., and Smith, P. J. (2001): Reversal of chloroquine resistance in *Plasmodium falciparum* using combinations of chemosensitizers. *Antimicrobial Agents and Chemotherapy*, *45*, 3171–3174.

Van Vugt, M., Looareesuwan, S., Wilairatana, P., McGready, R., Villegas, L., Gathmann, I., Mull, R., Brockman, A., White, N. J., and Nosten, F. (2000): Artemether-lumefantrine for the treatment of multidrug-resistant falciparum malaria. *Transactions of the Royal Society of Tropical Medicine and Hygiene*, (94), 545–548.

Vassiliev, S., Lee, C.-I., Brudvig, G. W., and Bruce, D. (2002): Structure-based kinetic modeling of excited-state transfer and trapping in histidine-tagged photosystem II core complexes from synechocystis. *Biochemistry*, *41*(40), 12236–12243.

Vaughan, A. M., Aly, A. S. I., and Kappe, S. H. I. (2008): Malaria parasite pre-erythrocytic stage infection: Gliding and Hiding. *Cell Host Microbe*, *4*(3), 209–218.

Vial, H. J., and Calas, M. (2001): Inhibitors of phospholipid metabolism. *In P. J. Rosenthal (Ed.), Antimalarial chemotherapy: Mechanisms of action, resistance, and new directions in drug discovery,* pages 347–365.

Vincensini, L., Richert, S., Blisnick, T., Van Dorsselaer, A., Leize-Wagner, E., Rabilloud, T., and Braun Breton, C. (2005): Proteomic analysis identifies novel proteins of the Maurer's clefts, a secretory compartment delivering *Plasmodium falciparum* proteins to the surface of its host cell. *Molecular Cellular Proteomics MCP*, *4*(4), 582–593.

Vitale, A., Ceriotti, A., and Denecke, J. (1993): The role of the endoplasmic reticulum in protein synthesis , modification and intracellular transport. *Review Literature and Arts of the Americas*, *44*(266), 1417–1444.

Vogel, C., Berzuini, C., Bashton, M., Gough, J., and Teichmann, S. A. (2004): Supra-domains: evolutionary units larger than single protein domains. *Journal of Molecular Biology*, *336*(3), 809–23.

Von Seidlein, L., Milligan, P., Pinder, M., Bojang, K., Anyalebechi, C., Gosling, R., Coleman, R., Ude, J. I., Sadiq, A., and Duraisingh, M. *et al.* (2000): Efficacy of artesunate plus

pyrimethamine-sulphadoxine for uncomplicated malaria in Gambian children: a double-blind, randomised, controlled trial. *Lancet*, *355*, 352–357.

Walsh, D. S., Looareesuwan, S., Wilairatana, P., Heppner, D. G., Tang, D. B., Brewer, T. G., Chokejindachai, W., Viriyavejakul, P., Kyle, D. E., Milhous, W. K., Schuster, B. G., Horton, J., Braitman, D. J., and Brueckner, R. P. (1999): Randomized dose-ranging study of the safety and efficacy of WR 238605 (Tafenoquine) in the prevention of relapse of *Plasmodium vivax* malaria in Thailand. *The Journal of Infectious Diseases*, *180*(4), 1282–7.

Wang, B.-L., Jiao, Y.-L., Li, X.-X., Zheng, F., Liang, H., Sun, Z.-Y., and Guo, G. (2009a): A universal method for directional cloning of PCR products. *Biotechnology and Applied Biochemistry*, *52*, 41–44.

Wang, F., Liu, Y., Ma, G., and Su, Z. (2009b): Glycerol-assisted hydrophobic interaction chromatography improving refolding of recombinant human granulocyte colony-stimulating factor. *Applied Biochemistry and Biotechnology*, *159*(3), 634–41.

Wang, J., Huang, L., and Al., L. J. et. (2010): Artemisinin directly targets malarial mitochondria through its specific mitochondrial activation. *PLoS One*, *5*(3), E9582.

Wang, L., Maji, S. K., Sawaya, M. R., Eisenberg, D., and Riek, R. (2008): Bacterial inclusion bodies contain amyloid-like structure. *PLoS Biology*, *6*(8), 11.

Wassler, M., Westman, J., and Fries, E. (1990): Permeabilization of hepatocytes by a saponin and the effects of dextran. *European Journal of Cell Biology*, *51*(2), 252–258.

Watanabe, J. (1997): Cloning and characterisation of heat shock protein DnaJ homologues from *Plasmodium falciparum* and comparison with ring infected erythrocyte surface antigen. *Molecular and Biochemical Parasitology*, *88*(1-2), 253–258.

Waterkeyn, J. G., Wickham, M. E., Davern, K. M., Cooke, B. M., Coppel, R. L., Reeder, J. C., Culvenor, J. G., Waller, R. F., and Cowman, A. F. (2000): Targeted mutagenesis of *Plasmodium falciparum* erythrocyte membrane protein 3 (PfEMP3) disrupts cytoadherence of malaria-infected red blood cells. *The EMBO Journal*, *19*(12), 2813–2823.

Weatherall, D. J., Miller, L. H., Baruch, D. I., Marsh, K., Doumbo, O. K., Casals-Pascual, C., and Roberts, D. J. (2002): Malaria and the red cell. *Journal of the Royal Society of Medicine*, *78*(2), 183.

Weber, J. L., Lyon, J. A., Wolff, R. H., Hall, T., Lowell, G. H., and Chulay, J. D. (1988): Primary structure of a *Plasmodium falciparum* malaria antigen located at the merozoite surface and within the parasitophorous vacuole. *The Journal of Biological Chemistry*, *263*(23), 11421–11425.

Wheeler, D. L. (2003): Database resources of the national center for biotechnology. *Nucleic Acids Research*, *31*(1), 28–33.

Wheeler, D. L., Church, D. M., Edgar, R., Federhen, S., Helmberg, W., Madden, T. L., Pontius, J. U., Schuler, G. D., Schriml, L. M., Sequeira, E., Suzek, T. O., Tatusova, T. A., and Wagner, L. (2004): Database resources of the national center for biotechnology information: update. *Nucleic Acids Research*, *32*, D35–D40.

White, N. J. (2008): *Plasmodium knowlesi*: The fifth human malaria parasite. *Clinical infectious diseases*, *46*(2), 172–173.

WHO | Insecticide-treated materials. (2012): World health organization. Retrieved September 24, 2012, from http://www.who.int/malaria/vector_control/itm/en/index.html

WHO | Malaria in pregnancy. (2012): World health organization. Retrieved August 31, 2012, from http://www.who.int/malaria/high_risk_groups/pregnancy/en/

WHO | MDG 6: combat HIV/AIDS, malaria and other diseases. (2012): World health organization. Retrieved August 31, 2012, from http://www.who.int/topics/millennium_development_goals/diseases/en/index.html

WHO | World Malaria Report. (2012): World health organization. Retrieved August 31, 2012, from http://www.who.int/malaria/world_malaria_report_2011/en/index.html

Wickert, H., Wissing, F., Andrews, K. T., Stich, A., Krohne, G., and Lanzer, M. (2003): Evidence for trafficking of PfEMP1 to the surface of *P. falciparum*-infected erythrocytes via a complex membrane network. *European Journal of Cell Biology*, *82*(6), 271–284.

Wickham, M. E., Rug, M., Ralph, S. A., Klonis, N., Mcfadden, G. I., Tilley, L., and Cowman, A. F. (2001): Trafficking and assembly of the cytoadherence complex in *Plasmodium falciparum*-infected human erythrocytes. *EMBO Journal*, *20*(20), 5636 – 5649.

Wilby, K. J., Lau, T. T. Y., Gilchrist, S. E., and Ensom, M. H. H. (2012): Mosquirix (RTS,S): A novel vaccine for the prevention of *Plasmodium falciparum* malaria. *The Annals of Pharmacotherapy*, *46*(3), 384–93.

Williamson, D. S., Borgognoni, J., Clay, A., Daniels, Z., Dokurno, P., Drysdale, M. J., Foloppe, N., Francis, G. L., Graham, C. J., Howes, R., Macias, A. T., Murray, J. B., Parsons, R., Shaw, T., Surgenor, A. E., Terry, L., Wang, Y., Wood, M., and Massey, A. J. (2009): Novel adenosine-derived inhibitors of 70 kda heat shock protein, discovered through structure-based design. *Journal of Medicinal Chemistry*, *52*(6), 1510–1513.

Wilson, C. G. M., Magliery, T. J., and Regan, L. (2004): Detecting protein-protein interactions with GFP-fragment reassembly. *Nature Methods*, *1*(3), 255–262.

Wilson, D. S., Keefe, A. D., and Szostak, J. W. (2001): The use of mRNA display to select high-affinity protein-binding peptides. *PNAS*, *98*, 3750 – 3755.

Wisén, S., and Gestwicki, J. E. (2008): Identification of small molecules that modify the protein folding activity of heat shock protein 70. *Analytical Biochemistry*, *374*(2), 371–377.

Wittung-Stafshede, P., Guidry, J., Horne, B. E., and Landry, S. J. (2003): The J-domain of Hsp40 couples ATP hydrolysis to substrate capture in Hsp70. *Biochemistry*, *42*(17), 4937–4944.

Worrall, D. M., and Goss, N. H. (1989): The formation of biologically active beta-galactosidase inclusion bodies in *Escherichia coli*. *Australian Journal of Biotechnology*, *3*(1), 28–32.

Worrall, L. J., and Walkinshaw, M. D. (2007): Crystal structure of the C-terminal three-helix bundle subdomain of C. elegans Hsp70. *Biochemical and Biophysical Research Communications*, *357*(1), 105–110.

Wright, C. M., Chovatiya, R. J., Jameson, N. E., Turner, D. M., Zhu, G., Werner, S., Huryn, D. M., Pipas, J. M., Day, B. W., Wipf, P., and Brodsky, J. L. (2008): Pyrimidinone-peptoid hybrid molecules with distinct effects on molecular chaperone function and cell proliferation. *Bioorganic and Medicinal Chemistry*, *16*(6), 3291–3301.

Wu, Y., Li, J., Jin, Z., Fu, Z., and Sha, B. (2005): The crystal structure of the C-terminal fragment of yeast Hsp40 Ydj1 reveals novel dimerisation motif for Hsp40. *Journal of Molecular Biology*, *346*(4), 1005–1011.

Xu, Z., Bae, W., Mulchandani, A., Mehra, R. K., and Chen, W. (2002): Heavy metal removal by novel CBD-EC20 sorbents immobilised on cellulose. *Biomacromolecules*, *3*, 462 – 465.

Yamauchi, L. M., Coppi, A., Snounou, G., and Sinnis, P. (2007): *Plasmodium* sporozoites trickle out of the injection site. *Cellular Microbiology*, *9*(5), 1215–1222.

Yochem, J., Uchida, H., Sunshine, M., Saito, H., Georgopoulos, C. P., and Feiss, M. (1978): Genetic analysis of two genes, dnaJ and dnaK, necessary for *Escherichia coli* and bacteriophage lambda DNA replication. *Molecular General Genetics*, *164*(1), 9–14.

Young, C. L., Britton, Z. T., and Robinson, A. S. (2012): Recombinant protein expression and purification: a comprehensive review of affinity tags and microbial applications. *Biotechnology Journal*, *7*(5), 620–34.

Young, J. C., Barral, J. M., and Ulrich Hartl, F. (2003): More than folding: localized functions of cytosolic chaperones. *Trends in Biochemical Sciences*, *28*(10), 541–547.

Zhang, Y., and Meshnick, S. R. (1991): Inhibition of *Plasmodium falciparum* dihydropteroate synthetase and growth *in vitro* by sulfa drugs. *Antimicrobial Agents and Chemotherapy*, *35*(2), 267–271.

Zhou, Z., Schnake, P., Xiao, L., and Lal, A. A. (2004): Enhanced expression of a recombinant malaria candidate vaccine in *Escherichia coli* by codon optimisation. *Protein Expression and Purification*, *34*(1), 87–94.

APPENDIX A

NUCLEOTIDE AND AMINO ACID NOMENCLATURE

Nucleotides were represented by single letter codes and the one and three-letter codes were used to represent amino acids as set forth by the Joint Commission of Biochemical Nomenclature (JBNC) of IUPAC (International Union of Pure and Applied Chemistry) and the IUBMB (International Union of Biochemistry and molecular Biology).

NUCLEOTIDE	SINGLE-LETTER CODE
Adenine	A
Cytosine	C
Guanine	G
Thymine	T
Uracil	U
Any Nucleotide	(A, C, G, T or U) N

AMINO ACID	SYMBOLS		MOLAR MASS (g/mol)	CHEMICAL FORMULAR
	3-letters	*1-letter*		
Alanine[1]	Ala	A	89.10	$C_3H_7NO_2$
Arginine[2]	Arg	R	174.20	$C_6H_{14}N_4O_2$
Asparagine[3]	Asn	N	132.12	$C_4H_8N_2O_3$
Aspartic acid[4]	Asp	D	133.11	$C_4H_7NO_4$
Cysteine[3]	Cys	C	121.16	$C_3H_7NO_2S$
Glutamic acid[4]	Glu	E	147.13	$C_5H_9NO_4$
Glutamine[3]	Gln	Q	146.15	$C_5H_{10}N_2O_3$
Glycine[5]	Gly	G	75.07	$C_2H_5NO_2$
Histidine[2]	His	H	155.16	$C_6H_9N_3O_2$
Isoleucine[1]	Ile	I	131.18	$C_6H_{13}NO_2$
Leucine[1]	Leu	L	131.18	$C_6H_{13}NO_2$
Lysine[2]	Lys	K	146.19	$C_6H_{14}N_2O_2$
Methionine[3]	Met	M	149.21	$C_5H_{11}NO_2S$
Phenylalanine[6]	Phe	F	165.19	$C_9H_{11}NO_2$
Proline[5]	Pro	P	115.13	$C_5H_9NO_2$
Serine[3]	Ser	S	105.09	$C_3H_7NO_3$
Threonine[3]	Thr	T	119.12	$C_4H_9NO_3$
Tryptophan[6]	Trp	W	204.23	$C_{11}H_{12}N_2O_2$
Tyrosine[6]	Tyr	Y	181.19	$C_9H_{11}NO_3$
Valine[1]	Val	V	117.15	$C_5H_{11}NO_2$

[1]Aliphatic amino acid with hydrophobic side chain
[2]Basic amino acid with electrically charged side chain
[3]Amino acid with polar neutral side chain
[4]Acidic amino acid with electrically charged side chain
[5]Unique amino acid
[6]Aromatic amino acid with hydrophobic side chain

APPENDIX B

SUPPLEMENTARY FIGURES

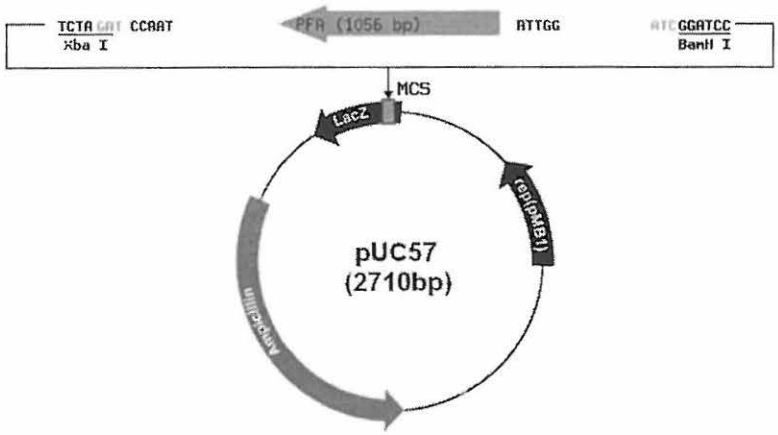

Figure B.1: Plasmid map of pUC57-PFA0660w.
The optimized coding sequences of PFA0660w were synthesized and cloned into pUC57 vector with BamHI (GGATCC), SphI (GCATGC) and KpnI (GGTACC) restriction sites included. Additional protective bases (ATTGG and CCAAT) are shown in blue text on the plasmid. The plasmid was reproduced as supplied by GeneScript®, USA.

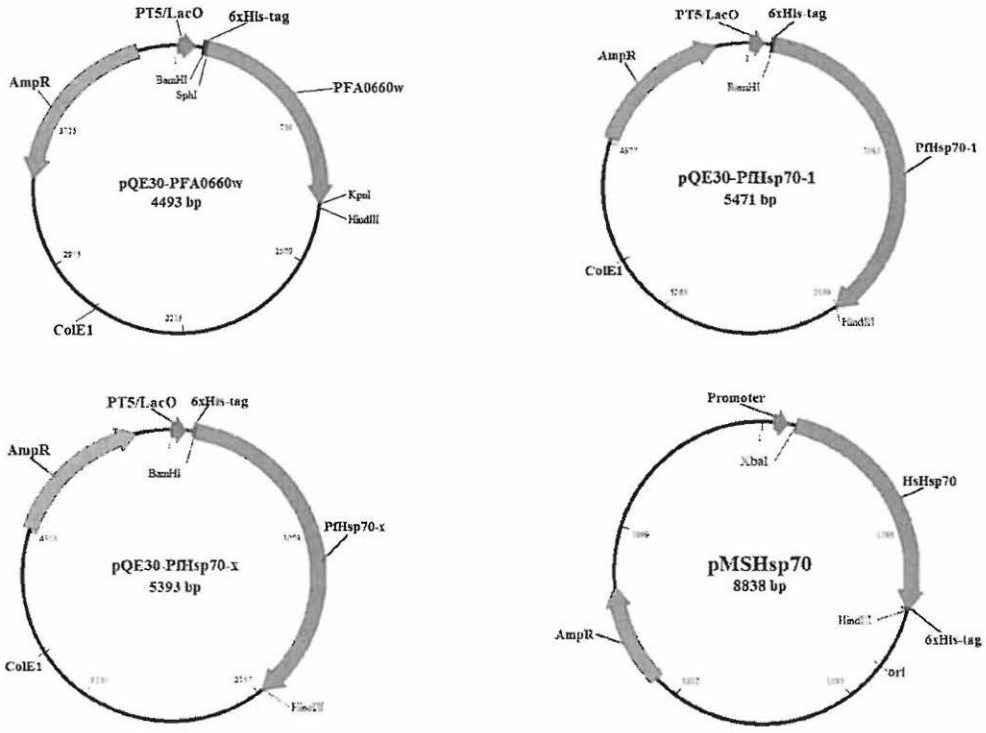

Figure B.2: Plasmid maps of the expression plasmids containing the inserted optimized coding sequences of PFA0660w, PfHsp70-1, PfHsp70-x and HsHs70.
Insertion of coding sequences into pQE30 vector was done downstream of the His-tag for PFA0660w, PfHsp70-1 and PfHsp70-x. The 6xHis-tag of the pMSHsp70 (HsHsp70) is located on the C-terminal end of the coding sequence, replacing EEVD motif and other terminal sequences. Thus the HsHsp70 produced lacked the EEVD motif. The plasmid was generated using BioEdit software (version 7.0.9.0).

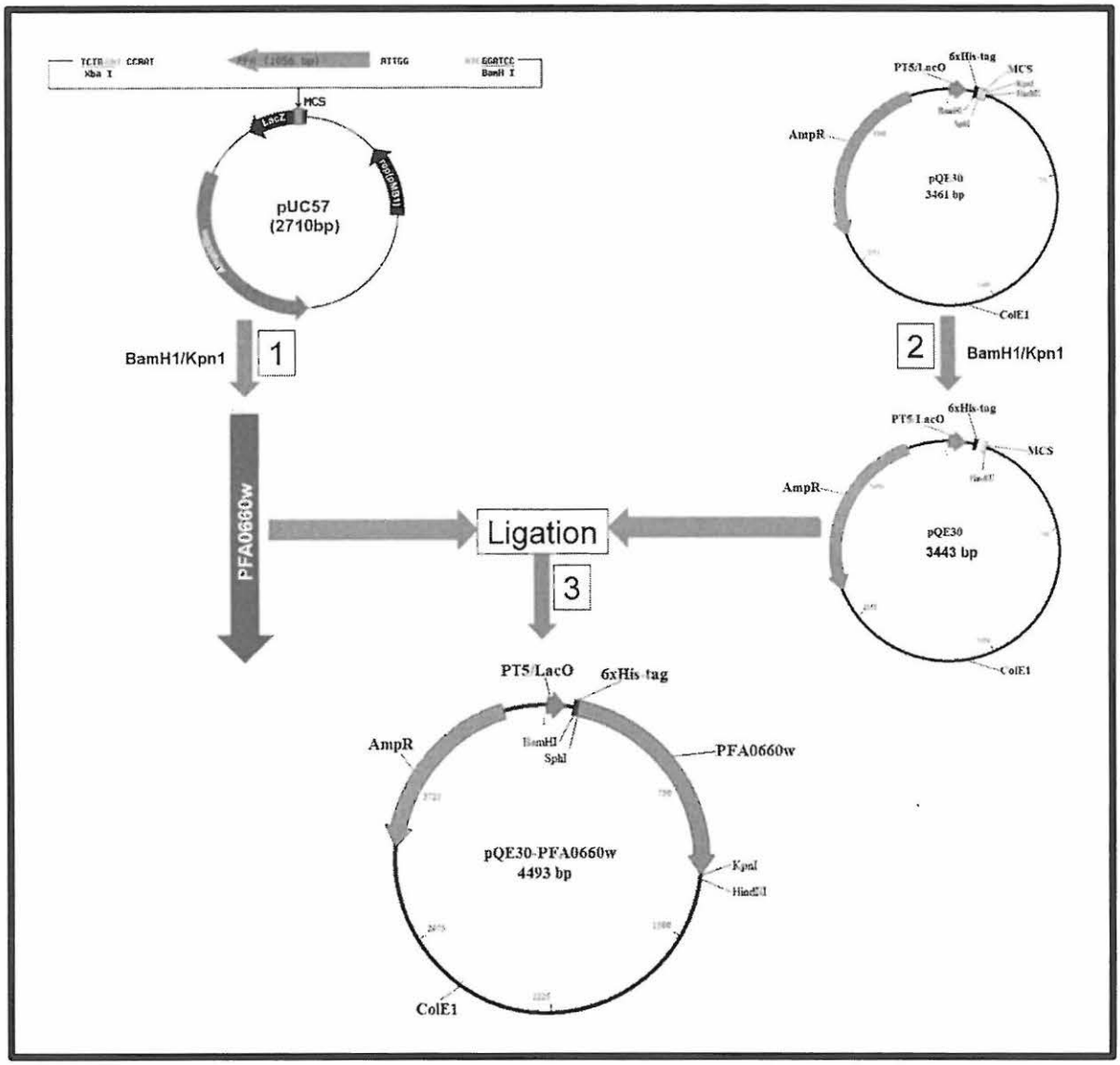

Figure B.3: Cloning strategy for the construction of pQE30-PFA0660w expression vector.
(1) Step wise digestion of pUC57-PFA0660w (3733 bp) cloning plasmid. Digestion was done first with BamHI, and purified using DNA clean and concentrate-5^{TM} kit (Zymo research). The linearized plasmid was then digested with KpnI to release PFA0660w coding DNA (1046 bp). (2) Direct double digestion of pQE30 (3461 bp) expression vector with BamHI/KpnI to produce linearized pQE30 (3443 bp). (3) Ligation of agarose gel purified coding fragment from (1) and linearized pQE30 vector from (2) to produce pQE30-PFA0660w (4493 bp). The pUC57-PFA0660w plasmid map is as supplied by GenScript®. Other plasmids maps were drawn using BioEdit software (version 7.0.0).

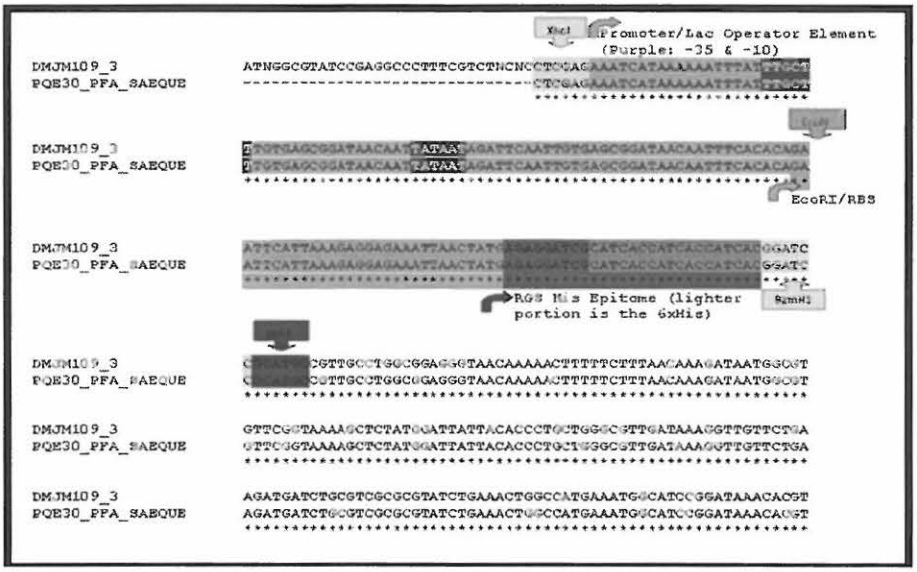

Figure B.4: Confirmation of pQE30-*PFA0660w* expression construct by sequencing.
Sequencing result showing the essential features of pQE30 expression vector and the N-terminal region of the encoded *PFA0660w* gene. The restriction sites are as indicated. Promoter/lac operator element (pink with purple identifying the critical regions), EcoRi/ribosome binding site (RBS - Turquoise) and 6xHis tag (light green). The insertion can be seen in the correct orientation and translational frame.

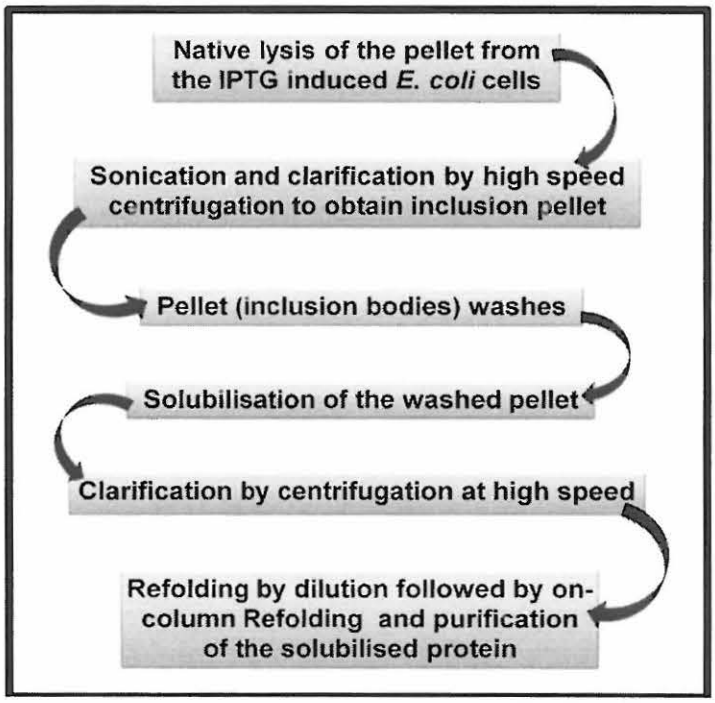

Figure B.5: Schematic diagram of Inclusion bodies purification steps
The schematic diagram of the various steps involved in purification from the inclusion bodies of which the isolation, solubilization and refolding are the critical steps. The isolation of inclusion bodies can be achieved by lysozyme (1 mg/ml) lysis of *E. coli* cells, followed by freezing at -80°C, rapid thawing, sonication and clarification by high speed centrifugation. Inclusion pellet wash was achieved with a buffer containing a low detergent (e.g. 1 – 5% Triton-X100) concentration supplemented with EDTA (10 mM) and low urea concentration (2 M). Triton X-100 is effective in extracting lipid and membrane-associated proteins while EDTA and urea help to prevent air catalysed metal oxidation and removal of other low abundant accompanied proteins respectively. Final washes of the inclusion pellet with distilled water are essential to remove contaminating salt and detergent. Refolding in a well optimized additive enhanced refolding buffer will enhance yield. Initial addition of low urea concentrations can help to prevent the formation of intermediate aggregates.

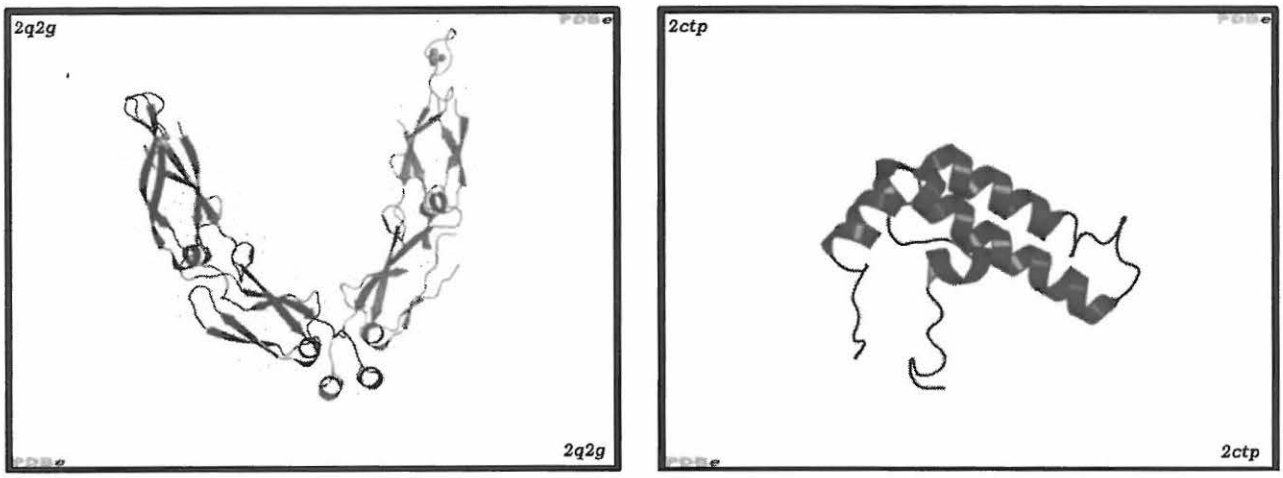

Figure B.6: Crystal structure of dimerization domain of HSP40 from *Cryptosporidium parvum* (2q2g) and solution structure of J-domain from human DnaJ subfamily B member 12 (2ctp).
2q2g and 2ctp were used as templates for comparative modelling of the J-domain and C-terminal domains of PFA0660w respectively.

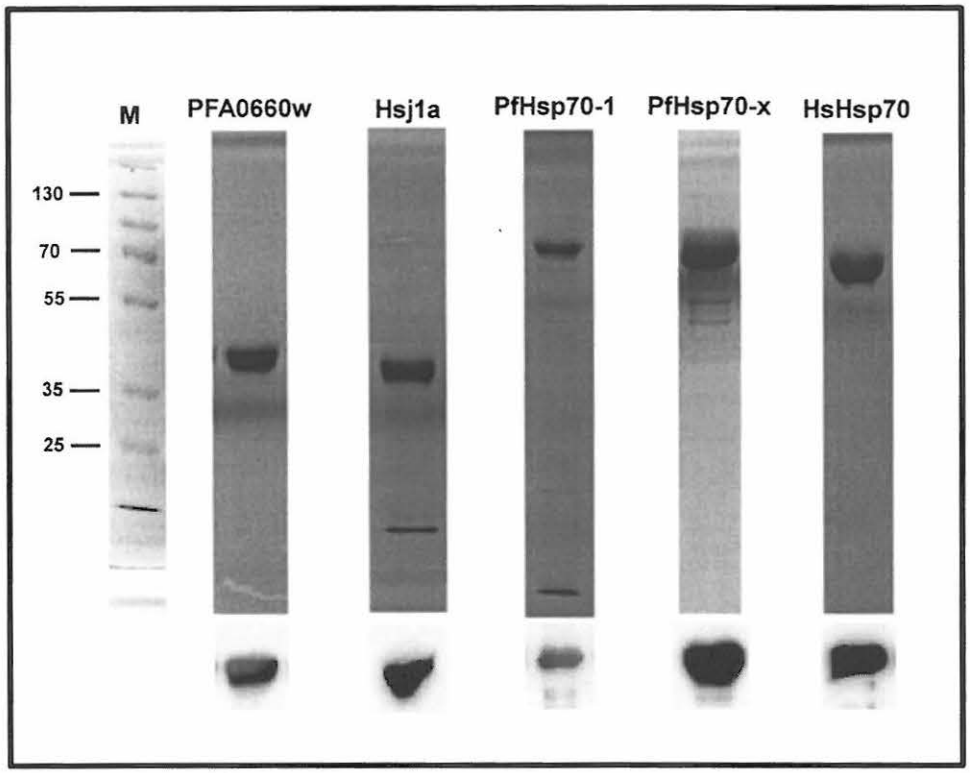

Figure B.7: Purification of PFA0660w, Hsj1a, PfHsp70-1, PfHsp70-x and HsHsp70
For purification, the plasmids bearing PFA0660w and PfHsp70-x genes were transformed into *E. coli* M15[pREP4] cells, while plasmids bearing PfHsp70-1 and Hsj1a were transformed into *E. coli* XL1 blue cells and HsHsp70 into *E. coli* BL21 cells. The $(His)_6$-PFA0660w was purified using additive enhanced inclusion bodies purification. All the Hsp70s and Hsj1a are soluble and are purified using native approaches as detailed in the *Appendix D15 and D16*. The purity of the protein was assessed by visualization on SDS-PAGE gel (upper panel) and western analysis (lower panel) with mouse monoclonal anti-His antibody (1 in 5,000) reveals the presence of the proteins of interest. Higher protein yields were obtained for PfHsp70-x, HsHsp70 and Hsj1a compared to PfHsp70-1. It should be noted that the last six residues, including the EEVD motif were replaced with the 6xHis-tag at the C-terminal end of the coding sequence in the plasmid encoding HsHsp70. Therefore, the recombinant HsHsp70 produced does not possess the EEVD motif. Generally, in 1 litre culture and with 6 ml elution volume, the average purified protein yield, expressed as mean ± standard error of mean, were 14.48 ± 0.84 mg/L for Hsj1a, 6.84 ± 0.26 mg/L for PfHsp70-1, 19.38 ± 1.20 mg/L for PfHsp70-x and 16.29 ± 1.05 mg/L for HsHsp70. M is the protein molecular weight marker in kDa

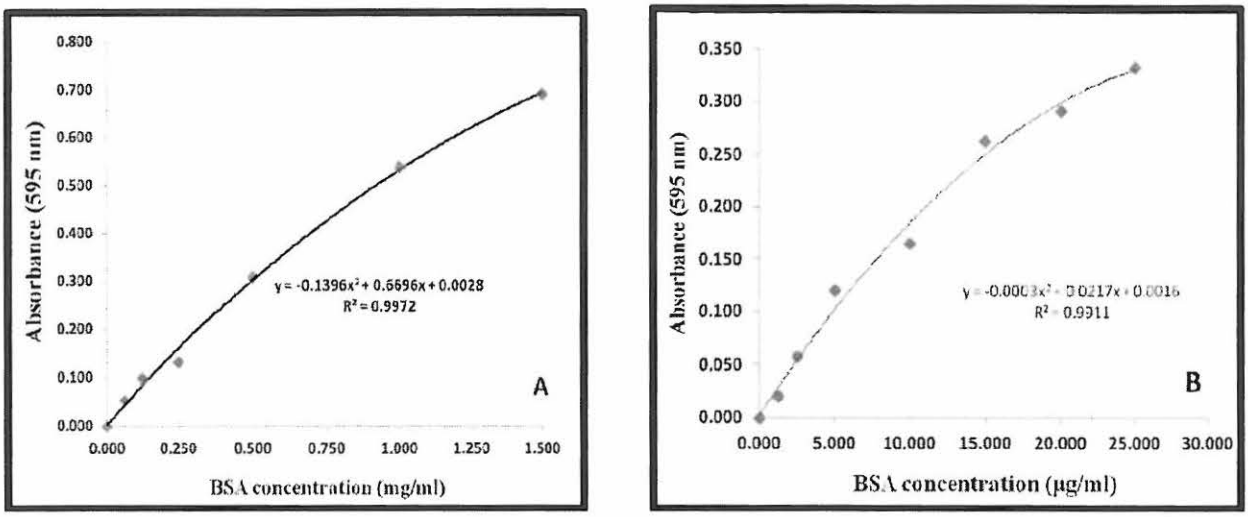

Figure B.8: Bovine serum albumin (BSA) standard curves for Bradford's assay.
Standard curves for Bradford's assay was generated using bovine serum albumin (BSA) for high (A) and low (B) yield protein estimation. The concentration range of 0 – 1.5 mg/ml and 0 – 25 µg/ml were used for (A) and (B) respectively and colour change was monitored spectrophotometrically at 595 nm. The plot of absorbance versus concentration produced the standard curve from where protein concentrations were estimated by extrapolation from the curve using the equation that described the line of best fit. The graph was generated on excel workbook.

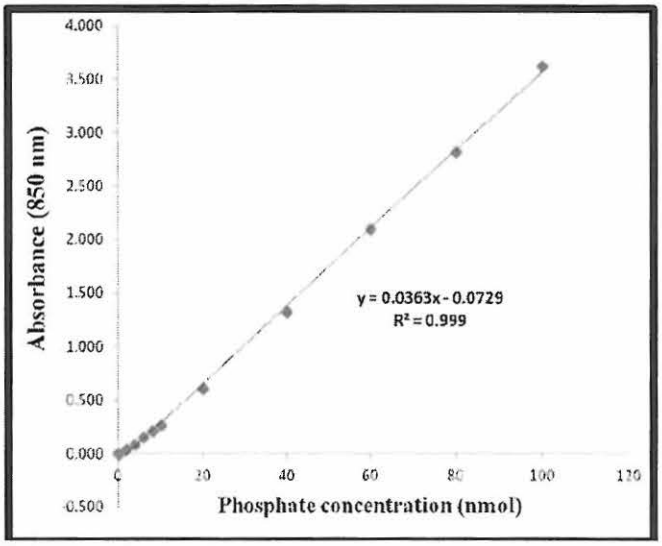

Figure B.9: Phosphate standard curve for ATPase assays.
Standard curves for ATPase assays were generated using potassium hydrogen phosphate. Phosphate (Pi) released in nmol by the ability of the chaperones to cause the hydrolysis of ATP (ATPase assay) were estimated by extrapolation from the graph using the equation that described the line of best fit. The graph was generated on excel workbook.

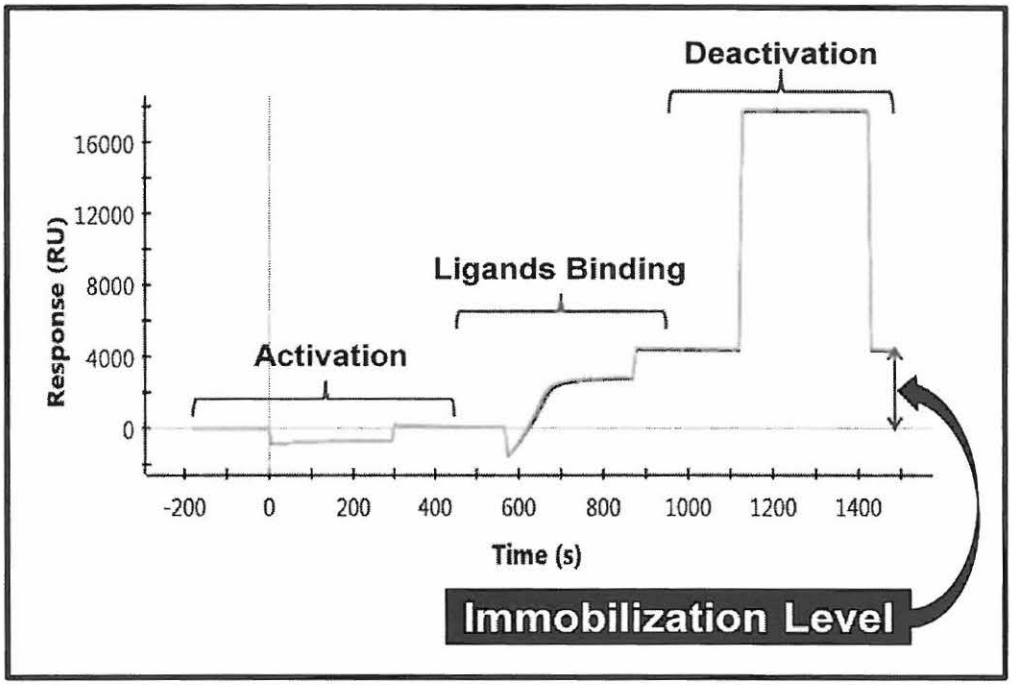

Figure B.10: Ligand immobilization sensorgram for SPR assay

The immobilization is an automated process of activation-coupling-deactivation sequence. Following activation of the GLC chip (as described in section 3.2.3.4), 10 µg/ml concentration of each ligand (PfHsp70-1 – Ligand 1, PfHsp70-x – Ligand 2 and HsHsp70 – Ligand 3) was passed over the chip at a flow rate of 30 µl/min. This was followed by deactivation. The sequence of steps and the immobilization level are as indicated. For each ligand used in this study, the level of immobilization (Table C.1 of Appendix C) was comparable across the analyte channel.

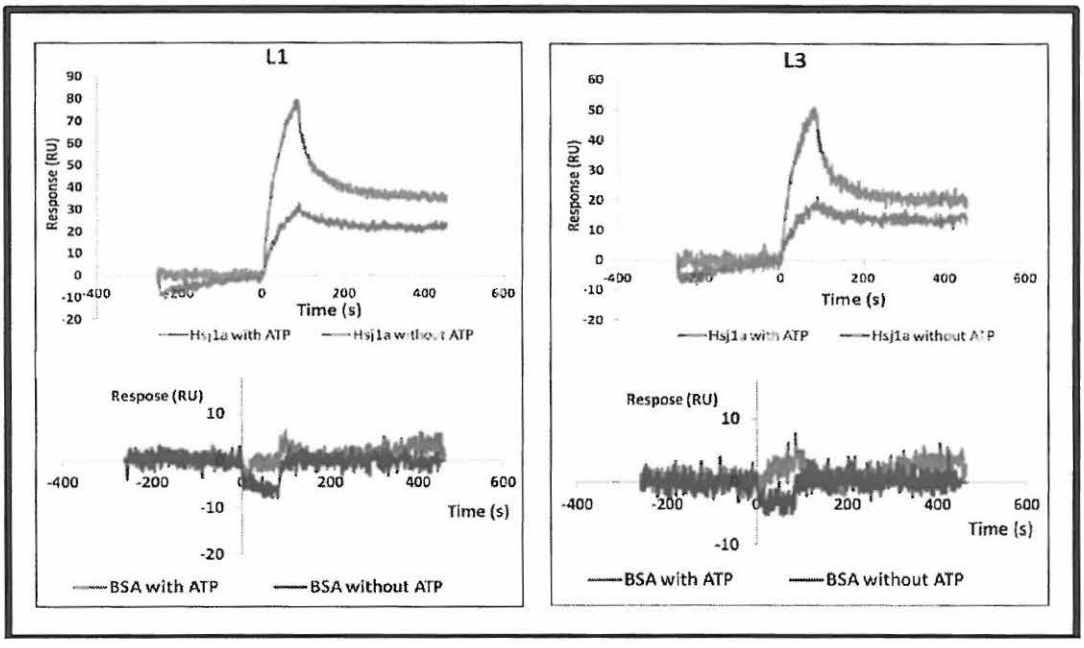

Figure B.11: The interaction of BSA and Hsj1a with PfHsp70-1 and HsHsp70

SPR analysis of the interaction of Hsj1a and BSA was performed by passing Hsj1a or BSA (1 µM; as analyte) over the immobilized PfHsp70-1 and HsHsp70 on GLC chip in the presence and absence of 1 mM ATP. The interactions of Hsj1a and BSA with the immobilized PfHsp70-x served as a control. The interaction assay was performed in triplicate and repeated at least three times. Hsj1a was freshly prepared for each set of triplicate runs while ATP and BSA concentrations were prepared just prior to use. All data were double referenced using buffer blanks (with or without ATP) and blank channel. All triplicate data overlapped and shown here is a representative sensograms for Hsj1a (upper panel) and BSA (lower panel), generated using the mean of a triplicate data obtained from one experiment.

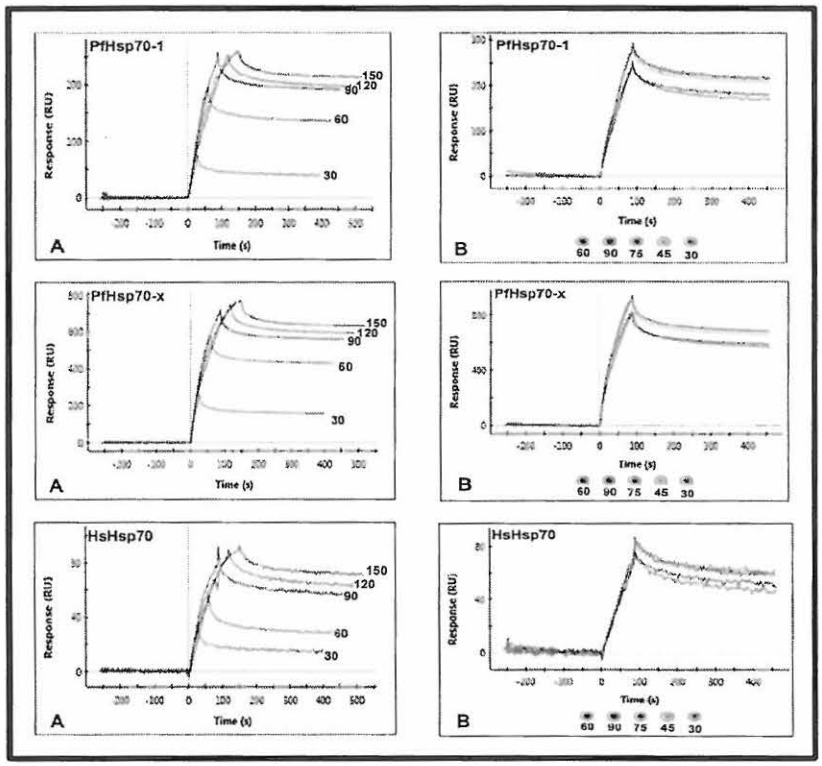

Figure B.12: Optimization of contact time and flow rate for SPR assay

As part of the optimization of the experimental procedures, contact time and flow rates were optimized using 1 μM concentration of $(His)_6$-PFA0660w as analyte for all the channels. By keeping all other parameters constant while either contact time or the flow rate was varied, it was possible to monitor changes in SPR interaction kinetics and to detect possible bulk shift and or mass transfer effects, when analyte was passed over the immobilized ligands (PfHsp70-1, PfHsp70-x and HsHsp70 as indicated) on GLC chip. For contact time, the flow rate was kept at 60 μl/min while for flow rate optimization the contact time was kept at 90 seconds with all other parameters maintained at default settings. The contact time in seconds used in (A) are shown at the end of each traces and the flow rates in μl/min used in (B) are indicated in the below the sensograms.

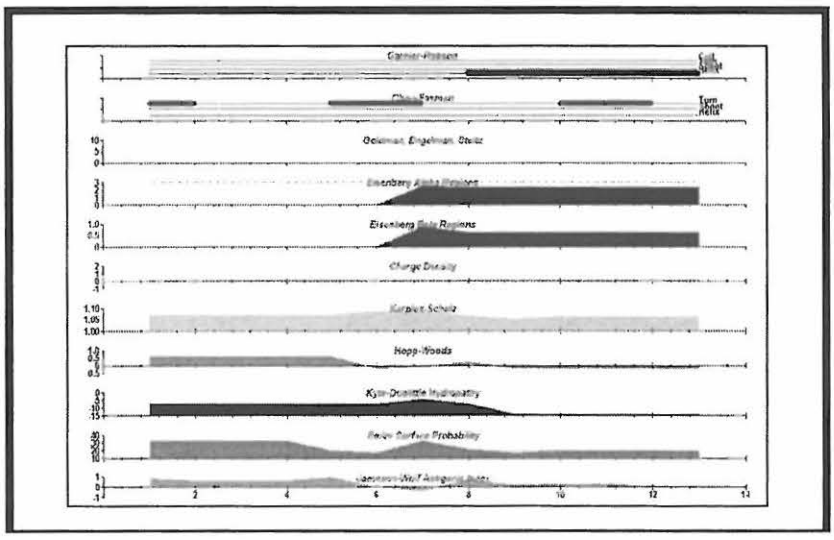

Figure B.13: Composite analysis of the PFA0660w specific peptide

Composite analysis of the peptide "DALKQSGFNSSNF" showing various algorithms used to access its antigenic properties as detailed in the text. Analysis was performed using Gene Runner software (version 3.05). The epitopic region showed high antigenic properties corresponding with Hopp-Wood positive peak (high hydrophilicity), Kyte and Doolittle negative value (high hydrophilicity) and Emini regions of highest surface probability (significant at value > 20). In addition, the peptide generally showed positive values of Karplus-Schultz chain flexibility, indicating a high antigenic determinant.

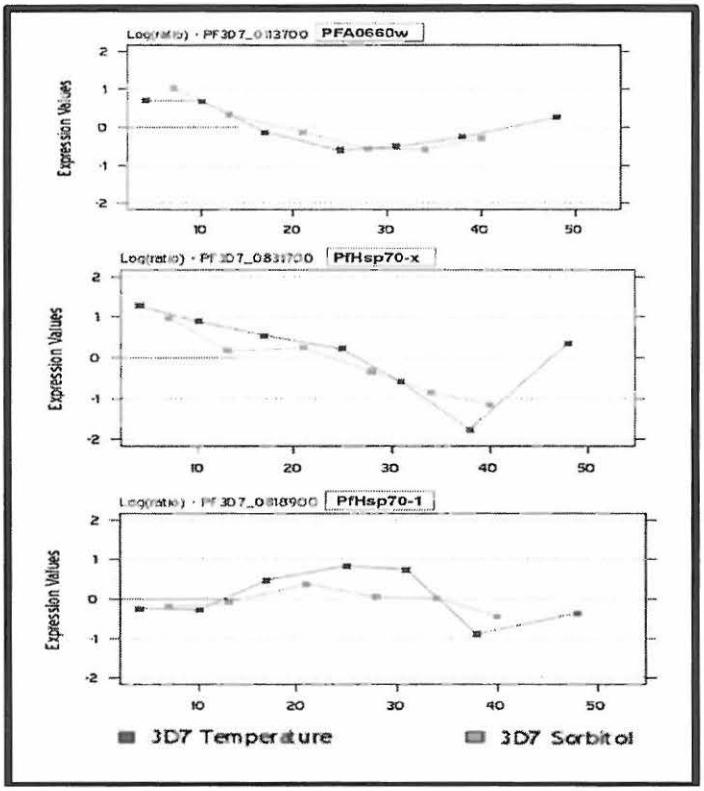

Figure B.14: Gene expression profiles of PFA0660w, PfHsp70-x and PfHsp70-1
The expression profiles were adapted from PlasmoDB as deposited by the authors (Aurrecoechea et al., 2009; Le Roch et al., 2003). Expression profiles of PFA0660w and PfHsp70-1 appear to correlate well with the western and densitometry analysis presented in Figure 4.4. Also, the expression profile of PFA06660w and PfHsp70-x using sorbitol synchronization correlated well with each other, indicating possible correlation in in vivo expression and export pattern.

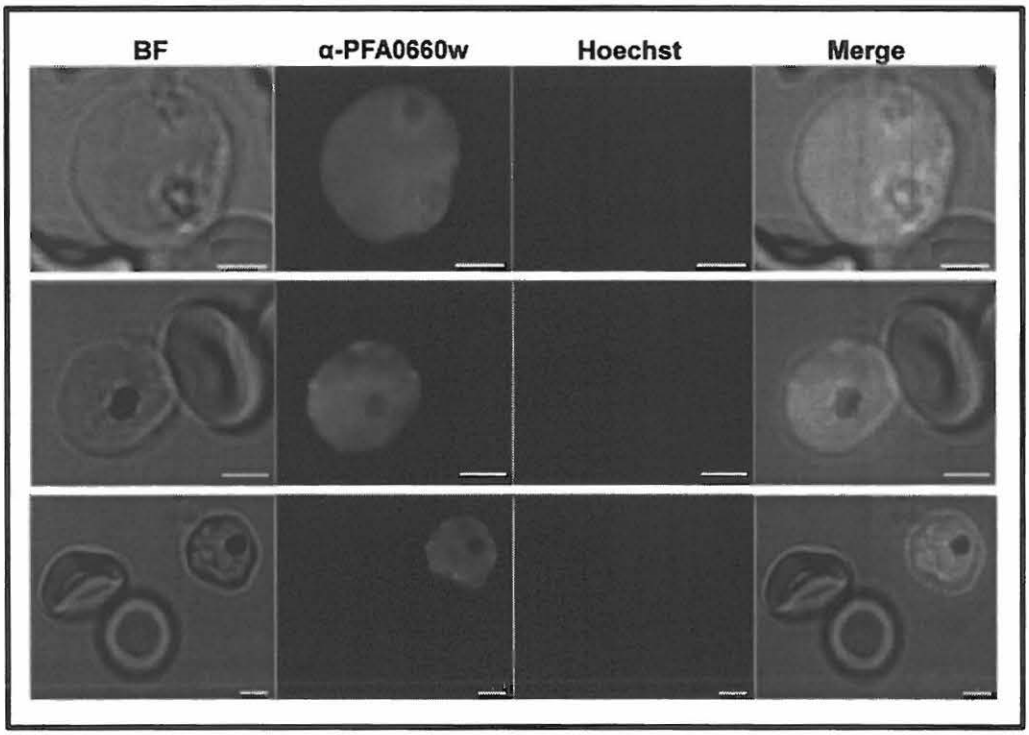

Figure B.15: Indirect immunofluorescence microscopy of PFA0660w and PfHsp70-1 using paraformaldehyde/glutaraldehyde fixation method.
Supplementary images obtained from paraformaldehyde/glutaraldehyde fixation method and anti-PFA0660w, showing localization within the cytosol of infected erythrocytes as expected. BF is bright field and the scale bars are as indicated. The white size bar in each frame indicates 5 μm.

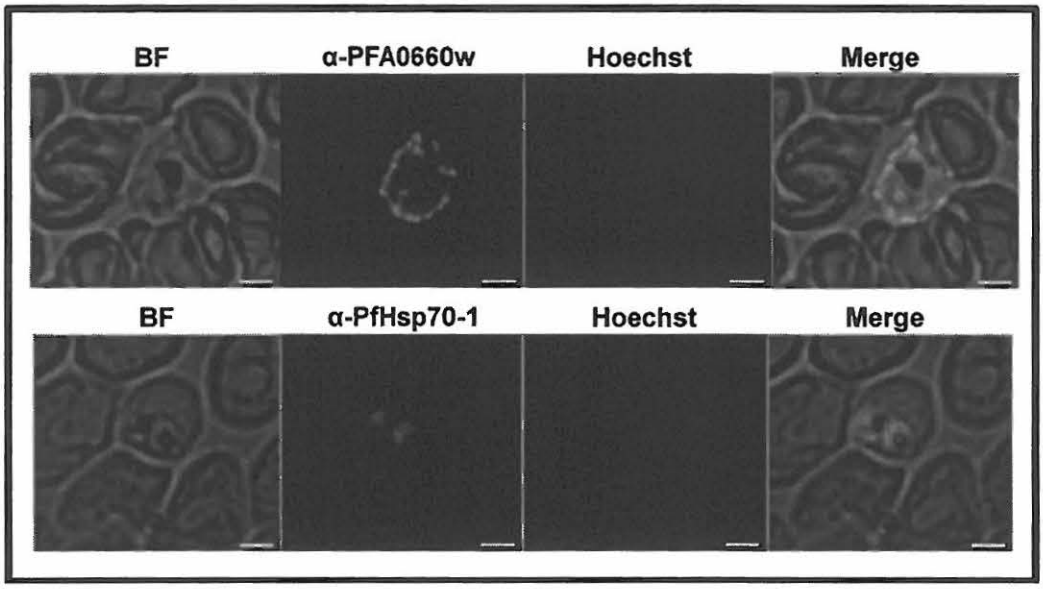

Figure B.16: Indirect immunofluorescence microscopy of PFA0660w and PfHsp70-1 using methanol fixation method.

Supplementary images obtained from methanol fixation method with anti-PFA0660w and anti-PfHsp70-1 antibodies, showing localization of PFA0660w into the cytosol of infected erythrocytes and PfHsp70-1 into the cytosol and nucleus of the parasite. The punctuate structures were well pronounced but the cells were crushed and there appeared to be some artefacts. BF is bright field and the scale bars are as indicated. The white size bar in each frame indicates 5 μm.

APPENDIX C

SUPPLEMENTARY TABLES

Table C.1: Ligand immobilization levels along the analyte (A) channels

Ligands		Level of Immobilization along Analytes Channels						Mean	Blanked Mean
		A1	A2	A3	A4	A5	A6		
L1	PfHsp70-1	4333.27	4313.39	4310.42	4392.82	4338.25	4428.31	4352.74	4306.23
L2	PfHsp70-x	3107.99	3126.84	3182.83	3193.78	3176.01	3104.4	3148.64	3102.12
L3	HsHsp70	3755.26	3856.42	4014.86	4056.01	4182.06	4222.1	4014.45	3967.93
L4	Blank	50	46.57	48.5	46.06	46.44	41.54	46.52	0.00
L5	PFA0660w	540.93	546.88	560.71	568.64	587.56	596.48	566.87	520.35
L6	PFB	803.33	814.69	828.97	841.07	867.42	888.69	840.70	794.18

Average Level of Ligands Immobilization

Table C.2: Analysis of the amino acids composition of PFA0660w and chaperones

		(His)6-PFA0660w		PfHsp70-1		PfHsp70-x		HsHsp70		PFA0660w	
Length		355 aa		677 aa		679 aa		641 aa		402 aa	
Molecular Weight		41299.58		73910.47		75048.17		70047.92		46983.9	
1 microgram =		24.213 pMoles		13.530 pMoles		13.325 pMoles		14.276 pMoles		21.284 pMoles	
Molar Extinction coefficient		42820		37350		35620		31180		49460	
1 A[280] corr. to		0.96 mg/ml		1.98 mg/ml		2.11 mg/ml		2.25 mg/ml		0.95 mg/ml	
A[280] of 1 mg/ml		1.04 AU		0.51 AU		0.47 AU		0.45 AU		1.05 AU	
Isoelectric Point		7.73		5.5		5.59		5.48		8.49	
Charge at pH 7		1.95		-10.59		-8.7		-10.56		5.41	
		F	% by W	F	% by W	F	% by W	F	% by W	F	% by W
Charged (RKHYCDE)		145	46.23	210	36.47	219	37.32	200	36.8	158	44.38
Acidic (DE)		50	14.63	95	15.55	97	15.61	92	15.82	54	13.93
Basic (KR)		51	16.4	84	15.24	88	15.51	81	15.58	59	16.69
Polar (NCQSTY)		105	29.69	166	24.76	193	28.73	152	24.13	121	30.28
Hydrophobic (AILFWV)		99	27.59	218	30.87	214	30.04	221	33.04	121	29.78
A	Ala	9	1.68	57	5.9	49	5	57	6.22	10	1.64
C	Cys	6	1.52	9	1.27	10	1.39	5	0.74	8	1.79
D	Asp	27	7.54	42	6.49	46	7.02	45	7.34	28	6.87
E	Glu	23	7.1	53	9.06	51	8.6	47	8.48	26	7.06
F	Phe	20	6.93	22	4.22	21	3.98	25	5.06	26	7.92
G	Gly	22	3.46	59	5.14	46	3.96	55	5.06	22	3.05
H	His	14	4.56	7	1.26	6	1.07	7	1.33	8	2.29
I	Ile	22	6.05	47	7.16	47	7.07	42	6.75	29	7.02
K	Lys	38	11.65	54	9.17	64	10.72	50	8.96	44	11.87
L	Leu	26	7.15	47	7.16	48	7.22	50	8.04	30	7.26
M	Met	4	1.25	19	3.29	12	2.05	9	1.65	6	1.65
N	Asn	25	6.93	37	5.68	49	7.42	30	4.86	30	7.31
P	Pro	10	2.41	29	3.88	23	3.03	24	3.39	11	2.34
Q	Gln	8	2.45	24	4.07	30	5.02	27	4.84	8	2.16
R	Arg	13	4.75	30	6.07	24	4.79	31	6.62	15	4.82
S	Ser	28	6.17	38	4.64	36	4.34	34	4.38	30	5.82
T	Thr	14	3.5	43	5.95	50	6.83	41	5.99	16	3.52
V	Val	20	4.91	42	5.72	47	6.31	45	6.46	24	5.19
W	Trp	2	0.86	3	0.71	2	0.47	2	0.5	2	0.75
Y	Tyr	24	9.12	15	3.16	18	3.74	15	3.33	29	9.69
B	Asx	52	14.46	79	12.17	95	14.43	75	12.2	58	14.19
Z	Glx	31	9.55	77	13.13	81	13.62	74	13.31	34	9.21
X	Xxx	0	0	0	0	0	0	0	0	0	0

F and W stands for frequency and weight respectively. The analysis was generated using Vector NTI Advance (TM) 11.0. The expected amino acids from coding sequence was used for (His)6-PFA0660w. Others are from PlasmoDB

Table C.3: Kinetic parameters generated for rhodanese aggregation assay

Dose response / Chaperone Effects													
Concentrations		PfHsp70-1			PfHsp70-X			HsHsp70			PFA0660w		
Rhodanese	Chaperones	K_1	$K_1.A_{lim}$	A_{lim}	K_1	$K_1.A_{lim}$	A_{lim}	K_1	$K_1.A_{lim}$	A_{lim}	K_1	$K_1.A_{lim}$	A_{lim}
1.5 μM	0 μM	1.10E-01	9.52E-03	8.66E-02	1.10E-01	9.52E-03	8.66E-02	1.10E-01	9.52E-03	8.66E-02	1.10E-01	9.52E-03	8.66E-02
		6.37E-03	3.68E-04	1.57E-03	6.37E-03	3.68E-04	1.57E-03	6.37E-03	3.68E-04	1.57E-03	6.37E-03	3.68E-04	1.57E-03
1.5 μM	0.25 μM	9.15E-02	7.02E-03	7.68E-02							1.04E-01	7.81E-03	7.51E-02
		2.06E-03	8.34E-05	8.27E-04							4.52E-04	4.30E-05	7.36E-04
1.5 μM	0.5 μM	8.63E-02	5.40E-03	6.26E-02	8.65E-02	8.09E-03	9.35E-02	8.35E-02	6.72E-03	8.06E-02	1.11E-01	6.02E-03	5.43E-02
		7.17E-05	3.66E-05	4.76E-04	5.52E-04	3.94E-05	1.49E-04	1.84E-03	8.52E-05	7.58E-04	1.55E-03	5.43E-05	2.72E-04
1.5 μM	1.0 μM	6.39E-02	2.56E-03	4.00E-02	1.00E-01	7.14E-03	7.15E-02	8.15E-02	5.20E-03	6.39E-02	1.93E-01	4.04E-03	2.10E-02
		1.21E-03	2.78E-05	3.35E-04	1.25E-03	1.66E-05	9.46E-04	2.15E-03	8.96E-05	6.24E-04	2.69E-03	4.57E-05	6.19E-05
1.5 μM	1.5 μM	-4.13E-02	4.04E-05	-9.81E-04	7.22E-02	4.23E-03	5.85E-02	8.26E-02	3.49E-03	4.23E-02	-6.07E-02	1.40E-05	-2.19E-04
		6.66E-04	1.75E-06	5.83E-05	7.57E-04	2.38E-05	2.83E-04	2.49E-03	7.33E-06	1.33E-03	2.21E-03	7.38E-06	1.14E-04
1.5 μM	2.0 μM				1.03E-01	2.37E-03	2.30E-02	5.22E-02	1.46E-03	2.79E-02			
					6.65E-04	1.60E-05	1.32E-04	1.91E-04	4.81E-06	1.02E-05			
Co-chaperone Effects of PFA0660w													
Concentrations		0.25 μM PfHsp70-1			1 μM PfHsp70-x			1 μM HsHsp70			1.5 μM Rhpdanese Alone		
Rhodanese	PFA0660w	K_1	$K_1.A_{lim}$	A_{lim}	K_1	$K_1.A_{lim}$	A_{lim}	K_1	$K_1.A_{lim}$	A_{lim}	K_1	$K_1.A_{lim}$	A_{lim}
1.5 μM		9.15E-02	6.02E-03	6.58E-02	1.00E-01	7.77E-03	7.77E-02	8.15E-02	5.20E-03	6.39E-02			
		2.06E-03	8.34E-05	5.82E-04	1.25E-03	6.28E-05	3.56E-04	2.15E-03	8.96E-05	6.24E-04			
1.5 μM	0.125 μM	8.23E-02	6.49E-03	7.88E-02									
		1.55E-03	6.92E-05	6.40E-04									
1.5 μM	0.25 μM	1.21E-01	4.26E-03	3.51E-02	1.05E-01	7.12E-03	6.78E-02	8.13E-02	6.57E-03	8.10E-02	1.10E-01	9.52E-03	8.66E-02
		5.72E-03	1.31E-04	5.74E-04	3.23E-03	1.25E-04	3.10E-03	2.39E-03	1.13E-05	2.24E-03	6.37E-03	3.68E-04	1.57E-03
1.5 μM	0.5 μM	3.95E-02	5.56E-04	1.43E-02	1.29E-01	5.43E-03	4.21E-02	1.05E-01	3.24E-03	3.09E-02			
		3.83E-03	2.45E-05	8.19E-04	3.43E-03	1.81E-05	1.00E-03	4.40E-04	2.80E-05	1.38E-04			
1.5 μM	1.0 μM				1.66E-01	2.44E-03	1.48E-02	-5.41E-02	-8.18E-06	1.52E-04			
					5.99E-03	6.69E-05	8.58E-04	3.66E-04	1.40E-06	2.69E-05			

*Results are presented in mean ± standard error of mean (SEM). SEM is shown in smaller fonts and highlighted.

Table C.4: Kinetic parameters for quantitative analysis of the aggregation suppression activity of $(His)_6$-PFA0660w, PfHsp70-1, PfHsp70-x and HsHsp70

	K_c (nm.min^{-1})	k_c (μM)	*Fold increase in k_c		R_{max}
			PFA0660w	Chaperones	
PFA0660w	0.0092	1.4535			1.0326
	2.51E-04	3.76E-01			0.0847
PfHsp70-1	0.0100	1.5835		2.8200	0.9500
	2.76E-04	4.14E-01			0.0508
HsHsp70	0.0062	0.9735		2.4677	1.5323
	2.41E-04	1.88E-01			0.0113
PfHsp70-x	0.0051	0.7984		2.1765	1.8627
	2.16E-04	1.32E-01			0.1096
PfHsp70-1 + PFA0660w	0.0282	4.4491	3.0652		0.3369
	7.54E-05	1.13E-01			0.0131
HsHsp70 + PFA0660w	0.0153	2.4141	1.6630		0.6209
	1.06E-04	1.59E-01			0.0060
PfHsp70-x + PFA0660w	0.0111	1.7519	1.2065		0.8559
	3.32E-05	4.98E-02			0.0234

The data obtained spectrophotometrically was transformed in line with equation 2 of section 3.2.3.3 to generate the plot of dA/dt versus A. The terminal phase of the plots (the last 12 minutes) were analysed using linear regression analysis to obtain the slope k_1, y-intercept k_1A_{lim} that were used to calculate A_{lim} (or extrapolated from x-axis). The k_1A_{lim} values for range of protein concentrations were plotted against ratio R (ratio of molar concentration of protein: rhodanese). The slope of the line of best fit was used to generate k_c in nmmin^{-1}or μM by applying equation 3 or 5 of section 3.2.3.3 respectively. R_{max} was calculated from y-intercept or extrapolated from the x-axis as intercept. R_{max} and k_c are two parameters that can be used to quantitatively determine the chaperone ability to suppress aggregation of rhodanese. Where co-chaperone was assessed using range of $(His)_6$-PFA0660w concentration on fixed chaperone concentration, R values were based on $(His)_6$-PFA0660w concentrations ($(His)_6$-PFA0660w : rhodanese). The results showed an increase in PfHsp70-1 activity by 2.82 fold, HsHsp70 by 2.47 fold and PfHsp70-x by 2.18 fold, indicating a comparable effect of $(His)_6$-PFA0660w on the aggregation suppression activities of the chaperones. The significant increase in the k_c values of the chaperone co-chaperone combination relative to the K_c value of $(His)_6$-PFA0660w which was higher with PfHsp70-1 (3.07 folds) as compared to HsHsp70 (1.67 folds) and PfHsp70-x (1.21 folds) may indicate a synergistic stimulation of $(His)_6$-PFA0660w by PfHsp70-1 and vice versa. *Fold increase was generated by dividing the values obtained when range of $(His)_6$-PFA0660w concentrations was assayed in the presence of fixed concentration for chaperones by the values obtained for each individual protein.

Table C.5: Analysis of sequence similarity of PFA0660w with other type II *P. falciparum* Hsp40s

	PFA0660w	PFE0055c	PFB0090c	PFB0595w	PF11_0099	PFL0565w	PF14_0137	PFF1415c	MAL13P1.277
PFA0660w		48.0	46.3	44.9	43.1	40.3	31.5	27.9	27.7
PFE0055c	48.0		47.7	60.6	41.0	40.9	40.0	29.4	26.6
PFB0090c	46.3	47.7		51.4	41.4	42.3	35.9	29.8	43.8
PFB0595w	44.9	60.6	51.4		47.6	39.0	30.1	43.4	25.2
PF11_0099	43.1	41.0	41.4	47.6		43.8	40.0	54.9	44.8
PFL0565w	40.3	40.9	42.3	39.7	43.8		43.3	42.2	32.7
PF14_0137	31.5	40.0	35.9	30.1	40.0	43.3		48.4	40.0
PFF1415c	27.9	29.4	29.8	43.4	54.9	42.2	48.4		31.6
MAL13P1.277	27.7	26.6	43.8	25.2	44.8	32.7	40.0	31.6	

The percentage similarity was generated by the local Blast search (Altschul et al., 1997) of the amino acid sequence of PFA0660w against other type II PfHsp40s as provided for by BioEdit sequence alignment editor (version 7.0.9.0.) software (Hall, 1999).

APPENDIX D

STANDARD MOLECULAR BIOLOGY PROTOCOLS

Standard molecular biology protocols were adapted from those described (Birnboim and Doly, 1979; Sambrook and Russell, 2001). Sterile technique was employed where applicable. Specialised materials and reagents utilised are listed in APPENDIX E.

D1: ISOLATION/EXTRACTION OF PLASMID DNA

D1.1 Alkaline Lysis Method

5 ml YT broth (1.6%w/v Tryptone, 1.0%w/v Yeast Extract and 0.5%w/v NaCl) supplemented with appropriate antibiotic for plasmid selection (100 ug/ml Ampicillin for DH5-alpha, XL1-blue and JM109 *E. coli* cells) was inoculated with *E. coli* colony transformed with the plasmid of interest (pQE30-PFA) and allow to grow at 37°C overnight with rigorous shaking. The cells were harvested by centrifugation for 60s at 13,000 rpm in the microcentrifuge. The supernatant was decanted and the pellet was resuspended in 100 µl of ice cold resuspension solution (50 mM glucose, 50 mM Tris-HCl pH 8.0 and 10 mM EDTA) premixed with RNase A to a final concentration of 0.1 mg/ml. To this was added 200 µl of lysis solution (200 mM NaOH, 1% SDS) and mix by inverting the tube several times for 2-3 minutes (not exceed 5 min) until becoming transparently viscous (indicating bacterial lysis has taken place). 150 µl of neutralizing solution (3 M potassium acetate and 5 M glacial acetic acid) was added to the suspension to precipitate the bacterial chromosomal DNA which is usually seen as a white precipitate. The resultant solution was clarified at 13,000 rpm for 10 minutes and the supernatant was carefully transferred into a new sterile tube containing 250 µl of Isopropanol. The tube was vortexed briefly and centrifuge at 13, 000 rpm for 60 s. (The plasmid DNA precipitates as a white pellet). The supernatant was decanted and to the pellet was added 750 µl of 70% ethanol, vortexed briefly, and centrifuged at 13, 000 rpm 60 s. The residual ethanol was removed from the pellet by aspiration and tube was allowed to air dried on the bench. The air dried pellet was resuspended in 50 µl of TE buffer (10 mM Tris-HCl pH 8.0 and 1 mM EDTA) and sample was analyzed for correctly ligated plasmid DNA by restriction digest followed by agarose gel electrophoresis. The purified DNA was quantified at 260 nm in a Helios Alpha UV-Vis Spectrophotometer (Thermo Scientific, USA).

D1.2 Smart Buffer Method

An overnight culture of plasmid DNA (pQE30-PFA) transformed *E. coli* colony in 5 ml YT broth (1.6%w/v Tryptone, 1.0%w/v Yeast Extract and 0.5%w/v NaCl) supplemented with appropriate antibiotic for plasmid selection (100 ug/ml Ampicillin for DH5-alpha, XL1-blue and JM109 *E. coli* cells was clarified by centrifugation for 2 minutes at 13,000 rpm to harvest the cells. The supernatant was decanted and the pellet was resuspended in 50 µl of Smart buffer (10mM TRIS-Cl pH 8.0, 1mM EDTA pH 8.0, 15%$^{w}/_{v}$ Sucrose, 0.1 mg/ml BSA, 0.2 mg/ml DNase free RNase and 2 mg/ml Lysozymes). The suspension was incubated at 37°C for 30 minutes, boiled for 1 minute and incubated on ice for 10 minutes. The suspension was clarified at 13, 000 rpm for 10 minutes and the supernatant was transferred into a sterile tube containing 100 µl of Isopropanol, vortexed briefly and allow to stand for 2-3 minutes and centrifuged at 13,000 rpm for 60 sec to pellet the plasmid DNA which appears as white precipitate. The supernatant was decanted and the pellet was washed with 500 µl of 70% ethanol. The ethanol was removed by decantation and air drying following centrifugation at 13,000 rpm for 60 s. The pellet (containing the plasmid DNA) was reconstituted in 50 µl of TE buffer (10 mM Tris-HCl pH 8.0 and 1 mM EDTA) and sample was analyzed for correctly ligated plasmid DNA by restriction digest followed by agarose gel electrophoresis. The purified DNA was quantified at 260 nm in a Helios Alpha UV-Vis Spectrophotometer (Thermo Scientific, USA.

D1.3 QIAprep Spin Miniprep Kit

The protocol for the isolation of plasmid DNA using QIAprep Spin Miniprep Kit was in accordance with the manufacturer's instruction. Briefly, a single colony of *E.coli* that has been transformed with the desired plasmid DNA was selected from a freshly streaked plate and inoculated into a 5 ml 2xYT culture medium containing the appropriate selective antibiotic. The culture was incubated overnight (16 hours) at 37°C with vigorous shaking. The culture was harvested by centrifugation at 10, 000 x g for 2 min at room temperature. The pelleted cells was resuspended in 250 µl Buffer P1 (having RNase A added to it) and transferred to a 1.5 ml microcentrifuge tube at room temperature. Following complete resuspension and vortexing, 250 µl Buffer P2 was added and mix thoroughly by inverting the tube 4–6 times. This was followed by the addition of 350 µl Buffer N3, thorough mixing by inverting the tube 4–6 times. The mixture was centrifuged for 10 min at 16, 000 x g to obtain the supernatant which was applied to the QIAprep spin column. The column was centrifuged for 30 s (10, 000 x g) and the flow through was discarded. The column was washed separately with 0.5 ml Buffer PB and 0.75 ml Buffer PE followed by centrifuging for 30 s (10, 000 x g) at every wash to remove the supernatant. Further centrifuging (10, 000 x g) for an additional 1 min to

remove residual wash buffer was followed by addition of 50 µl Buffer EB (10 mM Tris·Cl, pH 8.5) or water to elute the DNA by centrifugation (10, 000 x g) for 1 min.

D2: RESTRICTION ENZYMES DIGESTION OF DNA

Plasmid DNA was digested with the appropriate restriction endonuclease(s) (Kpn1 and/or BamH1) for 2-4 hours at the optimal temperature of 37°C (unless otherwise stated) in a digestion reaction containing: 200 - 500 ng of plasmid DNA, 2 µl (10%v/v) of the appropriate 10x restriction buffer (buffer A/J), 2 - 5 U of restriction endonuclease enzyme(s), 0.2 µl (1%v/v) of 10 mg/ml BSA (final concentration of 100 µg/ml) and distilled water to a final volume of 20 µl. The digested DNA was resolved by agarose gel electrophoresis as described in section D3. Sequential digestion at 37°C for 2 hours was used to achieve double digestion with BamHI/KpnI. Restriction buffers and added reagent (BSA) were used according to the enzymes supplier's recommendations. λ PstI DNA marker was prepared by the digestion of 20 µl of 526 µg.ml-1 λ DNA (Promega) for two hours/overnight at 37°C in a reaction containing 5 U of PstI restriction enzyme (Fermentas), 20 µl of the appropriate 10x restriction enzyme buffer (Fermentas) and distilled water to a final volume of 200 µl. Following digestion, the PstI restriction enzyme was heat inactivated by heating the solution to 100°C for 20 minutes on heating block The digested λ DNA was treated with 40 µl 10x DNA gel loading buffer (0.5% (w/v) bromophenol blue, 0.5% xylene cyanol FF and 50% (v/v) glycerol) for use in subsequent agarose gel electrophoresis (as per D3).

D3: AGAROSE GEL ELECTROPHORESIS

Agarose gels were prepared by melting molecular grade agarose (1.0% w/v) in TAE Buffer (45 mM Borate, 1 mM EDTA, 45 mM Tris-Cl, pH 8.3) and to this was added ethidium bromide to a final concentration of 0.5 μgml^{-1} on cooling prior to casting. For electrophoresis, enough TAE buffer was added to cover the cast gels in the electrophoresis tank and samples of DNA were treated with 6x DNA gel loading buffer (0.25% (w/v) bromophenol blue, 0.25% (w/v) xylene cyanol FF and 30% (v/v) glycerol) in a ratio of 5:1 respectively and loaded onto the gel with marker of λ PstI DNA marker (prepared as per section D2). The samples were resolved at 100 - 120 V for one hour, and visualised under ultra-violet light with a Chemidoc Imaging System (Bio-Rad).

D4: EXTRACTION AND PURIFICATION OF DNA FROM AN AGAROSE GEL

Resolved DNA fragments were isolated subsequent to agarose gel electrophoresis and purified using Gel DNA Extraction Kit (GE Healthcare, UK) in line with the manufacturer's instructions. Briefly, the DNA fragment of interest was identified by brief exposure to long-wave UV light, excised from the gel and transferred into pre-weighed tube. The tube containing excised gel was

weighed and the initial weight of the tube was subtracted to determine the weight of the excised gel containing the DNA fragment. The DNA fragment was incubated in Capture buffer (GE Healthcare, UK) (10 µl per 10 mg of excised gel) at 60°C for 15 minutes. The sample was applied to a GFXTM spin column (GE Healthcare, UK) and centrifuged at 16 000 xg for 1 minute. Bound DNA was washed with 500 µl of Wash buffer (GE Healthcare, UK) passed through the column by centrifugation (16 000 xg, 1 minute). The DNA was eluted from the column with 20-30 µl of Elution buffer (GE Healthcare, UK) by further centrifugation (16 000 xg, 1 minute). Quantification of the purified DNA was achieved in a Helios Alpha UV-Vis spectrophotometer (Thermo Scientific, USA) at 260 nm.

D5: LIGATION OF DNA FRAGMENTS

Vector and insert DNA fragments intended for ligation (at recommended values of 1:1, 1:3 or 3:1 molar ratio of vector:insert DNA when cloning a fragment into a plasmid vector. The ng value of insert can be calculated from [ng of vector x kb size of insert] x [molar ratio of insert/vector] / [kb size of vector]) were incubated for 16 hours (overnight) at 4°C, followed by 30 minutes at room temperature, in a ligation reaction comprising 1 µl of 10x ligation buffer (Roche Applied Sciences, Germany), 1 U of T4 DNA Ligase (Roche Applied Sciences, Germany) and distilled water to a final volume of 10 µl. Following incubation the resultant product was transformed into competent *E. coli* cells (section D8) and incubated at 37°C on antibiotic containing agar plate for 16 hours (overnight). Colonies were screened for successful ligation as per section D1.

D6: DNA SEQUENCING

Plasmid DNA was isolated for DNA sequencing using the QIAprep$^{(R)}$ Spin Miniprep Kit (Qiagen, USA) in line with the manufacturer's instructions. Sequencing reactions comprised of the plasmid DNA (200 - 500 ng), 3.2 pmol of primer (forward or reverse primer), 2 µl of 5 x Big DyeR Terminator Sequencing Buffer (Big Dye Terminator Cycle Sequencing Kit version 3.1, (Applied Bioscience, USA), 4 µl of Big Dye Terminator (Applied Bioscience, USA) and distilled water to a final volume of 10 µl. Thermal cycling was performed in a GeneAmp PCR System 9700 (version 3.05; Applied Bioscience, USA) as follows: one cycle of denaturation (94 °C, 3 minutes), 30 cycles of denaturation, annealing and extension (96 °C denaturation for 30 seconds, 55°C annealing for 30 seconds, and 72°C for 30 seconds) and a final elongation at 72oC for 7 minutes. Amplification product was purified from unincorporated big dye terminators using Zymo–Spin I TM columns (Zymo Research, UK) in line with the manufacturer's instructions. The DNA was eluted in 10 µl of water and vacumm dried. The purified DNA was resuspended in Hi–Di buffer for sequencing in ABIPRISM 3100 Genetic Analyser (Applied Bioscience, USA) and analysed by capillary

electrophoresis. DNA sequencing results were analysed using Chromas (version 2.33) and BioEdit Sequence Alignment Editor (version 7.0.4.1) (Hall, 1999).

D7: DNA CLEAN AND CONCENTRATOR

DNA clean and Concentrator–5™ kit (Zymo Research, UK) was used to clean up and concentrate DNA in line with the manufacturer's instructions. Briefly, in 1.5 ml microcentrifuge tube, to each volume of the DNA was added 2 volumes of DNA binding buffer, vortexed mixed briefly and the mixture was transferred to a Zymo-spin™ column in a collection tube and centrifuged at ≥ 10 000 rpm for 30 seconds. The flow-through was discarded and the column was washed twice with 200 µl wash buffer and centrifuged at ≥ 10 000 rpm for 30 seconds. The column was transfer to a new 1.5 ml microcentrifuge and the DNA was eluted by adding 6 - 10 µl of water directly to the column matrix followed by centrifugation at ≥ 10 000 rpm for 30 seconds.

D8: PREPARATION OF COMPETENT *E. COLI* CELLS

The protocol was as previously described (Dagert and Ehrlich, 1979). The *Escherichia coli* strain of interest was grown overnight (37°C, 200 rpm) in 5 ml of YT broth (1.6% w/v tryptone, 1% w/v yeast extract, 0.5%w/v NaCl) supplemented with the appropriate antibiotic for strain selection if required. 1.5 ml, 1.0 ml, 0.7 ml, and 0.3 ml of the overnight culture was inoculated into four flasks of 100 ml YT broth and incubated at 37°C with shaking until the flask inoculated with 1.5ml of the overnight culture reaches an OD_{600} of 0.6 - 0.8 Absorbance Unit (AU). Following the attainment of the correct optical density, 1.5 ml and 1.0 ml inoculated cultures were pooled together and 0.7 ml and 0.3 ml inoculated cultures were also pooled together into sterile 250 ml (Beckman JA 14 compatible) centrifuge tubes and centrifuged in the Beckman JA 14 Rotor at 5000 rpm for 10 minutes at 4°C. The pellets were resuspended in 4 ml of RF1 solution (100 mM KCl, 50 mM $MnCl_2$, 30 mM CH_3OOK, 10 mM $CaCl_2$ and 15% v/v Glycerol, pH 5.8) and incubated on ice for 20 minutes followed by centrifugation at 5000 rpm for 10 minutes in the Beckman JA 14 Rotor at 4°C. The content of the tubes were then pooled together by resuspending them in a total volume of 4 ml of RF2 solution (10 mM KCl, 10 mM MOPS, 80 mM $CaCl_2$ and 15% v/v Glycerol, pH 6.8). 300 µl aliquots the cells were store at -70°C until needed.

D9: TRANSFORMATION OF COMPETENT *E. COLI* CELLS

100 µl of competent *E. coli* cells (SECTION D7) were incubated with 100 ng of the plasmid DNA of interest (or 2 µl of ligation product) at 4°C for 30 minutes. Transformation controls included a sterile and a competent controls that were incubated with sterile distilled water and pUC18 plasmid DNA (Promega) respectively. This was followed by heat shock at 42°C for 45 seconds and second

incubation on ice (4°C) for 10 minutes. 900 µl (1 in 10 dilution) of YT broth (1.6%w/v tryptone, 1.0 %w/v yeast extract, 0.5%w/v NaCl) was added and were subsequently incubated for 60 minutes with shaking (200 rpm) at 37°C. The resultant cultures were centrifuged at 13,000 rpm for 2 minutes and the bacterial were resuspended in 100 µl of YT broth. The suspension was plated onto YT-agar plates (1.5% agar in YT broth) supplemented with the appropriate antibiotics (100 $\mu g.ml^{-1}$ ampicillin for pQE30-based plasmid selection; 50 $\mu g.ml^{-1}$ kanamycin for *E. coli* M15[*pREP4*] strain selection; and 34 $\mu g.ml^{-1}$ chloramphenicol and 50 $\mu g.ml^{-1}$ kanamycin for *E. coli* BB1994 strain selection). The plates were incubated overnight at 37°C.

D10: PROTEIN CONCENTRATION DETERMINATION BY BRADFORD'S ASSAY

Protein concentration determination was performed by Bradford's assay as previously described (Bradford, 1976) with Bradford reagent, ready to use (Fermentas). Each assay consisted of the BSA standard, blank (buffer) and test samples. Both standard and micro assay in 96 wells microplate were performed depending on the yield of the protein and in line with the manufacturer's protocols. Briefly, for standard assay, 5 µl (120 µl micro assay) of the samples were pipetted in triplicate in to the well of the microplate followed by the addition of 250 µl (120 µl micro assay) of Bradford reagent, ready to use, and mixing. Following incubation at room temperature for 10 minutes, the Absorbance of the samples was read at 595 nm in a PowerWave™ Microplate spectrophotometer (Biotek). Protein concentration was extrapolated from the Bovine Serum Albumin (BSA) standard curve (0 – 1.5 $mg.ml^{-1}$ for standard assay and 0 – 25 $\mu g.ml^{-1}$ for micro assay) prepared for the assay (represented in *Appendix B.8*).

D11: SODIUM-DODECYL SULPHATE – POLYACRYLAMIDE GEL ELECTROPHORESIS (SDS-PAGE)

The protocol for SDS-PAGE analysis is adapted from that previously described (Shapiro et al., 1967). Protein samples to be resolved by SDS-PAGE electrophoresis were first treated with 5x SDS-PAGE sample buffer (10% glycerol, 2% SDS, 5% β-mercaptoethanol, 0.05% bromophenol blue, 0.0625 M Tris, pH 6.8) in a ratio of 4:1 (protein:buffer) and loaded onto a polyacrylamide gel composed of a resolving gel (0.375 M Tris, pH 8.8, 0.1% (w/v) SDS, 10-12% (w/v) acrylamide-bis-acrylamide, 0.05% (w/v) ammonium persulphate (APS), 0.005% (v/v) N,N,N',N'-tetramethylethylenediamine (TEMED) in distilled water) and a stacking gel (0.125 M Tris, pH 6.8, 0.1% (w/v) SDS, 4% (w/v) acrylamide-bis-acrylamide, 0.05% (w/v) APS, 0.005% (v/v) TEMED in distilled water). Protein marker (Fermentas) was also loaded to serve as standard. The gel was resolved in a Mini Protean^{R} II system (Bio-Rad) at 160 V for one hour and stained or used for Western analysis (SECTION D11). Staining of the SDS-PAGE gel was done in Coomassie Blue

stain (40% (v/v) methanol, 7% (v/v) acetic acid, 0.25% (w/v) Coomassie Blue R250 in distilled water) overnight and destained using destaining solution (40% (v/v) methanol, 7% (v/v) acetic acid in distilled water) followed by gel visualisation using a Chemidoc chemiluminescence imaging system (Bio-Rad).

D12: PROTEIN DETECTION BY WESTERN ANALYSIS

The protocol for the detection of proteins by Western analysis was adapted from that described (Towbin et al., 1979). Proteins were resolved by SDS-PAGE as per section D10 and transferred onto nitrocellulose membrane (Hybond C-extra; GE Healthcare, UK) in transfer buffer (20% (v/v) methanol, 192 mM glycine, 25 mM Tris in distilled water) at 120 V for 60 minutes in a Mini Protean^{R} III Western trans-blot system (Bio-Rad). Protein transfer was verified with Ponceau S stain (0.5 % (w/v) Ponceau S, 1% (v/v) glacial acetic acid in distilled water). This was followed by membrane destaining with distilled water and overnight incubation at 4°C in blocking solution that was made up of 5% (w/v) fat-free milk powder in Tris Buffered Saline (TBS; 50 mM Tris, 150 mM NaCl, pH 7.5 in distilled water) except otherwise stated. The membrane was incubated with appropriate primary antibody (1:5000 in blocking solution unless otherwise stated in the text) for one hour at room temperature and washed four times (15 minutes each) with Tris Buffered Saline-Tween buffer (TBS-T; TBS containing 0.1% (v/v) Tween 20). This was followed by incubation of the membrane with the appropriate horse-radish peroxidise (HRP)-conjugated secondary antibody (1:10,000 in blocking solution unless otherwise stated in the text) for one hour at room temperature and washed with TBS-T as before. Chemiluminescence-based protein detection was achieved using the ECL^{TM} Western blotting kit (GE Healthcare, UK) as per the manufacturer's instructions, and captured with a Chemidoc chemiluminescence imaging system (Bio-Rad, USA).

D13: ANALYSIS OF RECOMBINANT PROTEIN EXPRESSION (INDUCTION STUDIES)

A colony of the specified *E. coli* strain transformed with the appropriate plasmid (pQE30-PFA0660w or other plasmid) as per section D8) was inoculated into 25 ml of 2xYT broth having the appropriate antibiotics selection pressure in the specified final concentration, and incubated overnight for about 16 hours at 180 rpm at the stated 37°C. The overnight culture was diluted to an A_{600} of 0.1 in 250 ml of the YT growth media supplemented with the appropriate concentration of antibiotic and incubated at 37°C to a cell density (A_{600}) of 0.6 – 0.8. Following the attainment of the desired cell density, protein expression was induced with 1 mM IPTG (except otherwise stated in the text) and 1 ml aliquots of the induced cells were harvested at 0 (pre-induction), 1, 2, 3, 4, 5 and 16 (overnight) hours post-induction. The harvested cells were pelleted by centrifugation at 13 000 x g for 1 minute and resuspended in phosphate buffered saline (PBS; 137 mM NaCl, 2.7 mM KCl, 10

mM Na_2HPO4, 2 mM KH_2PO4, pH 7.4) in volumes dependent on the cell density (150 µl of PBS per 0.5 recorded A_{600} absorbance units). Samples were analysed for recombinant protein expression by SDS-PAGE as per section D10 and Western analysis using a mouse anti-His primary mAb (1:5000; GE Healthcare) and an HRP-conjugated sheep anti-mouse secondary antibody (1:5000; GE Healthcare, UK) as per section D11.

D14: PREPARATION OF CHELATING SEPHAROSE FAST FLOW GEL FOR USE IN HIS-TAGGED PROTEIN PURIFICATION

Chelating Sepharose Fast Flow as supplied is approximately 75 % slurry in 20 % ethanol. The following procedure results in 50 % slurry of Chelating Sepharose Fast Flow charged with nickel. The gel is resuspended by gentle shaken and an aliquot is pipetted out into a new container/tube. The ethanol content was removed by decantation following centrifugation at 500 x g for 2-5 minutes. The gel is then resuspended in five gel volumes of distilled water and shaken gently by end-over-end rotation for 5 minutes (the use of magnetic stirrers must be avoided). The suspended gel was re-sedimented by centrifugation at 500 x g for 2-5 minutes and the supernatant was discarded. The washing process was repeated two more times. To charge the gel using nickel metal, 0.5 gel volume of 0.1 M $NiSO_4$ solution was added and shaken gently until the gel is fully re-suspended. The excess solution is removed by centrifugation at 500 x g for 2-5 minutes. The charged gel was washed by gently resuspending in five gel volumes of distilled water three times and water was removed at each round of washes by centrifugation at 500 x g for 2-5 minutes. Where necessary weakly bound nickel ions can be removed by the addition of buffer containing 1 M Imidazole, followed by washing in the buffer and finally again in distilled water. Finally, the nickel charged Sepharose gel was equilibrated in the desired start buffer (i.e. the buffer into which His-tagged protein was prepared), ready to be used for purification purposes. The binding capacity is about 5 mg histidine-tagged protein/ml gel.

D15: NATIVE OR NON-DENATURING PURIFICATION PROTOCOL

The native or non-denaturing purification of recombinant proteins were performed using the modification of a previously described procedure (Shonhai et al., 2008) as follows: 1 litre culture of *E. coli* transformants was maintained in 2xYT broth supplemented with appropriate antibiotics (to a final concentration of 100 µg/ml ampicillin for XL1 blue, and 100 µg/ml ampicillin + 50 µg/ml kenamycin for M15[pREP4]) and incubated at 37°C with shaking until the OD_{600} reached 0.6 – 0.8. Expression of protein was induced by the addition of IPTG to a final concentration of 1 mM and incubated for further 4 hours. The cells were then harvested by centrifugation (5,000 × *g* at 4 °C for 20 min). The cell pellet was resuspended in native lysis buffer (NLB - 2.5 ml; 10 mM Tris, pH 8.5,

300 mM NaCl, 50 mM Imidazole, 1 mM PMSF and 1 mg/ml lysozyme) and kept at -80°C overnight. The frozen pellet was rapidly thawed and sonication (5 times, 30 seconds each, at 30 second interval and 50 Hz) was performed at 4°C. The suspension was clarified by centrifugation (16,000 × *g* for 30 min at 4 °C) to obtain a clear supernatant. The supernatant was applied to nickel-charged sepharose beads (prepared as per Appendix D14) pre-incubated with NLB and binding was allowed for 4 hours at 4°C with gentle rocking. The unbound protein and contaminants were removed following centrifugation at 1,500 x g for 2 minutes, and the protein bound beads were washed 3 times with cold wash buffer (WB – 3 ml: 10 mM Tris, pH 8, 300 mM NaCl, 50 mM Imidazole) and recovered by centrifugation at 1500 x g for 2 minutes. The bound protein was eluted at least thrice with cold native elution buffer (NEB – 2 ml: 10 mM Tris, pH 8, 300mM NaCl, 1M Imidazole). All the eluted samples were analysed by SDS–PAGE and western analysis with the appropriate antibody (1 in 5,000) and dialysed into native dialysis buffer (NDB: 200 mM NaCl, 10 mM Tris-HCl, pH 8.0) or into the appropriate assay buffers for functional studies. Protein concentrations were determined by Bradford's assay (Bradford, 1976).

D16: OPTIMIZED NATIVE PURIFICATION PROTOCOL FOR HsHsp70

The protocol for the purification of 6xHis-tagged recombinant HsHsp70 was adapted from a previously published work (Chiang et al., 2009). 1 litre culture (divided into four 250 ml flask) of BL21 *E. coli* cells transformants was maintained in 2xYT broth supplemented with ampicillin to a final concentration of 100 µg/ml at 37°C until the OD_{600} 0.6-0.8. Protein expression was induced following the addition of IPTG to a final concentration of 1 mM and the cells were harvested after 3 hours by centrifugation (5,000 x g for 10 minutes at 4°C). The supernatant was discarded and each pellet was resuspended in 10 ml TEK_{50} (20 mM Tris-HCl pH 8.0, 0.1 mM EDTA, 50 mM KCl) and pooled together. The resuspended pellet was then divided into two 50 ml pre-weighed centrifuge tubes and clarified by centrifugation at 5,000 x g for 10 minutes at 4°C. The weight of the pellet containing tubes were determined and used to determine the mass of the pellet by subtraction from the initial weight. The pellet was stored at -80°C overnight. The pellet was then thawed on ice and resuspended in 3 ml/g final volume of TEK_{50} supplemented with lysozyme and PMSF to a final concentration of 1 mg/ml and 1 mM respectively. The suspension was incubated on ice for 30 minutes with slow intermittent mixing followed by 3 cycles (3 minutes in liquid nitrogen, 10 minutes in a 30°C water bath) of freeze-thawing. The resultant lysate was sonicated on ice (7 times, 15 seconds each, 30 second interval at 50 Hz) and centrifuged at 13,000 x g for 30 minutes at 4°C to obtained the clear supernatant. The pellet obtained was resuspended in total of 10 ml TEK_{50}, sonicated (5 times, 15 seconds each, at 30 second interval on ice using 50 Hz) and clarified again by centrifugation (13,000 x g for 30 minutes at 4°C). The supernatants were pooled together and the

protein was purified using nickel charged sepharose beads as Appendix D15. All the eluted samples were analysed by SDS–PAGE and western analysis with mouse monoclonal anti-His antibody (1 in 5,000) and dialysed into native dialysis buffer (NDB: 200 mM NaCl, 10 mM Tris-HCl, pH 8.0) or into the appropriate assay buffers for functional studies. Protein concentrations were determined by Bradford's assay (Bradford, 1976).

APPENDIX E

LIST OF MATERIALS AND SPECIALIZED REAGENTS

ANTIBODIES	SUPPLIER
Alexa FluorR 488 donkey anti–mouse	Invitrogen, USA
Alexa FluorR 488 chicken anti–rabbit	Invitrogen, USA
HRP–goat anti–mouse IgG	GE Healthcare, UK
HRP–conjugated sheep anti–mouse	GE Healthcare, UK
HRP–conjugated donkey anti–rabbit	GE Healthcare, UK
Mouse monoclonal anti–His primary antibody	GE Healthcare, UK
Mouse Anti–DnaK Monoclonal Antibody	Sigma–Aldrich, USA
Mouse His-probe (mouse anti His monoclonal IgG)	Santa Cruz Biotechnology
Rabbit α-glycophorin antibody	Thermo scientific, USA

REAGENT /MATERIAL	SUPPLIER
β–mercaptoethanol	Merck, Germany
λDNA	Promega, USA
Acetic Acid	Saarchem, South Africa
Adenosine triphosphate (disodium salt)	Sigma–Aldrich, USA
Agar (Bacteriological)	Biolab Diagnostics, South Africa
Agarose	Hispanagar, Spain
Ammonium per sulphate	Saarchem, South Africa
Ampicillin	Fisher Scientific, UK
30% Bis–Acrylamide	Bio–Rad, US
Bovine Serum Albumin	Sigma–Aldrich, USA
Bradford's Reagent	Fermentas, USA
Bromophenol Blue	Sigma–Aldrich, Germany
Calcium chloride	Saarchem, South Africa
AmiconR Ultra	UltracelR Centrifugal Filters Millipore, Ireland
Coomassie Brilliant Blue R250	Sigma–Aldrich, Germany
Hoescht	Invitrogen, USA
dNTP mix	Roche Applied Sciences, Germany
EDTA, sodium salt	Saarchem, South Africa
Ethanol	Saarchem, South Africa
Ethidium bromide	Sigma–Aldrich, Germany
Glacial acetic acid	Saarchem, South Africa
Glycerol	EMD Chemicals, USA

REAGENT /MATERIAL	SUPPLIER
Glycine	Sigma–Aldrich, Germany
HEPES	Fisher Scientific, UK
Hydrochloric Acid	Saarchem, South Africa
Imidazole	Sigma–Aldrich, Germany
Isopropyl–1–thio–β–D–galactopyranoside	Roche Applied Sciences, Germany
Kanamycin sulphate	Roche Applied Sciences, Germany
Lysozyme	Sigma–Aldrich, USA
Methanol	Saarchem, South Africa
Phenylmethylsulphonyl fluoride (PMSF)	Sigma–Aldrich, USA
Polyacrylamide	Bio–Rad, USA
Ponceau S	Sigma–Aldrich, Germany
Potassium chloride (KCl)	Saarchem, South Africa
Potassium hydroxide (KOH)	Saarchem, South Africa
Potassium phosphate (K2HPO4)	Merck, Germany
Potassium dihydrogen phosphate (KH2PO4)	Merck, Germany
Q–Sepharose Fast FlowTM	Sigma–Aldrich, USA
Sepharose Fast FlowTM	GE Healthcare, UK
Sodium chloride (NaCl)	Saarchem, South Africa
Sodium dodecyl sulphate (SDS)	Sigma–Aldrich, USA
Sodium phosphate (NaH2PO4 \ Na2HPO4)	Saarchem, South Africa
Sodium hydroxide (NaOH)	Saarchem, South Africa
SnakeskinTM dialysis tubing	Thermo Scientific, USA
TEMED (N,N,N‘,N‘‘–tetramethylethylenediamine)	Sigma–Aldrich, Germany
Tris (Tris–2–amino–2–hydroxymethyl–1,3–propanol)	Sigma–Aldrich, Germany
Tryptone	Oxoid, UK
Tween 20	Saarchem, South Africa
Urea	Sigma–Aldrich, Germany
Yeast extract	Oxoid, UK

RESTRICTION ENZYMES	SUPPLIER
BamHI	Fermentas, Lithuania
PstI	Fermentas, Lithuania
Kpn1	Fermentas, Lithuania

ESCHERICHIA COLI STRAINS	SUPPLIER
E. coli BL21(DE3)	Promega, USA
E. coli JM109	Promega, UK
E. coli XL1–Blue	Stratagene, USA
E. coli M15[pREP4]	Qiagen (USA)

PLASMIDS	SUPPLIER
pQE30	Qiagen, USA

ENZYMES	SUPPLIER
10x Buffer	Roche Applied Sciences, Germany
T4 DNA Ligase	Roche Applied Sciences, Germany
Ligation buffer	Roche Applied Sciences, Germany

COMMERCIAL KITS	SUPPLIER
Big DyeTM Terminator Cycle Sequencing Kit	Applied Biosciences, UK
ECL Western Blotting Kit	GE Healthcare, UK
ZymocleanTM Gel DNA Recovery Kit	Zymo Research,USA
DNA Clean & Concentrator–5TM	Zymo Research, USA
QIAPrepR Miniprep Kit	Qiagen, USA

PROTEIN MARKERS	SUPPLIER
PagerulerTM Protein Ladder	Fermentas, USA
Protein marker II peqGold	Fermentas, USA
Protein marker IV pre–stained	Invitrogen, USA

APPENDIX F

NUCLEOTIDE AND PROTEIN SEQUENCES IN FASTA FORMAT

F.1: PFA0660w Nucleotide and Protein sequences in fasta format

>PFA0660w Coding Sequence

ATGGCAACCTTAAGGAAAAGCTATGTACCAGAAATTTTATATTTTTCCAAATTTTTTATGAACGCATGTTT
TATTTCCCTTTTAATAATTACAGTGAATTGTTTTAATTATGAAAACTTTGTATGTAAGGATAAAGGAATAT
ATAATGAAAAGATAGTGATAAGATATAAACGATGTTTAGCAGAAGGTAATAAAAATTTCTTTTTTAATAA
GGACAATGGGGTTTTTGGAAAATCATCAATGGATTATTATACTTTATTGGGAGTTGATAAAGGGTGCTCA
GAAGACGATTTAAGAAGAGCATATTTAAAGCTAGCCATGAAATGGCATCCTGATAAACATGTTAACAAA
GGATCCAAAGTAGAAGCAGAAGAAAAGTTTAAAAATATTTGTGAAGCTTATAGTGTTTTGTCAGATAACG
AGAAAAGAGTAAAATATGATTTATTTGGAATGGATGCTTTAAAACAATCAGGATTTAATAGTTCAAATTT
TCAAGGAAATATTTCAATTAATCCGTTAGAAGTATTTACAAAAGCTTATAGTTTTTATAATAAATATTTTT
CAAAATCTAGTGGTGCTGGAAATCATAATATATTTACTCATATTAAAAATTTATACCCTTTGAGGAATGAC
TTTTCAGAAGATGAGAGCAGTTATAATGACGTGGAAGAATATGAAGTACCCCTTTACGTTACATTAGAAG
ATTTATACAACGGGTGCACAAAAACATTAAAAGTAACAAGAAAGAGATATGATGGATGCTACTTGTATTA
TGAGGATTATTTTATAAATGTCGATATAAAACAAGGATGGAATAATGGGACGAAGATTACTTTCCATGGG
GAAGGTGACCAGAGTTCTCCCGATTCTTATCCTGGTGATTTAGTTTTAGTATTACAAACAAAAAAGCATAG
TAAATTTGTAAGAAAGTCTCGAGATTTATATTATAGGCATATAATAACCTTAGAGCAATCATTAACAGGA
TTTGATTTTGTTATAAAATCATTAGATAATAGAGATATACATATACAAATAGATGAGGTGGTAAAACCTG
ACACAAAGAAGGTTATAAAAAATGAAGGAATGCCTTACTCAAGAGATCCAAGTATTAGAGGAAATTTGA
TTGTTGAATTTGATATTATATATCCTAATACAATAAAAAAGGAGCAAAAAAAATTGATAAAAGAGATATT
TAAAGAGAGTTATTAA

>PFA0660w Optimized Coding Sequence

GGATCC

GCATGCCGTTGCCTGGCGGAGGGTAACAAAAACTTTTTCTTTAACAAAGATAATGGCGTGTT**C**GGTAAAA
GCTCTATGGTATATTACACCCTGCTGGGCGTTGATAAAGGTTGTTCTGAAGATGATCTGCGTCGCGCGTAT
CTGAAACTGGCCATGAAATGGCATCCGGATAAACACGTGAACAAAGGCAGCAAAGTTGAAGCAGAAGAA
AAATTCAAAAACATCTGCGAAGCGTACTCTGTGCTGAGTGATAACGAAAAACGTGTTAAATACGATCTGT
TTGGCATGGATGCCCTGAAACAGAGTGGTTTCAACAGTAGCAATTTTCAGGGCAACATTAGCATCAATCC
GCTGGAAGTGTTTACCAAAGCCTACTCTTTCTACAACAAATACTTCAGTAAATCTAGTGGCGCAGGTAAC
CATAACATCTTCACGCACATCAAAAACCTGTACCCGCTGCGCAATGATTTTAGCGAAGATGAAAGCTCTT
ATAACGATGTGGAAGAATACGAAGTGCCGCTGTATGTTACCCTGGAAGATCTGTACAATGGTTGCACCAA
AACGCTGAAAGTGACGCGTAAACGCTACGATGGCTGTTACCTGTACTACGAAGATTACTTCATCAACGTT
GATATCAAACAGGGCTGGAACAATGGCACCAAAATCACGTTTCATGGCGAAGGTGATCAGAGTAGCCCG
GATAGCTATCCGGGTGATCTGGTGCTGGTTCTGCAGACCAAAAAACATAGTAAATTCGTGCGTAAAAGCC
GCGATCTGTATTACCGTCACATTATCACCCTGGAACAGAGCCTGACGGGCTTCGATTTTGTTATCAAATCT
CTGGATAACCGCGATATTCACATCCAGATTGATGAAGTGGTTAAACCGGATACCAAAAAAGTGATCAAAA
ACGAGGGTATGCCGTACAGCCGTGATCCGTCTATCCGCGGCAACCTGATCGTTGAATTCGATATCATCTAC
CCGAACACGATCAAAAAAGAACAGAAAAAACTGATCAAAGAAATTTTTAAAGAAAGCTATTAA
GGTACC

*Underlined are the BamHI (GGATCC) and KpnI (GGTACC) restriction sites used for the cloning

>PFA0660w Protein Sequence (PF3D7_0113700)

MATLRKSYVPEILYFSKFFMNACFISLLIITVNCFNYENFVCKDKGIYNEKIVIRYKRCLAEGNKNFFFNKDNGV
FGKSSMDYYTLLGVDKGCSEDDLRRAYLKLAMKWHPDKHVNKGSKVEAEEKFKNICEAYSVLSDNEKRVK
YDLFGMDALKQSGFNSSNFQGNISINPLEVFTKAYSFYNKYFSKSSGAGNHNIFTHIKNLYPLRNDFSEDESSYN
DVEEYEVPLYVTLEDLYNGCTKTLKVTRKRYDGCYLYYEDYFINVDIKQGWNNGTKITFHGEGDQSSPDSYP
GDLVLVLQTKKHSKFVRKSRDLYYRHIITLEQSLTGFDFVIKSLDNRDIHIQIDEVVKPDTKKVIKNEGMPYSRD
PSIRGNLIVEFDIIYPNTIKKEQKKLIKEIFKESY

F.2: Hsj1a Nucleotide and Protein sequences in fasta format

> Homo sapiens HSJ1a coding sequence

TCTAGA
CCCGCCTGACGACTGACCAGTTGCCATGGCATCCTACTACGAGATCCTAGACGTGCCGCGAAGTGCGTCC
GCTGATGACATCAAGAAGGCGTATCGGCGCAAGGCTCTCCAGTGGCACCCAGACAAAAACCCAGATAAT
AAAGAGTTTGCTGAGAAGAAATTTAAGGAGGTGGCCGAGGCATATGAAGTGCTGTCTGACAAGCACAAG
CGGGAGATTTACGACCGCTATGGCCGGGAAGGGCTGACAGGGACAGGAACTGGCCCATCTCGGGCAGAA
GCTGGCAGTGGTGGGCCTGGCTTCACCTTCACCTTCCGCAGCCCCGAGGAGGTCTTCCGGGAATTCTTTGG
GAGTGGAGACCCTTTTGCAGAGCTCTTTGATGACCTGGGCCCCTTCTCAGAGCTTCAGAACCGGGGTTCCC
GACACTCAGGCCCCTTCTTTACCTTCTCTTCCTCCTTCCCTGGGCACTCCGATTTCTCCTCCTCATCTTTCTC
CTTCAGTCCTGGGGCTGGTGCTTTTCGCTCTGTTTCTACATCTACCACCTTTGTCCAAGGACGCCGCATCAC
CACACGCAGAATCATGGAGAACGGGCAGGAGCGGGTGGAAGTGGAGGAGGATGGGCAGCTGAAGTCAG
TCACAATCAATGGTGTCCCAGATGACCTGGCACGTGGCTTGGAGCTGAGCCGTCGCGAGCAGCAGCCGTC
AGTCACTTCCAGGTCTGGGGGCACTCAGGTCCAGCAGACCCCTGCCTCATGCCCCTTGGACAGCGACCTC
TCTGAGGATGAGGACCTGCAGCTGGCCATGGCCTACAGCCTGTCAGAGATGGAGGCAGCTGGGAAGAAA
CCCGCAGATGTGTTCTGAGCTGGATGCCGGGTTCCAGAATCGCTGCACAGTTCCAACAGGACAGCGCCTT
CCCCCATGCGCTGGGAGGGGACCCTCCATTTCTCCCCCTCACCCATGCTGAGTGTAGAGCCGGGGCCTGG
GTGGCGGGTGGGGGCCGGGTGGGAGGTGGCAGTAGTCTTAGCCTGTGCACTCTCTTCCTTGGGTGTTTGG
TGCTGGCTCCTGGGGACTACAAATCCCAGAGTGCGGTGTGCCCGGCCTCATTTCTGATAGATCCCGCTTGG
GGGAGGTGGTGTATGGTTACGGAGCTGTGCATCTTGGGACATGTAGTAGCCCAGGTCTTGTCACTCGCTG
TGAGATGGGGAGATTTTGTCTTTTGATTTATCCCTGTAGGGCTGGCAGGGTTGTAGATGAAGGGGGAATG
ATCTGAGCCTTGGTTCCCCTGACACGTCTTGCTAGCCCCAGGGTTAGAGTGGGCAGGGCAGAGCCGCGCA
GCACCTGGGAGCGGTACCTTTCCCTTGGGCAGCCTGGGGTCCCAGGAACAAGCCAGGGCGAGTGGCATGT
CTGCCTGAGCAGGGTGTGGCCCCAGAAAGCTGAGGAGTGTGGGCTGGCAGAGAGCTTCGAGGGCAAGGC
CACCCGCGGGGGCGTGTGTGTGGTGGGGCTTGGCATGTGATGGCAGCTCCAGCTCCAGGCATGCCGCTGC
TTGTATGGCTTTCTTTGGCCTCTGACCCTGCTGCCCATTCTTTCCAACATCACAGATGAACTGCCTCTCCTC
CTCCCTGCCTGGGGAGCCCAGTGGCCAGGGAGGGAGTGGTGGAGCCAGTCGCTGTAACACTGAGCCTCA
GAGACGAACCAAAACCAGCTGGGCTGAGCTCAGATCCAGGGGGAAGAAATGCTGGAAGTCAATAAAACT
GAGTTTGAG
AAGCTT

*Underlined are the Xbal (TCTAGA) and HindIII (AAGCTT) restriction sites for cloning.

> Homo sapiens HSJ1a Protein sequence

MASYYEILDVPRSASADDIKKAYRRKALQWHPDKNPDNKEFAEKKFKEVAEAYEVLSDKHKREIYDRYGREG
LTGTGTGPSRAEAGSGGPGFTFTFRSPEEVFREFFGSGDPFAELFDDLGPFSELQNRGSRHSGPFFTFSSSFPGHS
DFSSSSFSFSPGAGAFRSVSTSTTFVQGRRITTRRIMENGQERVEVEEDGQLKSVTINGVPDDLARGLELSRREQ
QPSVTSRSGGTQVQQTPASCPLDSDLSEDEDLQLAMAYSLSEMEAAGKKPADVF

F.3: Protein sequences in fasta format of other Hsp40s

>PFE0055c Protein Sequence

MSILNKYEGKKNKIFLFIINIILFYTLEYVLIGSNYDKHNQSFGNEIFKNTKVFDFTSLRSLAEFNSGSSRESSKTD
ETDYYAVLGLTKDCTQDDIKKAYRKLAMKWHPDKHLNDEDKVEAERKFKLIGEAYEVLSDEEKRKNYDLFG
QSGLGGTTTNDEAYYTYSNIDPNELFSRFFSHDASSFFSQGFDDFPSFQGFASMNSRRPRSSRSNIFSRSFGRAAS
FEVPLQVTLEELYTGCRKKLKVTRKRFVGLNSYEDNTFITVDVKPGWSEGTKINFHGEGEQSSPNEQPGDLVFI
IKTKPHDRFIREGNNLIYKCYLPLDKALTGFQFSIKSLDNRDINVRVDDIINPNSKKIITNEGMPYSKSPSVKGDL
FIEFDIVFPKKLSPEQKRTLKETLENTY

>PFB0595w Protein Sequence

MGKDYYSILGVSRDCTTNDLKKAYRKLAMMWHPDKHNDEKSKKEAEEKFKNIAEAYDVLADEEKRKIYDT
YGEEGLKGSIPTGGNTYVYSGVDPSELFSRIFGSDGQFSFTSTFDEDFSPFSTFVNMTSRKSRPSTTTNINTNNYN
KPATYEVPLSLSLEELYSGCKKKLKITRKRFMGTKSYEDDNYVTIDVKAGWKDGTKITFYGEGDQLSPMAQP
GDLVFKVKTKTHDRFLRDANHLIYKCPVPLDKALTGFQFIVKSLDNRDINVRVDDIVTPKSRKIVAKEGMPSSK
YPSMKGDLIVEFDIVFPKSLTSEKKKIIRETLANTF

>PFB0090c Protein Sequence

MAIFKKYRFRENKIIFLFFIKIFLFSLFIWELCCFNKEKFQDQIQTSYYNKNNTSGNVSNLIIKRNLAQTQRNFKSK
NGKASTKKNEDYYSILGVSRDCTNEDIKKAYKKLAMKWHPDKHLNAASKKEADNMFKSISEAYEVLSDEEK
RDIYDKYGEEGLDKYGSNNGHSKGFKRTDPNDVFSKFFKTETKFYSNSPSSPNGNVLFEGSLFGGSSPFSGINPR
SGSGYTTSKSFSSMDKVEEYVVPLYVTLEDLYNGTQKKLKVTRKRCQGVTTYDDEFFVTVDIKSGWCDGTTIT
YKGEGDQTSPMSNPGDLVFTIKTVDHDRFVRSYNDLIYRCPITLEQALTGHKFTIITLDNRDIDIQVDEIVTPLTT
RVITSEGMPYMENPKMKGNLIIEFDIIFPKKLSDEQKELIKEALGGNGF

F.4: The Coding sequences of PfHsp70-1, PfHsp70-x and HsHsp70

>PfHsp70-1 coding sequence

GGATCC

ATGGCTAGTGCAAAAGGTTCAAAACCAAATTTACCAGAATCCAATATCGCTATTGGAATTGATTTAGGTA
CTACTTATTCTTGTGTTGGTGTATGGAGAAATGAAAATGTAGATATTATTGCTAATGACCAAGGTAATAGA
ACAACCCCATCTTATGTTGCTTTCACCGATACCGAAAGATTAATTGGAGATGCTGCTAAAAACCAAGTAG
CTAGGAATCCAGAAAATACAGTATTTGATGCTAAGAGATTAATTGGTAGAAAATTTACAGAATCATCAGT
ACAAAGTGATATGAAACATTGGCCATTCACTGTTAAATCAGGTGTTGATGAGAAACCAATGATTGAAGTT
ACCTATCAAGGAGAAAAGAAATTATTCCATCCAGAAGAAATTTCTTCTATGGTATTACAAAAAATGAAA
GAAAATGCTGAAGCATTTTTAGGAAAATCTATAAAGAATGCTGTCATTACCGTTCCAGCTTATTTTAACGA
TTCACAAAGACAAGCTACTAAAGATGCTGGTACAATTGCAGGATTAAATGTTATGAGAATTATTAATGAA
CCTACTGCAGCTGCTATTGCATATGGTTTACACAAAAAAGGAAAAGGTGAAAAGAACATTTTAATTTTCG
ACTTAGGAGGAGGTACATTTGATGTATCATTATTAACTATTGAAGATGGTATTTTTGAAGTAAAAGCTACT
GCTGGTGATACTCATTTAGGTGGTGAAGATTTCGATAACAGATTAGTAAATTTCTGTGTTGAAGATTTCAA
AAGAAAAAACAGAGGTAAAGATTTATCAAAAAATAGTAGAGCCTTAAGAAGATTAAGAACACAATGTGA
AAGAGCAAAACGTACTTTATCATCATCTACACAAGCTACAATTGAAATAGATTCCTTATTTGAAGGTATTG
ATTACAGTGTTACTGTAAGTAGAGCAAGATTTGAAGAATTATGTATCGACTATTTCCGTGATACTTTAATT
CCAGTAGAAAAAGTTTTAAAAGATGCTATGATGGATAAAAAAAGTGTACATGAAGTTGTTTTAGTTGGTG
GTTCTACAAGAATTCCAAAAATCCAAACTTTAATAAAAGAATTCTTTAATGGTAAAGAAGCATGCAGATC
AATTAACCCAGATGAAGCTGTTGCATATGGTGCAGCTGTACAAGCAGCCATTTTATCTGGTGACCAATCA
AATGCTGTCCAAGATTTATTATTATTAGATGTTTGCTCCTTATCATTAGGTTTAGAAACTGCTGGTGGTGTT
ATGACCAAATTAATTGAAAGAAACACAACCATACCTGCTAAAAAGAGTCAAATCTTTACTACTTATGCTG
ATAACCAACCAGGTGTCTTAATTCAAGTATATGAAGGTGAAAGAGCCTTAACCAAAGATAACAATTTATT
AGGAAAATTTCACTTAGATGGTATTCCACCTGCACCAAGAAAGGTACCACAAATCGAAGTTACATTCGAT
ATCGATGCTAACGGTATCTTAAACGTTACGGCTGTAGAAAAATCCACTGGTAAACAAAACCATATTACAA
TTACCAACGACAAAGGAAGATTATCTCAAGATGAAATTGATCGTATGGTTAATGATGCTGAAAAATACAA
AGCAGAAGATGAAGAAAACAGAAAAAGAATCGAAGCAAGAAACAGCCTTGAAAATTACTGCTATGGAG
TTAAAAGCTCATTAGAAGACCAAAAAATTAAAGAAAAATTACAACCAGCTGAAATTGAAACATGTATGA
AAACTATTACAACCATACTTGAATGGTTAGAAAAAAACCAACTTGCTGGAAAAGATGAATATGAAGCCA
AACAAAAAGAAGCAGAATCGGTTTGTGCTCCAATTATGTCTAAAATCTATCAAGATGCTGCTGGTGCAGC
CGGTGGTATGCCAGGAGGTATGCCCGGTGGAATGCCCGGTGGAATGCCAGGTGGTATGAATTTCCCAGGA
GGTATGCCCGGAGCAGGAATGCCAGGAAATGCCCCAGCTGGAAGTGGACCAACAGTTGAAGAAGTTGAT
TAA

AAGCTT

*Underlined are the BamHI (GGATCC) and HindIII (AAGCTT) restriction sites for cloning.

>PfHsp70-x coding sequence

GCATGCGGATCC

GCCTCTAATAACGCTGAAGAATCGGAAGTGGCAATCGGTATCGACCTGGGCACCACGTATAGTTGTGTTG
GCATCTGTCGTAACGGCGTGGTTGATATTATCGCAAACGACCAGGGTAATCGTACCACGCCGTCGTATGT
CGCTTTTACCGATACGGAACGTCTGATTGGTGATGCCGCAAAAAACCAGGCGAGCCGTAACCCGGAAAAT
ACCGTGTTTGATGCCAAACGTCTGATCGGTCGCAAATTCTCGGAAACCACGGTTCAGAGCGATATGAAAC
ATTGGCCGTTTACCGTCAAAGGCGGTTCTGACGGTAAACCGATGATTGAAGTTAGTTACCAGGGCGAAAA
GAAAACCTTCCACCCGGAAGAAATCAGCTCTATGGTGCTGAAGAAAATGAAAGAAGTTGCGGAAACCTA
TCTGGGTAAACCGGTTAAAAACGCGGTTATTACGGTCCCGGCCTACTTCAATGATTCTCAGCGTCAAGCG
ACCAAAGACGCCGGTGCAATTGCTGGCCTGAACGTCCTGCGCATTATCAATGAACCGACGGCAGCTGCGA
TCGCCTATGGCCTGGATAAAAAGGGTAAAGGCGAACAGAACATTCTGATCTTTGATCTGGGCGGTGGCAC
CTTCGACGTGTCTCTGCTGACGCTGGAAGATGGTATTTTTGAAGTTAAAGCAACCAGTGGCGACACGCAT
CTGGGTGGCGAAGATTTCGACAACAAACTGGTTAACTTCTGCGTCCAGGATTTCAAAAAGAAAAACGGTG

GCAAAGACGTTTCTAAAAATTCCAAATCACTGCGTCGCCTGCGTACCCAGTGTGAAAAAGCGAAACGCGT
GCTGAGTTCCTCAGCGCAAGCCACGATTGAAGTTGATAGTCTGTTTGATGGCATTGACTATAACGTCAATA
TCACCCGTGCAAAATTTGAAGAACTGTGCATGGATCAGTTCCGCAATACGCTGATTCCGGTGGAAAAAGT
TCTGAAAGATGCTAAAATGGACAAATCGCAAGTGCACGAAATCGTCCTGGTGGGTGGCAGCACCCGTATT
CCGAAAATCCAGCAACTGATCAAAGATTTCTTTAACGGTAAAGAACCGTGCAAAGCCATCAATCCGGACG
AAGCAGTTGCTTACGGTGCCGCAGTCCAGGCTGCGATTCTGTCCGGCGATCAATCGAGCGCGGTCAAAGA
TCTGCTGCTGCTGGACGTGTGTCCGCTGTCACTGGGCCTGGAAACCGCCGGTGGCGTTATGACGAAACTG
ATTGAACGCAACACCACGATCCCGACCAAGAAAAACCAGATTTTTACCACGTATGCGGATAACCAGCCGG
GTGTGCTGATCCAAGTTTACGAAGGCGAACGTGCCATGACCAAAGATAACAATCTGCTGGGTAAATTTCA
GCTGGAAGGCATTCCGCCGGCACCGCGCAGCGTCCCGCAAATCGAAGTGACCTTCGATATTGACGCAAAC
GGTATCCTGAATGTGACCGCTCTGGATAAGGGTACGGGCAAACAGAACCAAATTACCATCACGAATGAC
AAAGGCCGTCTGTCCAAAGATGACATTGATCGCATGGTTAACGACGCAGAAAAATACAAAGAAGAAGAT
GAACAGAACAAAAATCGTATCGAAGCTCGCAACAATCTGGAAAACTATTGCTACAACGTGAAAAATACC
CTGCAAGATGAAAATCTGAAAACGAAAATTCCGAAAGATGACTCCGAAAAATGTATGAAAACCGTCAAA
TCAGTGCTGGATTGGCTGGAGAAAAACCAGACCGCCGAAACGGAAGAATACAACGAAAAAGAAAAAGA
TATCTCTAGTGTGTATAACCCGATTATGACCAAAATCTACCAGGGTGCGAGCGCCCAGGAACCGCAAAAA
GCAGAAGCTACGAATCTGCGCGGCCGCAACTCCGAAAATAAAGAAGCACAAAACAATGGTCCGACGGTG
GAAGAAGTGAACTAA
AAGCTT
*Underlined are the SphI (GCATGC), BamHI (GGATCC) and HindIII (AAGCTT) restriction sites for cloning.

>HsHsp70 coding sequence

TCTAGA
ATAAAAGCCCAGGGGCAAGCGGTCCGGATAACGGCTAGCCTGAGGAGCTGCTGCGACAGTCCACTACCT
TTTTCGAGAGTGACTCCCGTTGTCCCAAGGCTTCCCAGAGCGAACCTGTGCGGCTGCAGGCACCGGCGCG
TCGAGTTTCCGGCGTCCGGAAGGACCGAGCTCTTCTCGCGGATCCAGTGTTCCGTTTCCAGCCCCCAATCT
CAGAGCGGAGCCGACAGAGAGCAGGGAACCGGCATGGCCAAAGCCGCGGCGATCGGCATCGACCTGGG
CACCACCTACTCCTGCGTGGGGGTGTTCCAACACGGCAAGGTGGAGATCATCGCCAACGACCAGGGCAAC
CGCACCACCCCCAGCTACGTGGCCTTCACGGACACCGAGCGGCTCATCGGGGATGCGGCCAAGAACCAG
GTGGCGCTGAACCCGCAGAACACCGTGTTTGACGCGAAGCGGCTGATTGGCCGCAAGTTCGGCGACCCGG
TGGTGCAGTCGGACATGAAGCACTGGCCTTTCCAGGTGATCAACGACGGAGACAAGCCCAAGGTGCAGG
TGAGCTACAAGGGGGAGACCAAGGCATTCTACCCCGAGGAGATCTCGTCCATGGTGCTGACCAAGATGA
AGGAGATCGCCGAGGCGTACCTGGGCTACCCGGTGACCAACGCGGTGATCACCGTGCCGGCCTACTTCAA
CGACTCGCAGCGCCAGGCCACCAAGGATGCGGGTGTGATCGCGGGGCTCAACGTGCTGCGGATCATCAA
CGAGCCCACGGCCGCCGCCATCGCCTACGGCCTGGACAGAACGGGCAAGGGGGAGCGCAACGTGCTCAT
CTTTGACCTGGGCGGGGGCACCTTCGACGTGTCCATCCTGACGATCGACGACGGCATCTTCGAGGTGAAG
GCCACGGCCGGGGACACCCACCTGGGTGGGGAGGACTTTGACAACAGGCTGGTGAACCACTTCGTGGAG
GAGTTCAAGAGAAAACACAAGAAGGACATCAGCCAGAACAAGCGAGCCGTGAGGCGGCTGCGCACCGC
CTGCGAGAGGGCCAAGAGGACCCTGTCGTCCAGCACCCAGGCCAGCCTGGAGATCGACTCCCTGTTTGAG
GGCATCGACTTCTACACGTCCATCACCAGGGCGAGGTTCGAGGAGCTGTGCTCCGACCTGTTCCGAAGCA
CCCTGGAGCCCGTGGAGAAGGCTCTGCGCGACGCCAAGCTGGACAAGGCCCAGATTCACGACCTGGTCCT
GGTCGGGGGCTCCACCCGCATCCCCAAGGTGCAGAAGCTGCTGCAGGACTTCTTCAACGGGCGCGACCTG
AACAAGAGCATCAACCCCGACGAGGCTGTGGCCTACGGGGCGGCGGTGCAGGCGGCCATCCTGATGGGG
GACAAGTCCGAGAACGTGCAGGACCTGCTGCTGCTGGACGTGGCTCCCCTGTCGCTGGGGCTGGAGACGG
CCGGAGGCGTGATGACTGCCCTGATCAAGCGCAACTCCACCATCCCCACCAAGCAGACGCAGATCTTCAC
CACCTACTCCGACAACCAACCCGGGGTGCTGATCCAGGTGTACGAGGGCGAGAGGGCCATGACGAAAGA
CAACAATCTGTTGGGGCGCTTCGAGCTGAGCGGCATCCCTCCGGCCCCCAGGGGCGTGCCCCAGATCGAG
GTGACCTTCGACATCGATGCCAACGGCATCCTGAACGTCACGGCCACGGACAAGAGCACCGGCAAGGCC
AACAAGATCACCATCACCAACGACAAGGGCCGCCTGAGCAAGGAGGAGATCGAGCGCATGGTGCAGGAG
GCGGAGAAGTACAAAGCGGAGGACGAGGTGCAGCGCGAGAGGGTGTCAGCCAAGAACGCCCTGGAGTC
CTACGCCTTCAACATGAAGAGCGCCGTGGAGGATGAGGGGCTCAAGGGCAAGATCAGCGAGGCGGACAA
GAAGAAGGTGCTGGACAAGTGTCAAGAGGTCATCTCGTGGCTGGACGCCAACACCTTGGCCGAGAAGGA
CGAGTTTGAGCACAAGAGGAAGGAGCTGGAGCAGGTGTGTAACCCCATCATCAGCGGACTGTACCAGGG
TGCCGGTGGTCCCGGGCCTGGGGGCTTCGGGGCTCAGGGTCCCAAGGGAGGGTCTGGGTCAGGCCCCACC
ATTGAGGAGGTAGATTAGGGGCCTTTCCAAGATTGCTGTTTTTGTTTTGGAGCTTCAAGACTTTGCATTTC
CTAGTATTTCTGTTTGTCAGTTCTCAATTTCCTGTGTTTGCAATGTTGAAATTTTTTGGTGAAGTACTGAAC
TTGCTTTTTTTCCGGTTTCTACATGCAGAGATGAATTTATACTGCCATCTTACGACTATTTCTTCTTTTTAAT
ACACTTAACTCAGGCCATTTTTTAAGTTGGTTACTTCAAAGTAAATAAACTTTAAAATTCAA
AAGCTT
*Underlined are the Xbal (TCTAGA) and HindIII (AAGCTT) restriction sites for cloning.

F.5: Proteins sequences of PfHsp70-1, PfHsp70-x and HsHsp70

>PfHsp70-1 (PF3D7_0818900)

MASAKGSKPNLPESNIAIGIDLGTTYSCVGVWRNENVDIIANDQGNRTTPSYVAFTDTERLIGDAAKNQVARN
PENTVFDAKRLIGRKFTESSVQSDMKHWPFTVKSGVDEKPMIEVTYQGEKKLFHPEEISSMVLQKMKENAEAF
LGKSIKNAVITVPAYFNDSQRQATKDAGTIAGLNVMRIINEPTAAAIAYGLHKKGKGEKNILIFDLGGGTFDVS
LLTIEDGIFEVKATAGDTHLGGEDFDNRLVNFCVEDFKRKNRGKDLSKNSRALRRLRTQCERAKRTLSSSTQA
TIEIDSLFEGIDYSVTVSRARFEELCIDYFRDTLIPVEKVLKDAMMDKKSVHEVVLVGGSTRIPKIQTLIKEFFNG
KEACRSINPDEAVAYGAAVQAAILSGDQSNAVQDLLLLDVCSLSLGLETAGGVMTKLIERNTTIPAKKSQIFTT
YADNQPGVLIQVYEGERALTKDNNLLGKFHLDGIPPAPRKVPQIEVTFDIDANGILNVTAVEKSTGKQNHITIT
NDKGRLSQDEIDRMVNDAEKYKAEDEENRKRIEARNSLENYCYGVKSSLEDQKIKEKLQPAEIETCMKTITTIL
EWLEKNQLAGKDEYEAKQKEAESVCAPIMSKIYQDAAGAAGGMPGGMPGGMPGGMPGGMPGGMNFPGGMPGAG
MPGNAPAGSGPTVEEVD

>PfHsp70-x (PF3D7_0831700)

MKTKICSYIHYIVLFLIATTTVHTASNNAEESEVAIGIDLGTTYSCVGICRNGVVDIIANDQGNRTTPSYVAFTDT
ERLIGDAAKNQASRNPENTVFDAKRLIGRKFSETTVQSDMKHWPFTVKGGSDGKPMIEVSYQGEKKTFHPEEI
SSMVLKKMKEVAETYLGKPVKNAVITVPAYFNDSQRQATKDAGAIAGLNVLRIINEPTAAAIAYGLDKKGKG
EQNILIFDLGGGTFDVSLLTLEDGIFEVKATSGDTHLGGEDFDNKLVNFCVQDFKKKNGGKDVSKNSKSLRRL
RTQCEKAKRVLSSSAQATIEVDSLFDGIDYNVNITRAKFEELCMDQFRNTLIPVEKVLKDAKMDKSQVHEIVL
VGGSTRIPKIQQLIKDFFNGKEPCKAINPDEAVAYGAAVQAAILSGDQSSAVKDLLLLDVCPLSLGLETAGGVM
TKLIERNTTIPTKKNQIFTTYADNQPGVLIQVYEGERAMTKDNNLLGKFQLEGIPPAPRSVPQIEVTFDIDANGIL
NVTALDKGTGKQNQITITNDKGRLSKDDIDRMVNDAEKYKEEDEQNKNRIEARNNLENYCYNVKNTLQDEN
LKTKIPKDDSEKCMKTVKSVLDWLEKNQTAETEEYNEKEKDISSVYNPIMTKIYQGASAQEPQKAEATNLRGR
NSENKEAQNNGPTVEEVN

>HSP71_HUMAN (P08107) – HsHsp70

MAKAAAIGIDLGTTYSCVGVFQHGKVEIIANDQGNRTTPSYVAFTDTERLIGDAAKNQVALNPQNTVFDAKRL
IGRKFGDPVVQSDMKHWPFQVINDGDKPKVQVSYKGETKAFYPEEISSMVLTKMKEIAEAYLGYPVTNAVIT
VPAYFNDSQRQATKDAGVIAGLNVLRIINEPTAAAIAYGLDRTGKGERNVLIFDLGGGTFDVSILTIDDGIFEVK
ATAGDTHLGGEDFDNRLVNHFVEEFKRKHKKDISQNKRAVRRLRTACERAKRTLSSSTQASLEIDSLFEGIDFY
TSITRARFEELCSDLFRSTLEPVEKALRDAKLDKAQIHDLVLVGGSTRIPKVQKLLQDFFNGRDLNKSINPD
EAVAYGAAVQAAILMGDKSENVQDLLLLDVAPLSLGLETAGGVMTALIKRNSTIPTKQTQIFTTYSDNQPGVL
IQVYEGERAMTKDNNLLGRFELSGIPPAPRGVPQIEVTFDIDANGILNVTATDKSTGKANKITITNDKGRLSKEE
IERMVQEAEKYKAEDEVQRERVSAKNALESYAFNMKSAVEDEGLKGKISEADKKKVLDKCQEVISWLDANT
LAEKDEFEHKRKELEQVCNPIISGLYQGAGGPGPGGFGAQGPKGGSGSGPTIEEVD

APPENDIX G

SUPPLEMENTARY PROTEIN SEQUENCE ALIGNMENTS

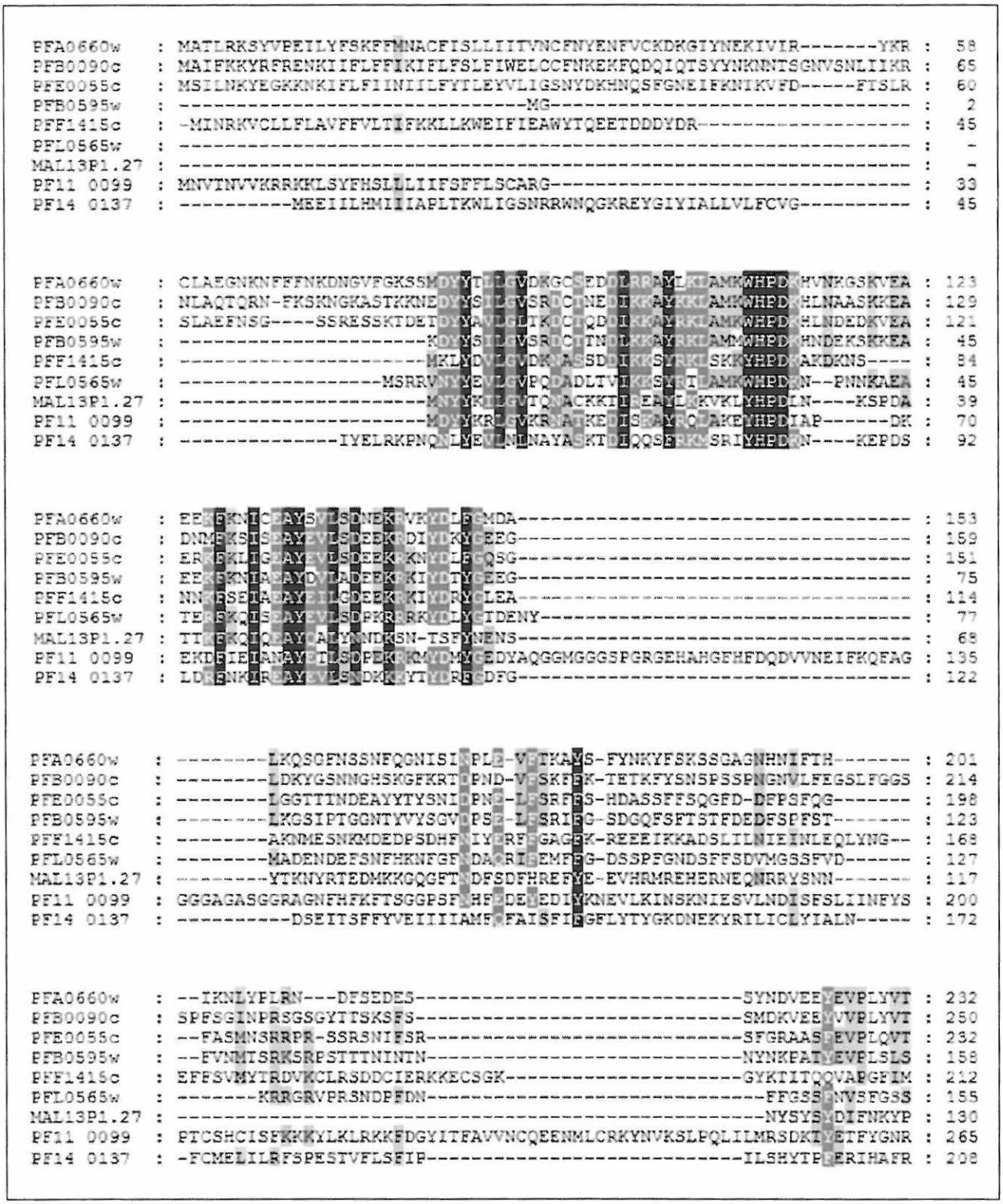

Continue next page.....

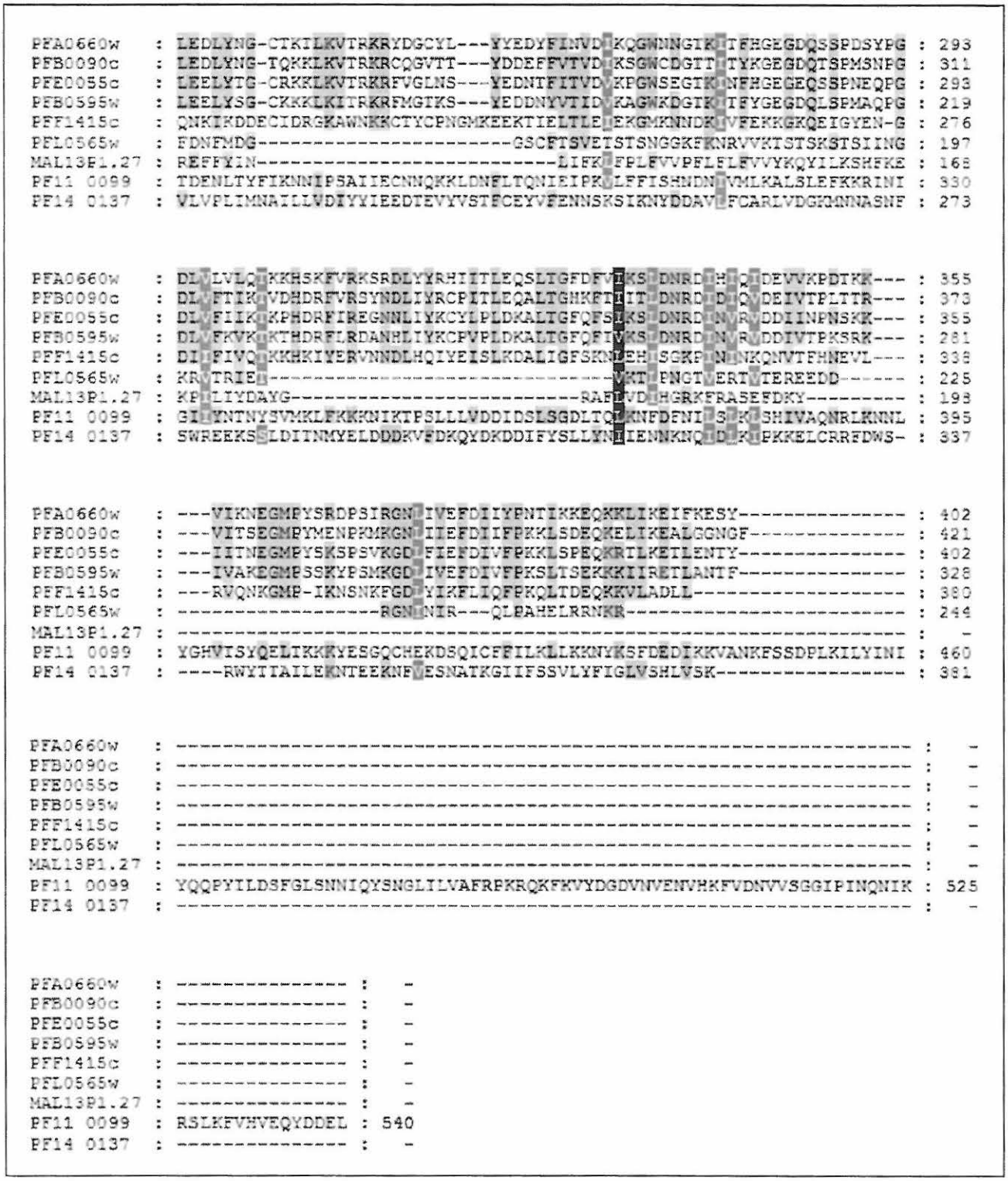

The amino acid multiple sequence alignment of type II *Plasmodium falciparum* Hsp40s. The level of sequence conservations are as shaded with the black background being the most conserved. The alignment was generated using ClustalW and shading was done using GeneDoc softwares (Larkin et al., 2007; Nicholas et al., 1995; Thompson et al., 1994).